The Coordination Chemistry of Pendant Aniline Aza-Macrocycles.

Thomas Tatchell B.Sc (Hons)

A thesis submitted to the University of Wales in accordance with the requirements for the degree of Doctor of Philosophy in the Faculty of Science, Department of Chemistry, University of Wales, Cardiff

December 2005

UMI Number: U584854

All rights reserved

INFORMATION TO ALL USERS
The quality of this reproduction is dependent upon the quality of the copy submitted.

In the unlikely event that the author did not send a complete manuscript
and there are missing pages, these will be noted. Also, if material had to be removed,
a note will indicate the deletion.

UMI®
Dissertation Publishing

UMI U584854
Published by ProQuest LLC 2013. Copyright in the Dissertation held by the Author.
Microform Edition © ProQuest LLC.
All rights reserved. This work is protected against
unauthorized copying under Title 17, United States Code.

ProQuest®

ProQuest LLC
789 East Eisenhower Parkway
P.O. Box 1346
Ann Arbor, MI 48106-1346

Abstract.

The selective functionalisation of triazamacrocycles is investigated herein, with the focus on 1, 4, 7-triazacyclononane (tacn). The ligands tris (5-fluoro, 2-aminophenyl) 1, 4, 7-triazacyclononane (L^1), tris (4-fluoro, 2-aminophenyl) 1, 4, 7-triazacyclononane (L^2) and tris (3-fluoro, 2-aminophenyl) 1, 4, 7-triazacyclononane (L^3) were studied. X-Ray crystal data was obtained for $[(L^1)M](ClO_4)_2.xMeCN$ where $M=Mn^{II}/Fe^{II}/Ni^{II}/Cu^{II}/Zn^{II}/Cd^{II}/Hg^{II}$, $[(L^2)M](ClO_4)_2.xMeCN$ where $M=Mn^{II}/Fe^{II}/Ni^{II}/Cu^{II}/Zn^{II}/Cd^{II}$ and $[(L^3)M](ClO_4)_2.xMeCN$ where $M=Mn^{II}/Ni^{II}/Cu^{II}/Zn^{II}/Cd^{II}/Pb^{II}$ complexes. The $[(L^1)Cu](ClO_4)_2$ complex exhibits a rare dynamic Jahn-Teller effect in the solid state. Selected compounds exhibit an interesting capping mode by their perchlorate counterions, with threefold-hydrogen bonding through the oxygen to the amine protons. The $[(L^3)Pb](ClO_4)_2$ crystal structure exhibits a typical geometry which accommodates a stereoactive lone pair from the lead centre. The variable temperature ^1H NMR of tris 1, 4, 7-(2-aminophenyl) 1, 4, 7-triazacyclononane zinc bis tetraphenylborate was carried out over 298K-193K and spectra are included within. All complexes characterized by ^1H NMR, ^{13}C NMR, ^{19}F NMR, IR, UV and where appropriate Mossbauer spectroscopy.

The investigation into the synthesis and chemistry of the novel sulphonamide pentaazamacrocycles 1-(*p*-tolylsulphonyl), bis 4, 7-(2-aminophenyl) - 1, 4, 7-triazacyclononane (L^4), 1-(*p*-methoxyphenylsulphonyl), bis 4, 7-(2-aminophenyl) - 1, 4, 7-triazacyclononane (L^5), 1-(*p*-fluorophenylsulphonyl), bis 4, 7-(2-aminophenyl) - 1, 4, 7-triazacyclononane (L^6) and 1-(2-mesitylsulphonyl) bis 4, 7-(2-aminophenyl) 1, 4, 7- triazacyclononane (L^7). The complexation with differing transition metals afforded the relevant complexes and X-Ray data was obtained for $[(L^4)Ni/Zn/Cd.MeCN](ClO_4)_2.MeCN$, $[(L^4)Pb(ClO_4)](ClO_4).2(MeCN)$, $2.[(L^4)Cu](ClO_4)_4..4MeCN.MeOH$, $[(L^5)Ni/Zn.MeCN](ClO_4)_2.MeCN$, and $[(L^6)Ni.MeCN](ClO_4)_2.MeCN.H_2O$. The $[(L^4)Zn/Hg/Pb.MeCN](ClO_4)_2.MeCN$, $[(L^5)Zn/Hg.MeCN](ClO_4)_2.MeCN$, $[(L^6)Zn.MeCN](ClO_4)_2.MeCN$ and $[(L^7)Zn.MeCN](ClO_4)_2.MeCN$ compounds exhibit an unusual amine pattern in the ^1H NMR. This was further studied by variable temperature ^1H NMR over the range of 298K-418K. The $[(L^4)Cu(ClO_4)_2$ crystal structure shows two complexes of the same compounds crystallizing in the same cell, each with slightly differing dimensions, but both of square based pyramidal geometry. The $[(L^4)Pb(ClO_4)]ClO_4.2.MeCN$ crystal structure exhibits a typical geometry which accommodates a stereoactive lone pair from the lead centre. The bis sulphonamide 1-(2-aminophenyl)-bis 4, 7-(*para*-tolylsulphonyl) 1, 4, 7-triazacyclononane (L^8) was also prepared and its complexation of $L^8Ni/Cu/Zn/Cd$ coordination chemistry expanded.

The fluorinated *N*-aryl tacn class was expanded by producing bis and tris *ortho meta para*-fluorinated phenyl ligands. This selective methodology led to the development of a tri substituted tacn ring with *meta* and *para*-fluorinated aromatic rings. We report the electronic spectroscopic examination of the autocatalytic oxidative degradation of the macrocyclic aniline moiety over 120hrs. The synthesis of mono 1-(5-fluoro, 2-aminophenyl) bis 4, 7, (2-aminophenyl) 1, 4, 7-

triazacyclononane (L^9), and mono 1-(4-fluoro, 2-aminophenyl) bis 4, 7, (2-aminophenyl) 1, 4, 7-triazacyclononane (L^{10}) are reported. The X-Ray single crystal data was collected for $[(L^9)Mn/Zn](ClO_4)_2$.

The synthesis of 1, 4-bis-(2-amino, 4-fluorophenyl) homopiperizene (L^{11}) and its X-Ray crystal structure of $(L^{11}Ni\ 2.MeCN)(ClO_4)_2$ is described. The conversion of *N, N'* bis (2-aminophenyl) 1, 4-diazacycloheptane by reaction with *p*-toluenesulphonyl chloride afforded *N, N'* bis (2-tosylaminophenyl) 1, 4-diazacycloheptane (L^{12}). Reaction with nickel perchlorate afforded the neutral complex $[(L^{12})Ni]$. This dianionic ligand is proposed as a porphyrin analogue.

Acknowledgements.

Firstly I would like to thank Dr Ian Fallis, without whose guidance and help this thesis would not have been completed. His enthusiasm for the subject is without equal, and without him, it would not have been an enjoyable experience.

I would like to thank PiezOptic Ltd for sponsoring my Postgraduate research. Drs Tim Carter, Steve Ross and Kelly Bearman at PiezOptic Ltd deserve special thanks for their cooperation and collaboration, as it made this thesis possible.

I would like to give a special thanks to Woody, Angelo and Simon for their advice and humour over my period in Cardiff University.

I have to mention my lab partners who made my working days (and nights out), a joy to be there. They are Anne, Cerys, Ruth, Glesni, Mark, Chris, Debs, Nat B, Neha, Nat C, Andrea, Dave, Dan, Jo, Matt L, James, Olli, Praba, Rob, Steve, Matt H and Graham.

A big thanks goes out for Rob Jenkins for his help and advice with VT ^{1}H NMR, and Mass Spec, it's much appreciated.

Thanks to Dr Nancy Dervisi for very helpful discussions.

The technical support staff of the chemistry department also deserves a huge thank you for all the times when I needed help or assistance with my work. Gaz, Robin, Alun, Steve, Jobo, Dave, Sham, Ricky, John and Mal.

Special thanks must be given to those who helped to gather results for this thesis. Dr Li-ling Ooi for her help and patience with crystallography and Dr Dave Evans (John Innes Centre) for running and intepreting Mossbäuer spectroscopy.

I now would like to give the biggest thanks to my family. They have supported me in so many ways throughout my life that I cannot list them. Mum, Dad, and Naomi thank you for everything, it's all greatly appreciated, and this thesis is for you.

Finally, another thank you for Vic. She has endured so much while I have been producing this thesis as well as when I was an undergraduate, and researching the content work. Thanks for listening when I was complaining and giving me advice when I needed it most.

For Mum and Dad

The journey, not the arrival, matters
--T. S. Eliot

Contents

Page.

Title page	**i**
Declaration	**ii**
Abstract	**iii**
Acknowledgements	**v**
Contents page	**vii**
Experimental declaration	**xi**
List of abbreviations	**xii**
Ligand Key	**xiv**

Chapter One-Introduction

Chemical sensors	**2**
PiezOptic technology	**2**
Piezoelectric effect	**6**
PiezOptic badge technology	**6**
Nitrous Oxide complexation chemistry	**9**
Introduction to nitrous oxide	**10**
Proposed system	**11**
Beta-carotene	**14**
Introduction to macrocycles	**17**
Azamacrocycles	**19**

The chelate effect 19

The macrocyclic effect 21

Cavity hole size 23

Octahedral and trigonal prismatic geometries of 6-coordinate complexes 24

Twist angle 25

Aims and objectives 26

Chapter Two- Experimental.

Synthesis of pendant fluoroaniline-1, 4, 7-triazacyclononane ligands and metal complexes 28

Synthesis of sulphonamide derivatives of bis 1, 4-(2-aminophenyl)- 1, 4, 7-triazacyclononane 42

Synthesis of bis 1, 4-tosyl 7-(2-nitrophenyl) 1, 4, 7-triazacyclononane 56

Synthesis of bis 1, 4-tosyl 7-(2-aminophenyl) 1, 4, 7-triazacyclononane 57

Functionalisation of 1, 4, 7-triazacyclononane with differing pendant fluoroaniline pendants 59

Complexation of pendant aminophenyl 1, 4, 7-triazacyclononane ligands bearing one fluorine 68

Synthesis of tetra-aza ligands and complexes 74

Synthesis of tosylated aminophenyl azamacrocyclic ligands 83

Complexation of nickel with tosylated aminophenyl homopiperazine ligand

86

Chapter Three-Pendant Fluoroaniline Derivatives of Triazacyclononane

Introduction	**88**
Aims and Objectives of Research	**97**
Results and Discussion	**98**
Ligand synthesis	**98**
Mn complexes	**105**
Fe complexes	**108**
Co complexes	**112**
Ni complexes	**116**
Cu complexes	**118**
Zn complexes	**121**
Cd complexes	**126**
Hg complexes	**129**
Pb complexes	**130**
^{19}F NMR spectra shifts of zinc complexes	**133**
Perchlorate counterion hydrogen bonding	**134**
Functionalisation of 1, 4, 7-triazacyclononane	**139**
Twist Angle (Φ)	**143**
Average metal-nitrogen length reference table	**148**
Average metal-nitrogen lengths	**149**
^{19}F NMR shift table	**150**
Complexation	**151**

Crystallography 153

Conclusions 153

Future work 155

Chapter Four-Synthesis of metal-sulphonamide bond complexes.

Introduction 157

Aims and Objectives of Research 160

Results and Discussion 160

Ni complexes 163

Cu complexes 167

Zn complexes 170

Cd complexes 174

Hg complexes 176

Pb complexes 177

Hydrogen bonding table 178

Bis-tosylated macrocyclic ligands 182

Metal-sulphonamide bond length table 182

Conclusions 183

Chapter Five-Tetra-aza ligands and complexes

Introduction 186

Aims and Objectives of Research 192

Results and Discussion 193

Ni complexes 195

Ni-N bond angles 196

Ni-N bond length comparison table 197

Tosylated Ni complex 197

Conclusions 200

Future work 200

Appendices

Appendix i 202

Appendix ii 203

Appendix iii 204

Appendix iv 205

Appendix v 206

Experimental declaration.

Non-synthesized reagents were purchased from Aldrich, Lancaster, and Avocado, and used as received. Solvents were pre-dried according to standards procedures. Mass spectra were obtained in APCI (Atmospheric Pressure Chemical Ionisation) mode or EI (Electronic Ionisation) mode. IR spectra in KBr discs using a Jasco

FTIR 110 series spectrometer. NMR spectra were obtained on Brűker 500 Ultrashield, Brűker Avance AMX 400, Brűker Avance 250 or JEOL Eclipse 300 spectrometers and referenced to external TMS. UV/Vis spectra was recorded on a Jasco V-750 UV/Vis/NIR spectrophotomer.

List of Abbreviations.

AcOH Acetic Acid.

Å Angstroms.

Al Aliphatic.

Ar Aromatic.

bpt Boiling point.

br Broad

^{13}C Carbon thirteen isotope.

cm^{-1} Wavenumbers.

$CDCl_3$ Deuterated Chloroform

CD_3CN Deuterated Acetonitrile.

CYCLEN 1,4,7,10-tetraazacyclododecane.

δ NMR chemical shift and definition of absolute conformation.

d Doublet.

d Deuterium.

DCM Dichloromethane.

DMF Diethylformamide.

D_2O Deuterated water.

Et Ethyl.

g Grams.

^1H Proton.

IR Infra red.

KBr Potassium Bromide.

m Multiplet.

mg Milligram.

MHz Mega Hertz.

mol Mole.

ml Millimole.

m/z mass / charge ratio.

NMR Nuclear Magnetic Resonance.

s Singlet.

t Tertiary.

TACN 1,4,7-triazacyclononane.

THF Tetrahydorfuran.

TLC Thin Layer Chromatography.

Ts Tosyl.

UV Ultra Violet.

Vis Visible

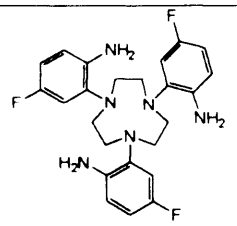	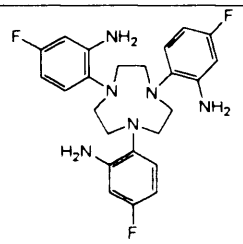	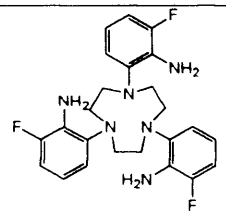
L^{1} = Tris 1, 4, 7-(5-fluoro, 2-aminophenyl) -1, 4, 7-triazacyclononane.	**L**^{2} = Tris 1, 4, 7-(4-fluoro, 2-aminophenyl)- 1, 4, 7-triazacyclononane.	**L**^{3} = Tris 1, 4, 7-(3-fluoro, 2-aminophenyl)- 1, 4, 7-triazacyclononane.
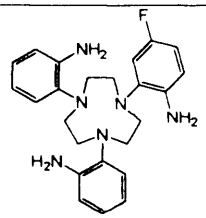	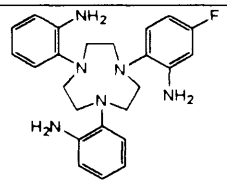	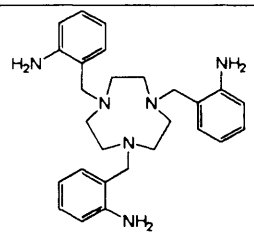
L^{9}=1-(5-fluoro, 2-aminofluorobenzene), 4, 7-bis aminobenzene, 1, 4, 7-triazacyclononane.	**L**^{10}=1-(2-amino, 4-fluorobenzene), 4, 7-bis aminobenzene, 1, 4, 7-triazacyclononane.	**L**^{KW} = Tris 1, 4, 7-(2-aminobenzyl) -1, 4, 7-triazacyclononane.

Ligand Key

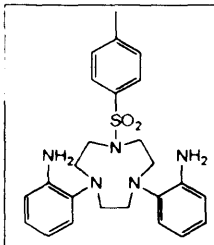 **L**^{4} = 1-Tosyl, 4, 7-bis (2-aminophenyl)- 1, 4, 7-triazacyclononane.	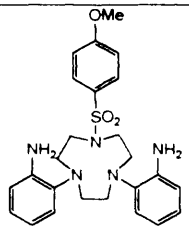 **L**^{5} = Mono 1-(4-methoxyphenylsulphonyl) bis 4, 7- (2-aminophenyl) 1, 4, 7-triazacyclononane.	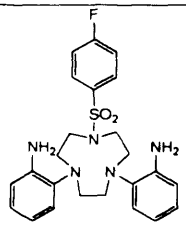 **L**^{6} = 1-(4-Fluorophenylsulphonyl), 4, 7 bis- (2-aminophenyl), 1, 4, 7-triazacyclononane.
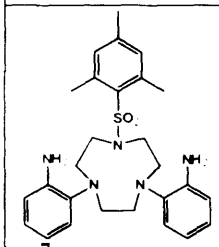 **L**^{7} = Mono 1-(2-mesitylsulphonylphenyl) bis 4, 7- (2-aminophenyl) 1, 4, 7-triazacyclononane.	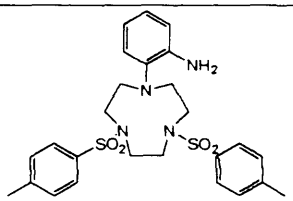 **L**^{8}=Bis 1, 4 –tosyl, mono 7-(2-aminophenyl)- 1, 4, 7-triazacyclononane	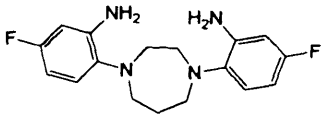 **L**^{11}=*N, N'*--bis-(2-amino, 4-fluorophenyl) – homopiperizene.

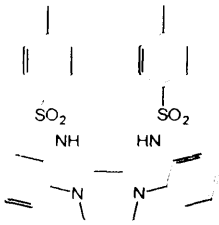

L^{12}=*N, N'*-bis (2-tosylaminophenyl) 1, 4-diazacycloheptane

Chapter One

Introduction

Try to learn something about everything and everything about something.

-- Thomas H. Huxley

The covers of this book are too far apart.

-- Ambrose Bierce, The Devil's Dictionary

Introduction

In a collaborative project between Cardiff University and PiezOptic Ltd, we set about to investigate the development of a colorimetric sensor for the detection of atmospheric nitrous oxide. We aimed to combine technology currently present at PiezOptic, with our azamacrocyclic chemistry, to develop a reagent to react with the target gas and produce a colour change that could be detected by the PiezOptic system.

Chemical sensors

A chemical sensor is a system which gives a specific response to a target reagent. Exposure to noxious gases has been an important area for health and safety regulations in recent years. This area has been focused upon further in light of harmful medical effects these gases have found to have on the human body. The health risks and effects of these gases have been recognised, and so the policies that govern exposure limits have been reviewed and revised every year, commonly reducing the exposure levels annually. Detection of these gases has been difficult due to many factors such as equipment standard, size and portability, interference from other gases, accuracy and the range of detection.

PiezOptic Technology

PiezOptic Ltd specialises in the development and supply of specific gas dosimeters for use in environments where toxic gases and vapours are present. The initial technology was invented at the Centre for Applied Microbiology Research (CAMR) at Porton Down in the early 1990's. Research is now also being carried out at PiezOptic Ltd in Ashford, Kent.

PiezOptic Ltd was formed to take advantage of a niche in the gas detection market[1]. Specific analytes covered by the PiezOptic system at the moment include glutaraldehyde, chlorine dioxide, formaldehyde, nitrogen dioxide, ozone, sulphur, dioxide and styrene. Examples include glutaraldehde

[1]Wright, J. D. Colin, F. Stöckle, R. M. Shepherd, P. D. Labayen, T. Carter, T. J. N. A. *Sensors and Actuators* B, **1998,** 51, 121-130. C. A. Gibson, T. J. N. Carter, P. D. Shepherd, J. D. Wright, *Sensors and Actuators* B, **1998**, 51, 238-243

which is a toxic and corrosive reagent used in the sterilisation of hospital equipment. Detection is achieved by using 2, 7-diaminofluorene.

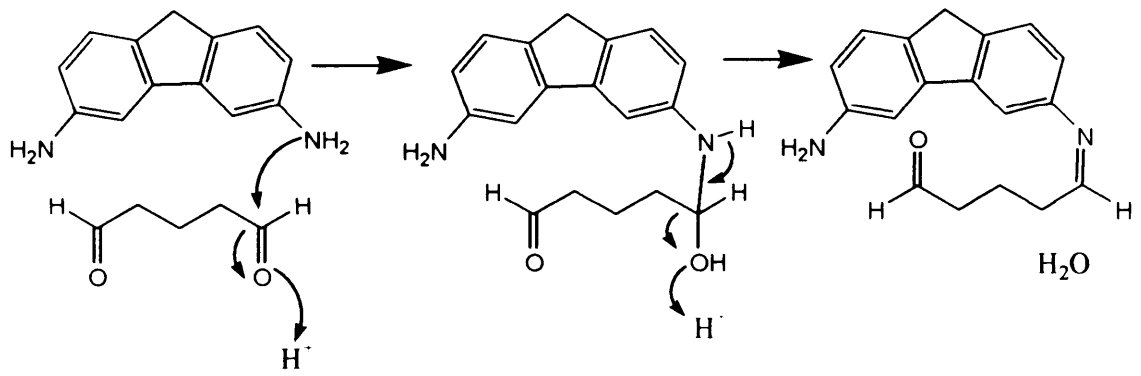

Figure 1.1: Reaction scheme of glutaraldehyde sensing by 2, 7-diaminofluorene.

Reaction with the difunctional aldehyde propyl chain affords the 2, 7-diaminofluorene/glutaraldehyde derivative, with the formation of imine bonds and the loss of water. Differing products are obtained when the ratios of reactants are altered. These products include the 1:1 adduct, 1:2 adduct, 2:1 adduct, polymeric material, oligomers, and cyclic oligomers. The colour change observed can be detected by the human eye, but is quantitatively calculated by the generic film reader so detecting the total exposure to the glutaraldehyde.

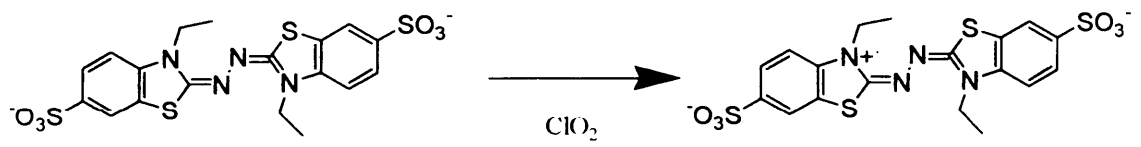

Figure 1.2: Reaction scheme of chlorine dioxide by of 2, 2-azino bis (3-ethylbenthiazoline)-6-sulphonic acid diammonium salt.

Chlorine dioxide is detected through the use of 2, 2-azino bis (3-ethylbenthiazoline)-6-sulphonic acid diammonium salt (ABTS)[2]. ABTS is oxidised from the colourless compound, in the presence of ClO_2 undergoing a one electron oxidation to form the stable radical cation, which is an overall anionic green compound.

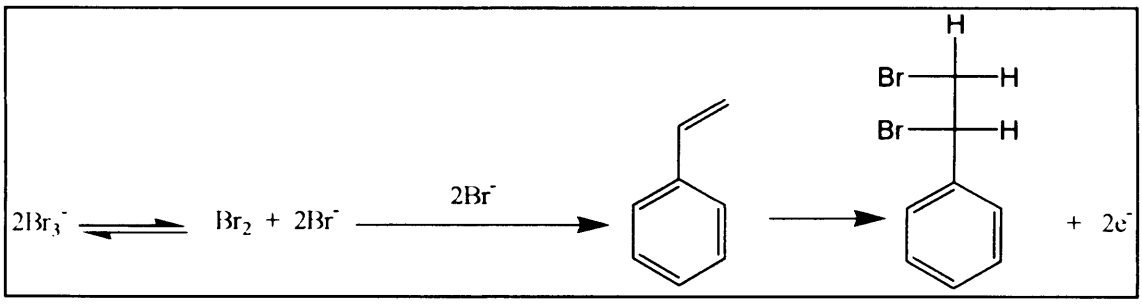

Figure 1.3: Reaction scheme of bromine sensing by styrene.

Styrene is detected through employing the tribromide ion suspended in a polyethylene glycol matrix[3]. Colour is lost as the reaction that occurs results in the halogenation of the alkene bond present in the styrene. The reaction can be detected by the naked eye, but the generic reader can identify the specific amount of colour change through the voltage generated across the piezofilm. The high toxicity and volatility of these gases make the need for their detection in the workplace paramount, in order to comply with legislation.

The sensors developed are used in the rapid monitoring of gases in the workplace, a test that was previously slow and expensive in both terms of time and money. The dosimeter badges (Figure 1.4) that have been developed require little training, are disposable, and give results in a short period of time.

---

[2] U. Pinkernell, B. Nowack, H. Gallard, U. Von Gunten, *Wat. Res*, **2000**, Vol. 34, No 18, 4343-4350.

[3] K. R. Bearman, D. C. Blackmore, T. J. N. Carter, F. Colin, J. D. Wright, S. A. Ross, *Chem. Commun.*, **2002**, 980-981.

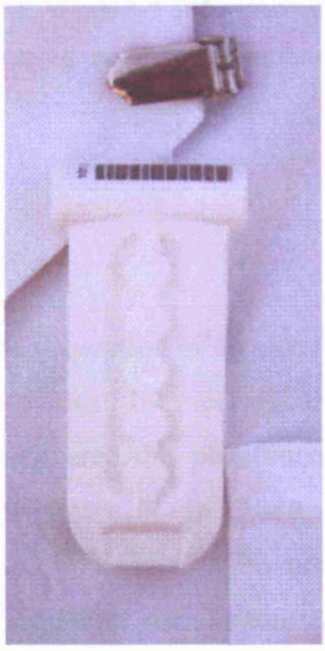

Figure 1.4: PiezOptic Dosimeter badge.

No equipment is needed other than a generic reader (Figure 1.5), that can be obtained with the badges from PiezOptic Ltd. These readers take a background reading of the badges before the employee starts work and a final reading after their shift.

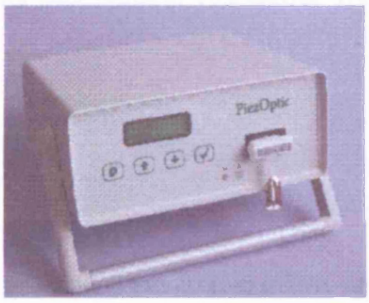

Figure 1.5: Dosimeter badge reader.

The reader then calculates the amount of contact that has been made with the target gas over this allotted time frame. The badges are developed for use over an 8 hour time period (time weighted average, TWA), or 15 minutes (short term exposure limits, STELs). The reader calculates the exposure by the change in colour intensity of the gas-specific reagent present in the spots on the

badge[4]. The PiezOptic system utilises a phenomenon called the *"Piezoelectric effect"*. This has been employed as the mechanism in the films, used in the badges.

The piezoelectric effect

The piezoelectric effect is the generation of an electric potential across certain faces of a crystal, which is induced by mechanical pressure and distortion[5]. Pierre and Jacques Curie discovered this phenomenon in quartz crystals and Rochelle's salt (potassium tartrate), in 1880. The effect is named piezoelectricity from the Greek "*peizein*" – to press. This effect has been found in several crystalline structures such as tourmaline and barium titanate. Ions present in the crystal lattices are displaced from the non-symmetrical unit cell. Electric polarisation occurs when the crystal is compressed. These effects accumulate as the crystal is of regular conformation. This accumulation produces an electric potential across the faces of the crystal. Piezoelectric crystals are used as transducers, record playing pickup elements, and in microphones, due to their capacity to convert mechanical deformation into electric voltages. They are also used in resonators in electric oscillation, and high frequency amplifiers, as mechanical resonance frequency of adequately cut crystals is well defined.

PiezOptic Badge Technology

The reagent spots are coated on a piezofilm sensor which is sputtered with indium tin oxide, (ITO)[6]. The reader illuminates the spot in the badge with

---

[4]J. D. Wright, C. Von Bültzingslöwen, T. J. N. Carter, F. Colin, P. D. Sheperd, J. V. Oliver, S. J. Holder, R. J. M. Nolte, *J. Mater. Chem.* **2000**, Vol 10, 175-182.

[5] Cady, W. G. *Piezoelectricity: An Introduction to the Theory and Applications of Electromechanical Phenomena in Crystals, New rev. ed., 2 vols.* New York: Dover, **1964**. Mason, W. P. *Piezoelectric Crystals and Their Application to Ultrasonics.* New York: Van Nostrand, **1950**. Rosen, C. Z.; Hiremath, B. V.; and Newnham, R. (Eds.). Piezoelectricity. New York: Springer-Verlag, **1992**. Halliday & Resnick, *Fundamentals of Physics* 3rd Ed p808 Tipler, *Physics*, 3rd Ed Extended Ch 36 p1211

[6]C. Yan, M. Zharnikov, A. Gölzhäuser, M. Grunze, *Langmuir* **2000,** 16, 6208-6215.

a complementary colour, and the signal is processed within the reader. The spot produces an amount of heat which has been generated by the absorbance of light energy from the reader. This heat distorts the sensor film and a voltage is produced. This electric charge is collected by the conductive ITO layer on the piezofilm. This charge travels to the conductive pads present at the end of this piezofilm. The gas exposure is calculated by the reader, since the voltage produced is proportional to the colour intensity of the spot. The reader has a built-in memory capable of recording results and storing exposures for up to 400 individuals. This data can then be read directly from the printed hard copy or downloaded to a PC.

The piezofilm is made from polyvinylidene fluoride, (PVDF), (Figure 1.6). The film is constructed so the effects of the target gas on the spot are heightened and a back to back construction of poled polymer layers means microphony effects are eliminated.

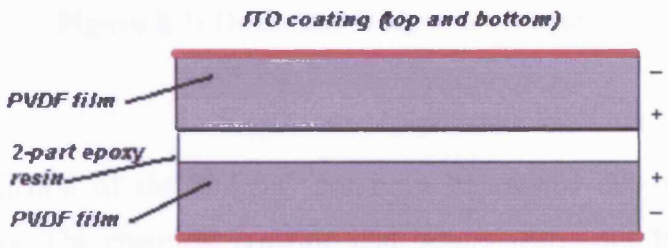

Figure 1.6: Cross section of PVDF piezofilm.

The reader uses "chopped light" at 10Hz, and the LED's emit at 470nm and 654nm, both in the visible region. This then generates the desired electrical signal.

K. L. Purvis, G. Lu, J. Schwartz, S. L Bernasek, *J. Am. Chem. Soc.* **2000**, 122, 1808-1809.
N. Biyikli, T. Kartaloglu. O. Aytur, I. Kimukin, E. Ozbay, *App. Phys. Lett.* **2001**, 79, 17, 2838-2840.

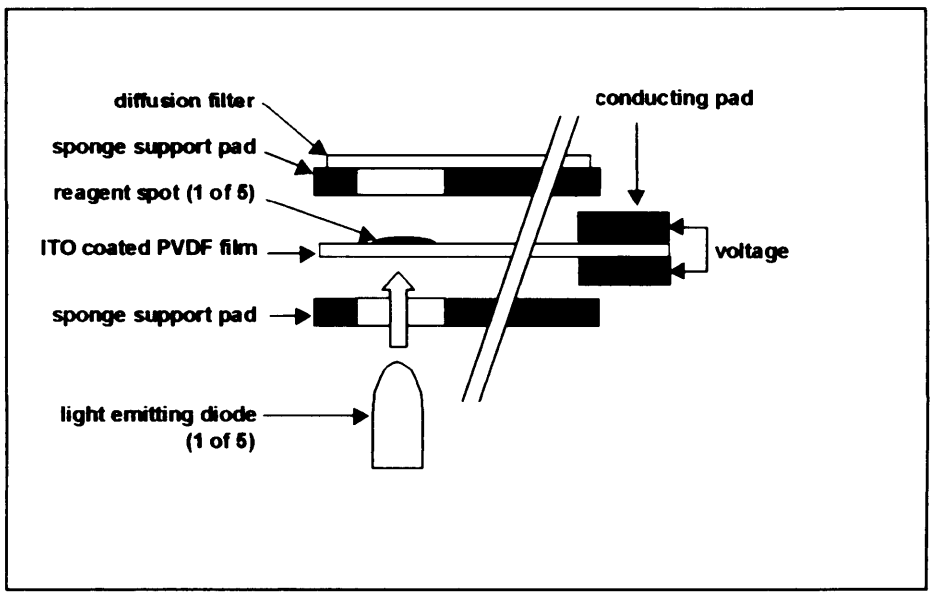

Figure 1.7: Dosimeter Badge construction.

Construction of the reagent spot must be carried out whilst meeting specific criteria. The chemical reaction that occurs within the badge must be *irreversible*. Since the dosimeter badges measure the accumulative exposure, and do not monitor the immediate levels of gases present. Systems that are currently available in the market employ charcoal absorber tubes, which after usage the exposure levels are calculated by either solvent extraction or by thermally desorbing the tube so that the sample can be run on GC/MS or HPLC. The reagent spot must be stable to light, temperature, humidity, mechanical shock and ambient gases. The colour change must complement the LED's in the reader, so the light is absorbed. The interaction between target gas must be fast and specific to the target gas only. The results obtained from the exposure must be quantitative and the reagent should be easy to synthesize, and precursors commercially available. When the spots are developed on the piezofilm, they must form a uniform spot, which is of even depth. These form porous matrices on the film, and form the desired spots. This allows good diffusion of the target gas into the matrix in order to react with the reagent. The solid formed is then

ground to a fine powder and made into a paste with a volatile solvent. The paste is then deposited onto the PVDF film and allowed to dry. Advantages of a uniform dispersant are that maximum accessibility is presented for the target gas when it diffuses into the badge spot matrix. The concentration of the reagent can be varied to control the sensitivity of the badge. The reagent spots are deposited onto the PVDF film that is a secured film piece in a spot-deposition jig. The spot solutions are deposited in 5μl aliquots, which are dispensed from an electronic micro pipette, which is also aligned by the jig. The employment of the jig allows the spots to be constructed within strict sizing parameters (approximately 5mm±10% diameter), and to also retain spot integrity.

Nitrous Oxide Complexation Chemistry.

The formation of nitrous oxide adducts are very rare and to date only one such complex has been formed and studied. Research in this field was carried out in the late 1960's by Armor and Taube[7]. They showed that synthesis of ruthenium monoaquo-pentammine reacted reversibly with N_2O. When passed under a stream of N_2O, the water molecule is displaced to form the nitrous oxide adduct.

$$(H_3N)_5RuOH_2^{2+} + N_2O \leftrightarrow (H_3N)_5RuN_2O^{2+} + H_2O$$

Figure 1.7: Reaction between Ruthenium monoaquapentammine and N_2O.

The use of other metals to form such adducts has resulted in the unwanted formation of oxides, nitrosyls and nitrides species. In the presence of a reducing agent such as Cr^{2+}, it has been shown that the nitrous oxide component of this adduct is reduced to the dinitrogen species with the loss of water. From the data shown in the literature[8], the formation of more stable nitrous oxide complexes would be a challenging and extensive field of research. N_2O is a weak σ and π donor and so a compound would have to be synthesised to produce a more

[7] Armor J T., Taube H., *J. Am. Chem. Soc.*, **1969**, 91, 6874-6876
[8] Paulat F., Kuschel T., Näther C., Praneeth V. K. K., Sander O., Lehnert N., *Inorg. Chem.*, **2004**, 43, 6979-6994.

stable metal-N_2O bond[9]. This would have to be achieved through the increase of π back bonding. The metal should be of low spin d^6 electronic configuration to strengthen this interaction[10]. This is why Ru^{2+} has shown to be the present within only nitrous oxide complex to date. Fe^{2+} or Os^{2+} could be good substitutes for Ru^{2+} as iron would be a cheaper compound, and osmium would exhibit stronger π bonding, but for our purposes would be unbeneficial to our long term goals due to the high levels of toxicity of Os^{2+} to the human body.

Introduction to Nitrous Oxide

Nitrous Oxide (N_2O) is used almost exclusively in the anaesthetisation of patients undergoing Medical/Dental treatment. Areas include operating theatres, dental surgeries, and by obstetricians. Exposure to N_2O by personnel in these areas will have long term effects, which are not experienced by patients who are administered it directly for short term anaesthesia[11]. Working area monitoring in hospitals could be achieved by the employment of the PiezOptic system. A target reagent is desired for their technology so to interact with the target gas and monitor N_2O levels. Other application areas include the production of N_2O as a by product from the synthesis of adipic acid and nitric acid. Adipic acid is formed by the oxidation of a ketone alcohol with nitric acid and N_2O is formed as a side product. Nitric acid is formed from the oxidation of ammonia with a platinum catalyst and so again N_2O is formed. The largest source of N_2O is through nitrogen fertilization of agricultural soils, catalytic conversion of waste gases from car exhaust fumes, crop residue burning, and the treatment of industrial wastewater.

N_2O was first isolated in 1772 by Joseph Priestly. Sir Humphrey Davy noted the analgesic effects in 1799 after testing the gas on himself. He experienced the relief from an erupting wisdom tooth pain after inhaling the gas.

---

[9] Armor J T., Taube H., *J. Am. Chem. Soc.*, **1969**, 91, 6874-6876. Armor J. N., Taube H., *Chem. Commun.*, **1971,** 287-288. Armor J. N., Taube H., *J. Am. Chem. Soc.*, **1969,** Vol 91, (24), 6874-6876. Armor J. N., Taube H., *J. Am. Chem. Soc.*, **1970,** Vol 92, (8), 2560-2562.

[10] Diamantis A A., Sparrow G J., *Chem. Commun.*, **1969**, 469-470. Diamantis A A., Sparrow G J., *Chem. Commun.*, **1970**, 819-820. Diamantis A A., Sparrow G J., Snow M R., Norman T R., *Aust. J. Chem.*, **1975**, 28, 1231-1244.

[11] *Bailleres Best Practice and Research in Clinical Anaesthesiology*, 15, 3, **2001**.

He then noted *"As nitrous oxide in its extensive operation appears capable of destroying physical pain, it may probably be used with advantage during surgical operations in which no great effusion of blood take place."* The properties of the gas were exploited in the field of public entertainment. During a sideshow tour in the US, a chemistry lecturer Gardner Quincy Colton inhaled the gas and while under its influence lacerated his leg after running into a bench. It appeared that he felt no pain and this was observed by Horace Wells. This led him to deliberate the prospect that the gas could be used the in the painless extraction of teeth. Colton administered the gas to Wells the following day and extracted one of his teeth. He declared after the effects of the gas wore off that *"A new era of teeth pulling. It did not hurt me as much as the prick of pain. It is the greatest discovery ever made."*

The use of N_2O replaced ether and chloroform as anaesthetics in the medical field. The long term exposure effects of using N_2O are: diffusion hypoxia, diffusion into closed body cavities (inner ear, intestinal gut), decreased methionine synthase activity (Vitamin B_{12} inhibition), nausea, and vomiting. There are occupational hazards such as the possibility of fetotxicity (injury to the foetus from a substance that enters the maternal and placental circulation and may cause death or retardation of growth and development), as well as the increased greenhouse effect. Long-term effects are that N_2O can suppress memory and consciousness, therefore decreasing awareness.

Other anaesthesia now used is desflurane, sevoflurane or using the short acting opiod remifentanil. There is a possibility that xenon may be a possible anaesthesia in the future. The need for monitoring of nitrous oxide is prevalent and so new methods of detection are needed to reduce exposure human exposure.

Proposed system

Some years ago, Groves reported that ruthenium tetramesitylporphyrins (Ru(TMP)) were capable of catalysing the oxidation of a range of olefins using nitrous oxide as an oxidant[12]. Groves found that this extension of Taube's

[12]Groves J T., Quinn R., *J. Am. Chem. Soc.*, **1985**, 107, 5790-5792.

ruthenium salt to be specific to nitrous oxide and did not produce the same results with the iron or osmium analogues. Groves found the dioxo-Ru(TMP) species can convert differing olefins (cyclooctene, norborene, methylstyrene, etc) to the relevant epoxide derivative through oxygen transfer.

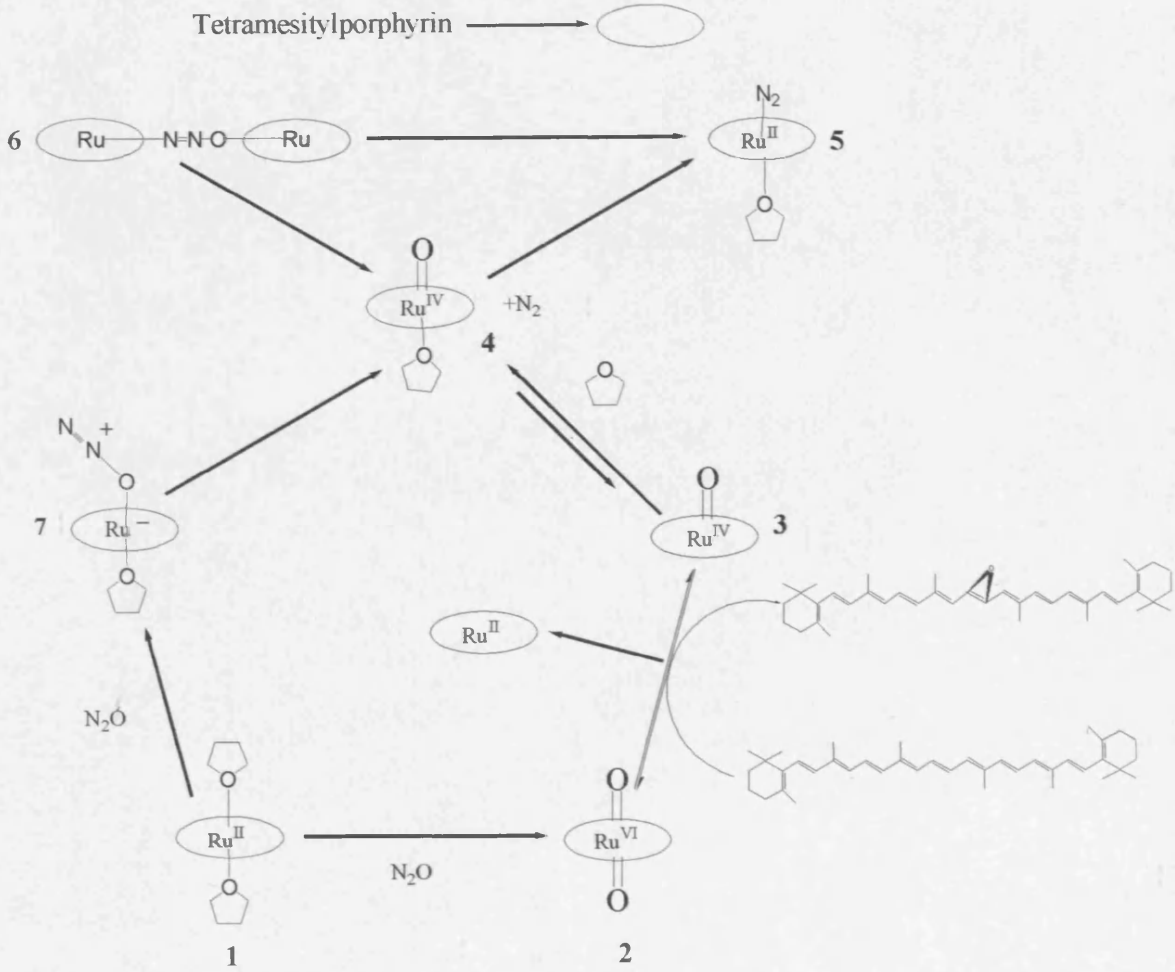

Figure 1.12: Groves' nitrous oxide oxidation cycle.

Figure 1.12 shows the proposed[13] reaction cycle for the binding of nitrous oxide to a ruthenium tetramesityl porphyrin. It was shown, via spectroscopic methods that under elevated pressures of N_2O (6 Psi), the dioxo species (**2**) is formed and that under anaerobic conditions oxidise *trans-β*-methylstyrene (We have inserted beta-carotene into the above scheme to illustrate our proposed system).

[13] Groves J T., Roman J S., *J. Am.. Chem. Soc.*, 117, **1995**, 5594-5595.

Groves has found the dioxoruthenium (VI) species has a limited shelf life[14]. There has been previous evidence that a bridged species is formed[15] ($(H_3N)_5RuN_2ORu(NH_3)_5$) which implies that when nitrous oxide is bound and cleavage of the N-O bond would lead to the formation of the dinitrogen species (**7**) and the Ru=O/THF adduct (**4**). Oxygen transfer from the dioxo species forms the monooxy species (**3**) whereby the oxygen is transferred to an olefin to epoxydise the alkene bond.

Tetramesitylporphyrin was reviewed by Lindsey *et al*[16] and they have devised a new synthetic route to its production from 2-mesitaldehyde and pyrrole. It oxidation from the porphryrinogen to the porphyrin was through employing *p*-chloroanil or DDQ. This method incurred a higher yield (29%) than its original method (4.5%)[17,18].

The synthesis and metallation of tetramesitylporphyrin will be discussed further in chapter five.

In a more recent study by Yamada *et al*[19] has shown that under elevated temperatures and pressure (100°C and 10atm), catalytic conversion of cholesteryl benzoate to the β-epoxide by ruthenium tetramesityl porphyrin occurs in good yield (30-99%) and in a range of solvents (toluene, benzene, fluorobenzene). Aside from olefin oxidation, Yamada *et al* [20] have shown the same system to work successfully with the oxidation of alcohols to aldehydes and ketones. Again higher pressures were used (10atm), a range of yields were produced (22-71%) for the conversion of 2-naphthylmethanol to 2-napthtaldehyde at 100°C. Reaction of nitrous oxide with differing transition metal complexes have also been recorded[21, 22, 23] but has been the inertness of nitrous oxide has resulted few viable systems.

We proposed that by synthesizing a ruthenium complex with 5 sites of coordination occupied by a ligand with a degree of steric hindrance, then

---

[14] Groves J T., Quinn R., *Inorg. Chem.*, 23, **1984**, 3844-3846.
[15] Armor J N., Taube H., *Chem. Commun.*, **1971**, 287-288.
[16] Wagner R W., Lawrence D S., Lindsey J S., *Tett.Lett.*, 28, 27, **1987**, 3069-3070.
[17] Lindsey J S., Hsu H C., Schreiman I C., *Tett. Lett.*, 27, **1986**, 4969-4970.
[18] Lindsey J S., Schrieman I C., Hsu H C., Kearney P C., Marguerettaz A M., *J. Org. Chem.*, 52, **1987**, 827-836.
[19] Yamada T., Hasimoto K., Kitaichi Y., Suzuki K., Ikeno T., *Chem. Lett.*, **2001**, 268.
[20] Hasimoto K., Kitaichi Y., Tanaka H., Ikeno T., Yamada T., *Chem. Lett.*, **2001**, 922-923.
[21] Banks R G S., Henderson R J., Pratt J M., *Chem. Commun.*, **1967**, 387-388.
[22] Banks R G S., Henderson R J., Pratt J M., *J. Chem. Soc (A).*, **1968**, 2886-2889.
[23] Bottomley F., Lin I J B., Mukaida M., *J. Am. Chem. Soc.*, **1980**, 102, 5238-5242.

formulation with beta carotene and a solid support such as silica or alumina, we would have our target reagent spot. Upon exposure with nitrous oxide the brown/orange colour of the composite would undergo a colour change to indicate the catalytic epoxidation of beta carotene within the matrix. This in essence, the proposed system, is a catalytic sensor.

The ruthenium complex will bind the nitrous oxide via the nitrogen terminus, and allow the oxygen end free to oxidise the double bonds present in the beta carotene. This loss of chromophore will then be observed in the UV/Vis spectra of the composite.

Beta carotene

The chromophore beta carotene (Figure 1.9) is found throughout nature as an orange pigment, and can be prepared synthetically[24]. It was first isolated in 1831 by Wackenroder, and since then many other compounds in its class, which are called carotinoids have been studied. The structure of the chromophore was solved by Karrer in 1931 and for his work on vitamins he received the Nobel Prize for chemistry. The first commercial synthesis of β-carotene was achieved in 1950[25,26] and Roche produced it in 1954. β-Carotene was found to exhibit antioxidant properties, and so suggested that it might have a role in the fight against cancer. In more recent times it has been found that β-carotene has a significant role in the prevention of cystic fibrosis and arthritis and has been used as a vitamin supplement.

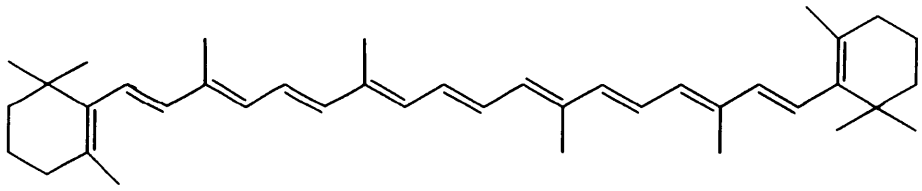

Figure 1.9: β-Carotene

[24] Johansen J E., Lianen-Jensen S., *Acta. Chem. Scand., Series B., Org. Chem.Biochem.*, **1974**, 28 (3), 349-356. Ahmad R., *J. Imp. Coll. Chem. Soc.*, **1953**, 31, 23-37.
[25] Karrer I P., Eugester C H., *Helv. Chim. Acta.*, **1950**, 33, 1172-1174.
[26] Karrer I P., Eugester C H., *Compt. Rend.*, **1950**, 230, 1920-1921.

The large chromophore system of β-carotene gives them colour due to them absorbing in the visible region. β-Carotene absorbs blue/green light therefore they are perceived as orange. The orange colour is seen in many aspects of nature, more notably in carrots, pumpkins, apricots and nectarines.

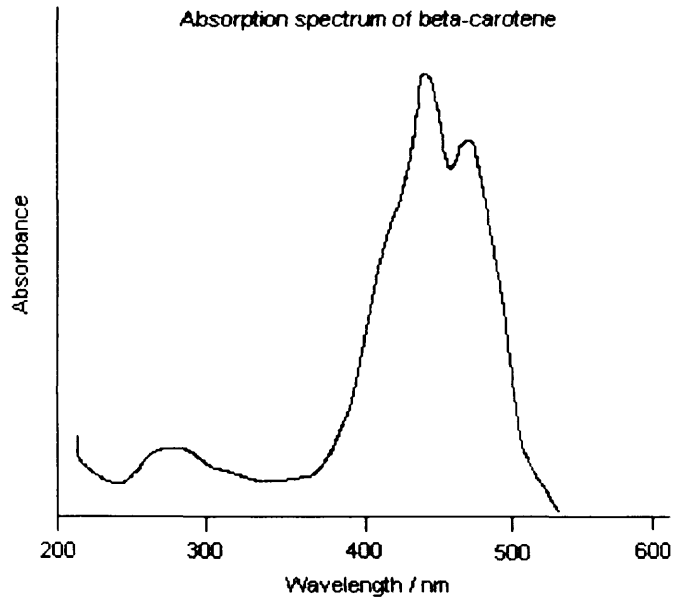

Figure 1.10: The UV/Vis spectrum of beta carotene.

The λ_{max} is 451nm, and has a molar extinction coefficient of 139,500 $M^{-1}cm^{-1}$. The large chromophore system of β-carotene is a good example of a coloured compound that could upon oxidation could produce a useful colour change. The 11 alkene bounds present are all susceptible to catalytic oxidation using N_2O as an oxygen atom donor (Figure 1.11). Such oxidation reduces the degree of conjugation in the chromophore so as to cause a blue shift in the electronic spectrum. Oxidation of β-carotene would also lead to a loss of extinction coefficient. The formation of epoxidised products have lower extinction coefficients and this can be detected by the PiezOptic reader.

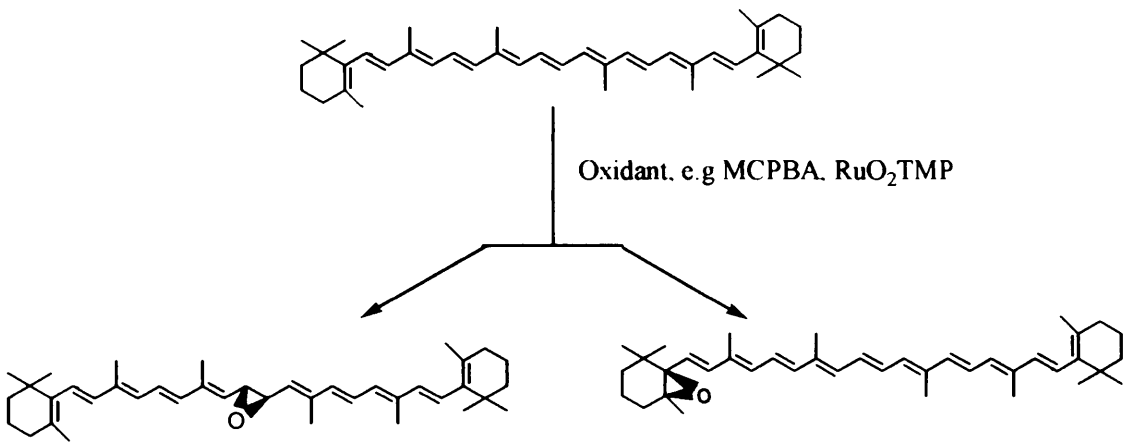

Figure 1.11: Epoxidation of β-carotene at 15, 15' and 5, 6 positions.

Marchon *et al*[27] and Burton *et al*[28] have shown by HPLC analysis that epoxidation can occur with $Ru^{VI}O_2(TMP)$, and that oxidation of β-Carotene forms the full range of epoxy products. The epoxy products exhibited λ_{max} over the range 409nm-446nm. If β-Carotene was to be used in the system, then a loss of colour would be the observed change. This colour change would not be discernable to the human eye, but the PiezOptic reader has sufficient sensitivity for quantifiable detection.

Application of this system for our purposes has problems associated such as the high extinction coefficient of the catalyst. This high ε value would saturate the system and detection of the epoxidised beta carotene products would not be detected by the reader. This reaction also takes place in the solution state. Our proposed system relies upon diffusion of the target gas into a porous solid matrix whereby the catalyst and chromophore are mixed and the catalytic oxidation occurs. Research into this catalysis chemistry would be novel for this field of nitrous oxide oxidative chemistry.

[27] Veyrat C C., Amiot M J., Ramasseul R., Marchon J C., *New. J. Chem.*, **2001**, 2, 203-206.
[28] Mordi R C., Walton J C., Burton G W., Hughes L., Ingold K U., Lindsay D A., Moffatt D J., *Tetrahedron.*, 49, 4, **1993**, 911-928.

Introduction to Macrocycles.

Macrocyclic chemistry is a relatively young field in chemistry, with its origins dating from the 1960's. A macrocycle is defined as a cyclic molecule, that within the ring of at least 9 atoms, has 3 or more potential donor atoms (e.g. N, O, P, S, As, and Se)

The potential applications of macrocyclic chemistry are vast and varied. The unusual co-ordination chemistry that the macrocycles adopt gives them differing properties that they exhibit spectroscopically and structurally. Application of macrocyclic ligands are found in biological systems[29], MRI agents[30], biological tracers[31], anti-HIV[32], tumour agents[33], protein labelling[34], and enzyme models[35], Also surfactants[36], metal extraction[37], and liquid crystals[38] are fields covered by macrocycle appliance.

Macrocycle classes include polyamines[39] (**1**), crown ethers[40] (**2**), mixed donor macrocycles[41] (**3**), catenates[42] (**4**), cryptands[43] (**5**), porphyrins[44] (**6**), and phthalocyanines[45] (**7**).

---

[29] B. Boitrel, R. Guilard, *Tett. Lett.*, **1994**, Vol 35, Issue 22, 3719-3722.
E. Bienvenue, S. Choua, M. A. Lobo-Recio, C. Marzin, P. Pacheco, P. Seta, G. Tarrago, *J. Inorg. Biochem.*, **1995**, Vol 57, Issue 3, 157-168.
[30] F. Benetello, G. Bombieri, L. Calabi, S. Aime, M. Botta, *Inorg. Chem.*, **2003**, 42, 148-157.
[31] S. J. DeNardo, G. L. DeNardo, A. Yuan, C. M. Richman, R. T. O'Donnell, P. N. Lara, D. L. Kukais, A. Natarajan, K. R. Lamborn, F. Jacobs, C. L. H. Sianter, *Clin. Can. Res.*, 9, 3938-3944, Sept 1, **2003**.
[32] M. Iwata, *Chem. Lett.*, **1999**, 1273-1274.
[33] K. P. Eisenwiener, M. I. M. Prata, I. Buschmann, H. W. Zhang, A. C. Santos, S. Wenger, J. C. Reubin, H. R. Mäcke, *Bioconjugate. Chem.*, **2002**, 13, 30-541.
[34] A. Levin, J. P. Hill, R. Boetzel, T. Georgiou, R. James, C. Kleanthous, G. R. Moore, *Inorg. Chim. Acta.*, **2002**, Vol 331, Issue 1, 123-130.
[35] J. P. Collman, L. Fu, P. C. Herrmann, X. Zhang, *Science*, Vol 275, **1997**. E. Kimura, T. Gostoh, S. Aoki, M. Shiro, *Inorg. Chem.*, **2003**, 41, 3239-3248. B. Graham, B. Moubarki, K. S. Murray, L. Spiccia, J. D. Cashian, D. C. R. Hockless, *J. Chem. Soc., Dalton Trans.*, **1997**, 887-893.
[36] I. A. Fallis, P. C. Griffiths, P. M. Griffiths, D. E. Hibbs, M. B. Hursthouse, A. L. Winnington, *Chem. Commun.*, **1998**, 665-666.
[37] H. Tsukube, Y. Mizutani, S. Shinoda, M. Tadokoro, K. Hori, *Tett. Lett.*, Vol 38, 28, 5021-5024, **1997**.
[38] G. H. Walf, R. Benda, F. J. Litterst, U. Stebani, S. Schmidt, G. Lattermann, *Chem. Eur. J.*, **1998**, 4, No 1, 93-99.
[39] Kimura E., *Tetrahedron*. 48, 30, **1992**, 6175-6217.
[40] Gokel G W., Leevy W M., Weber M E., *Chem. Rev.*, **2004**, 104, 2723-2750.
[41] Kauffmann T., Ennen J., *Tet. Lett.*, 22, 50, **1981**, 5035-5038.
[42] Amabilino D B., Ashton P R., Balzani V., Boyd S E., Credi A., Lee J Y., Menzer S., Stoddart J F., Venturi M., Williams D J., *J. Am. Chem. Soc.*, **1998**, 120, 4295-4307.
[43] McKee V., Town. R M., Nelson J., *Chem. Soc. Rev.*, **2003**, 32, 309-325.
[44] Sessler J L., Seidel D., *Angew. Chem. Int. Ed.*, **2003**, 42, 5134-5175.

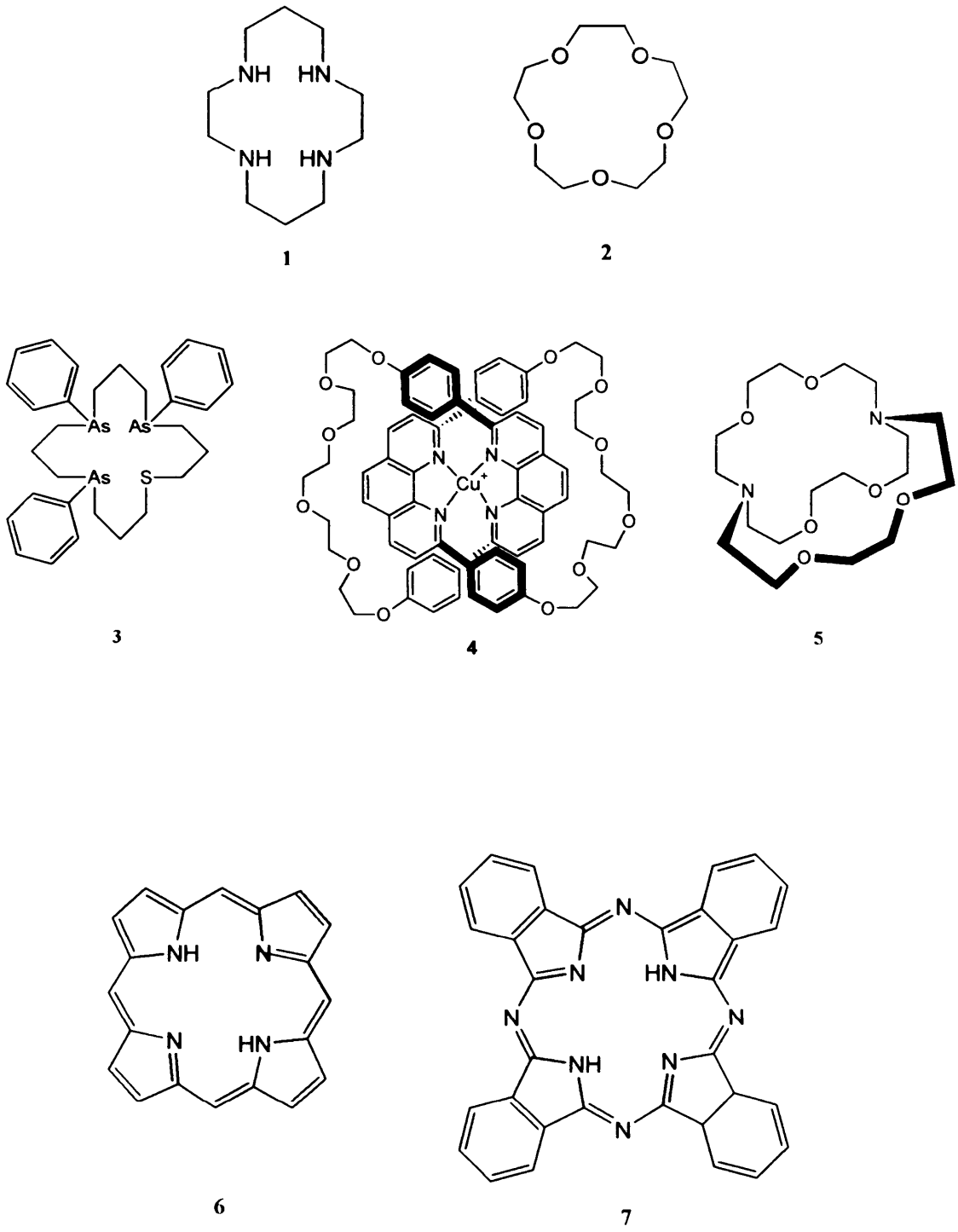

Figure 1.13: Examples of macrocycles.

[45] Inabe T., Tajima H., *Chem. Rev.*, 104, **2004**, 5503-5533. De La Torre G.,Vasquez P., Aguilo-Lopez F., Torres T., *Chem. Rev.*, 104, **2004**, 3723-3750. Cook M J., *The Chem. Rec.*, 2, **2002**, 225-236. Kobayashi N., *Coord. Chem. Rev.*, 227, **2002**, 129-152.

Azamacrocyles

1, 4, 7-Triazacyclononane (Tacn) was first synthesised by Koyama and Yoshino[46], then extensively examined by Richman and Atkins.[47] The chemistry of the free ligand tacn has been fully explored and is reviewed by Wieghardt and Chaudhuri[48]

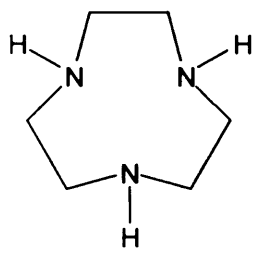

1, 4, 7-triazacyclononane=tacn

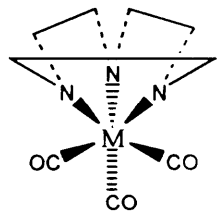

M = Mo, W

Figure 1.14: 1, 4, 7-triazacyclononane (Tacn) and W/Mo tacn tris carbonyl "piano stool" complexes.

The range of complexes formed with tacn is vast and varied, and due to the size of the macrocycle ring, the ligand typically adopts coordination geometries with metals by bonding to three *cis* sites of an octahedron. This is typified by the "piano stool" complexes[49] obtained when, for example tacn is reacted with $W/Mo(CO)_6$.

The Chelate Effect

The chelate effect is derived from the observed fact of the higher stability constants of chelates when compared with their free ligand analogues. From

[46] Koyama H., Yoshino T., *Bull. Chem. Soc. Jap.*, **1972**, 45, 481-484.
[47] Richman J. E., Atkins T. J., *J. Am. Chem. Soc.*, **1974**, 96, (7), 2268-2270.
[48] Chaudhuri P., Wieghardt K., *Prog. Inorg. Chem.*, **1987**, 35, 329.
[49] Roy P S., Wieghardt K., *Inorg. Chem.*, **1987**, 26, 1885-1888. Chaudhuri P., Wieghardt K., Tsai Y-H., Kruger C., *Inorg. Chem.*, **1984**, 23, 427-432. Wieghardt K., Guttmann M., Chaudhuri P., Gerbert W., Minelli M., Young C G., Enemark J H., *Inorg. Chem.*, **1985**, 24, 3151-3155.

figure 1.15, it can be seen that the most unfavoured system contains the 4 free ligands, but the highest stability constant is observed with the chelate analogue of the four ammonium atoms, 1, 4, 7, 10-triethylene tetraamine.

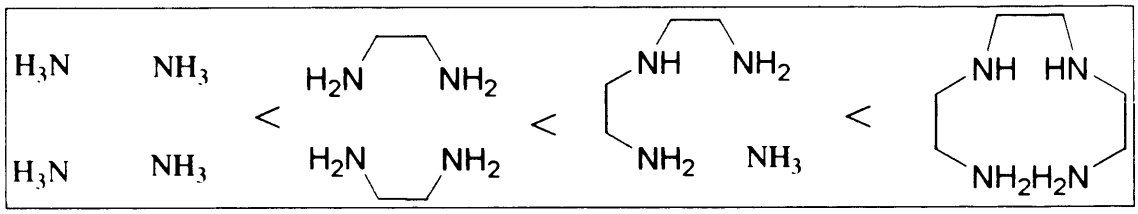

Figure 1.15: Scheme to show the greater stability of ammonia, ethylenediamine, diethylenetriamine and triethylenetetramine.

This arises from the higher likelihood of reattachment of the dissociated ligand, as the other end of the chelate will still be attached. Free ligands are less stable as they are unbound to the metal centre and so will constantly exchange with the metal centre faster than the chelate. The equilibrium constant will lie toward the right, when using the example of Ni, 6 ammonia molecules, and 3 ethane 1, 2-diamine (en) ligands in favour of the chelated metal complex.

$$[Ni(NH_3)_6]^{2+} + 3en \leftrightarrow [Ni(en)_3]^{2+} + 6NH_3$$

$$en = H_2NCH_2CH_2NH_2$$

Figure 1.16: Equilibrium of nickel hexaammonia and nickel tris ethylenediamine.

The entropy term of the system is the driving force behind the chelate effect. The example in scheme 1.17 shows the behaviour exhibited by cadmium, with it favouring complexation with 2 en bidentate chelate ligands over 4 methylamine

monodentate ligands. The stability constant shows a four fold increase in stability for the en ligands over the 4 free methylamine ligands.

1. $Cd^{2+}(aq) + 4CH_3NH_2(aq) = [Cd(NH_2CH_3)_4]^{2+}(aq)$ ($\log \beta = 6.52$)
2. $Cd^{2+}(aq) + 2H_2NCH_2CH_2NH_2(aq) = [Cd(en)_2]^{2+}(aq)$ ($\log \beta = 10.6$)

Ligands	**ΔH^o ($kJmol^{-1}$)**	**ΔS^o ($Jmol^{-1}deg^{-1}$)**	**ΔG^o ($kJmol^{-1}$)**
$4CH_3NH_2$	-57.3	-67.3	-37.2
2en	-56.5	+14.1	-60.7

Figure 1.17: Enthalpy, entropy, and Gibbs free energy of cadmium tetra methylamine and cadmium bis ethylenediamine.

It can be seen that the higher entropy gives more free energy for the multidentate systems.

The Macrocyclic Effect

This increase in stability constants for macrocyclic ligands over their free ligands is called the macrocyclic effect. The enthalpy of forming the macrocyclic product smaller than the acyclic counterpart (figure 1.18). When the hole size of the macrocycle and metal ion size are closely matched then a favourable enthalpy of formation occurs.

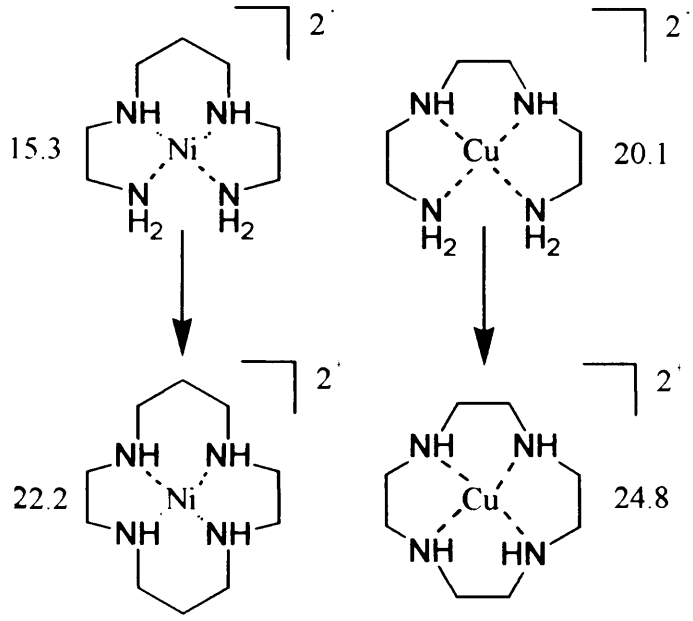

Figure 1.18: Nickel and copper acyclic and macrocyclic complexes with stability constants.

A good example is the formation cyclam and Ni^{2+} and cyclen and Cu^{2+}. When the enthalpy is decreased with a larger metal (Cu^{2+}) and a smaller macrocycle (Cyclen), the stability constant will increase slightly. If the macrocycle is to undergo some sort of reorganisation to accommodate the metal ion, then the enthalpy will increase. When Ni^{2+} complexes with cyclam, it fits within the plane of the macrocycle and so reorganisation is minimal, whereas Cu^{2+} and cyclen requires the ligand to flex so the nitrogen lone pairs all point toward the metal ion. It can so be perceived that the stability constant for Ni-Cyclam is higher than Cu-cyclen due to these factors, which arise from the macrocyclic effect.

Defining the factors solely responsible for the macrocyclic effect is hard and exists as contributions from pH, solvent, temperature, and degree of ligand solvation.

Cavity hole size

As metals bind in the macrocycle cavity, the metal centre will adopt a geometry that is dictated by the donor type, the macrocycle ring and any steric effects present on the ring. If the metal is too big for the hole in the macrocycle, then the metal will not be bonded in the plane of the ligand. The number of donor ligands will obviously dictate the geometry of the metal complex.

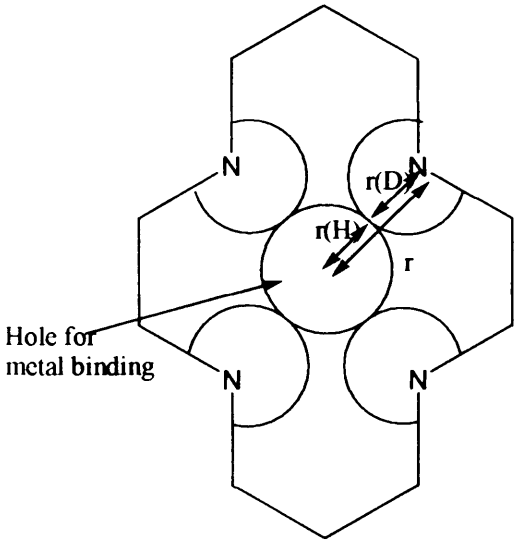

After taking the distance between opposite donors, d, and the perpendicular distance from the middle of d to one of the remaining donors, gives the cavity radius, r. The hole-size radius, r(H) is then determined by subtraction of the donor radius, r(D) from the cavity radius, r, r(H) = r - r(D) d for cyclam = 4.20 and 3.80Å (due to conformational differences)
Therefore, r = 2.10 and 1.90Å R(D) for N(amine) = 0.72Å
R(H) for cyclam = 1.18-1.38Å

Figure 1.19: Cavity hole size for cyclam.

Due to the difference of 2 methylene groups between the macrocycles of cyclen to cyclam, different geometries are adopted. Cyclam has a larger hole size so can adopt more configurations than cyclen. It can be square planar geometry. This allows trans complexes to be formed, although cyclam is flexible enough to permit *cis* complex formation. It can also configure so two *cis* sites are free but this geometry is less favoured due to the higher strain from the macrocyclic ring. The smaller ring of cyclen (1.31-1.42Å) means it can only arrange itself in a *cis* configuration with the metal centre bonding in 4 sites of an octahedral geometry, leaving two *cis* sites free to bond. This has a high strain on the ligand, but the metal cannot fit into the hole of the cyclen ring

Octahedral and Trigonal Prismatic geometries of six coordinate complexes.

Six coordinate metal complexes most commonly adopt an octahedral geometry. This is due to it being energetically favourable, with all 6 ligands being 90° apart. Occasionally 6 coordinate compounds arrange themselves in other geometries such as trigonal prismatic or rarely bicapped tetrahedral. In the trigonal prismatic arrangements, the e_g and t_{2g} levels split to an a'_1, level, and an e' level of slightly higher energy and the e_g level is lowered in energy to e'' when in a trigonal prismatic geometry[50], [51].

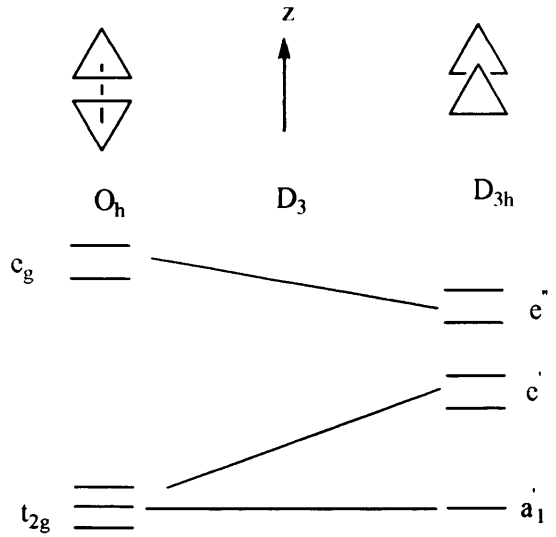

Figure 1.21: *d*-orbital diagram of octahedral and trigonal prismatic arrangements.

Ibers *et al*[52] discovered the complex tris (*cis*-1, 2-diphenylethene-1, 2-dithiolato)rhenium. The crystal structure showed the first example of trigonal prismatic geometry.

[50] Gillum W O., Wentworth R A D., Childers R F., *Inorg. Chem.*, 9, 8, **1970**, 1825-1832.
[51] Hoffman R., Howell J M., Rossi A R., *J. Am. Chem. Soc.*, 98, 9, **1976**, 2484-2492.
[52] Ibers J A., Eisenberg R., *J. Am. Chem. Soc.* **1965**, 3776-3778.

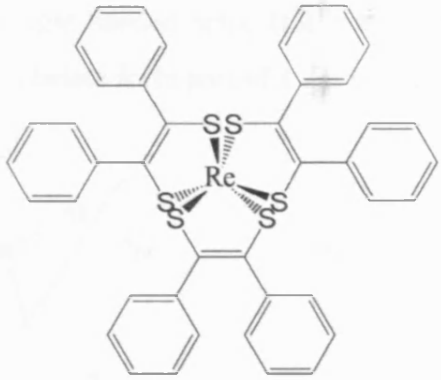

Figure 1.22: Tris (*cis*-1, 2-diphenylethene-1, 2-dithiolato)rhenium.

Twist Angle

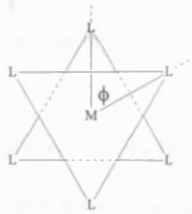

Figure 1.23: Definition of twist angle (Φ).

Twist angle (Φ) is defined as the torsional angle between opposite faces in the coordination polyhedra. Complexes with twist angles of 0° will be adopting a conformation of trigonal prismatic, whereas twist angles of 60° would be ideal octahedral conformations.

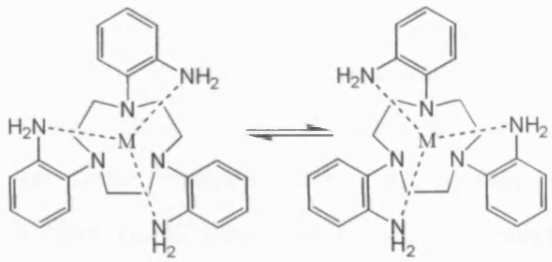

Figure 1.24: Λ twist of N_6 system and Δ twist.

If the complex (or ligand) is viewed down the C_3 axis and the pendant-arms are twisted clockwise relative to the nitrogen plane it is assigned as Δ. The atoms of

chelate form part of a right handed helix. If it is anti-clockwise it is assigned as Λ, as the atoms of this chelate form part of a left handed helix.

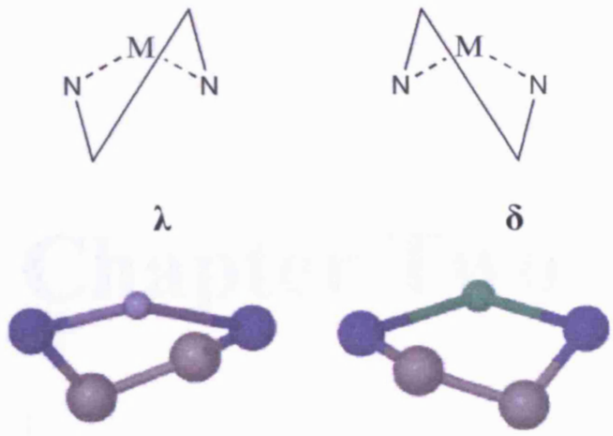

Figure 1.25: Chelate configuration of metal complexes.

We assign the configuration of chelate rings as λ and δ. The first CH_2 group from the left hand nitrogen when below the nitrogen (anticlockwise) is assigned as λ, and when above the nitrogen (clockwise) is δ. These chelates are found to be as δδδ or λλλ within the complex. The mixtures of chelate configurations such as δδλ or λλδ are not common due to the high degree of strain within these types of complex. The minimum strain is found when all three complexes are of the same orientation.

Aims and Objectives

Within this thesis we aim to develop new classes of potential ligands for complexation with ruthenium. Hopefully we can achieve this and run preliminary tests on these compounds to see if they can carry out the epoxidation of beta-carotene. If this were to occur, a potential colour change system could be suitable for Piez Optic technology.

We aim to extend work previously started by Fallis *et al* to see if this could be a potential route towards our nitrous oxide sensor. We will show the development of ligands with bulk to stop potential dimerisation, and a range of routes to these ligands.

Chapter Two

Experimental

The first time I see a jogger smiling, I'll consider it.
Joan Rivers

If God wanted us to fly, He would have given us tickets.
-- Mel Brooks

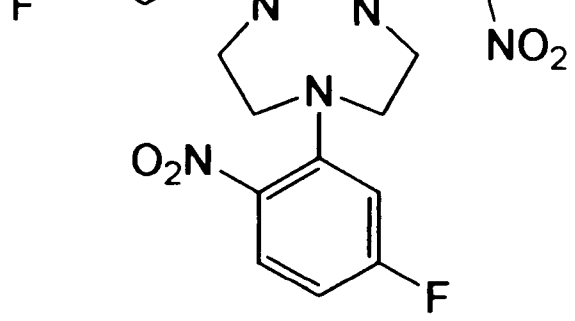

1, 4, 7-tris (2-nitro-5-fluorophenyl)-1, 4, 7-triazacyclononane ($L^{1'}$).

To a solution of 1,4,7-triazacyclononane (1.00 g, 7.75 mmol) in acetonitril ml) was added 2,4-difluoronitrobenzene (4.07 g, 25.58 mmol) and finely gr potassium carbonate (3.50 g, 25.58 mmol). The reaction mixture was heat reflux overnight. After cooling distilled water (50 ml) was added an resulting solution was extracted with chloroform (3 x 100 ml). The or extracts were combined, dried ($MgSO_4$) and the solvent removed to aff bright yellow solid. This material was purified by column chromatog (chloroform) isolating the first major band (R_f = 0.51). Recrystallisation acetone afforded a brilliant yellow fluffy powder ($L^{1'}$). Yield 3.30 g (78 % NMR (400 MHz, $CDCl_3$): δ 3.50 (s, 12H, Al), 6.59 (t, (J_{HH} = 8.25Hz), 3 H 6.70 (d, (J_{HH} = 8.55Hz), 3 H, Ar), and 7.65 (t, (J_{HH} = 8.09Hz), 3 H, Ar). NMR (400 MHz, $CDCl_3$): 54.33, 107.27, 107.89, 128.81, 128.92, 138.7 147.68 (J_{CF} = 986Hz). ^{19}F-NMR ($CDCl_3$): δ –102.45. IR (KBr disc, c 3130, 2963, 1625, 1565, 1513, 1479, 1438, 1343, 1302, 1262, 1244, 1178, 1082, 1015, 867, 799, 746 and 691. Mass spectrum: molecular ion peak a 546.5 (calc. 546).

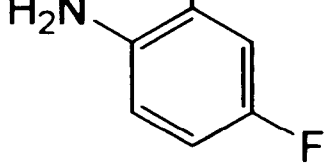

Tris 1, 4, 7-(2-amino, 5-fluorophenyl), 1, 4, 7-triazacyclononane) (L^1).

Tris 1, 4, 7-(2-nitro, 5-fluorophenyl), 1, 4, 7-triazacyclononane (L^1) (250 0.46mmol) was dissolved in a THF:MeOH solution (60:1ml), in a 250ml ro bottomed Schlenk tube. It was found that the use of HPLC grade THF essential, and the catalyst (Pt/C (75mg) was added to methanol (2ml) to crea slurry. CAUTION: minimum contact with methanol was exercised as in incident a small fire occurred, and so the catalyst was added below the surf of the THF:MeOH slurry with a pipette. The Schlenk tube was evacuated backfilled with hydrogen gas. This was stirred for 24 hours upon which complete reaction was indicated by a colour change of yellow to a c solution. The desired compound was filtered off via a cannula equipped glass fibre filter tip, into another Schlenk and the solvent was removed *in va* This afforded a colourless solid (L^1). This material was found to be air-sensit Degradation was indicated by a colour change from colourless to pink. Y 230mg, 92%. ^{1}H NMR: (250 MHz, $CDCl_3$) δ 3.30 (s, 12H, Aliphatic), δ 3.9 Br, 6H, NH_2), δ 6.50 (dd, 6H, (J_{HH} = 1.50 + 6.82), Ar), and δ 6.75 (dt, 3H, = 1.50 + 10.50), Ar). ^{13}C NMR: (250 MHz, $CDCl_3$) δ 54.48, 108.75, 109 114.99, 136.91, 140.52 and 155.14 (J_{CF} = 940). ^{19}F NMR: (300 MHz, CDCl -124.64. IR: (KBr disc, cm^{-1}) 3434, 2965, 1616, 1506, 1261, 1220, 1095, 1 802 and 728. E.I.-MS m/z 457.3 (M^++H^+ 457)

tube via filter cannula which contained manganese (II) perchlorate (52m 0.14mmol). This solution was a cream colour and was stirred vigorously for hour. The solvent was then removed *in vacuo* to yield an off-white precipita To this was added degassed ethanol (10ml), with vigorous stirring. The soluti allowed to settle, was filtered off via cannula, dried *in vacuo*, to afford the ti compound as an off-white solid. Single crystals suitable for X-Ray diffracti were grown by slow vapour diffusion of diethyl ether into an acetonitri solution. Yield 65mg, 70%. IR: (KBr disc, cm^{-1}) 3433, 1607, 1506, 1373, 126 1172, 1090, 866, 808, 770 and 726.

[(L^1)Fe](ClO_4)$_2$.1(MeCN)

This compound was prepared using a similar method to that of [(L^1)Mn](ClO_4 Iron (II) perchlorate (52mg, 0.14mmol), was added to the hydrogenati solution which formed a grey precipitate. Overnight the solid became deep blu Crystals of X-Ray quality were grown by slow vapour diffusion of diethyl eth into an acetonitrile solution. Yield 59mg, 63%. The Mossbäuer spectrum w recorded. IR: (KBr disc, cm^{-1}) 3450, 2963, 1261, 1095, 1019 and 802. UV/V (MeCN, nm (ε/dm^3 mol^{-1} cm^{-1})): 236 (1286), 268 (2135), 298 sh (857) and 7 (722).

[(L^1)Co](ClO_4)$_2$.

This compound was prepared using a similar method to that of [(L^1)Mn](ClO_4 Cobalt (II) perchlorate (53mg, 0.14mmol), was added to the hydrogenati solution which formed a blue precipitate. Attempts at growing crystals of X-Ra quality failed. Yield 67mg, 72%. IR: (KBr disc, cm^{-1}) 3434, 1507, 1464, 136 1305, 1269, 1172, 1100, 862, 811, 771 and 668. UV/Vis (MeCN, nm (ε/dn mol^{-1} cm^{-1})): 332 (347), 418 (168) and 594 (127). Upon addition of $HClO_4$, 46 (71).

[(L^1)Ni](ClO$_4$)$_2$.

This compound was prepared using a similar method to that of [(L^1)Mn](ClO$_4$)$_2$. Nickel (II) perchlorate (53mg, 0.14mmol), was added to the hydrogenation solution which formed a pink precipitate. Crystals of X-Ray quality were grown by slow vapour diffusion of diethyl ether into an acetonitrile solution. Yield 67mg, 72%. IR: (KBr disc, cm^{-1}) 3295, 3224, 3066, 2975, 1608, 1505, 1464, 1269, 1171, 1106, 970, 915, 863, 816, 771 and 725. UV/Vis (MeCN, nm (ε/dm^3 mol^{-1} cm^{-1})):328 (38), 518 (22), 817 (19) and 872 (25)

[(L^1)Cu](ClO$_4$)$_2$.

This compound was prepared using a similar method to that of [(L^1)Mn](ClO$_4$)$_2$. Copper (II) perchlorate (54mg, 0.14mmol), was added to the hydrogenation solution which formed a green precipitate. Crystals of X-Ray quality were grown by slow vapour diffusion of diethyl ether into an acetonitrile solution. Yield 61mg, 65%. IR: (KBr disc, cm^{-1}) 3424, 2964, 1607, 1506, 1265, 1173, 1095 and 725. Mass spectrum (ESI): molecular ion peak at *m/z* 518.1 (calc. 519.16) for M-2(ClO$_4$), 618.1 (calc. 618.11) for M-(ClO$_4$), 716.1 (calc. 717.06). UV/Vis (MeCN, nm (ε/dm^3 mol^{-1} cm^{-1})): 686 (69).

[(L^1)Zn](ClO$_4$)$_2$.

This compound was prepared using a similar method to that of [(L^1)Mn](ClO$_4$)$_2$. Zinc (II) perchlorate (54mg, 0.14mmol), was added to the hydrogenation solution which formed an off white precipitate. Crystals of X-Ray quality were grown by slow vapour diffusion of diethyl ether into an acetonitrile solution. Yield 70mg, 74%. ^{1}H-NMR (400 MHz, CD$_3$CN): δ 3.19 (m, 6 H, Al), 3.80 (m, 6 H, Al), 5.45 (s, 6 H, NH$_2$), 7.22 (dt, (J_{HH} = 2.68 + 8.65 Hz), 3 H, Ar), 7.49 (dd, (J_{HH} = 6.06 + 8.74 Hz), 3 H, Ar) and 7.78 (dd, (J_{HH} = 2.71 + 9.88 Hz), 3 H, Ar). ^{13}C-NMR (400 MHz, CD$_3$CN): δ 53.14, 115.14, 129.10, 131.92, 148.74, 159.98 and 162.40 (J_{CF} = 982Hz). ^{19}F-NMR (300 MHz, CD$_3$CN): δ – 112.92. IR (KBr disc, cm^{-1}): 3296, 3222, 3056, 2965, 1608, 1505, 1269, 1174, 1108, 972, 916, 863, 813, 772 and 726.

[(L^1)Cd](ClO$_4$)$_2$.

This compound was prepared using a similar method to that of [(L^1)Mn](ClO$_4$)$_2$. Cadmium (II) perchlorate (57mg, 0.14mmol), was added to the hydrogenation solution which formed a cream precipitate. Crystals of X-Ray quality were grown by slow vapour diffusion of diethyl ether into an acetonitrile solution. Yield 79mg, 78%. ^{1}H NMR: (400 MHz, CD$_3$CN) δ 3.10 (m, 6H, Al), δ 3.45 (m, 6H, Al), δ 4.65 (br s, 6 H, NH_2), δ 7.00 (m, 3H, Ar), δ 7.35 (m, 6H, Ar). ^{13}C NMR: (250 MHz, CDCl$_3$) δ 54.44, 113.99, 128.17, 128.86, 132.08, 155.65 and 160.20 (J_{CF} = 972Hz). ^{19}F NMR: (300 MHz, CD$_3$CN) δ -113.23. IR: (KBr disc, cm^{-1}) 3424, 2962, 1621, 1606, 1507, 1462, 1375, 1319, 1268, 1174, 1090, 868, 815, 771 and 726.

[(L^1)Hg](ClO$_4$)$_2$.

This compound was prepared using a similar method to that of [(L^1)Mn](ClO$_4$)$_2$. Mercury (II) perchlorate (58mg, 0.14mmol), was added to the hydrogenation solution which formed an off white precipitate. Crystals of X-Ray quality were grown by slow vapour diffusion of diethyl ether into an acetonitrile solution. Yield 75mg, 67%. ^{1}H NMR: (250 MHz, DMSO) δ 3.85 (m, 6H, Al), δ 4.05 (m, 6H, Al), δ 6.65 (br s, 6 H, NH_2), δ 7.55 (m, 3H, Ar), δ 8.10 (m, 6H, Ar). ^{199}Hg Satellite peaks at 6.60 + 6.70, (J_{HgH} = 55.29Hz). ^{13}C NMR: (400 MHz, DMSO) δ 52.86, 127.10, 128.38, 130.43, 134.61, 144.59 and 159.57 (J_{CF} = 968 Hz). ^{19}F NMR: (300 MHz, DMSO) δ -113.52. IR: (KBr disc, cm^{-1}) 3446, 2961, 1621, 1605, 1506, 1375, 1322, 1260, 1177, 1090, 868, 803, 772 and 725.

[(L^1)Pb](ClO$_4$)$_2$

This compound was prepared using a similar method to that of [(L^1)Mn](ClO$_4$)$_2$. Lead (II) perchlorate (59mg, 0.14mmol), was added to the hydrogenation solution which formed an off white precipitate. Crystals of X-Ray quality were grown by slow vapour diffusion of diethyl ether into an acetonitrile solution Yield 84mg, 74%. ^{1}H NMR: (400 MHz, CD$_3$CN) δ 3.70 (m, 6H, Al), δ 3.90 (m, 6H, Al), δ 4.55 (br s, 6 H, NH_2), δ 7.05 (m, 3H, Ar), δ 7.35 (m, 3H, Ar), δ 7.40 (dd, (J_{HH} = 2.71 + 10.91 Hz), 3H, Ar). ^{207}Pb Satellite Peaks at 4.50 and 4.60

(J_{PbH} = 11.02 Hz). ^{13}C NMR: (250 MHz, CD_3CN) δ 55.75, 111.05, 113.68, 129.83, 131.24, 147.73 and 147.88 (J_{CF} = 960Hz). ^{19}F NMR: (300 MHz, CD_3CN) δ - 115.05. IR: (KBr disc, cm^{-1}) 3465, 2963, 1506, 1261, 1095, 1023 and 801.

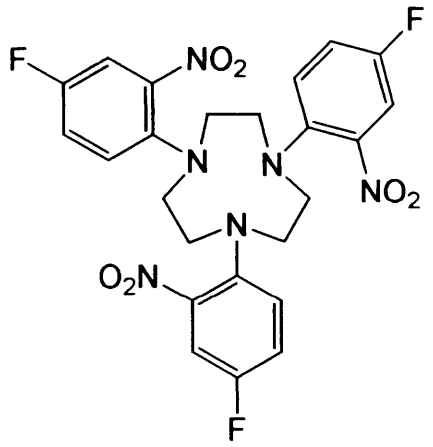

1, 4, 7 tris - (2-nitro, 4-fluorobenzene), 1, 4, 7- triazacyclononane ($L^{2'}$).

1, 4, 7- triazacyclononane (0.15g, 1.16mmol), 2, 5-difluoronitrobenzene (0.61g, 3.84mmol), potassium carbonate (0.497g, 3.60mmol), and acetonitrile (50ml) were all stirred vigorously under reflux, in a round bottomed flask at 85°C for 24 hours. After cooling distilled water (50 ml) was added and the resulting solution was extracted with chloroform (3 x 100 ml). The organic extracts were combined, dried ($MgSO_4$) and the solvent removed to afford an orange solid. This was recrystallized with hot ethanol ($L^{2'}$). X-Ray single crystals were grown by slow vapour diffusion of diethyl ether into acetonitrile. Yield 93%, 0.58g. ^1H NMR: (400 MHz, $CDCl_3$) δ 3.35 (s, 12H, Aliphatic), δ 7.15 (m, 3H, Ar), δ 7.25 (m, 3H, Ar), δ 7.75 (m, 3H, Ar). ^{13}C NMR: (400 MHz, $CDCl_3$) δ 56.32, 112.58, 121.18, 126.68, 142.89, 143.56, 156.10 (J_{CF} = 1124Hz). ^{19}F NMR: (300 MHz, $CDCl_3$) δ -118.39. IR: (KBr disc, cm^{-1}) 2951, 2911, 1570, 1395, 1339, 1305, 1281, 1266, 1222, 1199, 1163, 1130, 1098, 1060, 1031, 1000, 902, 875, 868, 829, 805, 794, 756, and 751. E.I.-MS m/z 547.0 (M^++H^+)

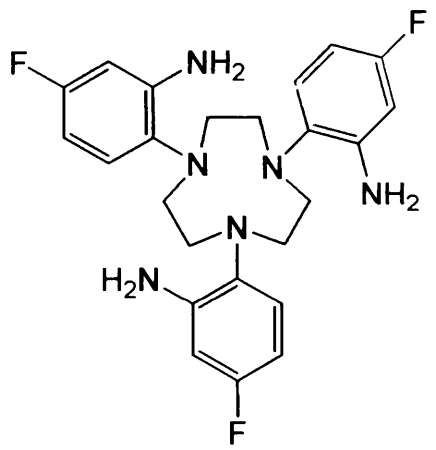

Tris 1, 4, 7-(2-amino, 4-fluorophenyl), 1, 4, 7-triazacyclononane (L^2).

Tris 1, 4, 7-(2-nitro, 4-fluorophenyl), 1, 4, 7-triazacyclononane ($L^{2'}$) (250mg, 0.46mmol) was dissolved in a THF:MeOH solution (60:1ml), in a 250ml round bottomed Schlenk tube. It was found that the use of HPLC grade THF was essential, and the catalyst (Pt/C (75mg) was added to methanol (2ml) to create a slurry. CAUTION: minimum contact with methanol was exercised so the catalyst was added below the surface of the THF:MeOH slurry with a pipette. The Schlenk tube was evacuated and backfilled with hydrogen gas. This was stirred for 24 hours upon which the complete reaction was indicated by a colour change of yellow to a clear solution. The desired compound was filtered off via a cannula equipped with glass fibre filter tip, into another Schlenk and the solvent was removed *in vacuo*. This afforded a colourless solid (L^2). This material was found to be air-sensitive. Degradation was indicated by a colour change from colourless to pink. Yield 181mg, 87%. ^{1}H NMR: (400 MHz, $CDCl_3$) δ 3.20 (s, 12H, Al), δ 4.40 (s Br, 6H, NH_2), δ 6.20-6.30 (m, 6H, Ar), and δ 6.95 (m, 3H, Ar). ^{13}C NMR: (400 MHz, $CDCl_3$) δ 55.76, 100.94, 103.55, 123.91, 136.37, 143.27, and 161.12 (J_{CF} = 780Hz). ^{19}F NMR: (300 MHz, $CDCl_3$) δ -117.52. IR: (KBr disc, cm^{-1}) 3476, 3357, 3040, 2962, 2902, 2813, 1614, 1501, 1440, 1373, 1287, 1261, 1188, 1163 and 1102. E.I.-MS m/z 457.4 (M^++H^+ 457)

[(L^2)Mn](ClO$_4$)$_2$.xMeCN

Manganese (II) perchlorate (74mg, 0.2mmol) was dissolved in ethanol (30n then transferred to another Schlenk tube, via cannula, which contained (60mg, 0.13mmol). The solution was heated with an air gun until the liga dissolved in the ethanol solution. The solution was a white colour and v stirred vigorously for 18 hours. The ethanolic solution was removed via cann carefully so to not disrupt the solid precipitate that had formed. This solid v then dried *in vacuo*. The solid was obtained in warm, degassed ethanol (15n and then re-decanted to leave the title compound as a white solid. Crystals of Ray quality were grown by slow vapour diffusion of diethyl ether into acetonitrile solution. Yield 69mg, 74%. IR: (KBr disc, cm^{-1}) 3447, 3287, 16 1568, 1498, 1458, 1373, 1262, 1086, 855, 805 and 700.

[(L^2)Fe](ClO$_4$)$_2$.xMeCN

This compound was prepared using a similar method to that of [(L^2)Mn](ClO. Iron (II) perchlorate (72mg, 0.2mmol), was added to the hydrogenation solut which formed a blue precipitate. Yield 55mg, 59%. The Mossbäuer spectr was recorded. IR: (KBr disc, cm^{-1}) 3389, 1627, 1502, 1261, 1089 and 8 UV/Vis (MeCN, nm (ε/dm^3 mol^{-1} cm^{-1})): 236 (1105), 270 (2225), 348 sh (8 and 735 (986).

[(L^2)Ni](ClO$_4$)$_2$.xMeCN

This compound was prepared using a similar method to that of [(L^2)Mn](ClO. Nickel (II) perchlorate (73mg, 0.2mmol), was added to the hydrogenat solution which formed a pink precipitate. Yield 59mg, 63%. IR: (KBr disc, c ^{1}) 3397, 1626, 1575, 1261, 1090 and 802. UV/Vis (MeCN, nm (ε/dm^3 mol^{-1} c ^{1})): 330 (31), 520 (14), 813 (15) and 870 (20)

618.1). UV/Vis (MeCN, nm (ε/dm^3 mol^{-1} cm^{-1})): 464 (90) and 700 (139).

[(L^2)Zn](ClO$_4$)$_2$.xMeCN

This compound was prepared using a similar method to that of [(L^2)Mn](ClC
Zinc (II) perchlorate (74mg, 0.2mmol), was added to the hydrogenation solut
which formed an off white precipitate. Yield 70mg, 74%. ^{1}H NMR: (400 M
CD$_3$CN) δ 3.00-3.20 (m, 6H, Al), δ 3.70-3.85 (m, 6H, Al), δ 5.60 (br s,
NH_2), δ 7.30-7.45 (m, 6H, Ar), δ 7.70-7.90 (m, 3H, Ar). ^{13}C NMR: (400 M
CD$_3$CN) δ 53.31, 114.25, 116.12, 127.03, 135.35, 143.06 and 160.30 (J_C
984Hz). ^{19}F NMR: (300 MHz, CD$_3$CN) δ -113.71. IR: (KBr disc, cm^{-1}) 34
3297, 1604, 1503, 1368, 1287, 1257, 1202, 1096, 1071, 860, 825 and 700.

[(L^2)Cd](ClO$_4$)$_2$.

This compound was prepared using a similar method to that of [(L^2)Mn](ClO
Cadmium (II) perchlorate (82mg, 0.2mmol), was added to the hydrogenat
solution which formed an off white precipitate. Yield 63mg, 63%. ^{1}H NM
(250 MHz, CD$_3$CN) δ 3.10 (m, 6H, Al), δ 3.60 (m, 6H, Al), δ 4.75 (br s,
NH_2), δ 7.10 (m, 6H, Ar), δ 7.60 (m, 3H, Ar). ^{13}C NMR: (400 MHz, CD$_3$CN
53.44, 112.67, 127.65, 131.60, 152.43, 156.87, 161.43 (J_{CF} = 988Hz). ^{19}F NM
(300 MHz, CD$_3$CN) δ -114.63. IR: (KBr disc, cm^{-1}) 3528, 2855, 1609, 14
1463, 1373, 1282, 1247, 1197, 1132, 1081, 850, 820, 725 and 700.

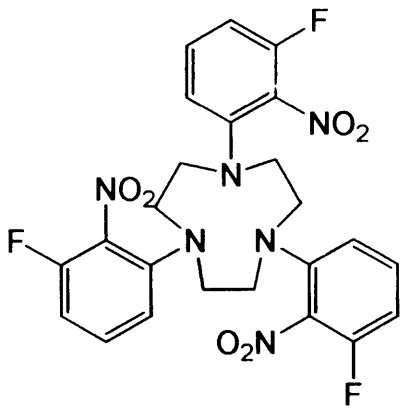

1, 4, 7 tris-(2-nitro, 3-fluorophenyl)- 1, 4, 7- triazacyclononane ($L^{3'}$).

1, 4, 7- triazacyclononane (24mg, 0.186mmol), 2, 6-difluoronitrobenzene (100mg, 0.63mmol), potassium carbonate (36mg, 0.621mmol), and acetonitrile (30ml) were all stirred vigorously in a pressure tube at 90°C for 24 hours. The flask was washed out DCM (15ml). The combined washings were filtered then dried *in vacuo*. The resulting yellow oil was recrystallized with hot ethanol, which afforded solid yellow flakes ($L^{3'}$). Crystals of x-ray quality were grown by slow vapour diffusion of diethyl ether into an acetonitrile solution. Yield 88%, 100mg. ^{1}H NMR: (400 MHz, $CDCl_3$) δ 3.35 (s, 12H, Al), δ 6.70 (t, (J_{HH} = 8.48 Hz), 3H, Ar), δ 6.80 (d, (J_{HH} = 8.61 Hz), 3H, Al), δ 7.25 (m, 3H, Ar). ^{13}C NMR: (400 MHz, $CDCl_3$) δ 54.89, 109.06, 109.20, 116.85, 131.75, 145.68, and 154.87 (J_{CF} = 1336 Hz). ^{19}F NMR: (300 MHz, $CDCl_3$) δ -122.82. IR: (KBr disc, cm^{-1}) 2963, 2900, 2849, 1613, 1520, 1495, 1475, 1445, 1407, 1371, 1261, 1228, 1184, 1147, 1102, 1062, and 1012. E.I.-MS m/z 547.0 (M^{+}+H^{+}).

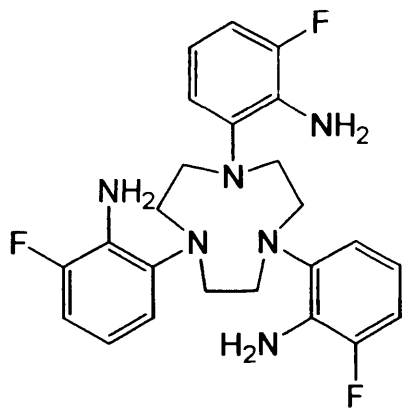

Tris 1, 4, 7-(2-amino, 3-fluorophenyl), 1, 4, 7-triazacyclononane (L^3).

Tris 1, 4, 7-(2-nitro, 3-fluorophenyl), 1, 4, 7-triazacyclononane (L^3) (250mg, 0.46mmol) was dissolved in a THF:MeOH solution (60:1ml), in a 250ml round bottomed Schlenk. It was found that the use of HPLC grade THF was essential, and the catalyst (Pt/C (75mg) was added to methanol (2ml) to create a slurry. CAUTION: minimum contact with methanol was exercised, so the catalyst was added below the surface of the THF:MeOH solution with a pipette. The Schlenk was evacuated and backfilled with hydrogen gas. This was stirred for 24 hours upon which the reaction was signalled by a colour change from yellow to clear. The desired compound was filtered off via a cannula equipped with glass fibre filter tip, into another Schlenk which was then dried *in vacuo*. This afforded a clear product (L^3). Yield 190mg, 91%. ^{1}H NMR: (250 MHz, $CDCl_3$) δ 3.35 (s, 12H, Aliphatic), δ 4.70 (s Br, 6H, NH_2), δ 6.05 (m, 3H, Ar), δ 6.15 (m, 3H, Ar), and δ 6.30 (d, 3H, (J_{HH} = 1.19 Hz), Ar). ^{13}C NMR: (250 MHz, $CDCl_3$) δ 54.88, 109.83, 115.95, 116.91, 129.74, 141.63, and 151.13 (J_{CF} = 945). ^{19}F NMR: (300 MHz, $CDCl_3$) δ -132.93. IR: (KBr disc, cm^{-1}) 3458, 2965, 1617, 1474, 1261, 1095, 1023, 802 and 726. E.I.-MS m/z 457 (M^++H^+)

then transferred to another Schlenk tube, via cannula, which contained (60mg, 0.13mmol). The solution was heated with an air gun until the lig dissolved in the ethanol solution. The solution was a white colour. This stirred vigorously for 18 hours and the ethanolic solution was removed cannula carefully so to not disrupt the solid precipitate that had formed. T solid was then dried *in vacuo*. The solid was obtained in warm, degassed etha (15ml), and then re-decanted to leave the title compound as a white so Crystals of X-Ray quality were grown by slow vapour diffusion of diethyl et into an acetonitrile solution. Yield 72mg, 78%. IR: (KBr disc, cm^{-1}) 3433, 32 1652, 1468, 1368, 1259, 1105, 1019, 862, 796 and 730.

[(L^3)Fe](ClO_4)$_2$.

This compound was prepared using a similar method to that of [(L^3)Mn](ClO Iron (II) perchlorate (52mg, 0.13mmol), was added to the hydrogenat solution which formed a blue precipitate. Crystals of X-Ray quality were grc by slow vapour diffusion of diethyl ether into an acetonitrile solution. Yi 74mg, 80%. The Mossbäuer spectrum was recorded. IR: (KBr disc, cm^{-1}) 34 2964, 1621, 1261, 1100, 797, 726 and 690. UV/Vis (MeCN, nm (ε/dm^3 m cm^{-1})): 236 (4271), 270 (2801), 349 sh (924) and 730 (1202).

[(L^3)Co](ClO_4)$_2$

This compound was prepared using a similar method to that of [(L^3)Mn](ClO Cobalt (II) perchlorate (53mg, 0.13mmol), was added to the hydrogenat solution which formed a blue precipitate. Crystals of X-Ray quality were gro by slow vapour diffusion of diethyl ether into an acetonitrile solution. Attem at growing crystals of X-Ray quality failed. Yield 77mg, 82%. IR: (KBr di cm^{-1}) 3433, 2962, 1263, 1231, 1095, 1042, 797 and 720. UV/Vis (MeCN,

solution which formed a pink precipitate. Crystals of X-Ray quality were gr by slow vapour diffusion of diethyl ether into an acetonitrile solution. Y 77mg, 83%. IR: (KBr disc, cm^{-1}) 3433, 1611, 1262, 1095, 803, 726 and UV/Vis (MeCN, nm ($\varepsilon/dm^3\ mol^{-1}\ cm^{-1}$)): 466 (74) and 812 (36).

[(L^3)Cu](ClO_4)$_2$.

This compound was prepared using a similar method to that of [(L^3)Mn](ClO Copper (II) perchlorate (54mg, 0.13mmol), was added to the hydrogena solution which formed a green precipitate. Crystals of X-Ray quality v grown by slow vapour diffusion of diethyl ether into an acetonitrile solut Yield 79mg, 85%. IR: (KBr disc, cm^{-1}) 3434, 2958, 1617, 1262, 1095, 801 725. Mass spectrum (ESI): molecular ion peak at *m/z* 518.1 (calc. 519.16) M-2(ClO_4), 616.1 (calc.618.11) for M-(ClO_4), 718.0 (calc. 717.06). UV (MeCN, nm ($\varepsilon/dm^3\ mol^{-1}\ cm^{-1}$)): 684 (106).

[(L^3)Zn](ClO_4)$_2$

This compound was prepared using a similar method to that of [(L^3)Mn](ClO Zinc (II) perchlorate (54mg, 0.13mmol), was added to the hydrogena solution which formed an off white precipitate. Crystals of X-Ray quality v grown by slow vapour diffusion of diethyl ether into an acetonitrile solut Yield 75mg, 81%. ^{1}H NMR: (400 MHz, CD_3CN) δ 3.10 (m, 6H, Al), δ 3.70 6H, Al), δ 4.60 (br s, 6 H, NH_2), δ 7.15 (m, 3H, Ar), δ 7.45 (m, 6H, Ar). NMR: (250 MHz, CD_3CN) δ 53.16, 114.25, 120.64, 122.54, 129.46, 148.47 157.87 (J_{CF} = 980Hz). ^{19}F NMR: (300 MHz, CD_3CN) δ -119.69. IR: (KBr d cm^{-1}) 3444, 2964, 1607, 1478, 1442, 1373, 1262, 1095, 859, 797, 726 and 69

6H, Al), δ 4.65 (br s, 6 H, NH_2), δ 7.00 (m, 3H, Ar), δ 7.35 (m, 6H, Ar). NMR: (250 MHz, CD_3CN) δ 53.20, 115.18, 117.69, 121.22, 123.72, 151.93 157.29 (J_{CF} = 960Hz). ^{19}F NMR: (300 MHz, CD_3CN) δ -119.66. IR: (KBr d cm^{-1}) 3539, 3246, 1479, 1374, 1263, 1084, 862, 792 and 725.

[(L^3)Hg](ClO$_4$)$_2$

This compound was prepared using a similar method to that of [(L^3)Mn](ClO Mercury (II) perchlorate (58mg, 0.13mmol), was added to the hydrogenat solution which formed an off white precipitate. Crystals of X-Ray quality w grown by slow vapour diffusion of diethyl ether into an acetonitrile soluti Yield 83mg, 74%. ^{1}H NMR: (400 MHz, CD_3CN) δ 3.10 (m, 6H, Al), δ 3.50 6H, Al), δ 4.90 (br s, 6 H, NH_2), δ 7.10 (m, 3H, Ar), δ 7.40 (m, 6H, Ar). 199 satellite peaks at δ 4.85 + 5.05, (54.77Hz). ^{13}C NMR: (250 MHz, CD_3CN 53.61, 113.44, 113.65, 121.91, 128.32, 148.30 and 158.14 (J_{CF} = 972Hz). NMR: (300 MHz, CD_3CN) δ -119.64. IR: (KBr disc, cm^{-1}) 3459, 3335, 16 1569, 1462, 1375, 1308, 1261, 1084, 802 and 726.

[(L^3)Pb](ClO$_4$)$_2$

This compound was prepared using a similar method to that of [(L^3)Mn](ClO Lead (II) perchlorate (59mg, 0.13mmol), was added to the hydrogenat solution which formed an off white precipitate. Crystals of X-Ray quality w grown by slow vapour diffusion of diethyl ether into an acetonitrile soluti Yield 84mg, 75%. ^{1}H NMR: (250 MHz, CD_3CN) δ 3.60 (m, 6H, Al), δ 3.90 6H, Al), δ 4.45 (br s, 6 H, NH_2), δ 7.15 (m, 3H, Ar), δ 7.35 (m, 6H, Ar). 207

triazacyclononane.

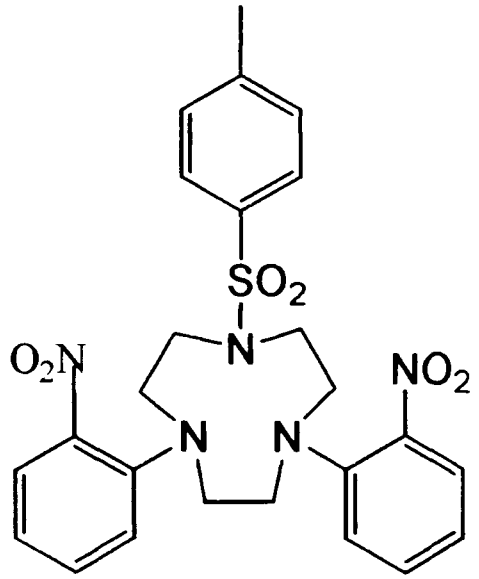

1-Tosyl, 4, 7-bis (2-nitrophenyl), 1, 4, 7-triazacyclononane ($L^{4'}$).

Mono 1-tosyl 1, 4, 7-triazacyclononane[1] (500mg, 1.77mmol), fluoronitrobenzene (498mg, 3.53mmol), potassium fluoride (205m 3.53mmol), and acetonitrile (30ml) were all refluxed vigorously in a 100 round bottomed flask at 100°C for 24 hours. The flask was washed out w DCM (15ml). The combined washings were filtered then dried *in vacuo*. T resulting orange oil was recrystallized with hot ethanol, which afforded orange powder ($L^{4'}$). Yield 1.26g, 92%. ^{1}H NMR: (400 MHz, $CDCl_3$) δ 2.30 3H, Methyl), δ 3.15 (m, 4H, Al), δ 3.55 (m, 8H, Al), δ 6.85 (t, (J_{HH} = 7.11 H 2H, Ar), δ 7.10 (d, (J_{HH} = 8.43 Hz), 2H, Ar), δ 7.15 (d, (J_{HH} = 8.02 Hz), 2 Ar), δ 7.35 (m, 2H, Ar), and δ 7.55 (dd, (J_{HH} = 1.63 + 8.12 Hz), 4H, Ar). ^{1} NMR: (250 MHz, $CDCl_3$) δ 21.51, 50.97, 54.14, 55.47, 120.75, 121.92, 125.9

[1] Lazar I., Takacs Z., *Synth .Commun.*, **2001**, 31 (20), 3141-3144.

127.25, 129.84, 133.26, 134.65, 142.84, 143.73 and 144.00. IR: (KBr disc, cm^{-1}) 1601, 1565, 1361, 1340, 1296, 1218, 1156, 1129, 1087, 1029, 1003, 867, 845, 813, 768, 746, 708 and 694. E.I.-MS m/z 526 ($M^{+}+H^{+}$)

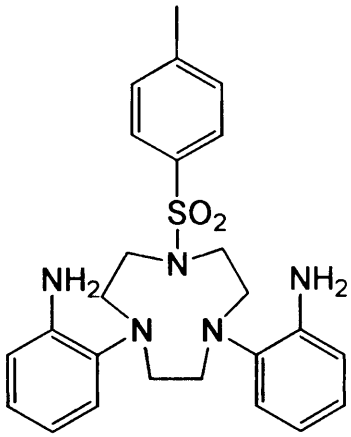

1-Tosyl, 4, 7-bis (2-aminophenyl), 1, 4, 7-triazacyclononane (L^4)

$L^{4'}$ (100mg, 0.19mmol) was dissolved in a THF: MeOH solution (40:1ml), in a 250ml round bottomed Schlenk. It was found that the use of HPLC grade THF was essential, and the catalyst (Pt/C (50mg) was added to methanol (2ml) to create a slurry. CAUTION: minimum contact with methanol was exercised as in one incident a small fire occurred, and so the catalyst was added below the surface of the THF:MeOH solution with a pipette. The Schlenk was evacuated and backfilled with hydrogen gas. This was stirred for 24 hours upon which the reaction was signalled by a colour change from yellow to clear. The desired compound was filtered off via a cannula equipped with glass fibre filter tip, into another Schlenk which was then dried *in vacuo*. This afforded a clear solid (L^4). Yield 83mg, 94%. ^{1}H NMR: (400 MHz, $CDCl_3$) δ 2.30 (s, 3H, Methyl), δ 3.20 (s, 8H, Al), δ 3.40 (s, 4H, Al), δ 4.00 (br s, 4H, NH_2), δ 6.60 (m, 4H, Ar), δ 6.80 (m, 2H, Ar), δ 7.05 (dd, (J_{HH} = 1.17 + 8.19 Hz), 2H, Ar), δ 7.15 (d, (J_{HH} = 8.04 Hz), 2H, Ar), and δ 7.55 (d, (J_{HH} = 8.25 Hz), 2H, Ar). ^{13}C NMR: (250 MHz, $CDCl_3$) δ 20.46, 52.10, 55.18, 55.26, 114.67, 117.64, 123.12, 124.15, 126.20, 128.72, 134.07, 139.77, 141.79 and 142.41. IR: (KBr disc, cm^{-1}) 3444, 1497, 1456, 1329, 1261, 1156 and 1089. E.I.-MS m/z 466 ($M^{+}+H^{+}$)

Synthesis of metal complexes of general formula $[(L^4)M](ClO_4)_2.x(MeCN)$, M=Ni, Cu, Zn, Cd, Hg and Pb.

$[(L^4)Ni.MeCN](ClO_4)_2.1(MeCN)$.

The solution of L^4 (100mg, 0.13mmol) was transferred directly into another Schlenk tube via filter cannula which contained nickel (II) perchlorate (63mg, 0.17mmol). This solution was a purple and was stirred vigorously for 18 hours. The solvent was removed *in vacuo*, and afforded a light purple precipitate. To this was added degassed ethanol (10ml), stirred vigorously then the solution allowed to settle. The solution was filtered off via cannula, again dried *in vacuo*, and produced the title compound as a lilac solid. Yield 102mg, 79%. Crystals of X-Ray quality were grown by layering of an acetonitrile solution by diethyl ether. IR: (KBr disc, cm^{-1}) 3484, 2965, 1617, 1594, 1575, 1498, 1367, 1263, 1165, 1100 and 1042. UV/Vis (MeCN, nm ($\varepsilon/dm^3\ mol^{-1}\ cm^{-1}$)): 496 (38) and 826 (26).

2.$[(L^4)Cu.]4.(ClO_4).4(MeCN)$ MeOH.

This compound was prepared using a similar method to that of $[(L^4)Ni](ClO_4)_2$. Copper (II) perchlorate (64mg, 0.17mmol) was used which formed a purple precipitate. Crystals of X-Ray quality were grown by slow vapour diffusion of diethyl ether into an acetonitrile solution. Yield 104mg, 81%. IR: (KBr disc, cm^{-1}) 3501, 3243, 1595, 1564, 1456, 1336, 1262, 1230, 1089, 883, 802, 766, 740 and 706. UV/Vis (MeCN, nm ($\varepsilon/dm^3\ mol^{-1}\ cm^{-1}$)): 499 (219).

$[(L^4)Zn.MeCN](ClO_4)_2.MeCN$.

This compound was prepared using a similar method to that of $[(L^4)Ni](ClO_4)_2$. Zinc (II) perchlorate (64mg, 0.17mmol) was used which formed an off white precipitate. Crystals of X-Ray quality were grown by layering of diethyl ether onto an acetonitrile solution. Yield 127mg, 85%. ^{1}H-NMR (250 MHz, CD_3CN): δ 2.65 (s, 3H, Me), 3.00-3.15 (m, 4H, Al), 3.35-3.55 (m, 4H, Al), 3.75-4.15 (m, 4H, Al), 5.10 (br d, (J_{NH} =13.12Hz), 2H, NH_2), 5.45 (br d, (J_{NH}=13.12Hz), 2H, NH_2), 7.60-7.80 (m, 8H, Ar), 7.90 (d, (J_{HH} =7.73Hz), 2H, Ar) and 8.10 (d, (J_{HH} =8.39Hz), 2H, Ar). ^{13}C-NMR (250 MHz, CD_3CN): δ 20.41, 47.16, 52.15, 54.55,

123.90, 127.18, 128.12, 128.87, 128.99, 129.21, 130.12, 133.25, 145.52 and 146.68. IR (KBr disc, cm^{-1}): 3499, 1575, 1497, 1455, 1342, 1294, 1261, 1090 and 876.

[(L^4)Cd.MeCN](ClO_4)$_2$.

This compound was prepared using a similar method to that of [(L^4)Ni](ClO_4)$_2$. Cadmium (II) perchlorate (72mg, 0.17mmol) was used which formed an off white precipitate. Crystals of X-Ray quality were grown by slow vapour diffusion of diethyl ether into an acetonitrile solution. Yield 106mg, 77%. ^{1}H NMR: (400 MHz, CD_3CN) δ 2.85 (m, 2H, Al), δ 3.05 (m, 2H, Al), δ 3.40 (s, 6H, Al), δ 3.65 (m, 2H, Al), δ 4.70 (br s, 2H, NH_2), δ 5.10 (br s, 2H, NH_2), δ 7.35 (m, 2H, Ar), δ 7.40-7.50 (m, 4H, Ar), δ 7.55 (d, (J_{HH} = 0.72Hz), 2H, Ar), δ 7.60 (d, (J_{HH} = 0.75Hz), 2H, Ar), and δ 7.85 (d, (J_{HH} = 8.34Hz), 2H, Ar). ^{13}C NMR: (400 MHz, CD_3CN) δ 20.43, 46.91, 50.17, 64.94, 123.75, 126.78, 127.32, 128.13, 128.84, 130.26, 133.36, 134.62, 144.90 and 146.87. IR: (KBr disc, cm^{-1}) 3521, 1616, 1497, 1458, 1337, 1294, 1262, 1228, 1089, 885, 831, 803, 763, 731, 709 and 697.

[(L^4)Hg.](ClO_4)$_2$.

This compound was prepared using a similar method to that of [(L^4)Ni](ClO_4)$_2$. Mercury (II) perchlorate (88mg, 0.17mmol) was used which formed an off white precipitate. Yield 116mg, 75%. ^{1}H NMR: (400 MHz, CD_3CN) δ 2.40 (m, 3H, Me), δ 2.95 (m, 4H, Al), δ 3.45 (m, 4H, Al), δ 3.70 (m, 4H, Al), δ 5.55 (br s, 2H, NH_2), δ 6.35 (br s, 2H, NH_2), δ 7.30 (d, (J_{HH} = 7.28Hz), 2H, Ar), δ 7.35-7.55 (m, 6H, Ar), δ 7.60 (t, (J_{HH} = 7.87Hz), 2H, Ar) and δ 7.75 (d, (J_{HH} = 8.04Hz), 2H, Ar). ^{201}Hg satellite peaks at δ 5.50 + 5.60, (51.28Hz) and δ 6.30 + 6.40, (53.83Hz). ^{13}C NMR: (250 MHz, CD_3CN) δ 21.56, 46.23, 49.84, 57.91, 124.58, 125.81, 126.53, 127.09, 128.26, 128.91, 130.20, 131.06, 144.29 and 146.21. IR: (KBr disc, cm^{-1}) 3501, 1496, 1456, 1372, 1331, 1263, 1089 and 889.

[(L^4)Pb.ClO_4](ClO_4) 2.(MeCN).

This compound was prepared using a similar method to that of [(L^4)Ni](ClO_4)$_2$. Lead (II) perchlorate (89mg, 0.17mmol) was used which formed a clear precipitate. Crystals of X-Ray quality were grown by slow evaporation of a concentrated acetonitrile solution. Yield 104mg, 67%. ^{1}H-NMR (250 MHz, CD_3CN): δ 2.55 (s, 3H, Me), 3.20-3.55 (m, *exo*, 6H, Al), 3.75-4.15 (m, *endo*, 6H, Al), 5.05-5.35 (br s, 4H, NH_2), 7.25-7.45 (m, 6H, Ar) 7.50 (d, (J_{HH} = 8.15Hz), 2H, Ar) 7.60 (m, 2H, Ar) and 7.80 (d, (J_{HH} = 8.32Hz), 2H, Ar). ^{13}C-NMR (100 MHz, CD_3CN): δ 28.13, 56.15, 58.19 59.23, 114.63, 115.36, 124.85, 126.42, 127.16, 127.90, 128.23, 129.36, 129.58 and 129.75. IR (KBr disc, cm^{-1}): 3465, 1652, 1498, 1331, 1261 and 1090.

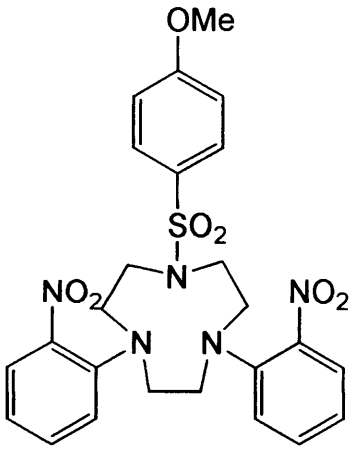

Mono 1-(4-methoxysulphonylphenyl) bis 4, 7-(2-nitrophenyl) 1, 4, 7-triazacyclononane ($L^{5'}$).

L^{32} (100mg, 0.27mmol), 4-methoxyphenylsulphonyl chloride (56mg, 0.27mmol), potassium fluoride (16mg, 0.27mmol), and acetonitrile (30ml) were all refluxed vigorously in a 100ml round bottomed flask for 24 hours. The flask was washed out with DCM (15ml). The combined washings were filtered then dried *in vacuo*. The resulting orange oil was recrystallized with hot ethanol,

which afforded an orange powder (L^5). Yield 131mg, 90%. ^{1}H-NMR (250 MHz, $CDCl_3$): δ 3.15 (m, 4H, Al), 3.50 (m, 8H, Al), 3.75 (s, 3H, Me), 6.85 (m, 2H, Ar), 7.10 (dd, (J_{HH} = 0.72 + 8.49Hz), 2H, Ar, 7.35 (m, 4H, Ar, 7.50 (dd, (J_{HH} = 1.56 + 8.07Hz), 2H, Ar) and 7.60 (d, (J_{HH} = 6.95Hz), 2H, Ar). ^{13}C-NMR (250 MHz, $CDCl_3$): δ 49.87, 53.03, 54.39, 54.89, 113.68, 119.61, 120.71, 128.28, 129.86, 132.23, 141.66, 142.88 and 161.98. IR (KBr disc, cm^{-1}): 3434, 2956, 1595, 1576, 1497, 1451, 1343, 1261, 1221, 1153, 1091, 1021, 831, 803, 731, 719 and 690. Mass spectrum: molecular ion peak at *m/z* 542.

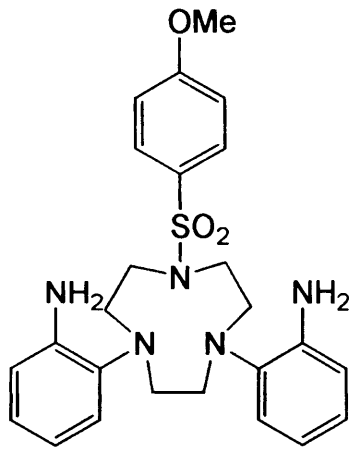

Mono 1-(4-methoxyphenylsulphonyl) bis 4, 7-(2-aminophenyl) 1, 4, 7-triazacyclononane. (L^5)

$L^{5'}$ (100mg, 0.185mmol) was dissolved in a THF:MeOH solution (40:1ml), in a 250ml round bottomed Schlenk. The THF used was of HPLC grade, and the catalyst washed on a sinter with methanol, (Pt/C (50mg). CAUTION: minimum contact with methanol was exercised as in one incident a small fire occurred, and so the catalyst was added below the surface of the THF:MeOH solution with a pipette. The Schlenk was evacuated and backfilled with hydrogen gas. This was stirred for 24 hours upon which the reaction was signalled by a colour change from yellow to clear. The desired compound was filtered off via a

cannula equipped with glass fibre filter tip, into another Schlenk which was then dried *in vacuo*. This afforded a clear solid (L^5). Yield 82mg, 92%. ^{1}H-NMR (400 MHz, $CDCl_3$): δ 3.30 (m, 4H, Al), 3.40 (m, 4H, Al), 3.75 (m, 4H, Al), 3.80 (s, 3H, Me), 3.95-4.50 (Br, 4H, NH_2), 6.60 (m, 2H, Ar), 6.65 (d, (J_{HH} = 7.37Hz), 2H, Ar), 6.85 (t, (J_{HH} = 8.21Hz), 2H, Ar), 6.90 (d, (J_{HH} = 8.88Hz), 2H, Ar), 7.05 (d, (J_{HH} = 8.11Hz), 2H, Ar) and 7.65 (d, (J_{HH} = 8.87Hz), 2H, Ar). ^{13}C-NMR (250 MHz, $CDCl_3$): δ 52.10, 54.58, 55.23, 55.29, 113.25, 114.67, 117.67, 123.14, 124.16, 128.26, 128.85, 139.80, 141.80 and 161.86. IR (KBr disc, cm^{-1}): 3463, 1595, 1496, 1452, 1261, 1090 and 1018. Mass spectrum: molecular ion peak at 483 *m/z*

Synthesis of metal complexes of general formula $[(L^5)M](ClO_4)_2.x(MeCN)$, M=Ni, Cu, Zn, Cd and Hg.

$[(L^5)Ni.MeCN](ClO_4)_2.2(MeCN)$.

L^5 (82mg, 0.17mmol) was transferred directly into another Schlenk tube via filter cannula which contained nickel (II) perchlorate (68mg, 0.187mmol). This solution was purple colour and was stirred vigorously for 18 hours. The solvent was removed *in vacuo*, and yielded a light purple precipitate. To this was added degassed ethanol (10ml), stirred vigorously then the solution allowed to settle. The solution was filtered off via cannula, again dried *in vacuo*, and produced the title compound as a lilac solid. Crystals of X-Ray quality were grown by layering of an acetonitrile solution by diethyl ether. Yield 119mg, 95%. IR (KBr disc, cm^{-1}): 3397, 1621, 1496, 1355, 1263, 1147, 1089, 804 and 625. UV/Vis (MeCN, nm (ε/dm^3 mol^{-1} cm^{-1})): 352 (57), 462 (49) and 866 (23).

$[(L^5)Cu](ClO_4)_2$.

This compound was prepared using a similar method to that of $[(L^5)Ni](ClO_4)_2$. Copper (II) perchlorate (73mg, 0.187mmol) was used which formed a purple precipitate. Yield 127mg, 80%. IR (KBr disc, cm^{-1}): 3434, 2955, 195, 1576, 1497, 1451, 1413, 1382, 1373, 1343, 1320, 1263, 1153, 1090, 1021, 884, 855, 831, 803, 749 and 690. UV/Vis (MeCN, nm (ε/dm^3 mol^{-1} cm^{-1})): 458 (312).

[(L^5)Zn.MeCN](ClO_4)$_2$.MeCN.

This compound was prepared using a similar method to that of [(L^5)Ni](ClO_4)$_2$. Zinc (II) perchlorate (70mg, 0.187mmol) was used which formed an off white precipitate. Crystals of X-Ray quality were grown by slow vapour diffusion of diethyl ether into an acetonitrile solution. Yield 119mg, 93%. ^{1}H-NMR (400 MHz, CD_3CN): δ 2.75-2.90 (m, 2H, Al), 3.15-3.20 (m, 2H, Al), 3.55-3.80 (m, 8H, Al), 4.85 (br d, (J_{HH} = 13.08Hz), 2H, NH_2), 5.15 (br d, (J_{HH} = 13.08Hz), 2H, NH_2), 7.15 (dd, (J_{HH} = 2.03 + 7.02Hz), 2H, Ar), 7.35-7.50 (m, 6H, Ar), 7.60 (d, (J_{HH} = 7.72Hz), 2H, Ar), and 7.90 (dd, (J_{HH} = 2.10 + 7.02Hz), 2H, Ar). ^{13}C-NMR (400 MHz, CD_3CN): δ 47.06, 52.00, 54.48, 55.60, 114.70, 122.88, 123.83, 127.09, 128.01, 128.88, 131.55, 133.22, 145.45 and 164.60. IR (KBr disc, cm^{-1}): 3434, 1496, 1260, 1090 and 1023

[(L^5Cd](ClO_4)$_2$.

This compound was prepared using a similar method to that of [(L^5)Ni](ClO_4)$_2$. Cadmium (II) perchlorate (78mg, 0.187mmol) was used which formed an off white precipitate. Yield 115mg, 84%. ^{1}H-NMR (400 MHz, CD_3CN): δ 2.85 (m, 2H, Al), 3.00 (m, 2H, Al), 3.20-3.65 (m, 8H, Al), 3.80 (s, 3H, Me), 4.70 (br s, 2H, NH_2), 5.10 (br s, 2H, NH_2), 7.10 (d, (J_{HH} = 9.01Hz), 2H, Ar), 7.25 (m, 2H, Ar), 7.35 (m, 2H, Ar), 7.40 (d, (J_{HH} = 7.82Hz), 2H, Ar), 7.55 (d, (J_{HH} = 7.21Hz), 2H, Ar) and 7.80 (dd, (J_{HH} = 2.09 + 6.95Hz), 2H, Ar). ^{13}C-NMR (400 MHz, CD_3CN): δ 50.10, 55.04, 55.59, 57.16, 114.90, 119.84, 123.72, 126.76, 127.25, 128.07, 131.22, 133.38, 144.90 and 164.79. IR (KBr disc, cm^{-1}): 3489, 1496, 1262 and 1089

[(L^5Hg](ClO_4)$_2$.

This compound was prepared using a similar method to that of [(L^5)Ni](ClO_4)$_2$. Mercury (II) perchlorate (95mg, 0.187mmol) was used which formed an off white precipitate. Yield 115mg, 76%. ^{1}H-NMR (400 MHz, CD_3CN): δ 3.35-3.45 (m, 6H, Al), 3.45-3.55 (M, 6h, Al), 3.80 (s, 3H, Me), 5.50 (br d, (J_{HH} = 11.13Hz), 2H, NH_2), 6.35 (br d, (J_{HH} = 12.00Hz), 2H, NH_2), 7.10 (dd, (J_{HH} = 1.91 + 7.04Hz), 2H, Ar), 7.30 (m, 2H, Ar), 7.40 (m, 2H, Ar), 7.45 (m, 2H, Ar), 7.60 (dd, (J_{HH} = 0.71 + 7.98Hz), 2H, Ar) and 7.65 (dd, (J_{HH} = 1.98 + 7.02HZ),

2H, Ar). ^{201}Hg satellite peaks at 5.40 + 5.65 (J_{HgH} = 109.65Hz), and 6.20 + 6.50 (J_{HgH} = 108.4Hz). ^{13}C-NMR (400 MHz, CD_3CN): δ 49.77, 55.15, 55.52, 56.89, 114.84, 119.74, 124.57, 125.81, 127.09, 128.89, 130.60, 131.05, 144.27, 164.43 and 119.74. IR (KBr disc, cm^{-1}): 3485, 1621, 1496, 1329, 1307, 1262, 1147, 1089 and 1023.

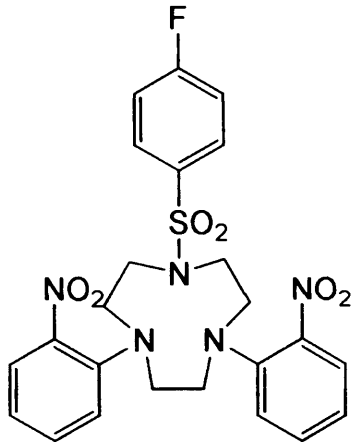

1-(4-Fluorophenylsulphonyl), 4, 7 bis-(2-nitrophenyl), 1, 4, 7-triazacyclononane ($L^{6'}$).

L^{32} (100mg, 0.27mmol), 4-Fluorophenylsulphonyl chloride (52mg, 0.27mmol), potassium fluoride (16mg, 0.27mmol), and acetonitrile (30ml) were all refluxed vigorously in a 100ml round bottomed flask at 90°C for 24 hours. The flask was washed out with DCM (15ml). The combined washings were filtered then dried *in vacuo*. The resulting orange oil was recrystallized with hot ethanol, which afforded an orange powder ($L^{6'}$). Yield 127mg, 89%. ^{1}H-NMR (400 MHz, $CDCl_3$): δ 3.25 (t, (J_{HH} = 4.38Hz), 4H, Al), 3.55 (m, 8H, Al), 6.90 (m, 2H, Ar), 7.10 (m, 4H, Ar), 7.35 (m, 2H, Ar), 7.55 (dd, (J_{HH} = 1.62 + 8.09Hz), 2H, Ar) and 7.70 (q, (J_{HH} = 5.03 + 8.88Hz), 2H, Ar). ^{13}C-NMR (250 MHz, $CDCl_3$): δ 50.91, 54.32, 55.40, 116.68, 120.92, 125.94, 129.83, 133.28, 133.80, 142.93, 143.99 and 165.19 (J_{CF}=1013Hz). ^{19}F-NMR ($CDCl_3$): δ -104.68. IR (KBr disc, cm^{-1}): 1601, 1517, 1342, 1293, 1224, 1154, 1087, 1051, 838, 742, 714 and 695. Mass spectrum: molecular ion peak at *m/z* 530.

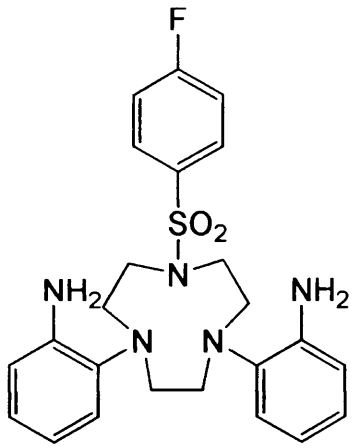

1-(4-Fluorophenylsulphonyl), 4, 7 bis-(2-aminophenyl), 1, 4, 7-triazacyclononane. (L^6)

$L^{6'}$ (100mg, 0.19mmol) was dissolved in a THF:MeOH solution (40:1ml), in a 250ml round bottomed Schlenk. The THF used was of HPLC grade, and the catalyst washed on a sinter with methanol, (Pt/C (50mg). CAUTION: minimum contact with methanol was exercised as in one incident a small fire occurred, and so the catalyst was added below the surface of the THF:MeOH solution with a pipette. The Schlenk was evacuated and backfilled with hydrogen gas. This was stirred for 24 hours upon which the reaction was signalled by a colour change from yellow to clear. The desired compound was filtered off via a cannula equipped with glass fibre filter tip, into another Schlenk which was then dried *in vacuo*. This afforded a clear solid. Yield 83mg, 94%. ^{1}H-NMR (400 MHz, $CDCl_3$): δ 3.25 (s, 4H, Al), 3.50 (m, 8H, Al), 4.10 (br s, 4H, NH_2), 6.65 (m, 4H, Ar), 6.85 (dt, (J_{HH} = 1.36 + 7.57Hz), 2H, Ar), 7.05 (m, 4H, Ar), and 7.70 (m, 2H, Ar). ^{13}C-NMR (250 MHz, $CDCl_3$): δ 52.12, 55.13, 55.32, 114.77, 115.20, 115.55, 117.77, 123.18, 124.27, 128.89, 139.71, 141.71 and 164.43 (J_{CF} = 1085Hz). ^{19}F-NMR ($CDCl_3$): δ – 105.06. IR (KBr disc, cm^{-1}): 3434, 1616, 1497, 1335, 1261, 1153, 1086, 1025, 802, 748 and 715. Mass spectrum: molecular ion peak at *m/z* 469.

Synthesis of metal complexes of general formula $[(L^6)M](ClO_4)_2.x(MeCN)$, M=Ni, Cu and Zn.

$[(L^6)Ni.MeCN](ClO_4)_2.MeCN.H_2O$.

The solution of L^6 (83mg, 0.18mmol) was transferred directly into another Schlenk tube via filter cannula which contained nickel (II) perchlorate (70mg, 0.19mmol). This solution was a purple and was stirred vigorously for 18 hours. The solvent was removed *in vacuo*, and yielded a light purple precipitate. To this was added degassed ethanol (10ml), stirred vigorously then the solution allowed to settle. The solution was filtered off via cannula, again dried *in vacuo*, and produced the title compound as a lilac solid. Yield 118mg, 93%. Crystals of X-Ray quality were grown by slow vapour diffusion of a diethyl ether solution into an acetonitrile solution. IR (KBr disc, cm^{-1}): 3433, 1587, 1498, 1261, 1095, 1019, 865, 801 and 698. UV/Vis (MeCN, nm ($\varepsilon/dm^3\ mol^{-1}\ cm^{-1}$)): 332 (25), 528 (12) and 840 (12).

$[(L^6)Cu](ClO_4)_2$.

This compound was prepared using a similar method to that of $[(L^6)Ni](ClO_4)_2$. Copper (II) perchlorate (71mg, 0.19mmol) was used which formed a dark purple precipitate. Yield 105mg, 65%. IR (KBr disc, cm^{-1}): 3433, 1495, 1339, 1261, 1095, 802, 713 and 619. UV/Vis (MeCN, nm ($\varepsilon/dm^3\ mol^{-1}\ cm^{-1}$)): 454 (462).

$[(L^6)Zn](ClO_4)_2$.

This compound was prepared using a similar method to that of $[(L^6)Ni](ClO_4)_2$. Zinc (II) perchlorate (71mg, 0.19mmol) was used which formed an off white precipitate. Crystals of X-Ray quality were grown by slow vapour diffusion of diethyl ether into an acetonitrile solution. Yield 114mg, 89%. ^{1}H-NMR (400 MHz, CD_3CN): δ 2.85-2.90 (m, 2H, Al), 3.05-3.10 (m, 2H, Al), 3.20-3.25 (m, 4H, Al), 3.70 (m, 3H, Al), 4.90 (br d, (J_{HH} = 13.10Hz), 2H, NH_2), 5.20 (br d, (J_{HH} = 13.07Hz), 2H, NH_2), 7.40-7.50 (m, 8H, Ar), 7.65 (d, (J_{HH} = 13.81Hz), 2H, Ar), 8.00 (m, 2H, Ar). ^{13}C-NMR (250 MHz, CD_3CN): δ 47.13, 53.01, 54.72, 117.13, 123.95, 127.20, 128.15, 129.03, 130.42, 131.70, 133.22, 145.58

and 163.89 (J_{CF} = 1080Hz). ^{19}F-NMR ($CDCl_3$): δ -103.14. IR (KBr disc, cm^{-1}): 3567, 1616, 1494, 1150, 1089, 878, 841, 765, 736, 712 and 697.

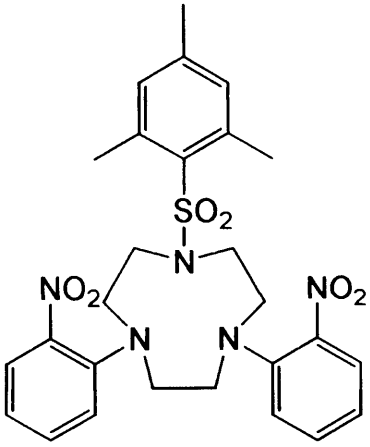

Mono 1-(2-mesitylsulphonylphenyl) bis 4, 7-(2-nitrophenyl) 1, 4, 7-triazacyclononane ($L^{7'}$).

L^{32} (100mg, 0.27mmol), 2-mesitylsulphonyl chloride (59mg, 0.27mmol), potassium fluoride (16mg, 0.27mmol), and acetonitrile (30ml) were all refluxed vigorously in a 100ml round bottomed flask at 90°C for 24 hours. The flask was washed out with DCM (15ml). The combined washings were filtered then dried *in vacuo*. The resulting orange oil was recrystallized with hot ethanol, which afforded an orange powder ($L^{7'}$). Yield 131mg, 88%. ^{1}H-NMR (400 MHz, $CDCl_3$): δ 2.15 (s, 3H, Me), 2.40 (s, 6H, Me), 3.35 (m, 4H, Al), 3.45 (m, 8H, Al), 6.80 (s, 2H, Ar), 6.85 (t, (J_{HH} = 7.74Hz), 2H, Ar), 7.05 (d, (J_{HH} = 8.38Hz), 2H, Ar), 7.30 (t, 2H, Ar) and 7.50 (dd, (J_{HH} = 1.45 + 7.99Hz), 2H, Ar). ^{13}C-NMR (250 MHz, $CDCl_3$): δ 19.86, 22.24, 47.73, 48.50, 53.63, 118.21, 119.26, 119.85, 120.98, 124.83, 131.18, 131.93, 138.99, 141.88 and 143.29. IR (KBr disc, cm^{-1}): 1601, 1522, 1357, 1261, 1206, 1152, 1083 and 1033. Mass spectrum: molecular ion peak at *m/z* 555.

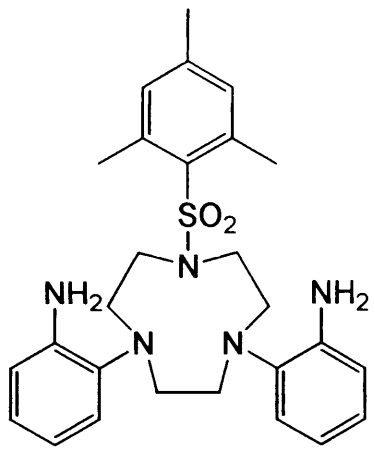

Mono 1-(2-mesitylsulphonylphenyl) bis 4, 7-(2-aminophenyl) 1, 4, 7-triazacyclononane. (L^7)

L^7 (100mg, 0.19mmol) was dissolved in a THF:MeOH solution (40:1ml), in a 250ml round bottomed Schlenk. The THF used was of HPLC grade, and the catalyst washed on a sinter with methanol, (Pt/C (50mg). CAUTION: minimum contact with methanol was exercised as in one incident a small fire occurred, and so the catalyst was added below the surface of the THF:MeOH solution with a pipette. The Schlenk was evacuated and backfilled with hydrogen gas. This was stirred for 24 hours upon which the reaction was signalled by a colour change from yellow to clear. The desired compound was filtered off via a cannula equipped with glass fibre filter tip, into another Schlenk which was then dried *in vacuo*. This afforded a clear solid. Yield 77mg, 91%. ^{1}H-NMR (400 MHz, $CDCl_3$): δ 2.20 (s, 3H, Me), 2.50 (s, 6H, Me), 3.20 (s, 4H, Al), 3.35 (m, 8H, Al), 4.0-4.20 (br d, 4H, NH_2), 6.55 (m, 4H, Ar), 6.80 (dt, (J_{HH} = 1.16 + 15.21Hz), 2H, Ar), 6.85 (s, 2H, Ar) and 6.95 (d, (J_{HH} = 6.81Hz), 2H, Ar). ^{13}C-NMR (250 MHz, $CDCl_3$): δ 19.85, 22.37, 50.88, 54.95, 55.05, 114.71, 117.68, 122.77, 124.09, 131.89, 131.83, 138.98, 139.85, 141.39 and 141.54. IR (KBr disc, cm^{-1}): 3434, 2962, 1606, 1497, 1456, 1316, 1261, 1148, 1100 and 1027. Mass spectrum: molecular ion peak at *m/z* 495.

Synthesis of metal complexes of general formula $[(L^7)M](ClO_4)_2.x(MeCN)$, M=Ni, Cu, Zn, Cd and Hg.

$[(L^7)Ni.MeCN](ClO_4)_2.MeCN$

The L^7 (77mg, 0.156mmol) was transferred directly into another Schlenk via filter cannula which contained nickel (II) perchlorate (63mg, 0.17mmol). This solution was a purple and was stirred vigorously for 18 hours. After this duration the solvent was removed *in vacuo*, and yielded a light purple precipitate. To this was added degassed ethanol (10ml), stirred vigorously then the solution allowed to settle. The solution was filtered off via cannula, again dried *in vacuo*, and produced the title compound as a lilac solid. Yield 105mg, 90%. IR (KBr disc, cm^{-1}): 3443, 1620, 1488, 1436, 1334, 1265 and 1106.

$[(L^7)Zn](ClO_4)_2$.

This compound was prepared using a similar method to that of $[(L^7)Ni](ClO_4)_2$. Zinc (II) perchlorate (63mg, 0.234mmol) was used which formed an off white precipitate. Yield 105mg, 89%. ^{1}H-NMR (400 MHz, CD_3CN): δ 2.30 (s, 3H, Me), 2.65 (s, 6H, Me), 2.95-3.10 (m, 2H, Al), 3.15-3.30 (m, 2H, Al), 3.35-3.45 (m, 4H, Al), 3.80 (m, 4H, Al), 4.95 (br d, (J_{HH} = 12.91Hz), 2H, NH_2), 5.45 (br d, (J_{HH} = 12.94Hz), 2H, NH_2), 7.20 (s, 2H, Ar), 7.35-7.50 (m, 6H, Ar), 7.65 (d, (J_{HH} = 0.90Hz), 2H, Ar). ^{13}C-NMR (400 MHz, CD_3CN): δ 19.71, 23.98, 46.06, 50.95, 55.41, 123.52, 125.59, 126.95, 127.92, 128.70, 133.19, 133.46, 141.24, 144.94 and 145.27. IR (KBr disc, cm^{-1}): 3450, 1616, 1496, 1454, 1332, 1261 and 1110.

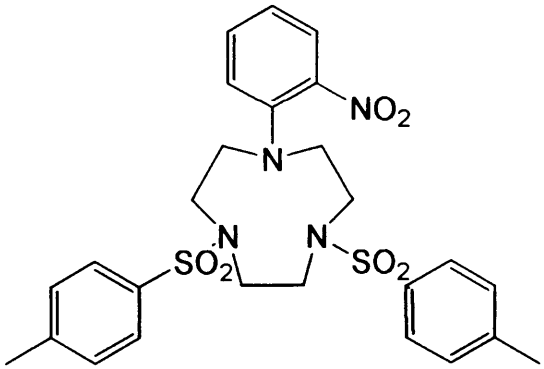

Bis 1, 4 –tosyl, mono 7-(2-nitrophenyl)-1, 4, 7-triazacyclononane $L^{8'}$

Bis 1, 4-Tosyl, 1, 4, 7-triazacyclononane (1g, 2.29mmol), fluoronitrobenzene (323mg, 2.29mmol), potassium fluoride (133mg, 2.29mmol), and acetonitrile (50ml) were all refluxed vigorously in a 100ml round bottomed flask for 24 hours. The flask was washed out with DCM (15ml). The combined washings were filtered then dried *in vacuo*. The resulting yellow oil was recrystallized with hot ethanol, which afforded a bright yellow powder ($L^{8'}$). Yield 1.17g, 92%. ^{1}H-NMR (250 MHz, $CDCl_3$): δ 2.40 (s, 6H, Me), 3.15 (s, 2H, Al), 3.20 (s, 2H, Al), 3.40 (s, 8H, Al), 6.90 (t, 1H, Ar), 7.10 (d, (J_{HH} = 8.39Hz), 1H, Ar), 7.25 (m, 4H, Ar), 7.40 (t, (J_{HH} = 8.40Hz), 2H, Ar) and 7.55 (d, (J_{HH} = 8.11Hz), 4H, Ar). ^{13}C-NMR (250 MHz, $CDCl_3$): δ 20.45, 49.65, 51.20, 54.00, 119.53, 120.49, 126.31, 128.91, 129.01, 129.49, 132.03, 133.63, 142.23 and 142.92. IR (KBr disc, cm^{-1}) 2857, 1600, 1565, 1522, 1451, 1372, 1337, 1223, 1157, 1089, 1050, 871, 840, 812, 770, 746, 711 and 694. Mass spectrum: molecular ion peak at 559 *m/z* .

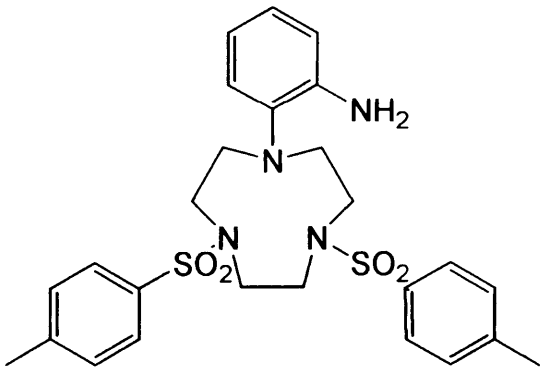

Bis 1, 4 –tosyl, mono 7-(2-aminophenyl)-1, 4, 7-triazacyclononane L^8.

$L^{8'}$ (100mg, 0.18mmol) was dissolved in a THF:MeOH solution (40:1ml), in a 250ml round bottomed Schlenk. The THF used was of HPLC grade, and the catalyst washed on a sinter with methanol, (Pt/C (50mg). CAUTION: minimum contact with methanol was exercised as in one incident a small fire occurred, and so the catalyst was added below the surface of the THF:MeOH solution with a pipette. The Schlenk was evacuated and backfilled with hydrogen gas. This was stirred for 24 hours upon which the reaction was signalled by a colour change from yellow to clear. The desired compound was filtered off via a cannula equipped with glass fibre filter tip, into another Schlenk which was then dried *in vacuo*. This afforded a clear solid (L^8). Yield 95mg, 95%. ^{1}H-NMR (250 MHz, $CDCl_3$): δ 2.30 (s 6H, Me), 3.05-3.25 (m, 4H, Al), 3.30-3.45 (m, 8H, Al), 4.20 (br s, 2H, NH_2), 6.60 (d, (J_{HH} = 6.18Hz), 1H, Ar), 6.85 (t, (J_{HH} = 6.49Hz), 1H, Ar), 7.15 (d, (J_{HH} = 7.15Hz), 1H, Ar), 7.20-7.30 (m, 5H, Ar) and 7.50-7.60 (m, 4H, Ar). ^{13}C-NMR (250 MHz, $CDCl_3$): δ 39.42, 52.05, 53.01, 53.81, 114.68, 117.38, 123.38, 124.62, 126.18, 128.82, 133.74, 138. 75, 142.72 and 143.01. IR (KBr disc, cm^{-1}) 3446, 3369, 1596, 1500, 1336, 1260, 1159, 1090 and 1024. Mass spectrum: molecular ion peak at *m/z* 530.

Synthesis of metal complexes of general formula $[(L^8)M](ClO_4)_2.x(MeCN)$, M=Ni, Cu, Zn, Cd and Hg.

$[(L^8)Ni](ClO_4)_2$.

The solution of L^8 (95mg, 0.18mmol) was transferred directly into another Schlenk via filter cannula which contained nickel (II) perchlorate (72mg, 0.2mmol). This solution was off white and was stirred vigorously for 18 hours. After this duration the solvent was removed *in vacuo*, and yielded an off-white precipitate. To this was added degassed ethanol (10ml), stirred vigorously then the solution allowed to settle. The solution was filtered off via cannula, again dried *in vacuo*, and produced the title compound as an off-white solid. Crystals of X-Ray quality were grown by slow vapour diffusion of diethyl ether into an acetonitrile solution. Yield 148mg, 92%. IR (KBr disc, cm^{-1}): 3388, 1622, 1261, 1095, 1019 and 801.

$[(L^8)Cu](ClO_4)_2$.

This compound was prepared using a similar method to that of $[(L^8)Ni](ClO_4)_2$. Copper (II) perchlorate (53mg, 0.2mmol) was used which formed a purple precipitate. Crystals of X-Ray quality were grown by slow vapour diffusion of diethyl ether into an acetonitrile solution. Yield 146mg, 86%. IR (KBr disc, cm^{-1}): 3465, 1261, 1150, 1089 and 1019.

$[(L^8)Zn](ClO_4)_2$.

This compound was prepared using a similar method to that of $[(L^8)Ni](ClO_4)_2$. Zinc (II) perchlorate (73mg, 0.2mmol) was used which formed an off white precipitate. Yield 142mg, 88%. ^{1}H-NMR (400 MHz, CD_3CN): δ 2.30 (s, 6H, Me), 3.05-3.80 (m, 12H, Al), 4.30-4.95 (br s, 2H, NH_2), 7.05 (m, 4H, Ar), 7.30 (d, (J_{HH} = 7.99Hz), 2H, Ar) and 7.60 (d, (J_{HH} = 8.14Hz), 4H, Ar). ^{13}C-NMR (100 MHz, CD_3CN): δ 20.13, 57.19, 57.86, 58.29, 120.85, 123.52, 125.42, 126.05, 126.35, 126.82, 127.07, 129.50, 134.16 and 143.79. IR (KBr disc, cm^{-1}): 3542, 1652, 1496, 1452, 1336, 1261, 1157, 1089 and 1022.

[(L^8)Cd](ClO$_4$)$_2$.

This compound was prepared using a similar method to that of [(L^8)Ni](ClO$_4$)$_2$. Cadmium (II) perchlorate (82mg, 0.2mmol) was used which formed an off white precipitate. Yield 146mg, 86%. ^{1}H-NMR (400 MHz, CD_3CN): δ 2.40 (s, 6H, Me), 3.15 (m, 2H, Al), 3.30 (m, 2H, Al), 3.65 (m, 8H, Al), 4.20-4.75 (br s, 2H, NH_2), 7.40 (d, (J_{HH} = 10.67Hz), 4H, Ar), 7.45 (m, 2H, Ar) and 7.70 (d, (J_{HH} = 11.06Hz), 4H, Ar). ^{13}C-NMR (400 MHz, CD_3CN): δ 46.44, 51.11, 51.55, 54.56, 120.38, 124.14, 126.01, 126.90, 129.58, 129.69, 132.94, 138.32, 143.94 and 144.21. IR (KBr disc, cm^{-1}): 3433, 1329, 1261, 1159, 1089 and 1031.

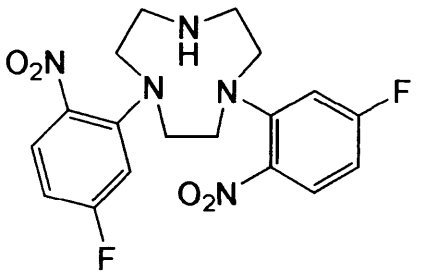

1, 4-bis (2-nitro, 5-fluorophenyl) 1, 4, 7-triazacyclononane.

1, 4, 7 - Triazacyclononane (0.5g, 3.88mmol), 2, 4-difluoronitrobenzene (1.29g, 8.11mmol), K_2CO_3 (1.12g, 8.11mmol), and MeCN (30ml) were all stirred vigorously in a round bottomed flask at 110°C for 24 hours under a nitrogen atmosphere. The flask was washed with DCM (30ml). The combined washings were dried *in vacuo*. An orange solid was afforded. This solid was dissolved in $CHCl_3$ (50ml), and washed with 4M HCl (3 × 70ml). The aqueous extracts were combined and basified with 1M NaOH until the pH 12 was reached. This aqueous solution was washed with $CHCl_3$ (150ml), and the organic extract dried $MgSO_4$. This was filtered and dried *In Vacuo*. This afforded an orange oil which after recrystallisation with hot ethanol afforded an orange solid. Yield 97%, 1.53g. ^{1}H NMR: (400 MHz, $CDCl_3$) δ 2.80 (t, (J_{HH} = 4.83Hz), 4H, Al), δ 3.30

(t, (J_{HH} = 4.85Hz), 4H, Al), δ 3.50 (s, 4H, Al), δ 6.40 (m, 2H, Ar), δ 6.60 (dd, (J_{HH} = 2.38 +11.95Hz), 2H, Ar), δ 7.60 (m, 2H, Ar). ^{13}C NMR: (400 MHz, $CDCl_3$) δ 45.53, 51.77, 54.21, 103.48, 104.07, 127.13, 136.54, 144.01, and 163.49 (J_{CF} = 1008Hz). ^{19}F-NMR ($CDCl_3$): δ - 102.83. IR: (KBr disc, cm^{-1}) 3092, 2843, 1568, 1491, 1430, 1385, 1347, 1305, 1251, 1170, 1151, 1130, 1119, 1083, 1011, 887, 842, 835, 812, 796, 748, and 716. E.I.-MS m/z 408.0 (M^++H^+)

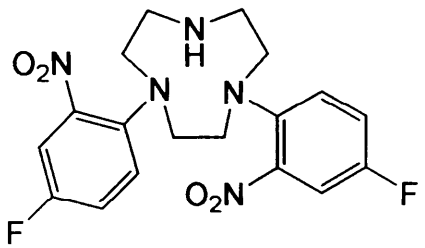

1, 4 bis - (2-nitro, 4-fluorophenyl) -, 1, 4, 7- triazacyclononane.

1, 4, 7- triazacyclononane (0.1g, 0.78mmol), 2, 5-difluoronitrobenzene (0.26g, 1.64mmol), K_2CO_3 (0.22g, 1.59mmol), and MeCN (15ml) were all stirred vigorously in a pressure tube at 85°C for 24 hours. The tube was washed with DCM (15ml). The combined washings were dried *in vacuo*. An orange crystalline solid was afforded, which was recrystallized with hot ethanol. Crystals of X-ray quality were grown by slow vapour diffusion of diethyl ether into an acetonitrile solution. Yield 26%, 81mg. ^{1}H NMR: (400 MHz, $CDCl_3$) δ 3.00 (s, 4H, Aliphatic), δ 3.30 (s, 4H, Al), δ 3.35 (m, 4H, Al), δ 7.05-7.20 (m, 2H, Ar), δ 7.25 (m, 2H, Ar), δ 7.40 (m, 2H, Ar). ^{13}C NMR: (400 MHz, $CDCl_3$) δ 49.11, 54.93, 56.73, 112.49, 120.28, 124.19, 141.56, 143.04, and 156.23 (J_{CF} = 1216Hz). ^{19}F NMR: (300 MHz, $CDCl_3$) δ -121.18. IR: (KBr disc, cm^{-1}) 3419, 2962, 1575, 1538, 1533, 1354, 1264, 1222, 1195, 1163, 1130, 1099, and 1032. E.I.-MS m/z 408.0 (M^++H^+)

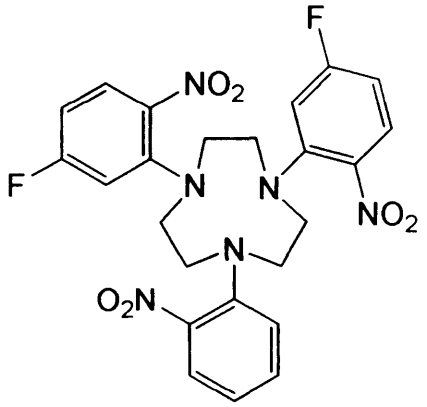

1-(2-nitrophenyl), 4, 7- bis (2-nitro, 5-fluorophenyl), 1, 4, 7, triazacyclononane.

1, 4-bis (2-nitro, 5-fluorophenyl), 1, 4, 7, triazacyclononane (0.2g, 0.49mmol), 2-fluoronitrobenzene (83mg, 0.59mmol), potassium fluoride (30mg, 0.52mmol), and MeCN (30ml) were all stirred vigorously in a pressure tube for 24 hours at 85°C. The tube was washed with DCM (15ml), filtered to remove the potassium fluoride and the resulting solution was dried *in vacuo*. Yield 107mg, 41%. ^{1}H NMR: (400 MHz, $CDCl_3$) δ 3.35 (m, 4H, Al), δ 3.40 (m, 4H, Al), δ 3.50 (s, 4H, Al), δ 6.80 (t, (J_{HH} = 2.85Hz), 1H, Ar), δ 7.00 (d, (J_{HH} = 4.30Hz), 1H, Ar), δ 7.10 (m, 1H, Ar), δ 7.20-7.25 (m, 2H, Ar), δ 7.35 (m, 2H, Ar), δ 7.40 (m, 2H, Ar), δ 7.95 (m, 1H, Ar). ^{13}C NMR: (400 MHz, $CDCl_3$) δ 48.63, 53.47, 55.90, 104.90, 105.77, 107.53, 122.21, 125.73, 128.94, 133.34, 136.99, 145.69, 145.69, 146.44, and 165.18 (J_{CF} = 1008Hz). ^{19}F-NMR ($CDCl_3$): δ - 102.64. IR: (KBr disc, cm^{-1}) 3087, 2927, 1617, 1565, 1515, 1430, 1346, 1305, 1244, 1180, 1130, 1119, 1082, 1011, 835, 796, 746 and 709. E.I.-MS m/z 529.0 (M^{+}+H^{+})

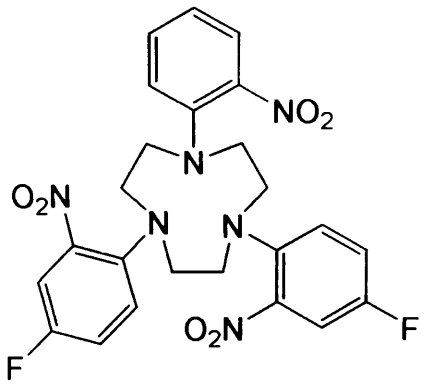

1-(2-nitrophenyl), 4, 7-(bis 2-nitro, 4-fluorophenyl), 1, 4, 7-triazacyclononane.

1, 4-bis 2-nitro, 4-fluorobenzene, 1, 4, 7- triazacyclononane (0.01g, 0.02mmol), fluoronitrobenzene (3.8mg, 0.02mmol), K_2CO_3 (4mg, 0.02mmol), and MeCN (15ml) were all stirred vigorously in a pressure tube at 85°C for 24 hours. The tube was washed with DCM (15ml). The combined washings were dried *in vacuo*. An orange solid was afforded. This was recrystallized with hot ethanol. Yield 5.9mg, 45%. ^{1}H NMR: (400 MHz, $CDCl_3$) δ 3.30 (m, 4H, Al), δ 3.40 (m, 4H, Al), δ 3.50 (s, 4H, Al), δ 6.85 (t, (J_{HH} = 2.92Hz), 1H, Ar), δ 7.05 (d, (J_{HH} = 4.18Hz), 1H, Ar), δ 7.15-7.25 (m, 2H, Ar), δ 7.30 (m, 2H, Ar), δ 7.50 (m, 2H, Ar), δ 8.00 (m, 2H, Ar). ^{13}C NMR: (400 MHz, $CDCl_3$) δ 55.03, 55.74, 55.82, 112.49, 118.36, 118.56, 120.47, 124.60, 126.18, 133.16, 135.58, 135.66, 142.11, and 156.08 (J_{CF} = 1444Hz). ^{19}F NMR: (300 MHz, $CDCl_3$) δ -117.39. IR: (KBr disc, cm^{-1}) 3106, 2926, 1573, 1538, 1349, 1269, 1222, and 1165. E.I.-MS m/z 529.0 (M^++H^+)

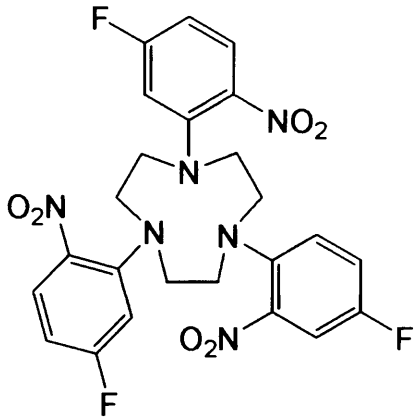

1-(2-nitro, 4-fluorophenyl), 4, 7-bis (2-nitro, 5-fluorophenyl), 1, 4, 7-triazacyclononane.

1, 4-bis 2-nitro, 5-fluorophenyl, 1, 4, 7- triazacyclononane (0.2g, 0.49mmol), 2, 5-difluoronitrobenzene (94mg, 0.59mmol), K_2CO_3 (72mg, 0.52mmol), and MeCN (15ml) were all stirred vigorously in a pressure tube at 85°C for 24 hours. The tube was washed out with DCM (15ml). The combined washings were dried *in vacuo*. Initially the product was recrystallized with chloroform and diethyl ether. The removal of the yellow by product was then followed with a second Recrystallisation of hot methanol. A yellow/orange crystalline powder was afforded. Yield 99%, 265mg. ^{1}H NMR: (400 MHz, $CDCl_3$) δ 3.35 (m, 4H, Aliphatic), δ 3.50 (m, 4H, Al), δ 3.65 (s, 4H, Al), δ 6.55 (m, 2H, Ar), δ 6.60 (dd, (J_{HH} = 2.37 + 11.61Hz), 2H, Ar), δ 6.70 (dd, (J_{HH} = 2.41 + 11.52Hz), 1H, Ar), δ 7.10 (m, 1H, Ar), δ 7.30 (m, 1H, Ar), δ 7.60 (m, 2H, Ar). ^{13}C NMR: (400 MHz, $CDCl_3$) δ 53.89, 54.64, 56.12, 105.77, 106.24, 107.42, 111.29, 121.63, 125.94, 128.77, 140.03, 145.83, 146.50, 158.62 and 166.34. ^{19}F NMR: (300 MHz, $CDCl_3$) δ -115.81. IR: (KBr disc, cm^{-1}) 2962, 1624, 1565, 1512, 1342, 1302, 1243, 1153, 1079, and 1014. E.I.-MS m/z 547.0 (M^++H^+)

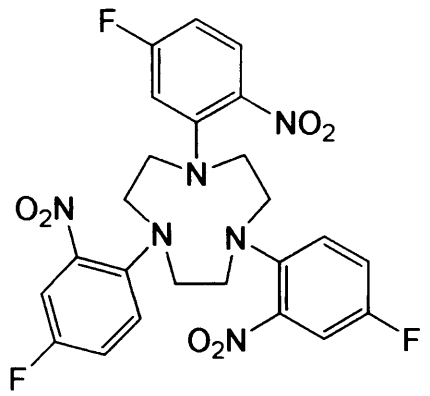

1-(2-nitro, 5-fluorophenyl), 4, 7-bis (2-nitro, 4-fluorophenyl), 1, 4, 7-triazacyclononane.

1, 4-bis 2-nitro, 4-fluorophenyl, 1, 4, 7- triazacyclononane (0.2g, 0.49mmol), 2, 4-difluoronitrobenzene (94mg, 0.59mmol), K_2CO_3 (72mg, 0.52mmol), and MeCN (15ml) were all stirred vigorously in a pressure tube at 85°C for 24 hours. The tube was washed out DCM (15ml). The combined washings were dried *in vacuo*. An orange crystalline powder was afforded. Yield 99%, 265mg. ^{1}H NMR: (400 MHz, $CDCl_3$) δ 3.25 (s, 4H, Al), δ 3.45 (m, 4H, Al), δ 3.55 (m, 4H, Ar), δ 6.40 (m, 1H, Ar), δ 6.60 (dd, (J_{HH} = 2.49 + 11.66Hz), 1H, Ar), δ 6.95 (m, 1H, Ar), δ 7.05-7.15 (m, 2H, Ar), δ 7.30 (dd, (J_{HH} = 3.00 + 7.59Hz), 2H, Ar), δ 7.60 (m, 2H, Ar). ^{13}C NMR: (400 MHz, $CDCl_3$) δ 54.46, 55.44, 56.38, 105.29, 105.55, 106.43, 112.25, 120.43, 126.33, 129.06, 142.12, 144.75, 146.17, 157.11 (J_{CF} = 980Hz), and 165.25 (J_{CF} = 1008Hz). ^{19}F NMR: (300 MHz, $CDCl_3$) δ - 117.24. IR: (KBr disc, cm^{-1}) 3087, 2916, 1621, 1533, 1520, 1445, 1415, 1339, 1282, 1240, 1223, 1187, 1160, 1072, 1034, 1008, 900, 873, 839, 806, 746, and 714. E.I.-MS m/z 547.0 (M^++H^+)

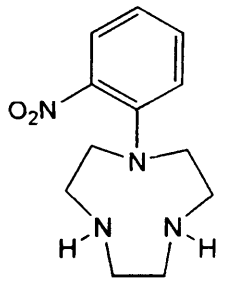

1-mono (2-nitrophenyl)- 1, 4, 7- triazacyclononane.

1, 4, 7- triazacyclononane (0.3g, 2.3mmol), 2-fluoronitrobenzene (0.328g, 2.3mmol), K_2CO_3 (0.321g, 2.3mmol), and MeCN (40ml) were all stirred vigorously in a round bottomed flask at 95°C for 24 hours. The flask was washed out DCM (25ml). The combined washings were filtered and dried *in vacuo*. The orange residue was taken up in chloroform (30ml) and washed with distilled water (3 × 40ml). The organic layer was dried ($MgSO_4$), filtered and dried *in vacuo*. Red coloured oil was afforded which was then purified by acid extraction (4M HCl). The solution was washed with dichloromethane (3 × 50ml), NaOH was added and basified to pH 12, and extracted with $CHCl_3$ (3 × 50ml). This was dried with $MgSO_4$, filtered, and dried *in vacuo*, which then afforded the desired compound as an orange coloured oil. Yield 81%, 489mg. ^{1}H NMR: (400 MHz, $CDCl_3$) δ 2.70 (s, 4H, Aliphatic), δ 2.80 (t, (J_{HH} = 2.40Hz), 4H, Al), δ 3.35 (t, (J_{HH} = 2.35Hz), 4H, Al), δ 6.75 (m, 1H, Ar), δ 7.10 (d, (J_{HH} = 8.39Hz), 1H, Ar), δ 7.30 (m, 1H, Ar), δ 7.50 (d, (J_{HH} = 6.50Hz), 1H, Ar). ^{13}C NMR: (400 MHz, $CDCl_3$) δ 46.90, 48.71, 53.91, 118.19, 120.06, 124.79, 131.79, 141.27, and 143.03. IR: (KBr disc, cm^{-1}) 2964, 1522, 1362, 1260, 1095, 802 and 706. E.I.-MS m/z 250.0 (M^++H^+)

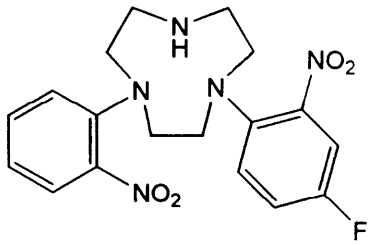

1-(2-nitro, 4-fluorophenyl), 4-(2-nitrophenyl), 1, 4, 7- triazacyclononane.

1-(2-nitrophenyl)- 1, 4, 7- triazacyclononane (469mg, 1.88mmol), 2, 5-difluoronitrobenzene (283mg, 1.78mmol), K_2CO_3 (246mg, 1.78mmol), and MeCN (30ml) were all stirred vigorously in a round bottomed flask at 95°C for 24 hours. The flask was washed out DCM (20ml). The combined washings were filtered then dried *in vacuo*. The resulting orange oil was taken up in chloroform (30ml) and washed with distilled water (3 × 40ml). The organic layer was dried ($MgSO_4$), filtered, and dried *in vacuo*. Recrystallisation with hot ethanol afforded an orange crystalline powder. Yield 26%, 185mg. ^{1}H NMR: (400 MHz, $CDCl_3$) δ 3.30 (s, 4H, Al), δ 3.40 (m, 4H, Al), δ 3.50 (m, 4H, Al), δ 6.90 (t, (J_{HH} = 7.33Hz), 1H, Ar), δ 7.05 (d, (J_{HH} = 2.92Hz), 1H, Ar), δ 7.10 (m, 1H, Ar), δ 7.15 (m, H, Ar), δ 7.20 (d, (J_{HH} = 4.01 Hz), H, Ar), δ 7.25 (dd, (J_{HH} = Hz), 1H, Ar), 7.35 (t, (J_{HH} = Hz) , 1H, Ar), 7.55 (dd, (J_{HH} = 1.55 + 8.07 Hz), 1H, Ar). ^{13}C NMR: (400 MHz, $CDCl_3$) δ 53.98, 54.52, 54.77, 111.74, 112.02, 119.91, 120.40, 121.01, 125.25, 125.62, 133.31, 141.37, 142.83, 143.82, and 155.63 (J_{CF} = 964 Hz). ^{19}F NMR: (300 MHz, $CDCl_3$) δ - 118.18. IR: (KBr disc, cm^{-1}) 2965, 2913, 2850, 1604, 1560, 1533, 1440, 1355, 1335, 1297, 1263, 1222, 1166, 1105, 1048, 873, 807, 735, and 709. E.I.-MS m/z 390.0 (M^++H^+)

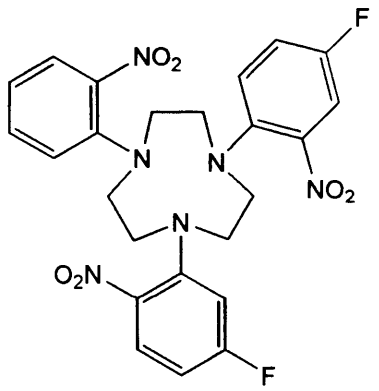

1-(2-nitro, 4-fluorophenyl), 4-(2-nitrophenyl), 7-(2-nitro, 5-fluorophenyl) 1, 4, 7- triazacyclononane.

1-(2-nitro, 4-fluorophenyl), 4-(2-nitrophenyl), 1, 4, 7- triazacyclononane (150mg, 0.39mmol), 2, 4-difluoronitrobenzene (61mg, 0.38mmol), K_2CO_3 (56mg, 0.41mmol), and MeCN (30ml) were all stirred vigorously in a pressure tube at 90°C for 24 hours. The flask was washed out with DCM (15ml). The combined washings were filtered then dried *in vacuo*. The resulting orange oil was taken up in chloroform (15ml) and washed with distilled water (3 × 25ml). The organic layer was dried ($MgSO_4$), filtered, and dried *in vacuo*. Recrystallisation with hot ethanol afforded an orange crystalline powder. Yield 33%, 66mg. ^{1}H NMR: (400 MHz, $CDCl_3$) δ 3.20 (s, 4H, Al), δ 3.30 (m, 4H, Al), δ 3.40 (m, 4H, Al), δ 6.85 (m, 1H, Ar), δ 7.05 (m 1H, Ar), δ 7.10 (m 1H, Ar), δ 7.13 (m 1H, Ar), δ 7.15 (m 1H, Ar), δ 7.17 (m 1H, Ar), δ 7.20 (m 1H, Ar), δ 7.30 (m 1H, Ar), δ 7.35 (m 1H, Ar), δ 7.55 (dd, (J_{HH} = 1.55 + 8.06 Hz), 1H, Ar). ^{13}C NMR: (500 MHz, $CDCl_3$) δ 53.82, 54.13, 54.88, 111.23, 111.44, 119.41, 119.44, 119.52, 119.61, 119.62, 120.27, 124.83, 124.89, 124.96, 132.11, 141.12, 141.14, 141.58, 143.16, 143.23, 143.56, 154.79 and 156.75 (J_{CF}=980Hz). ^{19}F NMR: (300 MHz, $CDCl_3$) δ -118.19. IR: (KBr disc, cm^{-1}) 2917, 1605, 1533, 1520, 1439, 1411, 1355, 1339, 1295, 1263, 1222, 1166, 1101, 1050, 1030, and 1000. E.I.-MS m/z 529.0 (M^++H^+)

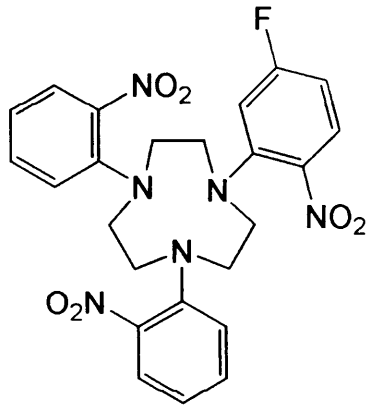

1-(2-nitro, 5-fluorobenzene), 4, 7-bis 2-nitrobenzene, 1, 4, 7-triazacyclononane ($L^{9'}$).

1, 4 – bis (2-nitrobenzene), 1, 4, 7- triazacyclononane (0.1g, 0.27mmol), 2, 4-difluoronitrobenzene (64mg, 0.4mmol), K_2CO_3 (17mg, 0.29mmol), and MeCN (15ml) were all stirred vigorously in a pressure tube at 85°C for 24 hours. The tube was washed out DCM (15ml). The combined washings were dried *in vacuo*. This was recrystallised with hot ethanol, a fluffy orange solid was afforded ($L^{9'}$). Yield 64%, 87mg. ^{1}H NMR: (400 MHz, $CDCl_3$) δ 3.35 (s, 4H, Al), δ 3.50 (m, 8H, Al), δ 6.45 (m, 1H, Ar), δ 6.60 (dd, (J_{HH} = 2.56 + 11.58 Hz), 1H, Ar), δ 6.85 (t, (J_{HH} = 7.25 Hz), 2H, Ar), δ 7.05 (d, (J_{HH} = 0.80 Hz), 2H, Ar), δ 7.30 (t, (J_{HH} = 1.14 Hz), 2H, Ar), δ 7.50 (dd, (J_{HH} = 1.68 Hz) + 8.08, 2H, Ar), δ 7.60 (m, 1H, F). ^{13}C NMR: (400 MHz, $CDCl_3$) δ 54.16, 54.49, 55.38, 106.34, 106.70, 121.43, 122.42, 125.86, 129.09, 133.28, 137.30, 143.37, 144.78, 146.32, and 165.23 (J_{CF} = 1012Hz). ^{19}F-NMR ($CDCl_3$): δ - 103.41. IR: (KBr disc, cm^{-1}) 3460, 2978, 2920, 1622, 1560, 1509, 1438, 1339, 1294, 1259, 1244, 1156, 1073, 869, 851, 797, 771, 733, and 707. E.I.-MS m/z 511.0 (M^++H^+)

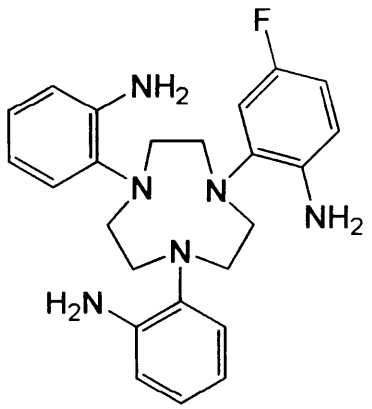

1-(2-amino, 5-fluorobenzene), 4, 7-bis aminobenzene, 1, 4, 7-triazacyclononane. (L^9)

$L^{9'}$ (250mg, 0.46mmol) was dissolved in a THF:MeOH solution (60:1ml), in a 250ml round bottomed Schlenk. The THF was of HPLC grade, and the catalyst washed on a sinter with methanol, (Pt/C (75mg). CAUTION: Minimum contact with methanol was exercised as in one incident a small fire occurred, and so the catalyst was added below the surface of the THF:MeOH solution with a pipette, as a methanol slurry. The Schlenk was evacuated and backfilled with hydrogen gas. This was stirred for 24 hours upon which the reaction was signalled by a colour change of yellow to a clear solution. The desired compound was filtered off via a cannula equipped with glass fibre filter tip, into another Schlenk which was then dried *in vacuo*. This afforded a clear solid (L^9). Degradation of the ligand was seen by the product being a pink/red colour, thus generating an unusable sample. Yield 190mg, 92%. ^{1}H NMR: (400 MHz, $CDCl_3$) δ 3.30 (m, 12H, Aliphatic), δ 4.00 (s Br, 6H, NH_2), δ 6.50 (m, 2H, Ar), δ 6.60 (m, 4H, Ar), δ 6.70 (m, 1H, Ar), δ 6.80 (m, 2H, Ar) δ 7.05 (d, 2H, (J_{HH} = 7.28 Hz), Ar). ^{13}C NMR: (250 MHz, $CDCl_3$) δ 55.00, 56.27, 56.55, 109.62, 109.92, 110.60, 110.87, 115.82, 115.85, 115.97, 118.78, 123.21, 124.95, 138.20, 141.85 (J_{CF} = 302Hz). ^{19}F NMR: (300 MHz, $CDCl_3$) δ -124.73. IR: (KBr disc, cm^{-1}) 3434, 2963, 1606, 1497, 1450, 1260, 1095, 1018, 863, 802, 707 and 660. E.I.-MS m/z 421.0 (M^++H^+)

Synthesis of metal complexes of the general formula $[(L^9)M](ClO_4)_2$. M=Mn and Zn.

$[(L^9)Mn](ClO_4)_2$.

The solution of L^9 (80mg, 1.9mmol) was transferred directly into another Schlenk via filter cannula which contained manganese (II) perchlorate (76mg, 2.1mmol). This solution was a cream colour and was stirred vigorously for 1 hour. After this duration the solvent was removed *in vacuo*, and yielded an off-white precipitate. To this was added degassed ethanol (10ml), stirred vigorously then the solution allowed to settle. The solution was filtered off via cannula, again dried *in vacuo*, and produced the title compound as an off-white solid. Crystals of X-Ray quality were grown by slow vapour diffusion of diethyl ether into an acetonitrile solution. Yield 104mg, 81%. IR: (KBr disc, cm^{-1}) 3427, 3299, 3233, 1617, 1506, 1463, 1261, 1095, 1018 and 802.

$[(L^9)Zn](ClO_4)_2$.

This compound was synthesised in the same manner as $[(L^9)Mn](ClO_4)_2$. Zinc (II) perchlorate (77mg, 2.1mmol), was added and formed a white precipitate. Crystals of X-Ray quality were grown by slow vapour diffusion of diethyl ether into an acetonitrile solution. Yield 99mg, 78%. ^1H NMR: (400 MHz, CD_3CN) δ 3.05 (m, 16H, Aliphatic), δ 3.70 (m, 6H, Aliphatic), δ 4.70 (s Br, 6H, NH_2), δ 7.10 (m, 1H, Ar), δ 6.60 (m, 4H, Ar), δ 7.25 - 7.35 (m, 4H, Ar), δ 7.40 - 7.50 (m, 4H, Ar) δ 7.65 (d, 2H, (J_{HH} = 7.69 Hz), Ar). ^{13}C NMR: (250 MHz, CD_3CN) δ 53.04, 53.10, 53.19, 111.54, 112.64, 114.95, 115.09, 124.97, 127.38, 127.92, 128.94, 129.96, 133.52, 146.50, 148.01 and 149.00 (J_{CF} = 988Hz). ^{19}F NMR: (300 MHz, CD_3CN) δ -112.76. IR: (KBr disc, cm^{-1}) 3433, 3305, 1465, 1383, 1369, 1267, 1234, 1110, 859, 762 and 731.

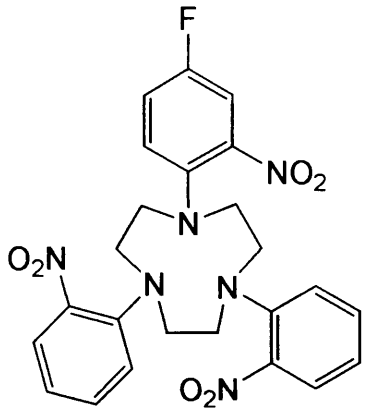

1-(2-nitro, 4-fluorophenyl), 4, 7-bis (2- nitrophenyl), 1, 4, 7-triazacyclononane.

1, 4-bis nitrobenzene, 1, 4, 7- triazacyclononane (0.05g, 0.13mmol), 2, 5-difluoronitrobenzene (23mg, 0.14mmol), K_2CO_3 (195mg, 0.14mmol), and MeCN (15ml) were all stirred vigorously in a pressure tube at 85°C for 24 hours. The tube was washed with DCM (15ml). The combined washings were dried *in vacuo*. An orange solid was afforded. This was recrystallized with hot ethanol. Yield 37%, 25mg. ^{1}H NMR: (400 MHz, $CDCl_3$) δ 3.35 (m, 4H, Aliphatic), δ 3.45 (m, 4H, Al), δ 3.50 (s, 4H, Al), δ 6.85 (t, (J_{HH} = 7.17Hz), 2H, Ar), δ 7.05 (d, (J_{HH} = 7.92Hz), 2H, Ar), δ 7.10 (m, 1H, Ar), δ 7.20 (m, 1H, Ar), δ 7.25 (m, 1H, Ar), δ 7.35 (m, 2H, Ar) , δ 7.55 (dd, (J_{HH} = 1.55 + 8.08Hz), 2H, Ar). ^{13}C NMR: (400 MHz, $CDCl_3$) δ 54.87, 54.95, 55.55, 112.26, 112.53, 120.49, 120.73, 121.18, 126.01, 126.53, 126.61, 133.10, 133.19, 142.59, 143.91 and 144.50 (J_{CF} = 994Hz). ^{19}F-NMR ($CDCl_3$): δ -120.65. IR: (KBr disc, cm^{-1}) 2911, 1606, 1560, 1509, 1339, 1296, 1260, 1223, 1168, 1103, and 1051. E.I.-MS m/z 511.0 (M^++H^+)

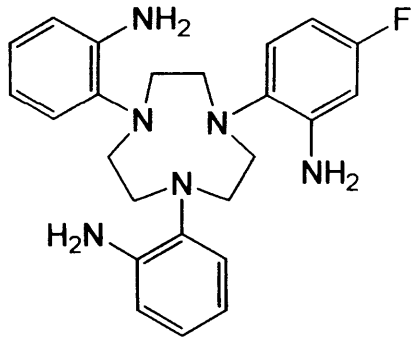

1-(2-amino, 4-fluorobenzene), 4, 7-bis aminobenzene, 1, 4, 7-triazacyclononane (L^{10}).

$L^{10'}$ (250mg, 0.46mmol) was dissolved in a THF:MeOH solution (60:1ml), in a 250ml round bottomed Schlenk. The THF was of HPLC grade, and the catalyst washed on a sinter with methanol, (Pt/C (75mg). CAUTION: Minimum contact with methanol was exercised as in one incident a small fire occurred, and so the catalyst was added below the surface of the THF:MeOH solution with a pipette, as a methanol slurry. The Schlenk was evacuated and backfilled with hydrogen gas. This was stirred for 24 hours upon which the reaction was signalled by a colour change of yellow to a clear solution. The desired compound was filtered off via a cannula equipped with glass fibre filter tip, into another Schlenk which was then dried *in vacuo*. This afforded a clear solid. Yield 188mg, 91%. ^{1}H NMR: (400 MHz, $CDCl_3$) δ 3.35 (s, 12H, Aliphatic), δ 4.05 (s Br, 6H, NH_2), δ 6.55 (m, 2H, Ar), δ 6.60 (m, 4H, Ar), δ 6.75 (m, 1H, Ar), δ 6.85 (m, 2H, Ar) δ 7.00 (d, 2H, (J_{HH} = 7.35 Hz), Ar). ^{13}C NMR: (250 MHz, $CDCl_3$) δ 56.12, 56.98, 57.13, 109.13, 109.89, 110.89, 111.43, 115.23, 115.92, 116.27, 117.79, 121.66, 124.55, 139.58 and 140.94 (J_{CF} = 880Hz). ^{19}F NMR: (300 MHz, $CDCl_3$) δ -123.49. IR: (KBr disc, cm^{-1}) 3450, 3335, 1611, 1497, 1441, 1325, 1299, 1261, 1192, 1144, 1095, 1028, 798 and 747. E.I.-MS m/z 421.0 (M^++H^+)

Synthesis of metal complexes of the general formula $[(L^{10})M](ClO_4)_2$. M=Mn and Zn.

$[(L^{10})Mn](ClO_4)_2$.

The solution of L^{10} (80mg, 1.9mmol) was transferred directly into another Schlenk via filter cannula which contained manganese (II) perchlorate (76mg, 2.1mmol). This solution was a blue colour and was stirred vigorously for 1 hour. After this duration the solvent was removed *in vacuo*, and yielded a blue precipitate. To this was added degassed ethanol (10ml), stirred vigorously then the solution allowed to settle. The solution was filtered off via cannula, again dried *in vacuo*, and produced the title compound as a blue solid. Yield 98mg, 79%. IR: (KBr disc, cm^{-1}) 3444, 1652, 1506, 1261, 1095, 1025, 802 and 621. UV/Vis (MeCN, nm ($\varepsilon/dm^3\ mol^{-1}\ cm^{-1}$)): 604 (359).

$[(L^{10})Zn](ClO_4)_2$.

This compound was synthesised in the same manner as $[(L^{10})Mn](ClO_4)_2$. Zinc (II) perchlorate (77mg, 2.1mmol), was added and formed a white precipitate. Yield 95mg, 75%. ^1H NMR: (400 MHz, CD_3CN) δ 3.05 (m, 6H, Aliphatic, *Endo*), δ 3.70 (m, 6H, Aliphatic, *Exo*), δ 4.20 (s Br, 4H, NH_2), δ 4.75 (s Br, 2H, NH_2), δ 7.10 (dd, (J_{HH} = 2.92 + 8.98Hz), 2H, Ar), δ 7.20 (m, 2H, Ar), δ 7.35 (m, 1H, Ar), δ 7.45 (m, 2H, Ar) δ 7.60-7.70 (m, 4H, Ar). ^{13}C NMR: (250 MHz, CD_3CN) δ 53.12, 54.35, 54.89, 111.23, 112.50, 114.63, 115.38, 124.62, 127.41, 127.89, 128.66, 130.41, 132.62, 146.22, 148.35 and 149.22 (J_{CF} = 996Hz). ^{19}F NMR: (300 MHz, CD_3CN) δ -113.98. IR: (KBr disc, cm^{-1}) 3463, 3305, 1611, 1575, 1497, 1370, 1261, 1095, 919, 810, 768, 739, 702 and 624.

Porphyrin analogues and complexes.

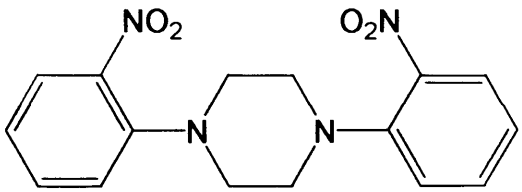

***N, N'* bis (2-nitrophenyl) 1, 4-diazacyclohexane.**

Piperizene (2.0g, 23.3mmol), 2 - fluoronitrobenzene (6.72g, 47.7mmol), potassium fluoride (2.77g, 47.7mmol), and acetonitrile (50ml) were all stirred vigorously together in a round bottom flask, refluxed at 90°C for 36 hours and under nitrogen. The resulting solution was filtered and the flask washed with DCM (30ml). The MeCN and DCM washings were combined and dried *in vacuo*. This afforded an orange crystalline solid, which was used without further purification. ^{1}H-NMR (400 MHz, DMSO): δ 3.15 (s, 8 H, Al), 7.30 (t, (J_{HH} = 7.62HZ), 2H, Ar), 7.40 (d, (J_{HH} = 8.26HZ), 2H, Ar), 7.65 (t, (J_{HH} = 7.43HZ), 2H, Ar), and 7.85 (d, (J_{HH} = 8.01HZ), 2 H, Ar). ^{13}C (400MHz, DMSO): δ 51.17, 121.68, 122.27, 125.37, 133.81, 143.07 and 144.95. IR (KBr disc, cm^{-1}): 3460, 3354, 2956, 2836, 1604, 1500, 1445, 1371, 1301, 1276, 1214, 1147, 1051, 937 and 761. E.I.-MS m/z 329 (M^{+}+H^{+})

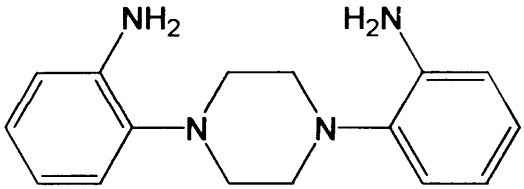

<u>*N, N'* bis (2-aminophenyl) 1, 4-diazacyclohexane.</u>

N, N' Bis (2-nitrophenyl) 1, 4-diazacyclohexane (200mg, 0.61mmol) was charged in a 250ml round bottom Schlenk with THF:MeOH (30ml:0.5ml) and Pt/C (50mg). This was evacuated and backfilled with hydrogen. This reaction vessel was left to stir for 24hrs until the reaction had ended with a colour change from yellow to clear. The solution was filtered by cannula which had been equipped with a filter tip into another Schlenk with a stirrer bar. The solvent was removed *in vacuo* to yield a clear solid that was used without further purification. Yield 93%, 152mg. ^{1}H NMR: (400 MHz, $CDCl_3$) δ 3.05 (s, 8H, Al), δ 4.65 (s br, 4H, NH_2), δ 6.15-6.25 (m, 4H, Ar), δ 6.90 (t, (J_{HH} = 7.25 Hz), 4H, Ar), δ 7.00 (d, (J_{HH} = 7.20 Hz), 2H, Ar). ^{13}C NMR: (250 MHz, $CDCl_3$) δ 51.85, 115.27, 118.65, 119.94, 124.79, 139.73 and 141.57. IR: (KBr disc, cm^{-1}) 3459, 2957, 1601, 1585, 1500, 1457, 1445, 1383, 1371, 1356, 1300, 1275, 1255, 1213, 1146, 1128, 1051, 1025, 761 and 668. E.I.-MS m/z 269 (M^++H^+)

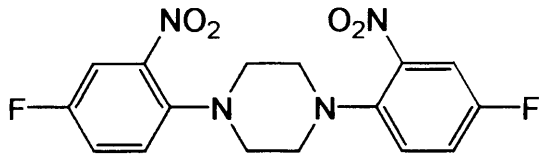

<u>*N, N'* bis (2-nitro, 4-fluorophenyl) 1, 4-diazacyclohexane.</u>

Piperizene (2.0g, 23.3 mmol), 2, 5-difluoronitrobenzene (7.58g, 47.7 mmol), potassium fluoride (2.77g, 47.7 mmol), and acetonitrile (50ml) were all stirred vigorously together in a round bottom flask, refluxed at 90°C for 36 hours and under nitrogen. The resulting solution was filtered and the flask washed with DCM (60ml). The MeCN and DCM washings were combined and dried *in vacuo*. This afforded an orange solid which was washed with methanol to afford an orange crystalline product. Yield 54%, 4.58mg. ^{1}H NMR: (400 MHz, $CDCl_3$) δ 3.05 (s, 8H, Al), δ 7.20-7.25 (m, 4H, Ar), δ 7.45-7.50 (m, 2H, Ar). ^{13}C NMR: (250 MHz, $CDCl_3$) δ 44.29, 50.81, 51.98, 112.30, 113.44, 120.48, 123.33, 124.64 and 143.08 (J_{CF} = 1124Hz). ^{19}F NMR: (300 MHz, $CDCl_3$) δ -116.73. IR: (KBr disc, cm^{-1}) 1522, 1447, 1380, 1328, 1292, 1265, 1213, 1199, 1149, 1121, 1067, 1034, 886, 833, 811, 760 and 720. E.I.-MS m/z 365 (M^{+}+H^{+})

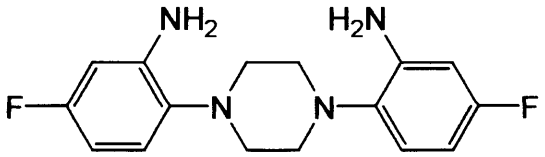

<u>*N, N'* bis (2-amino, 4-fluorophenyl) 1, 4-diazacyclohexane.</u>

N, N' Bis (2-nitro, 4-fluorophenyl) 1, 4-diazacyclohexane (200mg, 0.55mmol) was charged in a 250ml round bottom Schlenk with THF: MeOH (30ml: 0.5ml) and Pt/C (50mg). This was evacuated and backfilled with hydrogen. This reaction vessel was left to stir for 24hrs until the reaction had ended with a colour change from yellow to clear. The solution was filtered by cannula which

had been equipped with a filter tip into another Schlenk with a stirrer bar. The solvent was removed *in vacuo* to yield a clear solid that was used without further purification. Yield 90%, 150mg. ^{1}H NMR: (250 MHz, $CDCl_3$) δ 2.90 (s, 8H, Al), δ 3.90-4.20 (br s, 4H, NH_2), δ 6.30-6.40 (m, 2H, Ar), 6.45-6.50 (m, 2H, Ar), 6.85 (m, 2H, Ar). ^{13}C NMR: (250 MHz, DMSO) δ 50.77, 117.31, 119.74, 133.91, 143.73 and 159.07 (J_{CF} = 940Hz). ^{19}F NMR: (300 MHz, $CDCl_3$) δ-118.98. IR: (KBr disc, cm^{-1}) 3444, 1606, 1500, 1367, 1261, 1219, 1153, 1133, 1047, 845, 808, 753 and 716. E.I.-MS m/z 305 (M^++H^+)

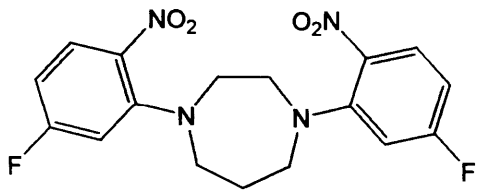

<u>*N, N'*-bis-(2-nitro, 5-fluorophenyl) – homopiperizene.</u>

Homopiperizene (0.5g, 5 mmol), 2,4-difluoronitrobenzene (1.83g, 11.51 mmol), potassium carbonate (1.5g, 10.87 mmol), and acetonitrile (50ml) were all stirred vigorously together in a round bottom flask, refluxed at 110°C for 24 hours and under nitrogen. The resulting solution was filtered and the flask washed with DCM (30ml). The MeCN and DCM washings were combined and dried *in vacuo*. This afforded a green/yellow solid. The title product was purified further by column chromatography, using chloroform as an elutant. This removed any mis-inserted products which gave a yellow pure product. Crystals of X-ray quality were grown by slow vapour diffusion of diethyl ether into an acetonitrile solution. Yield 57%, 1.08g. ^{1}H NMR: (400 MHz, $CDCl_3$) δ 2.05 (m, 2H, Al), δ 3.35 (t, (J_{HH} = 5.57Hz), 4 H, Al), δ 3.40 (s, 4H, Al), δ 6.50 (m, 2H, Ar), δ 6.70 (dd, (J_{HH} = 2.52 + 11.14Hz), 2H, Ar), δ 7.75 (dd, (J_{HH} = 6.12 + 9.09Hz), 2H, Ar). ^{13}C NMR: (400 MHz, $CDCl_3$) δ 27.20, 52.04, 52.05, 105.52, 105.85, 128.15, 135.81, 147.01, and 164.12 (J_{CF} = 1012Hz). ^{19}F-NMR ($CDCl_3$): δ -102.70. IR: (KBr disc, cm^{-1}) 3080, 2962, 2920, 1617, 1568, 1514, 1489, 1346, 1303, 1285, 1246, 1167 and 1077. E.I.-MS m/z 378.0 (M^++H^+)

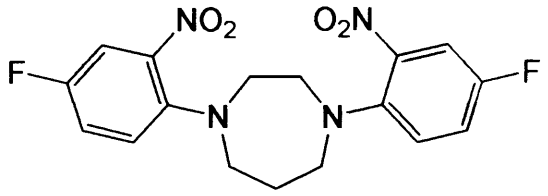

<u>*N, N'*-bis - (2-nitro, 4-fluorophenyl) - homopiperizene.</u>

Homopiperizene (0.5g, 5 mmol), 2, 5-difluoronitrobenzene (1.67g, 10.5 mmol), potassium carbonate (1.41g, 10.2 mmol) and acetonitrile (50ml) were all stirred vigorously in a round bottom flask, under reflux at 85°C for 24 hours. The resulting solution was filtered and the flask washed with DCM (30ml). The organic washings were combined and dried *in vacuo*. This afforded an orange, crystalline solid. Slow vapour diffusion of diethyl ether into an acetonitrile solution afforded crystals of X-ray quality. Yield 96%, 1.87g. ^{1}H-NMR (400 MHz, $CDCl_3$): δ 1.95-2.05 (m, 2H, Al), δ 3.20 (t, (J_{HH} = 6.10Hz), 4H, Al), δ 3.35 (s, 2H, Al), δ 7.05-7.20 (m, 4H, Ar), δ 7.40 (dd, (J_{HH} = 2.85 + 7.98Hz), 2H, Ar). ^{13}C-NMR (400 MHz, $CDCl_3$): δ 28.95, 54.35, 54.87, 112.59, 120.43, 123.30, 142.33, 143.18, and 156.04 (J_{CF} = 976Hz). ^{19}F NMR (300 MHz, $CDCl_3$): δ -120.02. IR (KBr disc, cm^{-1}): 2971, 2901, 1621, 1575, 1520, 1395, 1336, 1294, 1261, 1209, 1177, 1142, 1099, 1061, and 1032. E.I.-MS m/z 379 (M^++H^+)

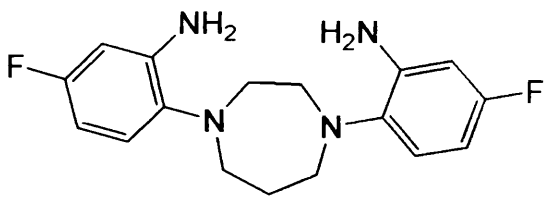

<u>*N, N'*-bis-(2-amino, 4-fluorophenyl) – homopiperizene L^{11}.</u>

N, N' bis - (2-nitro, 4-fluorobenzene) - homopiperizene (50mg, 0.13mmol), and Pd/C catalyst (10mg) were placed in a 250ml round bottom Schlenk, in a THF:MeOH solution (80ml:1ml). The catalyst had been washed beforehand in a sinter with methanol, and was added as slurry to prevent ignition. The THF used was HPLC grade and had been thoroughly dry and degassed. The Schlenk was evacuated and then backfilled with hydrogen gas. This was stirred continuously under an atmosphere of hydrogen for 24 hours. Completion was signalled by loss of colour of the solution. After this period of hydrogenation, a cannula was equipped with a glass fibre filter. The solution was filtered into another Schlenk and dried *in vacuo*. The resulting product was an off-white clear solid (L^{11}). Yield 37mg, 89%. ^{1}H-NMR (400 MHz, $CDCl_3$): δ1.95 (m, 2H, Al), δ 3.05 (s, 4H, Al), δ 3.10 (t, (J_{HH} = 6.05Hz), 2H, Al), δ 4.15 (br s, 4H, Amine), δ 6.30-6.40 (m, 4H, Ar), δ 6.90 (m, 2H, Ar). ^{13}C-NMR (400 MHz, $CDCl_3$): δ 29.00, 53.53, 56.32, 100.50, 103.58, 121.77, 136.69, 142.26, 159.12 (J_{CF} = 956Hz). ^{19}F NMR (300 MHz, $CDCl_3$): δ - 118.12. IR (KBr disk, cm^{-1}): 3475, 1616, 1590, 1506, 1376, 1256, 1203 and 1004. E.I.-MS m/z 319 (M^{+}+H^{+})

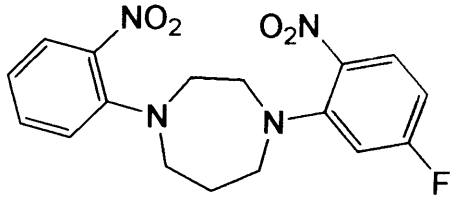

<u>*N*-(2-Nitrophenyl), *N'*-(2-nitro, 5-fluorophenyl)-homopiperizene.</u>

N-(2-nitrobenzene)-homopiperizene (0.2g, 0.905 mmol), 2, 4-difluoronitrobenzene (0.158g, 0.99 mmol), potassium carbonate (0.13g, 0.94 mmol) and acetonitrile (15ml) were all stirred vigorously in a pressure tube at 85°C for 24 hours. The resulting solution was filtered and the pressure tube washed with DCM (10ml). The MeCN and DCM washings were combined and dried *in vacuo*. This afforded an orange/brown oil. Yield 93%, 0.302g. ^{1}H-NMR (400 MHz, $CDCl_3$): δ 2.05 (m, 2H, Al), δ 3.20 (m, 2H, Al), δ 3.35 (m, 2H, Al), δ 3.40 (m, 4H, Al), δ 6.45 (m, H, Ar), δ 6.95 (m, H, Ar), δ 7.05 (dd, (J_{HH} = 2.53 + 11.43Hz), H, Ar), δ 7.30 (m, H, Ar), δ 7.60 (dd, (J_{HH} = 1.55 + 8.08Hz), H, Ar), δ 7.70 (t, (J_{HH} = 6.14 + 9.07Hz), H, Ar), δ 8.05 (m, H, Ar). ^{13}C-NMR (400 MHz, $CDCl_3$): δ 42.40, 43.57, 47.20, 48.59, 56.24, 106.14, 120.58, 120.89, 125.86, 128.25, 133.18, 136.27, 142.09, 146.00, 147.83, 162.56, and 165.14 (J_{CF} = 1008Hz). ^{19}F-NMR ($CDCl_3$): δ -103.03. IR (NaCl plates), 2918, 1604, 1558, 1464, 1430, 1410, 1396, 1347, 1277, 1260, 1242, 1214, 1177, 1105, 1090, 1077, 1043 and 1021 cm^{-1}. E.I.-MS m/z 361.0 (M^++H^+)

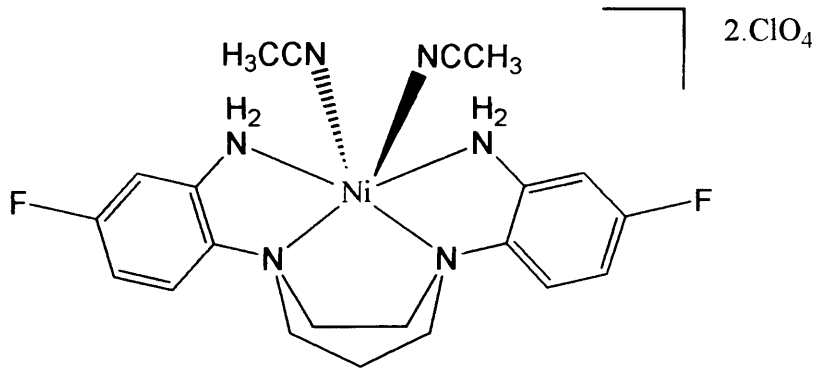

<u>*N, N'*-bis (2-amino, 4-fluorophenyl), 1, 4, diazacycloheptane nickel perchlorate bis acetonitrile adduct.</u>

The solution of L^{11} (50mg, 0.16mmol) was transferred directly into another Schlenk tube via filter cannula which contained nickel (II) perchlorate (63mg, 0.17mmol). This solution was light orange and was stirred vigorously for 18 hours. After this duration the solvent was removed *in vacuo*, and yielded a light orange precipitate. To this was added degassed ethanol (10ml), stirred vigorously then the solution allowed to settle. The solution was filtered off via cannula, again dried *in vacuo*, and produced the title compound as an orange solid. Crystals of X-ray quality were grown from a concentrated solution of MeCN by vapour diffusion of diethyl ether. Yield 45mg, 76%. IR (KBr disc, cm^{-1}): 3469, 1502, 1412, 1260, 1095, 1023, 862, 797, 701 and 623.

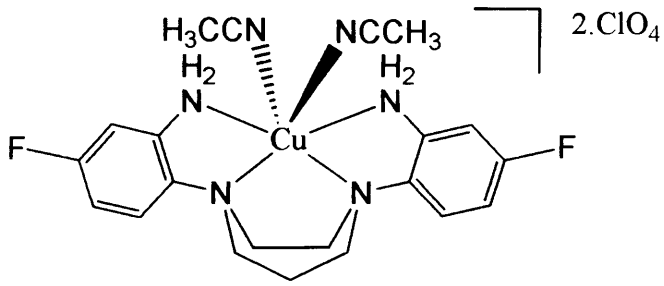

<u>*N, N'*-bis (2-amino, 4-fluorophenyl), 1, 4, diazacycloheptane copper perchlorate bis acetonitrile adduct.</u>

The hydrogenation solution of L^{11} (50mg, 0.16mmol) was transferred directly into another Schlenk tube via filter cannula which contained copper (II) perchlorate (64mg, 0.17mmol). This solution was purple and was stirred vigorously for 18 hours. After this duration the solvent was removed *in vacuo*, and yielded a purple precipitate. To this was added degassed ethanol (10ml), stirred vigorously then the solution allowed to settle. The solution was filtered off via cannula, again dried *in vacuo*, and produced the title compound as a purple solid. Yield 44mg, 74%. IR (KBr disc, cm^{-1}): 3437, 3276, 1614, 1568, 1498, 1537, 1091, 1026, 855 and 800.

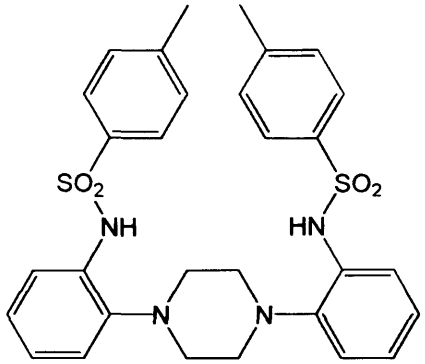

<u>*N, N'* bis (2-tosylaminophenyl) 1, 4-diazacyclohexane.</u>

Under anaerobic conditions, a solution of DCM (30ml) was added to triethylamine (309mg, 3.06mmol), and tosyl chloride (584mg, 3.07mmol) in a pressure equalising dropping funnel. This was connected to a Schlenk which was charged with N, N' bis (2-aminophenyl)-piperazine (412mg, 1.46mmol). To this was added the solution from the dropping funnel slowly over 30 minutes. This was kept at 0°C for 1 hour and allowed to warm to room temperature overnight with continual stirring of the dark red solution. This solution was then washed with 0.1M sodium hydroxide, and the organic layer separated, dried ($MgSO_4$), and filtered. The solvent was removed *In Vacuo* to yield a brown residue, which was recrystallized with hot ethanol with a few drops of glacial acetic acid. This afforded a pink/brown solid which was found to be air stable. Yield 81%, 72mg. ^{1}H NMR: (250 MHz, $CDCl_3$) δ 2.25 (s, 6H, Me, Al), δ 2.55 (s, 8H, Macrocyclic ring), δ 6.95 - 7.10 (m, 6H, Ar), δ 7.15 (d, (J_{HH} = 6.74 Hz), 4H, Ar), δ 7.50 (dd, (J_{HH} = 1.63 + 7.83 Hz), 2H, Ar), δ 7.65 (d, (J_{HH} = 8.32 Hz), 4H, Ar). ^{13}C NMR: (250 MHz, $CDCl_3$) δ 22.13, 53.67, 119.67, 122.83, 124.43, 126.87, 127.49, 128.55, 129.82, 133.11, 136.99 and 143.58. IR: (KBr disc, cm^{-1}) 2944, 1591, 1496, 1454, 1382, 1381, 1337, 1280, 1260, 1234, 1173, 1156, 1136, 1090, 1059, 1037, 813, 775, 755, 742 and 708. E.I.-MS m/z 577.48 (M^++H^+)

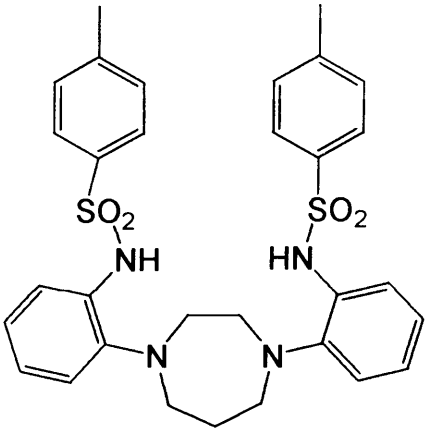

<u>*N, N'* bis (2-tosylaminophenyl) 1, 4-diazacycloheptane L^{12}.</u>

Under anaerobic conditions, a solution of DCM (30ml) was added to triethylamine (309mg, 3.06mmol), and tosyl chloride (584mg, 3.07mmol) in a pressure equalising dropping funnel. This was connected to a Schlenk tube which was charged with *N, N'* bis (2-aminophenyl)-homopiperazine (412mg, 1.46mmol). To this was added the solution from the dropping funnel slowly over 30 minutes. This was kept at 0°C for 1 hour and allowed to warm to room temperature overnight with continual stirring of the dark red solution. This solution was then washed with 0.1M sodium hydroxide, and the organic layer separated, dried ($MgSO_4$), and filtered. The solvent was removed *in vacuo* to yield a brown residue, which was recrystallized with hot ethanol with a few drops of glacial acetic acid. This afforded a pink/brown solid which was found to be air stable L^{12}. Yield 85%, 733mg. ^{1}H NMR: (400 MHz, $CDCl_3$) δ 1.80 (m, 2H, Al), δ 2.25 (s, 6H, Me), δ 2.70 (s, 4 H, Al), δ 2.85 (t, (J_{HH} = 5.63 Hz), 4H, Al), δ 6.95-7.10 (m, 6H, Ar), δ 7.15 (d, (J_{HH} = 8.13 Hz), 4H, Ar), δ 7.50 (d, (J_{HH} = 7.68 Hz), 2H, Ar), δ 7.60 (d, (J_{HH} = 8.21 Hz), 2H, Ar). ^{13}C NMR: (250 MHz, $CDCl_3$) δ 29.20, 39.67, 55.34, 57.65, 118.43, 123.27, 124.68, 126.01, 127.02, 129.67, 132.77, 136.63, 144.01 and 144.14. IR: (KBr disc, cm^{-1}) 3434, 2946, 1596, 1492, 1337, 1286, 1222, 1166, 1091, 1044, 812 and 755. E.I.-MS m/z 591.45 (M^++H^+)

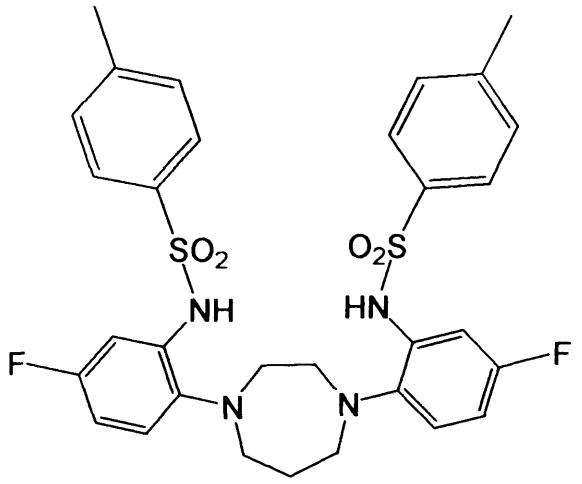

N, N' bis (2-tosylamino, 4-fluorophenyl) 1, 4-diazacycloheptane.

Under anaerobic conditions, a solution of DCM (30ml) was added to triethylamine (100mg, 0.99mmol), and tosyl chloride (189mg, 0.99mmol) in a pressure equalising dropping funnel. This was connected to a Schlenk which was charged with *N, N'* bis (2-amino, 4-fluorophenyl)-homopiperazine (150mg, 0.47mmol). To this was added the solution from the dropping funnel slowly over 30 minutes. This was kept at 0°C for 1 hour and allowed to warm to room temperature overnight with continual stirring of the dark red solution. This solution was then washed with 0.1M sodium hydroxide, and the organic layer separated, dried ($MgSO_4$), and filtered. The solvent was removed *In Vacuo* to yield a brown residue, which was recrystallized with hot ethanol with a few drops of glacial acetic acid. This afforded a pink/brown solid which was found to be air stable. Yield 79%, 233mg. ^{1}H NMR: (250 MHz, $CDCl_3$) δ 1.80 (m, 2H, Al), δ 2.35 (s, 6H, Me), δ 2.70 (s, 4 H, Al), δ 2.80 (t, (J_{HH} = 5.60Hz), 4H, Al), δ 6.65 (m, 2H, Ar), δ 7.05 (m, 2H, Ar), δ 7.10 (d, (J_{HH} = 7.70Hz), 4H, Ar), δ 7.15 (m, 2H, Ar), δ 7.65 (d, (J_{HH} = 8.24Hz), 4H, Ar). ^{13}C NMR: (250 MHz, $CDCl_3$) δ 28.94, 38.22, 55.64, 57.38, 117.87, 122.32, 124.11, 126.82, 127.37, 129.88, 132.11, 135.61, 144.90 and 156.43 (J_{CF} = 980Hz). ^{19}F NMR: (300 MHz, $CDCl_3$) δ -113.18. IR: (KBr disc, cm^{-1}) 3452, 2954, 1597, 1503, 1329, 1265, 1218, 1138, 1067, 1028, 798 and 748. E.I.-MS m/z 627 (M^++H^+)

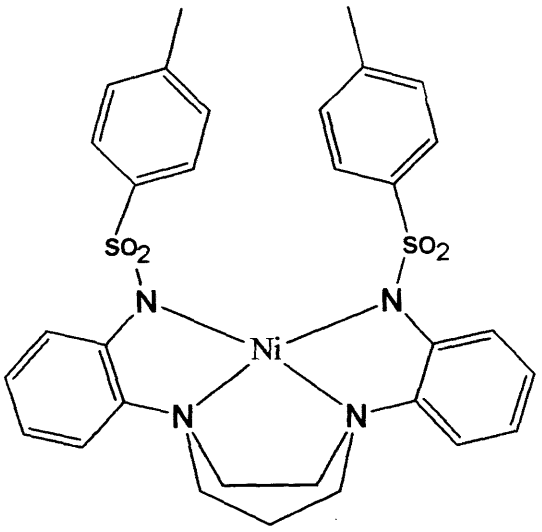

<u>*N, N'* bis (2-tosylaminophenyl) 1, 4-diazacycloheptane nickel complex.</u>

Under anaerobic conditions, degassed acetone (10ml) was added to L^{12} (50mg, 0.008mmol), nickel (II) perchlorate (34mg, 0.008mmol), and triethylamine (17.5mg, 0.017mmol) in a Schlenk tube. This light red solution was stirred vigorously at room temperature for 10 minutes then dried *in vacuo* to yield a purple residue. Acetonitrile (10ml) was added to the residue and allowed to stand, upon which purple crystals of X-Ray quality were afforded. Yield 85%, 47mg. IR: (KBr disc, cm^{-1}) 1450, 1299, 1286, 1258, 1147, 1105, 1086, 1038, 1020, 848, 817, 752 and 710.

Chapter Three

Pendant Fluoroaniline derivatives of triazacyclononane.

I am returning this otherwise good typing paper to you because someone has printed gibberish all over it and put your name at the top.
-- An English Professor, Ohio University

Reminds me of my safari in Africa. Somebody forgot the corkscrew and for several days we had to live on nothing but food and water.
-- W. C. Fields

Introduction

The selective functionalisation of macrocycles has been an area of increased interest over past years. The desire to synthesise ligands with specific differing pendants has increased due to heightened interest to tune the properties of metal-ligand complexes[53].

The reaction scope to produce multi substituted azamacrocycles has widened so to produce ligands in higher yields an in fewer steps. Many applications of azamacrocyclic ligands require functionalisation of the parent ligand[54, 56]. The addition of differing pendant donor groups to the macrocyclic ring can be achieved in one of two ways. Firstly the carbon backbone of the ring can be tailored to different aims, but this incurs multi step syntheses to form the azamacrocycle ring. Parker *et al* have synthesised a variety of *N* and *C* functionalised macrocycles for the derivitisation of antibodies[55]. Pendant addition at the carbon backbone allows additional groups to be incorporated into the macrocycle, whereas addition to the nitrogen terminus then is dictated by the number of nitrogen's in the ring. The second point of functionalisation of the macrocyclic ring is at the nitrogen[56].

The main focus of this thesis is concentrating on *ortho*-aniline group addition to 1, 4, 7-triazacyclononane. Fallis *et al*[57] originally synthesised the parent ligand L^{33} that was prepared using 2-fluoronitrobenzene and reduced under standard (H_2/Pd/C) conditions. Reaction with divalent metal perchlorates in ethanolic solutions yielded the desired metal complexes in good yield of general formula $[(L^{33})M](ClO_4)_2.xMeCN$.

---

[53] Bombieri G., Artali R., *J. Alloy and Compounds.*, 344, **2002**, 9-16.
[54] Fallis I A., *Supramolecular Chemistry,* Atwood J L., Steed J W., *Annual Reports on the Progress of Chemistry. Section A., Inorg. Chem.*, 94, **1998**, 351-387.
[55] Cox J P L., Craig A S., Helps I M., Jankowski K J., Parker D., Eaton M A W., Millican A T., Millar K., Beeley N R A., Boyce B A., *J. Chem. Soc., Dalton Trans.*, **1990**, 2567-2576.
[56] Wainwright K P., *Coord. Chem. Rev.*, **1997**, 166, 35-90.
Fallis I A., *Annu. Rep. Prog. Chem., Sect. A*, **2001**, 97, 331-369.
[57] Fallis I A., Farley R D., Malik K M A., Murphy D M., Smith H J., *J. Chem. Soc., Dalton Trans.*, **2000**, 3632.

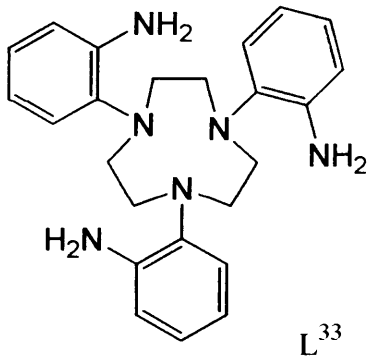

Figure 3.1: 1, 4, 7-tris (2-aminophenyl) 1, 4, 7-triazacyclononane (L^{33})

Fallis and co workers have investigated the chemistries of the Fe, Ni, Cu and Zn complexes. A range of spectroscopic methods were used to investigate this class of complex with interesting results obtained. The iron complex crystal structure showed a mean Fe-N bond length of 2.10Å which is intermediate between the normal ranges of low and high spin Fe^{II} complexes. EPR and magnetometry studies revealed that 5% of the sample was Fe^{III}. Fallis *et al* then suggest that this could be the mono deprotonated anilide species $[(L^{33-H})Fe](ClO_4)_2$. The Ni complex exhibited a short average Ni-N bond length of 2.09Å, and a high ligand field strength of 12,330cm^{-1} (B=850cm^{-1}). The Cu structure showed a mainly axial species with a slight rhombic distortion. The ^{1}H NMR spectra was recorded for the zinc complex, over a temperature range of -40°C-(+70°C) in CD_3CN and showed non fluxional behaviour.

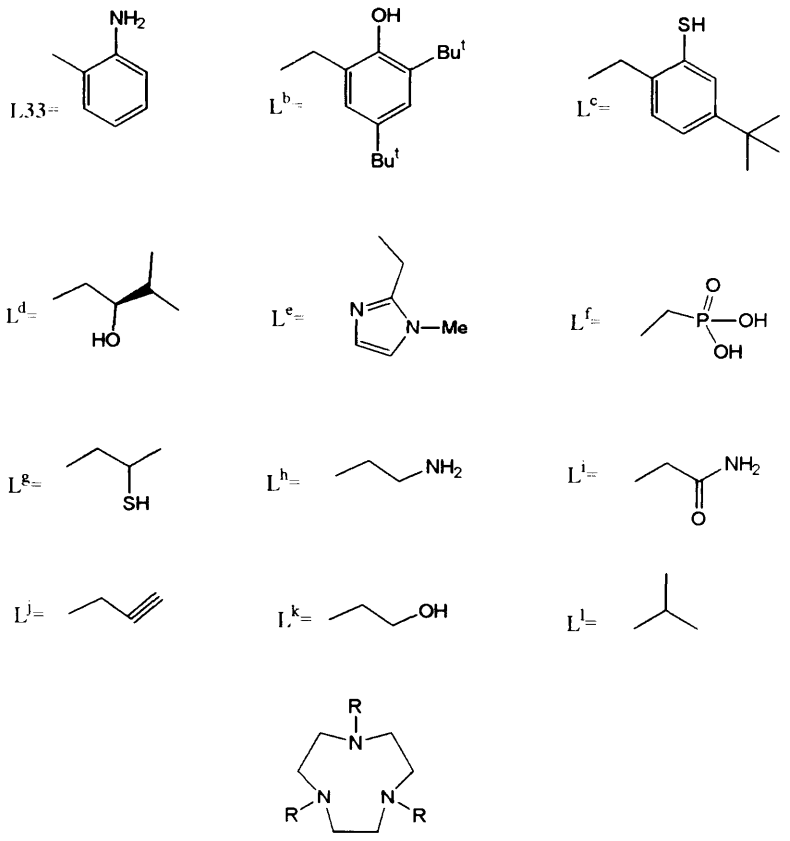

Figure 3.2: Pendant donor derivatives of 1, 4, 7-triazacyclononane.

Groups other than anilines such as (Figure 3.1) phenols[58] (L^b), thiophenols[59] (L^c), alcohols[60] (L^d), thiols[61] (L^g), *N*-methyl pyrazoles[62] (L^e), phosphonic acids[63] (L^f), amino alkyls[64] (L^h), amides[65] (L^i), alkynes[66] (L^j), alkyl alcohols[67], [60] (L^k) and isopropyl pendants[68] (L^l) are all some of the diverse groups that make up this field of study. These are all examples of tris substitution of the nitrogens present in the tacn ring.

---

[58] Moore D A., Fanwick P E., Welch M J., *Inorg. Chem.*, **1989**, 28, 1504.
[59] Bessel T., Bürger K S., Voight G., Weighardt K., Butzlaff C., Trautwein A X., *Inorg. Chem.*, **1993**, 32, 124.
[60] Fallis I A., Farrugia L J., MacDonald N M., Peacock R D., *J. Chem. Soc., Dalton Trans.*, **1993**, 2759.
[61] Mabeza G F., Loyevsky M., Gordeuk V R., Weiss G., *Pharmacol. Ther.*, **1999**, 81, 53.
[62] Norante G de M., Di Vaira M., Mani F., Mazzi S., Stoppionoi P., *J. Chem. Soc., Dalton Trans.*, **1992**, 361.
[63] Prata M I M., Santos A C., Geraldes C F G C., de Lima J I P., *Nucl. Med. Biol.*, **1999**, 26, 707.
[64] Tei L., Baum G., Blake A J., Fenske D., Schröder M., *J. Chem. Soc., Dalton Trans.*, **2000**, 2793.
[65] Bakyal U., Akkaya M S., Akkaya E U., *J. Mol. Catal A.*, **1999**, 145, 309.
[66] Ellis D., Farrugia L J., Peacock R D., *Polyhedron*, **1999**, 18, 1229.
[67] Belal A A., Chaudhuri P., Fallis I A., Farrugia L J., Hartung R., MacDonald N M., Nuber B., Peacock R D., Weiss J., Weighardt K., *Inorg. Chem.*, **1991**, 30, 4397.
[68] Haselhorst G., Stoetzel S., Strassburger A., Walz W., Weighardt K., Nuber B., *J. Chem. Soc., Dalton Trans.*, **1993**, 83.

The Spiccia group[69] have extended methodologies by Schröder *et al*[70] to make biomimetic ligands resembling amino acids. The ligands L^{mnp} are all derived from 1, 4, 7-triazatricyclo[5.2.1.^{0,4,10}]decane and through the addition of one pendant to then form the monoamidinium salt. The formyl group formed is then removed by hydrolysis after addition of the second pendant to the free macrocyclic nitrogen. All reactions are over four steps and with overall yields of 22%(L^m), 44%(L^n) and 46%(L^p) respectively.

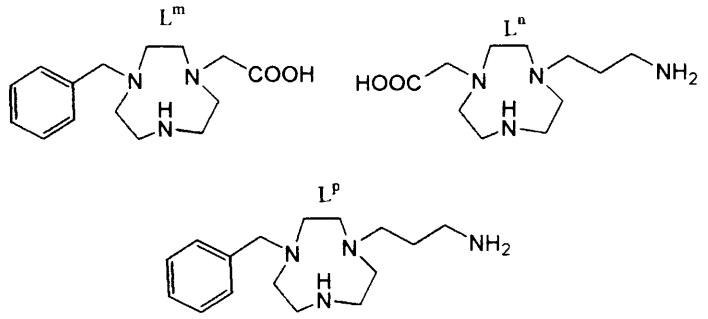

Figure 3.3: Bis substituted tacn ligands by Spiccia *et al.*

The use of 1, 4, 7-triazatricyclo[5.2.1.^{04,10}]decane as a multifunctionalised tacn precursor is well published[71], whereby after addition of the first desired pendant or more notably reaction with benzyl bromide, the formyl species formed has a nitrogen available for further reaction. After formation of the formyl tacn species through acid hydrolysis, Schröder *et al* subsequently added two equivalents of 2, 2-dimethyl oxirane formed the bis *iso*-butyl 2-ol intermediate. Base hydrolysis cleaved the formyl group to form the desired pentadentate macrocycle 1, 4-bis (2-hydroxy-2-methylpropyl)-1, 4, 7-triazacyclononane (L^q). The mono alcohol pendant version was synthesised by blocking one of the tacn nitrogen's with a pendant benzyl group (L^r).

[69] Warden A., Graham B., Hearn M T W., Spiccia L., *Org. Lett.*, **2001**, 3, 18, 2855-2858.
[70] Blake A J., Fallis I A., Gould R O., Parsons S., Ross S A., Schröder M., *J. Chem. Soc., Chem.. Commun.*, **1994**, 2467-2469.
[71] Atkins T J., *J. Am. Chem. Soc.*, 102, **1980**, 6364-6365.

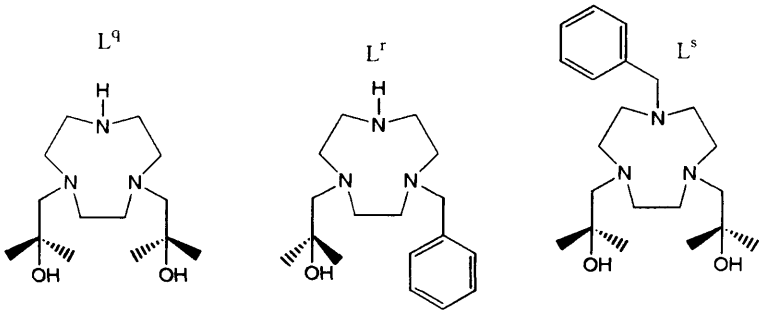

Figure 3.4: Schröder *et al*-bis and tris substituted tacn ligands.

Formation of L^s was achieved by the addition of benzyl bromide to 1, 4, 7-triazatricyclo [5.2.1.$^{04,\ 10}$] decane, hydrolysis of the formyl group to produce the mono benzyl tacn intermediate, then subsequent addition of 2 equivalents of the epoxide to form the aforementioned ligand.

Penta and hexadentate ligands bearing phenolate and carboxylate donors have been prepared by Wieghardt *et al*[72].

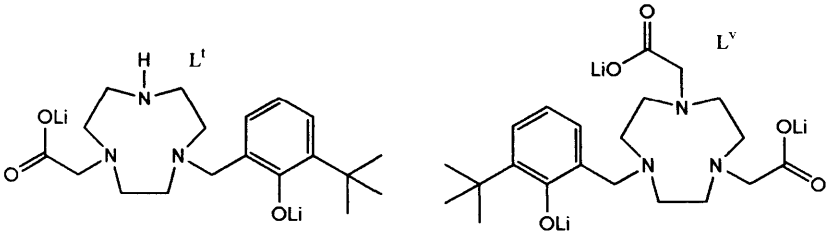

Figure 3.5: Wieghardt's mixed phenolate and carboxylate pendant tacn macrocycle.

L^t and L^v are of the N_3O_2 and N_3O_3 donor set, and were reacted to form the compounds [(L^t)Fe] and [(L^v)V/Mn/Fe/Co]. These anionic ligands react well to produce the desired metal complexes in moderate yields (32%-62%). The mono addition of the phenolate pendant is achieved by using a large excess of tacn (5:1) then recouping the macrocycle through collection of the chloroform layer. Interestingly Wieghardt states that by addition of one or two equivalents of the corresponding ethyl bromoacetate in a LiOH

[72] Stockheim C., Hoster L., Weyermuller T., Wieghardt K., Nuber B., *J. Chem. Soc., Dalton Trans.*, **1996**, 4409-4416.

solution, the ligands L^t and L^v are formed. Further explanation of formation of the bis substituted product with one equivalent is not included.

Benniston *et al*[73] have explored the region of addition of soft donors to macrocycles such as tacn, cyclen, and cyclam. Lithiation of the macrocycle and subsequent addition of vinyl aromatic pendants afford the mono and bis substituted ligands $L^{wxyz(aa)}$.

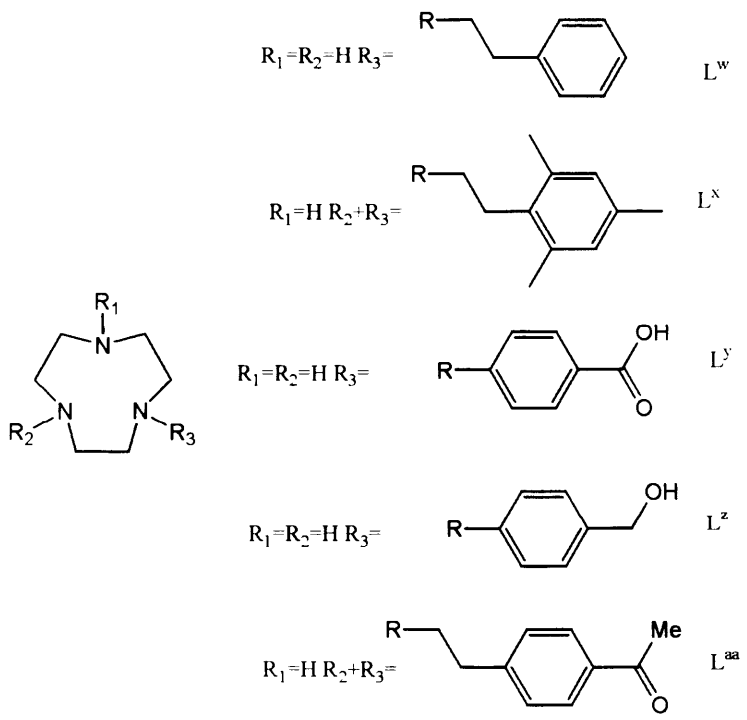

Figure 3.6: Mono and bis substituted tacn with electron rich arene pendants.

The ligands shown in figure 3.6 have been synthesised without the need for column chromatography and in reasonable yields (43%-68%). Reaction of $L^{wxyz(aa)}$ with transition metal perchlorates (2:1) afforded tacn sandwich type complexes with the pendant arenas showing interesting crystal packing. A coordinated polymer is shown to form though the repeated cell of $[2.L^1Cu_2(H_2O)_2]$.

[73] Benniston A C., Ellis D., Farrugia L J., Kennedy R., Peacock R D., Walker S., *Polyhedron*, 21, **2002**, 333-342.

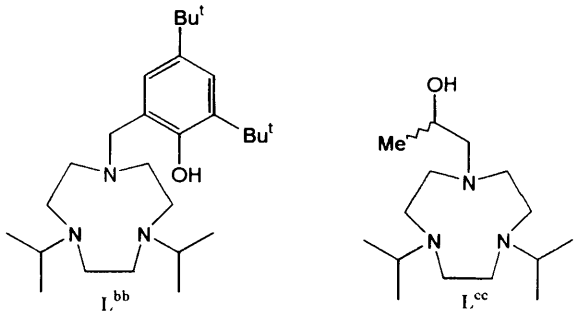

Figure 3.7: Cationic tacn ligands for aluminium complexation by Mountford *et al.*

Mountford *et al*[74] have monofunctionalised bisprotected tacn with an aromatic (L^{bb}) and alkyl (L^{cc}) alcohols. Reaction of $L^{(bb)(cc)}$ with $AlMe_3$ or [$AlMe_3$.Py] afforded four and five coordinate complexes respectively. Interestingly the complexation only occurred through the macrocycle nitrogen that was attached to the pendant and not the one tethered to the *iso*-propyl group. Crystallographic data of [$L^{bb}AlMe_2$] shows a distorted tetrahedral arrangement with the two methyl groups is a *cis* arrangement to each other. Reaction of L^{cc} generated the dimeric structure with both aluminium centres sharing the oxygen's present on the phenolate pendants. [$L^{cc}Al_2Me_4$]. As stated before, the two *iso*-propyl bearing nitrogen's do not contribute to the coordination of the metal and are left to dangle away from the coordination centre.

[74] Robson D A., Rees L H., Mountford P., Schröder M., *Chem. Commun.*, **2000**, 1269-1270.

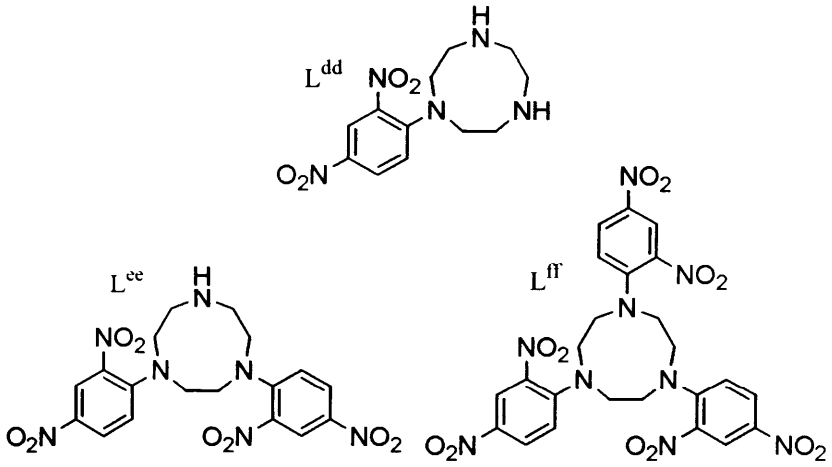

Figure 3.8: Tacn macrocycles bearing the Sanger's pendants 2, 4-bisnitrobenzene.

Research is in progress by Fallis *et al*[75] into the addition of Sanger's reagent (1-Fluoro, 2, 4-dinitrobenzene) to tacn and forming the mono, bis and tris substituted macrocycle. Addition of differing groups to the free macrocyclic nitrogen's could lead to mixed donor sets (N_4O_2, N_5O_1) and so design of specific ligands. The increased degree of electron richness of the ligand, compared to L^{33}, leads to more air sensitive samples upon hydrogenation but further functionalisation of the outer amine groups could be attempted to form larger dendrimers[76].

[75] Fallis I A., Tatchell T., *Unpublished Results*, **2004**.
[76] Beer P D., Gao D., *Chem. Commun.*, **2000**, 443-444.

CARDIFF UNI

Wieghardt et al[77, 88, 133] explored the pendant aniline class of ligand first by making the aminobenzyl derivative (L^{KW}). Extensive research has shown the complexation of $[(L^{KW})M](ClO_4)_2$ (M=Mn/Fe/Co/Ni/Cu/Pd/Zn/Cd/Hg) and subsequent addition of triethylamine to the metal complexes produced the compounds $[L^{KW-3H}]$ (M=Fe/Co).

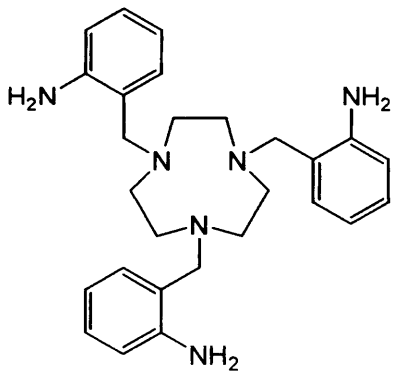

L^{KW}

Figure 3.9: Tris 1, 4, 7-(2-aminobenzyl) 1, 4, 7-triazacyclononane.

2-nitrobenzaldehyde was reduced with sodium borohydride to form the relevant alcohol which was subsequently brominated with phosphorus trichloride in carbon tetrachloride. Three equivalents of 2-nitrobenzyl bromide were then reacted with potassium hydroxide and the macrocycle 1, 4, 7-triazacyclononane, then reduced with hydrazine hydrate over a graphite catalyst to afford L^{KW}. This ligand was dissolved in methanol and stirred with ethanolic metal perchlorate solutions. Refluxing and subsequent cooling of the reaction solutions afforded the desired metal complexes.

In depth investigation of the zinc sample revealed interesting fluxional behaviour over the temperature range of -30°C-(+90°C). Broad resonances for the benzylic and amine protons at room temperature are well resolved upon cooling and produce sharp peaks at elevated temperatures. At low temperature the protons of the benzylic and amine groups are locked into a preferred conformation and the 6-membered chelate forces these protons into different environments. Similar behaviour was observed for the cadmium sample. Characteristic *H-Hg* coupling was found straddling the amine peak for the mercury sample satellite peaks and was found to be

[77] Schlager O., Wieghardt K., Nuber B., *Inorg. Chem.* **1995**, 34, 6456-6462.

J_{HHg} =45Hz. Crystal data was obtained for the nickel, copper and palladium samples. The copper and palladium structures were found to be of square based pyramidal geometry. Coordination of the metal to the macrocycle nitrogen's and to two of the benzylanilines generated the N5 donor set, and the third benzylaniline is left to dangle away from the metal centre and does not participate in bonding.

Addition of base to the metal complexes afforded the tris deprotonated species. Crystal data was obtained for the Mn^{IV} species, it was synthesised from manganese III acetate and the counterion exchanged for tetraphenylborate. Wieghardt states that the deprotonation of these ligands is reversible and was confirmed by UV/Vis spectroscopy.

Aims and Objectives

Our aim was to produce a class of ligands with similar structures to see if the alteration of peripheral groups on the pendant arms would have an effect upon the nature of the metal complex. With the incorporation of fluorine bearing aniline pendant we hypothesize that the metal-nitrogen bond lengths would alter depending on the electron withdrawing nature of the attached pendant. When the fluorine is *ortho/para* to the amino group, electron withdrawal from the phenyl ring should lead to weaker interaction from the metal centre and the aniline nitrogen, thus longer bonding should be evident. When the fluorine is *meta* to the amino group, it is not activated therefore does should not have an effect on the $N_{aniline}$-M bond lengths. However, this fluorine will be *para* to the nitrogen of the macrocyclic ring and so should increase the N_{ring}-M bond lengths by withdrawing electron density from the phenyl ring.

We chose to combine methods from Perkins[78] to produce mono, bis and tris fluorinated aromatic aniline pendant tacn ligands. Our interest lay in the possibility of producing such multifluorinated ligands with the aim of complexation and then comparison of these complexes metal ligand environments. The coordination centre of any crystallographic data obtained will be evaluated to assess the extent of the alteration of ligand has upon the overall complex

[78] Perkins W T S., *Ph.D Thesis*, **2002.**

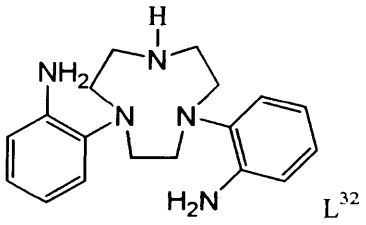

Figure 3.10: 1, 4-bis (2-aminophenyl) 1, 4, 7-triazacyclononane (L^{32}).

Developing potential nitrous oxide compounds required us to investigate the possibility of making differing hexaamine ligands capable of complexing ruthenium. These can be seen as mimics for the initial $[Ru(NH_3)_5X]^{2+}$ salt Taube developed. If complexation were to occur using L^{33}, then there could be the possibilities that in future work the pentammine ligand (L^{32})[79] (Figure 3.10) could be synthesised allowing the sixth coordination site free for possible nitrous oxide bonding.

Results and discussion

Ligand Synthesis

Reaction of fluorinated nitrobenzenes with tacn in the presence of potassium fluoride afforded the nitro ligands in good yield. The reaction proceeded via aromatic nucleophillic substitution (SNAr) to afford the bright yellow/orange powders. Reaction conditions have been optimised since the initial publication of L^{33}, and so higher yields of the nitro precursor and amine ligands have been achieved.

Ligand	$L^{1'}$	$L^{2'}$	$L^{3'}$	L^{1}	L^{2}	L^{3}
Yield (%)	78	93	88	92	87	91

Figure 3.11: Table of yields for nitro precursors and aniline ligands.

Production of the ligands with the pendant 2-amino, 6-fluorophenyl could not occur due to no such precursor 2, 3-difluoronitrobenzene being available commercially. The

[79] Fallis I A., Perkins W T S., Longhurst S L., Malik K M A., *Unpublished Results*, **2000**.

closest derivative is 2, 3, 5 tri fluoronitrobenzene but unfortunately the synthetic route was not able to be repeated due to the high toxicity and corrosiveness of the reagents used by Olah *et al*[80]. Reaction at room temperature with the aromatic in superacid produced a wide variety of differing fluorinated and other substituted nitrobenzenes in generally good yields (52%-99%). We feel the prospect of synthesising this final family of ligands appealing but due to lack of equipment, this could not be attempted.

Palladium catalysts were used in the primary reactions, but were found to produce samples that degraded quickly upon transfer. We chose to then employ a platinum catalyst which was found to produce more stable samples. The more reactive catalyst used was platinum on carbon and of 5% loading. The palladium catalyst was bought from different commercial suppliers and tested with $L^{33'}$. The results showed a variety of unstable samples. The palladium catalyst (10%) was loaded on carbon and was also washed with methanol. This isolation of this catalyst when employed, produced more stable L^{33} samples but not as stable as the platinum reduced samples.

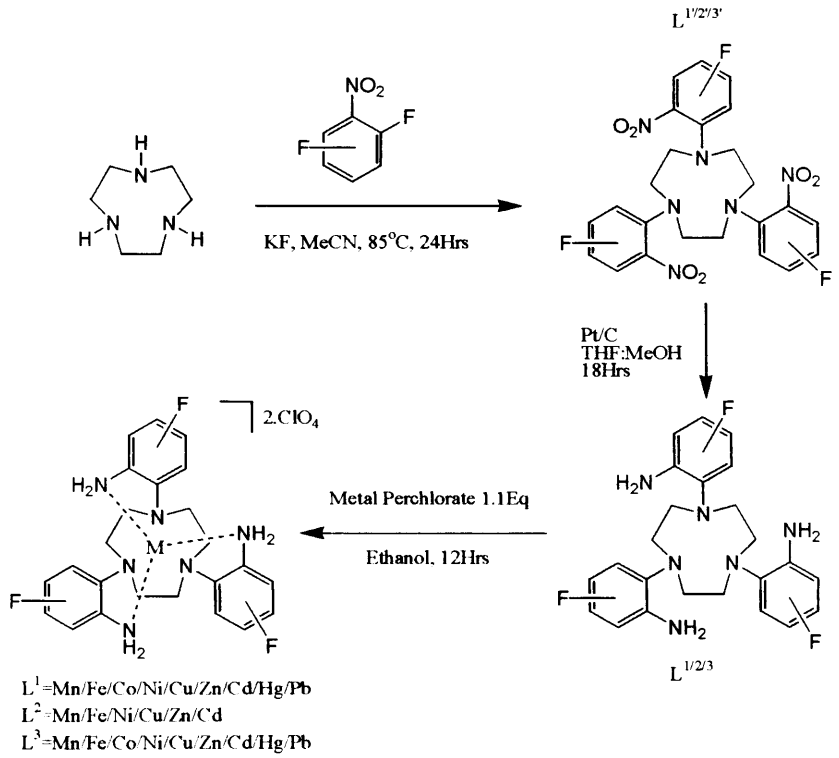

[80] Olah G. A., Orlinkov A., Oxyzoglou A B., Prakash G K S., *J. Org. Chem.*, **1995**, 60 (22), 7348-7350.

Figure 3.12: Reaction scheme for ligand synthesis and metal complexation.

Small test reactions were carried out upon the hydrogenation of nitro precursor compounds against the same batch of precursor but with a small trace of 2-fluoronitrobenzene added. After 24 hours the sample without the 2-fluoronitrobenzene had hydrogenated well, but the sample with a trace did not undergo completion. This gave us the indication that any excess fluoronitrobenzene starting material present in the precursor would not allow the hydrogenation reaction to proceed. Purity of the nitro precursor was an overriding factor to the conversion, and so batches of the nitro ligand were often successively recrystallised with hot ethanol. A reaction scheme of the route taken to synthesise the compounds in the chapter is shown in figure 3.12.
Synthesis of $L^{1'}$ (IAF0303) was carried out under standard conditions, but was then purified by column chromatography, to remove any mis-inserted fluoronitrobenzene groups[81].

[81] Davey D D., Erhardt P W., Cantor E H., Greenberg S S., Ingebresten W R., Wiggins J., *J. Med. Chem.*, **1991**, 34, 2671-2677. Longhurst S L., Fallis I A., Perkins W T S., Malik K M A., *Unpublished Results*, **2001**.

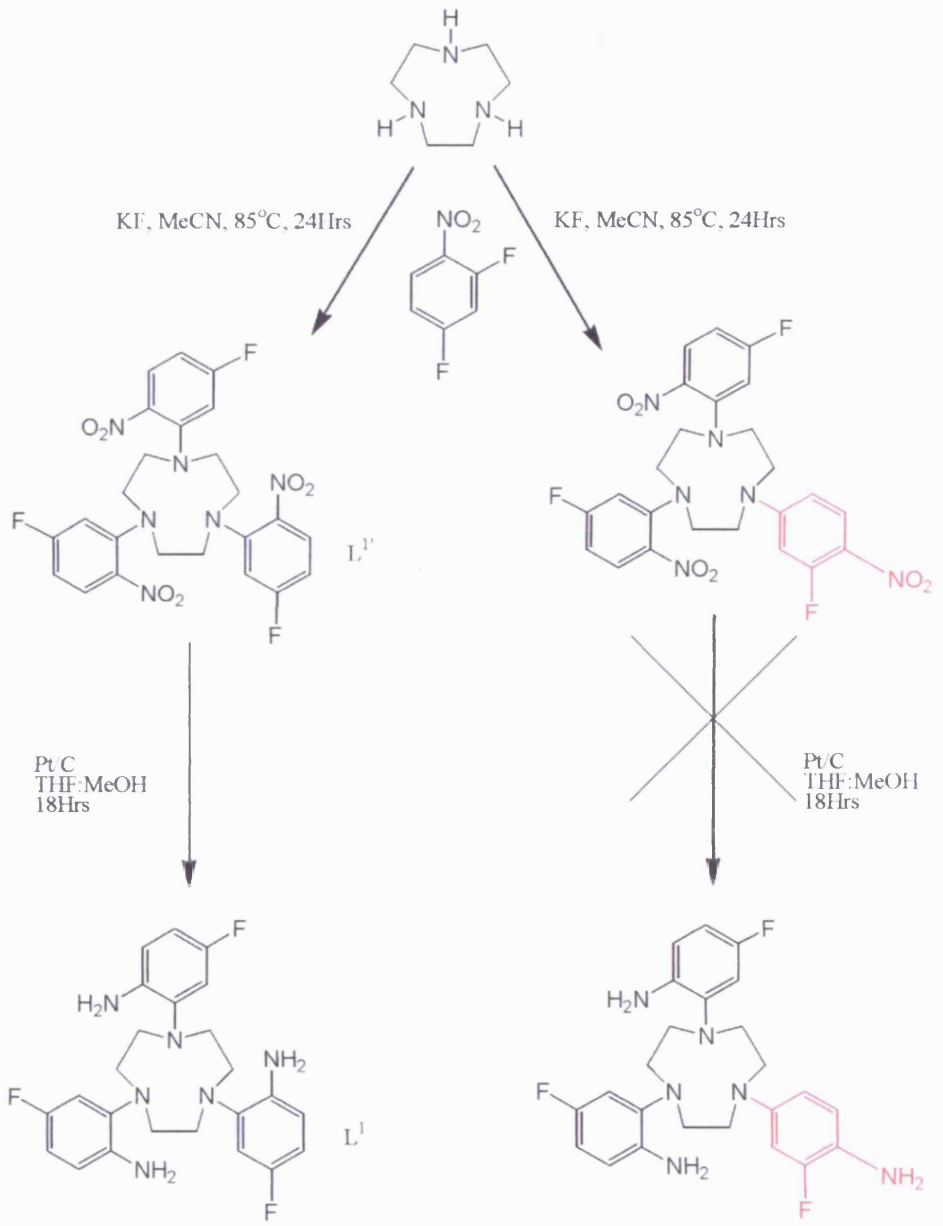

Figure 3.13: Reaction scheme showing the mis-inserted by-product in the synthesis of $L^{2'}$.

The red fragment (Figure 3.13) indicates the mis-inserted pendant. Thus elution of the product on silica with chloroform (R_f = 0.51) isolated the ligand as the main bright yellow band, which was further purified with acetone. The crystal structure of $L^{1'}$ is included as appendix i. The arrangement appears that two aromatic rings are "stacked" but no π stacking is present due to an interplanar ring distance of 3.788Å. The structures for $L^{1'}$ and $L^{2'}$ are similar with two aromatic rings stacking, and the macrocycle ring folding to pack within the crystal.

The synthesis of $L^{2'}$ (IAF0402) was carried out in analogous fashion to $L^{1'}$ but there was no need for chromatography as the fluorine is in the *meta* position to the nitrobenzene and thus is deactivated. Substitution would not occur at this position and we feel any sort of by products would be minimal (~1%) and removed by recrystallisation.

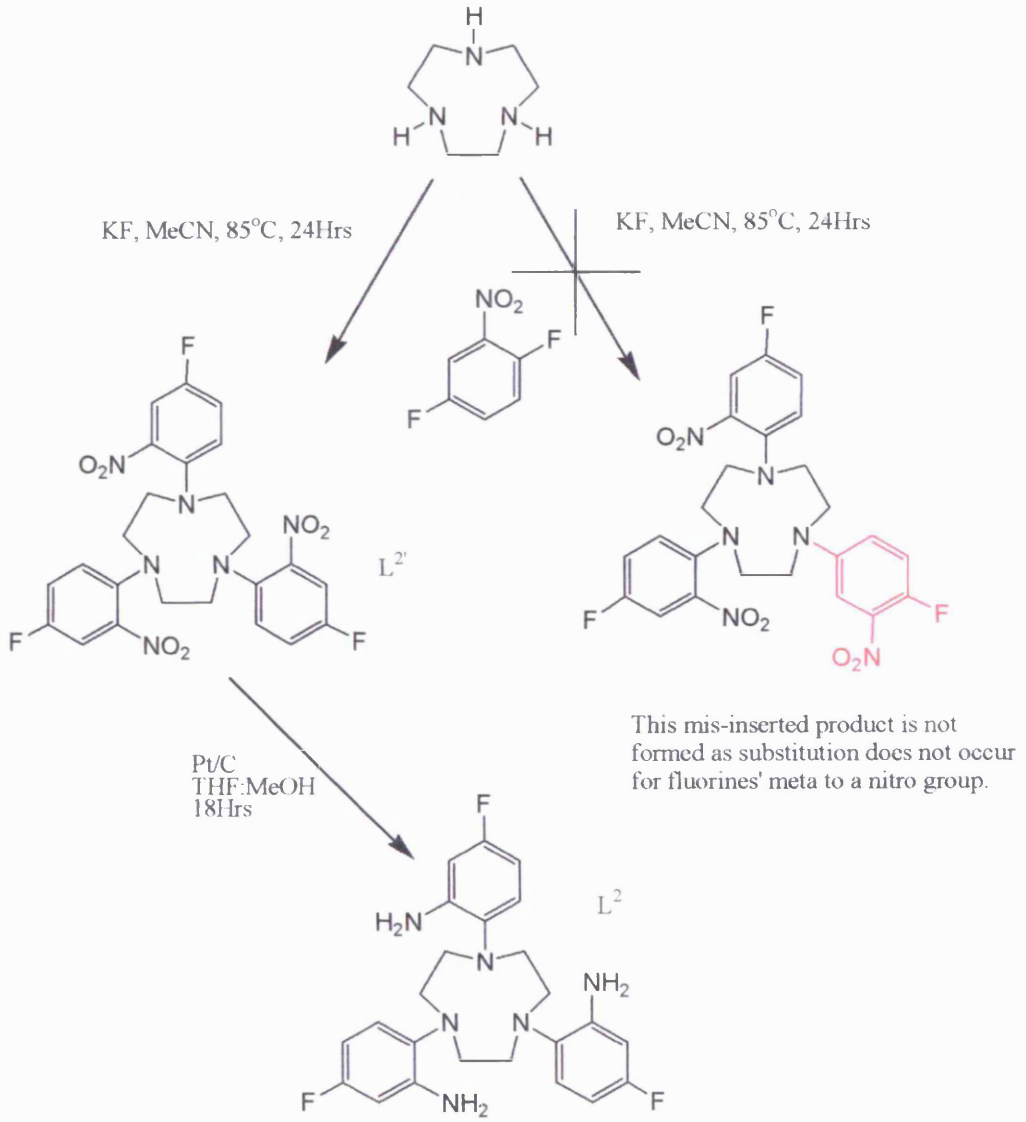

Figure 3.14: Reaction scheme for the synthesis of $L^{2'}$ and L^{2}. The potential mis-inserted fragment is indicated in red.

The crystal structure of $L^{2'}$ (Included as appendix ii) indicates a like packing with two aromatic rings "stacking" but with minimal π interaction as the rings are a closer interplanar distance of 3.374Å. Again the tacn ring is "folded" with one aromatic ring free.

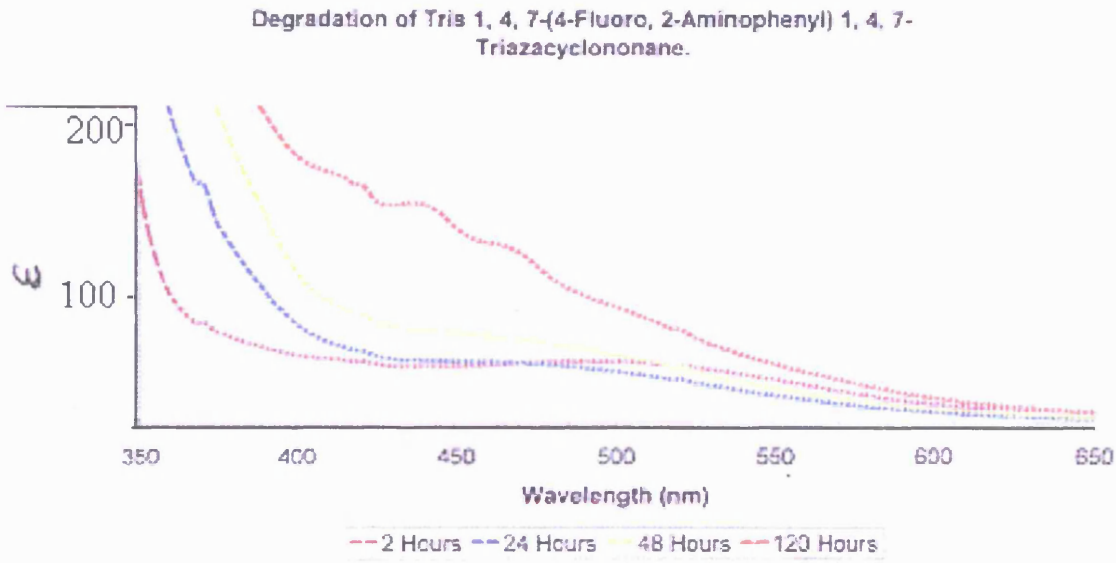

Figure 3.15: UV/Vis spectra of L^2 degradation over 120 hours.

The initial sample of L^2 was clear, and pure ligands could then be used to form metal complexes. Problems occurred after the initial transfer of the hydrogenated solution, and the clear sample was seen to degrade in the Schlenk tube and change to a bright pink colour. Figure 3.15 shows the UV/Vis spectra of L^2 degrading over a period of 5 days. This colour then changed to a dark brown after 5 days exposure. At a λ_{max} at 492nm, the extinction coefficient can be seen to increase gradually. After 2 hours exposure (purple trace) $\varepsilon = 40$, 24hrs exposure (blue trace) $\varepsilon = 36$, 48hrs exposure (yellow trace) $\varepsilon = 48$ and after 5 days (red trace) $\varepsilon = 80$. Subsequent attempts at hydrogenation also produced unworkable ligands also turned pink upon transfer. New batches of ligand were made, and this problem still occurred. We would like to hypothesize that this degradation is due some sort of free radical reaction (e.g polymerisation of diaminobenzene/Würsters blue/red)[82]. All complexes made were

[82] Eggers J., Frieser H., *Physikalische Chemie*., **1956**, 60, 372-376. Michealis L., *J. Am. Chem. Soc.*, **1931**, 2953-2962. Michealis L., Granick S., *J. Am. Chem. Soc.*, **1943**, 1747-1755.

from the same initial batch of hydrogenated ligand, and have since not been able to be reproduced.

The ligand $L^{3'}$ (IAF0410) was produced in a like manner with potassium fluoride and refluxed in acetonitrile, again without the need for chromatography (Included as appendix i). There is the possibility of the difluoronitrobenzene reacting twice and thus tethering two tacn rings together, but a TLC of the reaction mixture showed no visible side-products and the ^{1}H NMR spectra indicated a single product with a lone singlet present in the aliphatic region. This shows a triply substituted macrocycle, whereas tethered tacn rings would show a triplet, triplet, singlet arrangement in the aliphatic region.

Differing methods of hydrogenation were attempted to convert the nitro groups to amines. Initial tests were carried out with toluene:methanol, but this solvent mix was dispensed with as the higher volatility of THF allowed faster transfer of the air sensitive hydrogenation solutions. The THF grade used was found to be vital in the reduction of the nitro groups. When HPLC grade THF was used, a stable sample was afforded. The absence of stabilizers in the solvent was found to be paramount in the completion of this reaction.

The formation of metal complexes was achieved by the transfer of the amine ligand in THF solution via cannula onto the metal perchlorate salt. This was done anaerobically as to prevent and ligand degradation. The salt was allowed to dissolve over one hour in the THF solution with the aid of stirring. The volatile solvent was then removed *in vacuo* and degassed ethanol was added via cannula onto the dry precipitate. This solution was stirred overnight at room temperature (sometimes the solution was warmed with a heat gun to aid the ligand and salt to completely dissolve) upon which the desired metal complex has precipitated. After this time the ethanolic solution was decanted as it contained any unreacted perchlorate salt and the metal complex was washed with several batches of dry ether. This protocol was used for the formation of all metal complexes.

Manganese complexes

Complexation around the metal centres within this class involves six nitrogen ligators, three tertiary amine from the tacn ring, and three coordinated bonds from the pendant aniline groups. Each set of donor nitrogen's occupy three *cis* sites on the manganese, thus forming three five membered rings. Wentworth *et al*[83] have shown that trigonally prismatic geometries are adopted by compounds that have empty, half-filled or full d-orbitals ($d^{0/5/10}$). Octahedral orientations are adopted when a complex has ligand field stabilisation energy.

The average manganese-nitrogen bond lengths shown (L^2-2.256Å, L^3-2.264Å) are all comparable to the other literature compounds of Weihe[115], bis (2-pyridylmethyl)amine (2.261Å) and Li[84], trisethylenediamine manganese (2.272Å). The twist angles (Φ) are $[(L^1)Mn](ClO_4)_2$ =20.8°, $[(L^2)Mn](ClO_4)_2.MeCN$ =35.6° and $[(L^3)Mn](ClO_4)_2$ =12.4°. The geometry is nearing trigonal prismatic as the ligand system approaches the *othro* fluorine ligand (L^3). Preference for the trigonal prismatic geometry has been observed with N_6 hexadentate ligand 1, 4, 7-triazacyclononane-*N*, *N'*, *N''*-triacetate[85]. The $[(L^1)Mn](ClO_4)_2$ bond lengths are found to be the longest with an average of 2.292Å. The chelate formed upon complexation with L^1 (Figure 3.16) generates a conformation which we assign to be (λλλ). As this was found to crystallise in a chiral fashion (C_3), no crystals of (δδδ) orientation were found in the crystal lattice. The chelates formed for $L^{2/3}Mn$ (Figure 3.16) were found to be achiral in the crystal lattice due to a centre of inversion within the crystal cell.

[83] Gillum W O., Wentworth R A D., Childers R F., *Inorg. Chem.*, **1970**, 9, 1825-1832.
[84] Li J., *Inorg. Chim. Acta.*, 273, **1998**, 310-315.
[85] Van Der Meuwe M J., Boeyens J C A., Hancock R D., Inorg. Chem., 1983, 22, 1208.

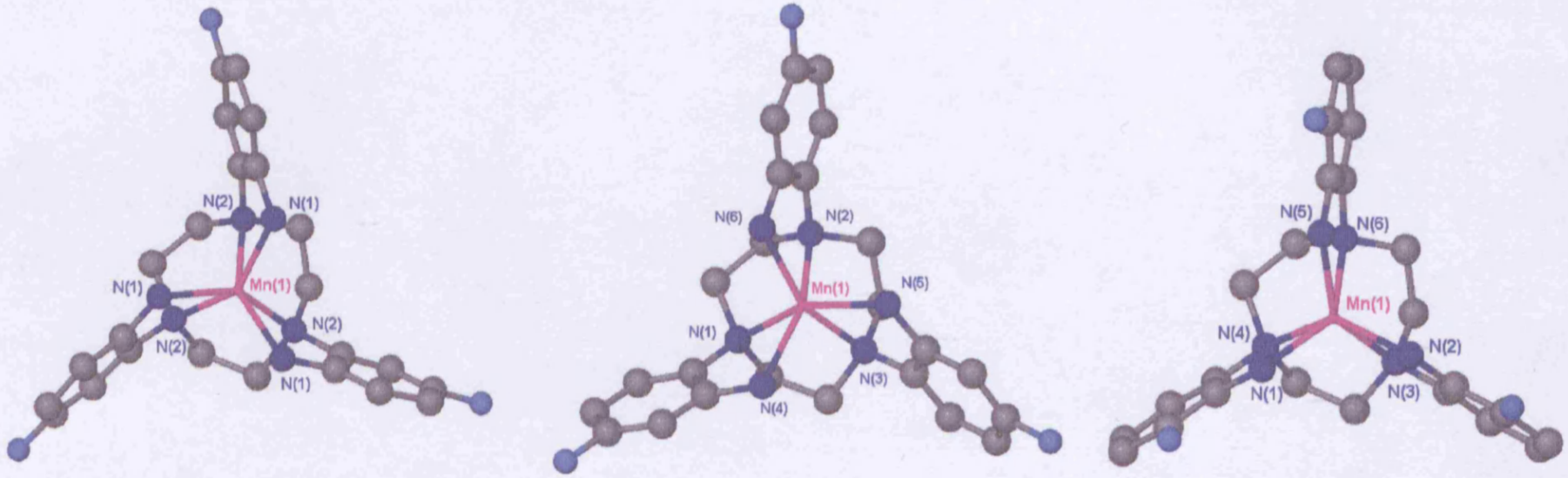

$[(L^1)Mn](ClO_4)_2$ **$[(L^2)Mn](ClO_4)_2.MeCN$** **$[(L^3)Mn](ClO_4)_2$**

Figure 3.16: $[(L^1)Mn](ClO_4)_2$ selected bond lengths; N(1)-Mn(1) 2.219(3), N(2)-Mn(1) 2.308(3). Crystal configuration is of the geometry (Λ). $[(L^2)Mn](ClO_4)_2.MeCN$ selected bond lengths; N(1)-Mn 2.308(3), N(2)-Mn 2.274(3), N(3)-Mn 2.309(3), N(4)-Mn 2.220(3), N(5)-Mn 2.205(3) and N(6)-Mn 2.222(3). Crystal configuration is of the geometry (Δ). $[(L^3)Mn](ClO_4)_2$ selected bond lengths; N(1)-Mn(1) 2.270(3), N(2)-Mn(1) 2.239(3), N(3)-Mn(1) 2.333(3), N(4)-Mn(1) 2.320(3), N(5)-Mn(1) 2.257(3), N(6)-Mn(1) 2.331(3). Crystal configuration is of the geometry (Δ). Hydrogen atoms, counter ions and solvent molecules have been removed for clarity.

We were able to synthesize $[(L^9)M](ClO_4)_2$, (M=Mn/Zn) metal complexes which exhibit a single fluorinated aniline. Reaction of the aza-macrocycle with two equivalents of 2-fluoronitrobenzene and base afforded the bis substituted ligand after acid-base work up. Further reaction with one equivalent of 2, 4-difluoronitrobenzene generated the mono fluoro derivative. Hydrogenation under standard conditions and reaction in the same manner as listed before afforded the mono fluorinated complexes.

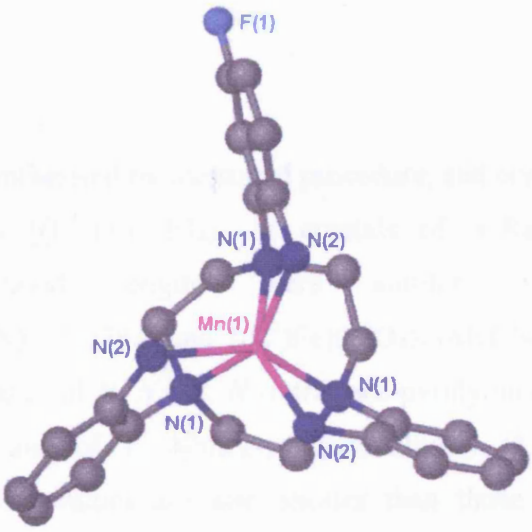

Figure 3.17. $[(L^9)Mn](ClO_4)_2$. Hydrogen atoms and counter ions have been removed for clarity. Due to 1/3 occupancy per cell, the fluorine atom is shown on one phenyl ring as 3/3 occupancy. Selected Bond Lengths; N(1)-Mn(1) 2.313(4), N(2)-Mn(1) 2.216(4).

The $[(L^9)Mn](ClO_4)_2$ complex exhibits a Φ of 22° therefore a pseudo trigonal-prismatic environment. This complex is highly comparable with it's triply fluorinated $[(L^1)Mn](ClO_4)_2$ analogue. With its Φ of 21°, chelate configuration and natural orientation the mono fluorinated version exhibits exactly the same geometrical preferences as $[(L^1)Mn](ClO_4)_2$. The chelates formed are of the configuration ($\lambda\lambda\lambda$). This type of crystal packing has shown to be highly organised as the single fluorine atom is found to have 1/3rd occupancy within the cell. The Mn-$N_{aniline}$ and Mn-N_{ring} bond lengths show minimal deviation from $[(L^1)Mn](ClO_4)_2$ structure.

	L^9	L^1
$Mn\text{-}N_{Ring}$	2.313Å	2.308Å
$Mn\text{-}N_{Aniline}$	2.216Å	2.219Å

Figure 3.18: Comparison of $Mn\text{-}N_{Ring/Aniline}$ average bond lengths for the mono fluorinated (L^9) and triply fluorinated (L^1) complexes

Iron complexes

All complexes were synthesised by the stated procedure, and crystal data collected for all complexes except $[(L^3)Fe](ClO_4)_2$ as crystals of X-Ray quality were not forthcoming. The bond lengths were similar with averages of $[(L^1)Fe](ClO_4)_2.(MeCN)$ =1.978Å and $[(L^2)Fe](ClO_4)_2.(MeCN)$=1.983Å. These are comparable with averages of *N, N, N', N'*-tetrakis(2-pyridylmethyl)ethylene-diamine (1.978Å)-Toftlund[116], and of 1, 4-bis(2-pyridylmethyl)-1, 4, 7-triazacyclononane (1.988Å)-Spiccia[118]. The values are also shorter than those found in the parent $[(L^{33})Fe](ClO_4)_2.(MeCN)$ (2.103Å), and so more indicative of Fe^{II} low spin compounds (~2.00Å). The Φ for the crystal structures obtained were both similar with $[(L^1)Fe](ClO_4)_2.(MeCN)$ =47.5°and $[(L^2)Fe](ClO_4)_2.(MeCN)$ =46.6°. These angles are the closest of this class of complex to octahedral geometry. From the crystal data generated, we can assign the chelate geometry to be (δδδ) $[(L^1)Fe](ClO_4)_2.(MeCN)$ and (λλλ) $[(L^2)Fe](ClO_4)_2.(MeCN)$ for the figure 3.19. Both crystal structures were found to be of an achiral spacegroup, therefore having both compounds with both chelates formed within the same crystal lattice. The compound $[(L^1)Fe](ClO_4)_2.(MeCN)$ was the only metal complex for this ligand (L^1) to not complex in a chiral spacegroup.

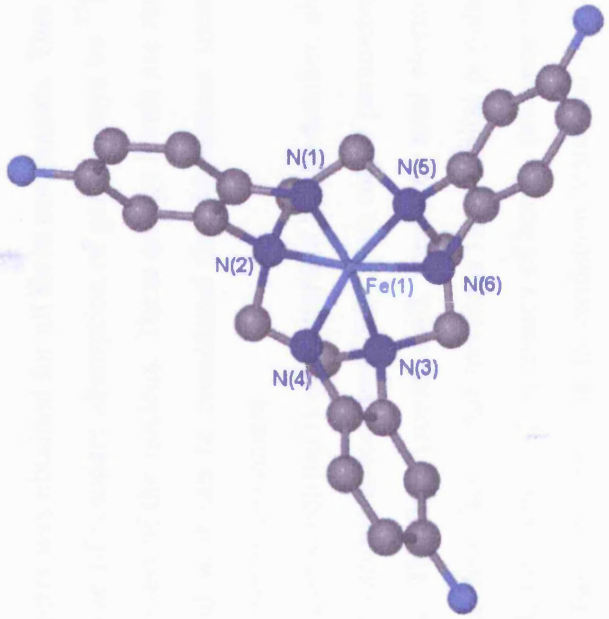

[(L^1)Fe](ClO$_4$)$_2$.MeCN

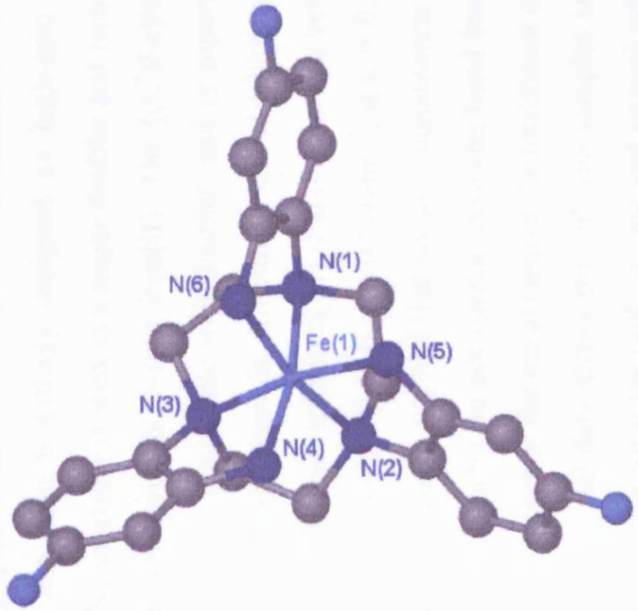

[(L^2)Fe](ClO$_4$)$_2$.MeCN

Figure 3.19: [(L^1)Fe](ClO$_4$)$_2$.MeCN selected Bond Lengths; N(1)-Fe 1.839(4), N(2)-Fe 2.004(4), N(3)-Fe 2.033(4), N(4)-Fe 2.000(4), N(5)-Fe 1.991(4) and N(6)-Fe 2.008(4). Crystal configuration is of geometry (Λ). [(L^2)Fe](ClO$_4$)$_2$.MeCN selected Bond Lengths; Fe-N(1) 2.011(4), Fe-N(2) 2.013(4), Fe-N(3) 2.006(4), Fe-N(4) 1.960(4), Fe-N(5) 1.951(4) and Fe-N(6) 1.957(4). Crystal configuration is of geometry (Δ). Hydrogen atoms, counter ions and solvent molecules have been removed for clarity.

The ^{57}Fe Mossbauer spectra was obtained for all three compounds. This spectroscopic technique employs the use of resonant absorption of gamma rays by ^{57}Fe in order to investigate the energy levels of the nucleus. These energy levels are modified by the nuclei's environment and so it can be considered that Mossbauer spectroscopy uses the nucleus to probe its own environment.

A typical Mossbauer spectrum is characterised by the number, shape, position, and relative intensity of various absorption lines. Two major parameters are used in Mossbauer spectroscopy. The first, isomer shift, measures total electron density (s-electrons) at the nucleus. Any factor that increases the s-orbital population will also increase the isomer shift. i.e. increased covalency of bonds, presence of lone pairs of electrons with high S-character, increase in oxidation state and a decrease in co-ordination number. The second parameter, quadrupole splitting, gives information on the electric field gradient. The quadrupole splitting therefore reflects the symmetry of the bonding environment and the local structure of the Mossbauer atom.

Dr Dave Evans of the John Innes Centre, Norwich, ran the Mossbauer Spectroscopy of the iron complexes and from the results, derived the d-orbital configuration of the metal centres. The $[(L^1)Fe](ClO_4)_2.(MeCN)$ Mossbauer spectrum shows two overlapping quadrupole split doublets. The second doublet is very broad and so the complex has been tentatively assigned as high-spin iron (III). The $[(L^2)Fe](ClO_4)_2.(MeCN)$ spectrum is seen as a major doublet and two minor doublets. These values are consistent with high-spin iron(II). The $[(L^3)Fe](ClO_4)_2$ spectrum exhibits a major feature of a quadrupole split doublet, and is superimposed upon a broad unresolved feature. Assignment is difficult of the *d*-orbital arrangement and could be low-spin iron(II) or high-spin iron(III). Parameters are very similar to the mossbauer recorded for $[(L^{33})Fe](ClO_4)_2$ (i.s. = $0.56mms^{-1}$, q.s. = $0.20mms^{-1}$). From all the mossbauer spectra obtained, we feel that some contamination has occurred as crystal data and mossbauer spectra do not concur. Average bond lengths found from the crystal data are not indicative of the metal centres the mossbauer seems to suggest. The single crystal X-Ray crystal data shows that all iron samples are low spin Fe^{II}. The mossbauer samples are ran from the bulk sample and ground with boron nitride. Possible oxidation of the samples upon preparation shows the air-sensitive nature of the compounds and is confirmed by the mossbauer data.

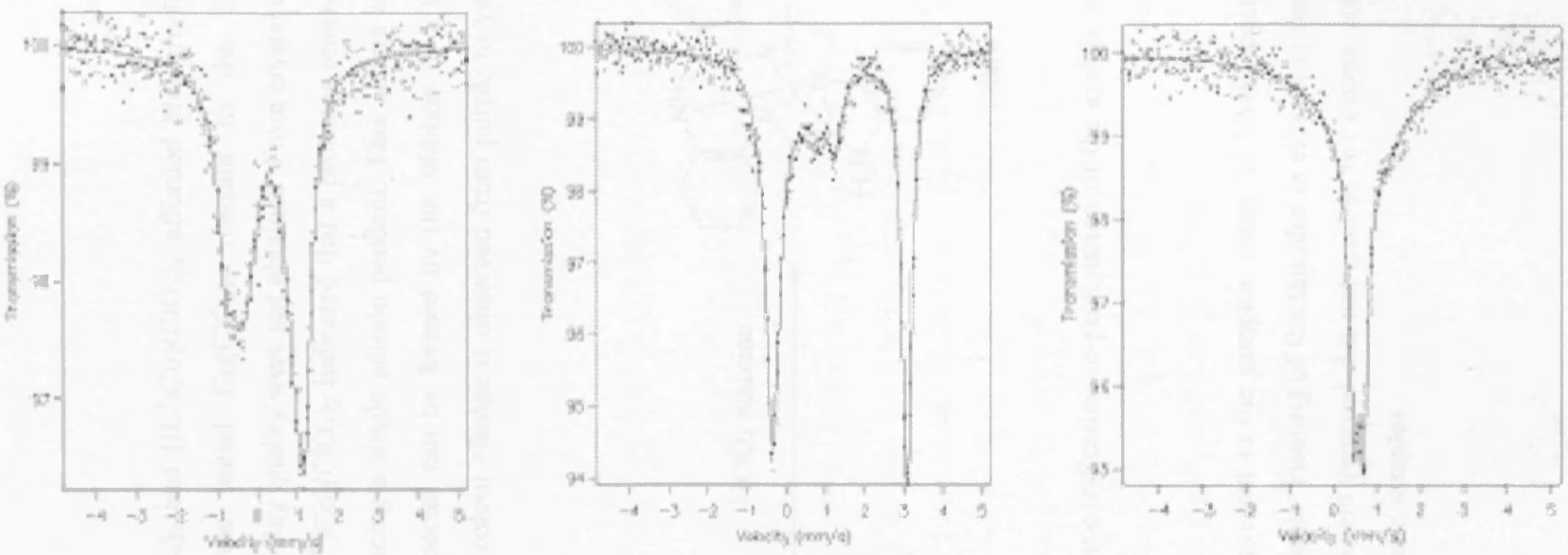

$[(L^1)Fe](ClO_4)_2.1(MeCN)$ **$[(L^2)Fe](ClO_4)_2.1(MeCN)$** **$[(L^3)Fe](ClO_4)_2$**

Figure 3.20: The Mossbauer spectra for $[(L^1)Fe](ClO_4)_2.(MeCN)$, $[(L^2)Fe](ClO_4)_2.(MeCN)$ and $[(L^3)Fe](ClO_4)_2$.

	$[(L^1)Fe](ClO_4)_2.1(MeCN)$	$[(L^2)Fe](ClO_4)_2.1(MeCN)$	$[(L^3)Fe](ClO_4)_2$
Isomer shift (mms^{-1})	0.19 and 0.34	1.36	0.57
Quadrupole splitting (mms^{-1})	1.95 and 1.31	3.43	0.23
Assigned d electron configuration	High spin Fe^{III}	High spin Fe^{II}	Low spin Fe^{II}/High spin Fe^{III}

Cobalt complexes

Synthesis of $[(L^1)Co](ClO_4)_2$ and $[(L^3)Co](ClO_4)_2$ afforded blue/green precipitates indicating oxidation of the initial $Co(ClO_4)_2$ reactant to the Co^{III} species. Unfortunately crystals of X-Ray quality were not obtained. From crystal data obtained by Perkins *et al*[79] for $[(L^{33\text{-}H})Co](ClO_4)_2$ indicated that a proton is removed from one of the anilines hence producing a single anilido pendant. This occurs at neutral pH, and the fully protonated species can be formed by the addition of a few drops of perchloric acid. An instant colour change is observed from purple to yellow (Figure 3.21).

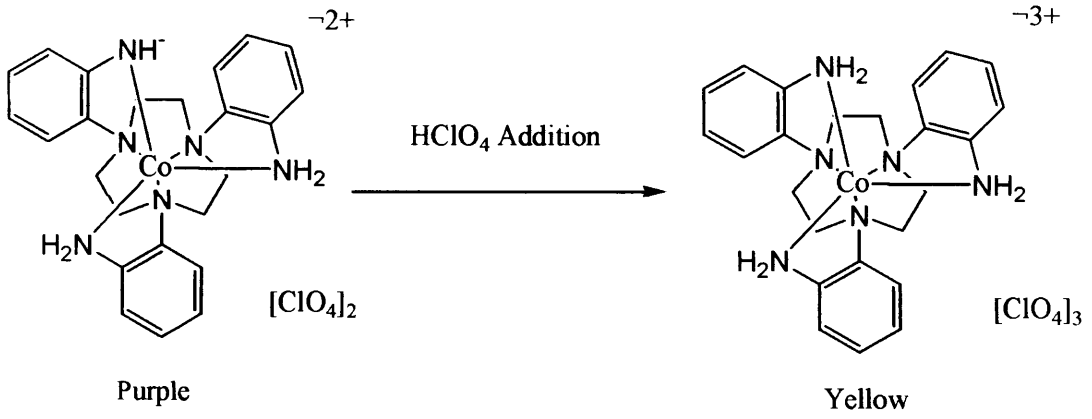

Figure 3.21: Reaction scheme indicating re-protonation of the anilide species to the amine moiety.

Due to some residual Co^{II} present in the samples, clean ^1H NMR spectra for $[(L^{1/3\text{-}H})Co](ClO_4)_2$ were unobtainable. Heating of the samples in ethanol in the presence of oxygen, then subsequent solvent removal did not oxidise the excess cobalt salts, so did not afford pure diamagnetic samples.

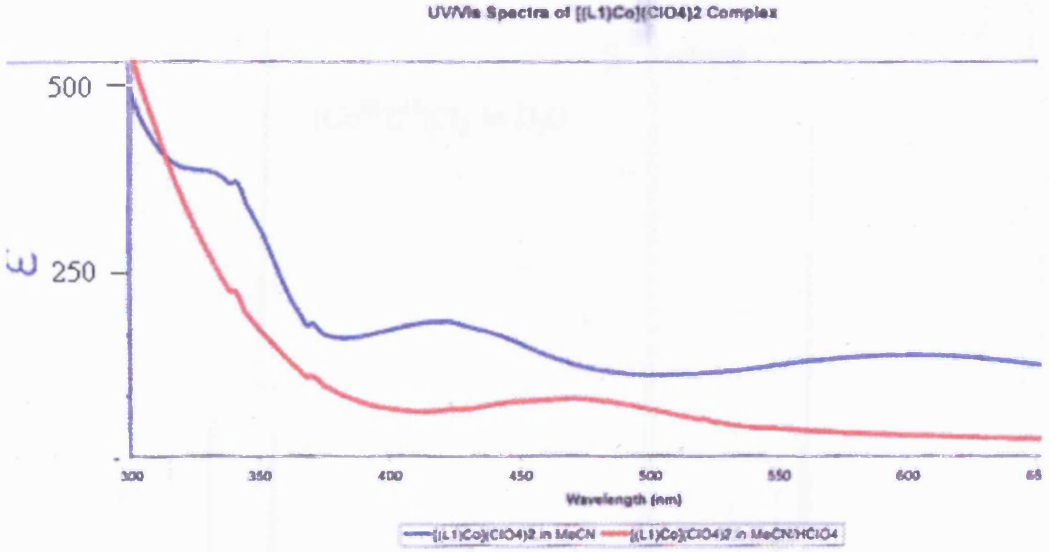

Figure 3.22: UV/Vis spectra of $[(L^1)Co](ClO_4)_2$ complex.

Both UV/Vis spectra of $[(L^1)Co](ClO_4)_2$, and $[(L^3)Co](ClO_4)_2$ (Figure 3.22) were identical and exhibited the same behaviour as the parent $[(L^{33\text{-}H})Co](ClO_4)_2$ sample. The mono deprotonated species (blue trace) has peaks at 332nm(347), 418nm(168), and 594nm(127). Upon the addition of $HClO_4$, (red trace) one peak is seen at 468nm(71). Upon the addition of NaOD to the neutral sample in the NMR tube, a purple precipitate was observed to form in the solution. We would hypothesise that this is the triply deprotonated neutral species$[(L^{33\text{-}3H})Co]$. ^1H NMR data was highly unclear with no assignable peaks.

From the ^1H NMR spectrum (Figure 3.23) it can be seen that there are three sets of protons in the aliphatic region which integrate to 3:3:6.

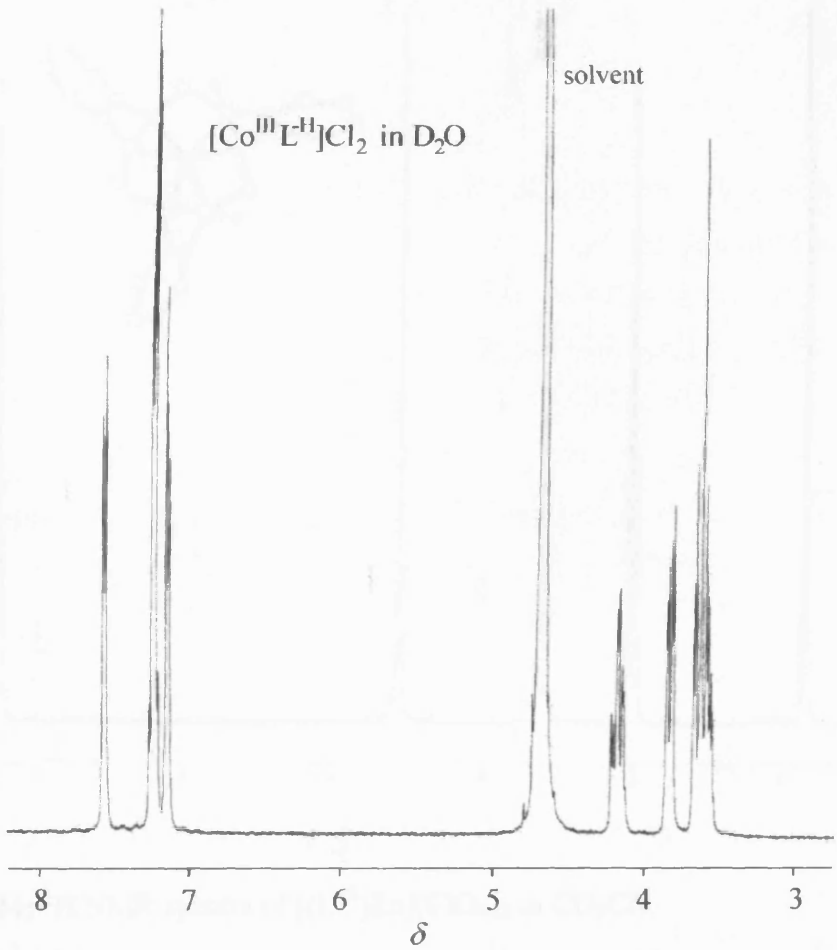

Figure 3.23: ^{1}H NMR spectra of $[(L^{33\text{-}H})Co]Cl_2$ in D_2O.

The unusual aliphatic arrangement observed we hypothesise to be protons present on the tacn ring to be of three differing environments. Further in depth investigation by ^{1}H NOE NMR must be carried out to confidently assign these protons. The ^{1}H NMR spectra of the free amine ligand shows a single aliphatic peak (12 protons on macrocylic ring). Upon complexation, the aliphatic protons are locked into a tetrahedral arrangement and therefore generate different signals in the aliphatic region of the 1H NMR spectra. From the crystal structure obtained by Perkins the Φ for $[L^{33}Co^{-H}]$ is 51°. This indicates an almost octahedral geometry, therefore the metal when complexed, may force the ligands macrocyclic ring to distort in a fashion not observed in the ^{1}H NMR of group twelve metal complexes of this class.

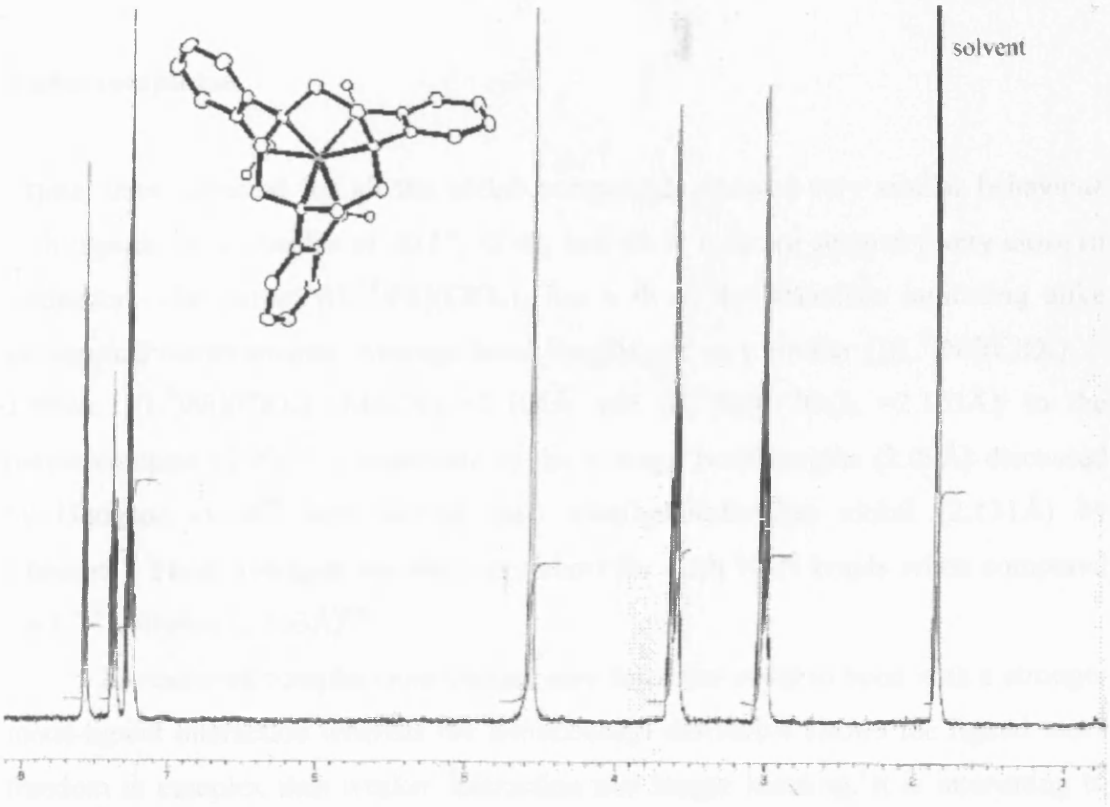

Figure 3.24: ^{1}H NMR spectra of $[(L^{33})Zn](ClO_4)_2$ in CD_3CN.

The two aliphatic peaks observed for $[(L^{x})Zn/Cd/Hg/Pb](ClO_4)_2$ complexes are assigned to the equatorial and axial protons from the macrocyclic ring and so integrate to 2 × 6H. These can be observed in the spectra above at ~3.00ppm and ~3.60ppm. We tentatively assign these to be the *endo* and *exo* protons present on the aliphatic ring, but it can evidently be seen as that the complex forms a more defined and symmetrical geometry.

Nickel complexes

Crystal data collected for all the nickel compounds showed very similar behaviour with regards to Φ. Angles of 40.3°, 43.0°, and 44.1° indicate geometry very close to octahedral. The parent $[(L^{33})Ni](ClO_4)_2$ has a Φ of 44° therefore indicating alike geometrical environments. Average bond lengths are very similar $\{[(L^1)Ni](ClO_4)_2$ = 2.099Å, $[(L^2)Ni](ClO_4)_2.(MeCN)$ =2.105Å and $[(L^3)Ni](ClO_4)_2$ =2.103Å} to the parent complex (2.09Å), comparable to the average bond lengths (2.09Å) discussed by Hodgson *et al*[86], and shorter than trisethylenediamine nickel (2.131Å) by Chesnut[87]. These averages are also very short for such Ni-N bonds when compared the L^{KW} complex (2.163Å)[88].

Its restricted complexation chelate may force the metal to bond with a stronger metal-ligand interaction whereas the aminobenzyl derivative allows the ligand more freedom to complex thus weaker interaction and longer bonding. It is interesting to note that the non-bonding distances between the ortho fluorine's show uneven puckering of the metal chelate rings. F (1)-F (2) =6.550Å, F (1)-F (3) = 7.383Å and F (2)-F (3) =8.480Å. The chelate formed is of (λλλ) for both $[(L^{2/3})Ni](ClO_4)_2$ structures shown are enanatiomorphus. As with all of the L^1 metal complexes $[(L^1)Ni](ClO_4)_2$ is found to be chiral and so only (δδδ) is found within the crystal unit cell.

[86] Arulsamy N., Glerup J., Hodgson D J., *Inorg. Chem.*, **1994**, 33, 3043-3050.
[87] Chesnut D J., Haushatter R C., Zubieta J., *Inorg. Chim. Acta.*, 292, **1999**, 41-51.
[88] Schlager O., Wieghardt K., Nuber B., *Inorg. Chem.*, **1995**, 34, 6449-6455.

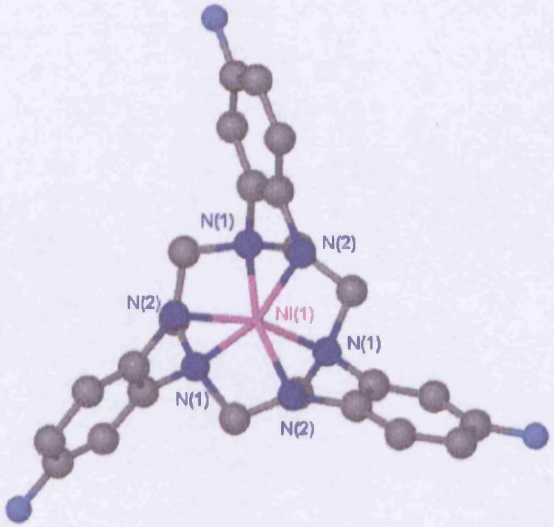

$[(L^1)Ni](ClO_4)_2$

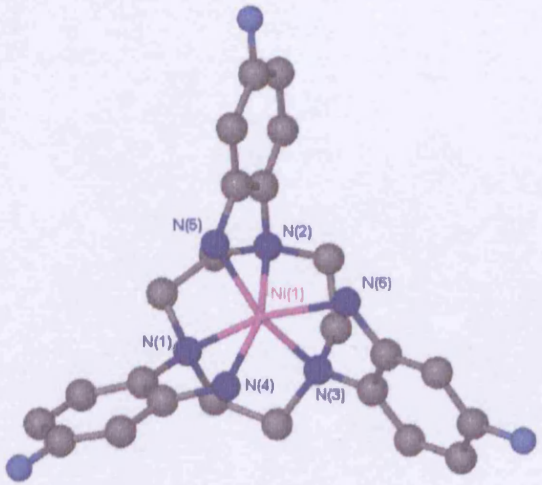

$[(L^2)Ni](ClO_4)_2.MeCN$

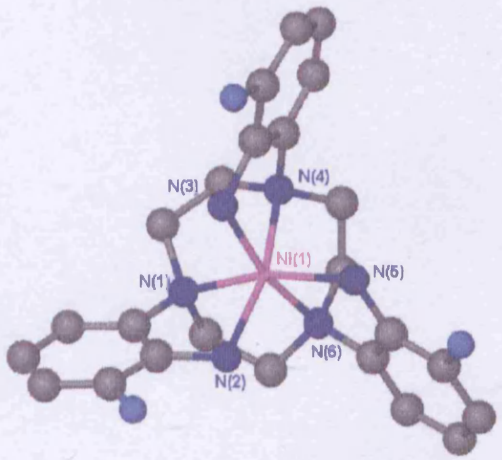

$[(L^3)Ni](ClO_4)_2$

Figure 3.25: $[(L^1)Ni](ClO_4)_2$ selected Bond Lengths; Ni(1)-N(1)2.114(3), Ni(1)-N(2) 2.092(3). Crystal configuration is of the geometry (Λ). $[(L^2)Ni](ClO_4)_2.MeCN$ selected Bond Lengths; N(1)-Ni 2.092(4), N(2)-Ni 2.112(4), N(3)-Ni 2.106(4), N(4)-Ni 2.112(4), N(5)-Ni 2.094(4) and N(6)-Ni 2.111(4). Crystal configuration is of the geometry (Δ). $[(L^3)Ni](ClO_4)_2$ selected Bond Lengths; N(1)-Ni 2.103(5), N(2)-Ni 2.089(5), N(3)-Ni 2.113(5), N(4)-Ni 2.088(5), N(5)-Ni 2.115(5) and N(6)-Ni 2.088(4). Crystal configuration is of the geometry (Δ). Hydrogen atoms, counter ions and solvent molecules have been removed for clarity.

Copper complexes

The research into copper complexes has been widely investigated, in which a geometrical distortion arises from the devised theory of Jahn-Teller. This distortion arises from the d-orbital arrangement of e_g^1 complexes (e.g.: high-spin Cr^{II}/Mn^{III}, low-spin Co^{II}/Ni^{III} and Cu^{II}). The lone electron present in the e_g orbitals can occupy the $d_{x^2-y^2}$ or d_{z^2} orbital. In a symmetrical geometry this orbital degeneracy renders the molecule unstable and so will distort to remove this degeneracy. The energy of the system is lowered by an asymmetric distortion of the complex geometry in the form of lengthening or shortening of bonds present along the z-axis. Within the d^9 configuration, Cu^{2+} complexes generally exhibit two trans bonds longer than the four equatorial bonds. The complex $[Cu(NO_2)_6]^{2+}$ exhibits this behaviour with four equatorial bonds of 2.05Å and two bonds along the *z*-axis of 2.31Å length. Theoretically a compression can also occur along the *z*-axis but complexes of this nature are very rare. This was reported first by H A Jahn and E Teller[89], and recently Falvello[90] reviews this theorem.

[89] Jahn H E., Teller E., *Proc. R. Soc. London A.*, 161, 220, **1937**.
[90] Flavello L R., *J. Chem. Soc., Dalton Trans.*, **1997**, 4463-4475.

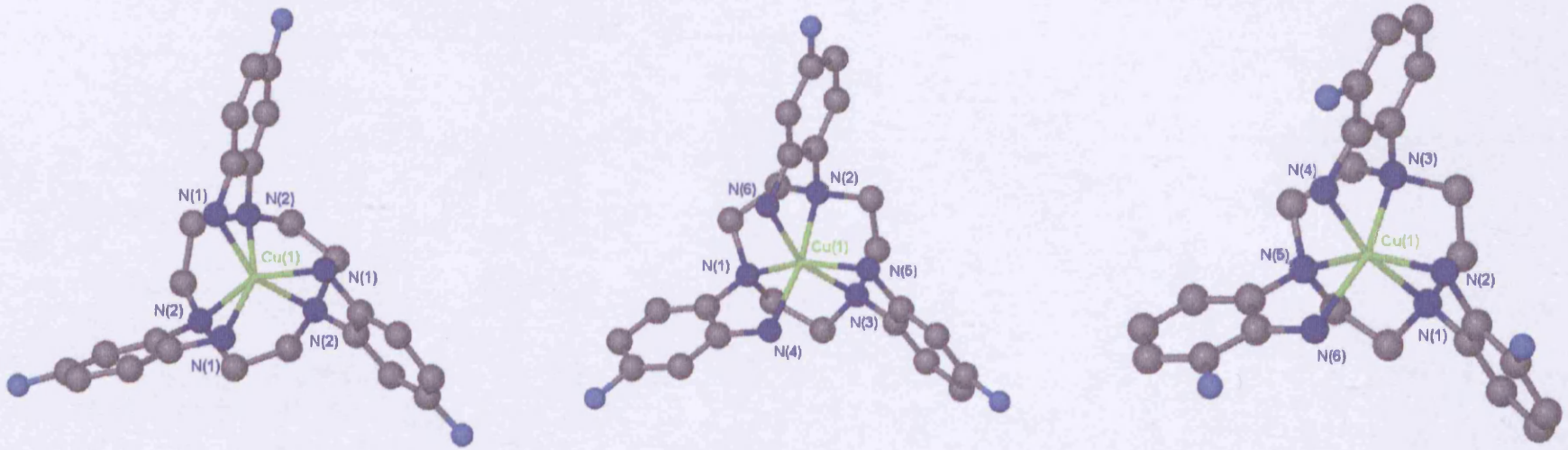

$[(L^1)Cu](ClO_4)_2$ **$[(L^2)Cu](ClO_4)_2.MeCN$** **$[(L^3)Cu](ClO_4)_2$**

Figure 3.26; $[(L^1)Cu](ClO_4)_2$ selected Bond Lengths; Cu(1)-N(1) 2.106(4), Cu(1)-N(2) 2.176(4). Crystal configuration is of the geometry (Δ). $[(L^2)Cu](ClO_4)_2.MeCN$ selected Bond Lengths; N(1)-Cu 2.090(2), N(2)-Cu 2.085(2), N(3)-Cu 2.291(2), N(4)-Cu 2.036(2), N(5)-Cu 2.095(2) and N(6)-Cu 2.249(2). Crystal configuration is of the geometry (Δ). $[(L^3)Cu](ClO_4)_2$ selected Bond Lengths; Cu-N(1) 2.094(2), Cu-N(2) 2.244(2), Cu-N(3) 2.107(2), Cu-N(4) 2.024(2), Cu-N(5), 2.236(2) and Cu-N(6) 2.111(2). Crystal configuration is of the geometry (Δ). Hydrogen atoms, counter ions and solvent molecules have been removed for clarity

The dynamic Jahn-Teller effect is observed in compounds where this effect is "dampened out" and so not displayed. This symmetry is the result of time-averaged distortions that arises from the electronic-vibrational coupling. Distortions of this kind are very rare and to date only a few compounds have been synthesised which show this non-distortion. Parker *et al* [91] have shown that in a C_3 symmetric tris phosphinic acid tacn species the Jahn-Teller distortion can be suppressed. Other such compounds have been investigated by Cullen[92,93], Bertini[94] and Sheldon[95].The $[(L^1)Cu](ClO_4)_2$ complex has revealed an interesting result. $[(L^1)Cu](ClO_4)_2$ (Figure 3.23) displays two sets of bond lengths, the metal-macrocycle ring, metal-aniline bonds, and crystallises in the chiral cubic space group P21/3. The crystal structure shows that in the solid state this compound exhibits a dynamic Jahn-Teller distortion. The lack of a Jahn-Teller effect is observed for this compound and further investigation to fully research the true nature of the complex must be carried out by Q-band EPR spectroscopy. $[(L^2)Cu](ClO_4)_2.(MeCN)$ (Figure 3.26) exhibits similar pairs of bond lengths comparable to the parent ligand $L^{33}Cu$. N6-Cu-N3=2.249+2.291Å (long x axis), N5-Cu-N1=2.095+2.090Å (medium Y axis), and N4-Cu-N2=2.036+2.085Å (short z axis). These three pairs of bond length sets indicate a distorted rhombic system. This is stated as the medium and short bond groups are very close in length and the N6 and N3 donors are very long within the complex. The $[(L^3)Cu](ClO_4)_2$ structure (Figure 3.26) also exhibits a pronounced rhombic distortion. The three sets of bond lengths are N2-Cu-N5=2.244Å+2.236Å (Long x axis), N6-Cu-N3=2.111Å+2.107Å (medium y axis) and N4-Cu-N1=2.024Å+2.094Å (short z axis). The average bond lengths for the copper compounds ($L^{1/2}$=2.141Å, L^3=2.136Å) were all found to be shorter than trisethylenediamine copper[96] (2.160Å). The non-bonding distances for the ortho fluorine's are F (1)-F (2) =6.768Å, F (2)-F (3) =6.760Å and F (1)-F (3) =6.913Å. We find these non-bonding distances to be the closet of all $[(L^3)M](ClO_4)_2$ complexes,

[91] Cole E., Parker D., Ferguson G., Gallagher J F., Kaitner B., *J. Chem. Soc., Chem. Commun.*, **1991**, 1473.
[92] Cullen D L., Lingafelter B C., *Inorg. Chem.*, 10, 6, **1971**, 1264-1268.
[93] Cullen D L., Lingafelter E C., *Inorg. Chem.*, 9, 8, **1970**, 1858-1864.
[94] Bertini I., Dapporto P., Gatteschi D., Scozzafava A., *J. Chem. Soc., Dalton Trans.*, **1979**, 1409-1414.
[95] Sheldon R I., Jircitano A J., Beno M A., Williams J M., Mertes K B., *J. Am. Chem. Soc.*, **1983**, 105, 3028-3031.
[96] Bertini I., Dapporto P., Gatteschi D., Scozzafava A., *J. Chem. Soc., Dalton Trans.*, **1979**, 1409.

indicating an even geometry within the structure. The chelate formed is of (λλλ) for both $[(L^{2/3})Cu](ClO_4)_2$ structures shown that they are enantiomorphous. As with all of the L^1 metal complexes $[(L^1)Cu](ClO_4)_2$ is found to be chiral and so only (δδδ) is found within the crystal unit cell.

Zinc complexes

The crystal structures of $[(L^2)Zn](ClO_4)_2.(MeCN)$ (Figure 3.27) and $[(L^3)Zn](ClO_4)_2$ were obtained and the values of Φ indicate geometry closer to octahedral than trigonal prismatic. The Φ for $[(L^2)Zn](ClO_4)_2.(MeCN)$ and $[(L^3)Zn](ClO_4)_2$ were 38.4° and 37.4° respectively, whereas the geometry for $[(L^1)Zn](ClO_4)_2$ could be best described as an intermediate between octahedral and trigonal prismatic as it has a Φ of 25.8°. The parent complex $[(L^{33})Zn](ClO_4)_2$ is much closer to octahedral than trigonally prismatic with a Φ of 50°. Upon complexation five membered chelates are formed between the *N*-aryl *ortho* aniline and the tacn backbone. Due to the rigidity of this system it may be restricting the complex to adopt a natural trigonally prismatic geometry as when compared to the L^{KW} complexes researched by Wieghardt *et al*[133]. The 6 membered chelates formed show more flexibility and so the Zn complex has a Φ of 13.6°. The non-bonding distances are F (1)-F (2) =6.875Å, F (1)-F (3) =7.030Å and F (2)-F (3) =6.933Å. The chelate formed upon complexation is of (λλλ) for both $[(L^{2/3})Zn](ClO_4)_2$ structures. They are both of an achiral spacegroup so are enantiomorphous. As with all of the L^1 metal complexes $[(L^1)Zn](ClO_4)_2$ is found to be chiral and so only (λλλ) is found within the crystal unit cell.

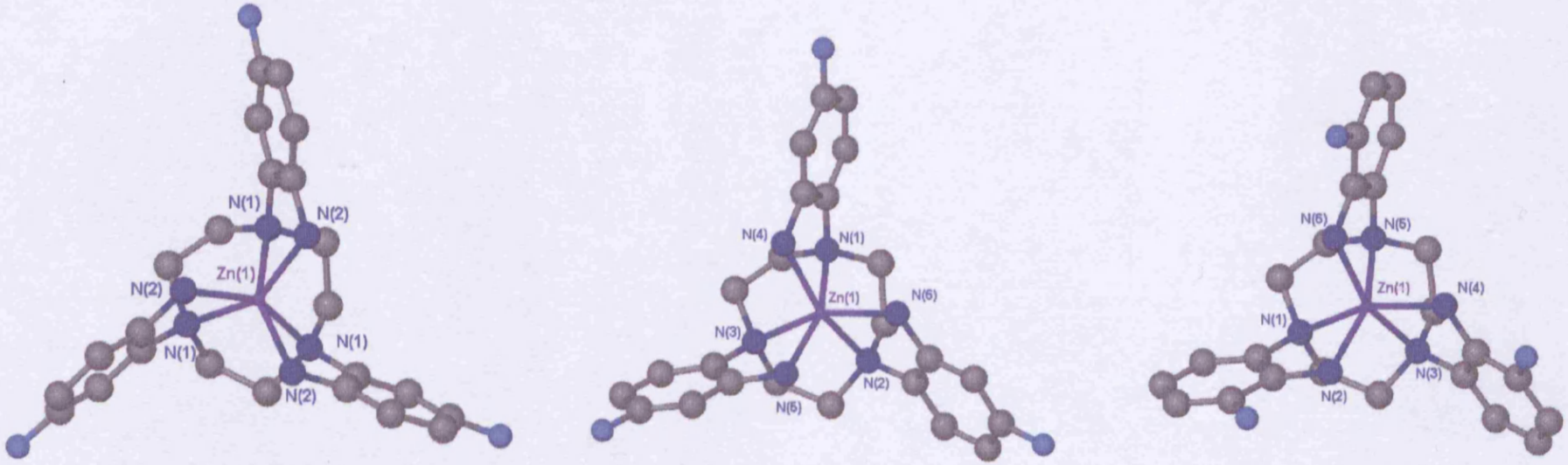

$[(L^1)Zn](ClO_4)_2$ **$[(L^2)Zn](ClO_4)_2.MeCN$** **$[(L^3)Zn](ClO_4)_2$**

Figure 3.27. $[(L^1)Zn](ClO_4)_2$ selected bond lengths; Zn(1)-N(1) 2.241(3), Zn(1)-N(2) 2.125(2). Crystal configuration is of the geometry (Λ). $[(L^2)Zn](ClO_4)_2.MeCN$ selected bond lengths; N(1)-Zn 2.218(3), N(2)-Zn 2.182(3), N(3)-Zn 2.227(3), N(4)-Zn 2.130(3), N(5)-Zn 2.117(3) and N(6)-Zn 2.143(3). Crystal configuration is of the geometry (Δ). $[(L^3)Zn](ClO_4)_2$ selected bond lengths; Zn-N(1) 2.187(3), Zn-N(2) 2.158(3), Zn-N(3) 2.205(3), Zn-N(4) 2.120(3), Zn-N(5) 2.194(3) and Zn-N(6) 2.143(3).Crystal configuration is of the geometry (Δ). Hydrogen atoms, counter ions and solvent molecules have been removed for clarity.

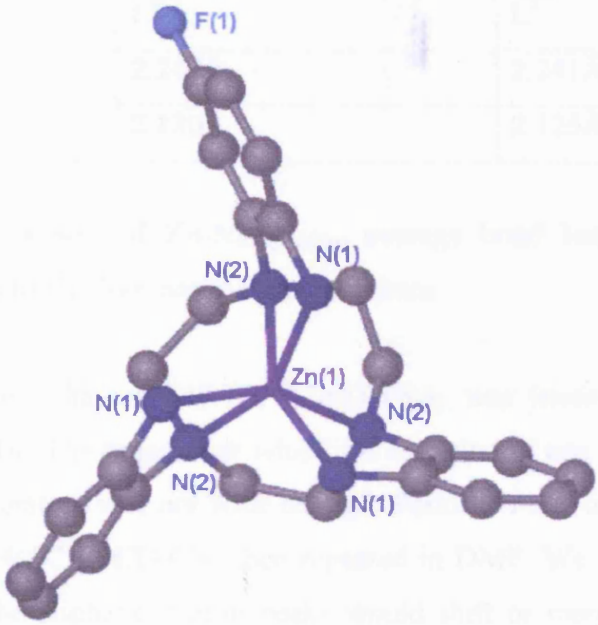

Figure 3.28. $[(L^9)Zn](ClO_4)_2$. Hydrogen atoms and counter ions have been removed for clarity. Due to 1/3 occupancy per cell, the fluorine atom is shown on one phenyl ring as 3/3 occupancy. Selected Bond Lengths; Zn(1)-N(1) 2.130(5), Zn(1)-N(2) 2.247(5).

The $[(L^9)Zn](ClO_4)_2$ complex exhibits a Φ of 27° and is very similar to $[(L^9)Zn](ClO_4)_2$ with 26°. Its chelate configuration is $\lambda\lambda\lambda$ and natural orientation is Λ. It is found to crystallise in a chiral spacegroup, therefore no Δ enantiomers are found in the cell. This type of crystal packing has again shown to be highly organised as the single fluorine atom is found within the cell as 1/3rd occupancy. The average bond lengths (L^1=2.183Å, L^2=2.170Å, L^3=2.168Å) are shorter in this class of compounds when compared to trisethelenediamine zinc[97] (2.190Å). This could be due to the increased electron density present with the *ortho*-phenylenediamine analogous ligands we have synthesised. As can be seen from figure 3.29, the bond lengths between the L^9 and L^1 complexes are highly similar.

[97] Li J., *Inorg. Chim. Acta.*, 273, **1998**, 310-315.

	L^9	L^1
$Zn\text{-}N_{Ring}$	2.247Å	2.241Å
$Zn\text{-}N_{Aniline}$	2.130Å	2.125Å

Figure 3.29: Comparison of $Zn\text{-}N_{Ring/Aniline}$ average bond lengths for the mono fluorinated (L^9) and triply fluorinated (L^1) complexes.

The solution behaviour of $[(L^{33})Zn](BPh_4)_2$ was investigated by variable temperature ^1H NMR. The range over which the experiment was carried out initially, upon further consideration was not wide enough. Perkins *et al*[79] originally carried out the experiment to -40°C in CD_3CN, then repeated in DMF. We envisioned at lower temperatures that the aliphatic proton peaks would shift or merge, indicating some behaviour at even lower temperatures. This data might give an insight into the nature of the fluxionality of the metal complexes.

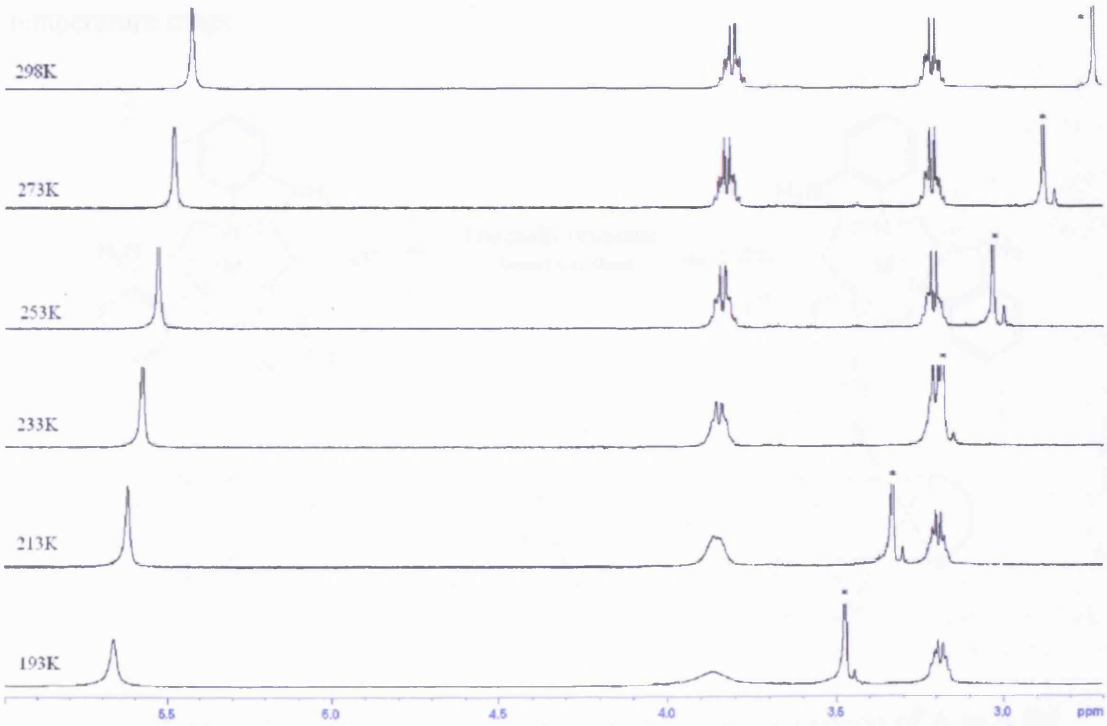

Figure 3.30: Variable Temperature ^1H NMR of $[(L^{33})Zn](BPh_4)_2$ in d_6-Acetone. Temperature range -80°C-25°C and * denotes water peak.

The initial measurement was carried out in d_7-DMF which has a lower limit of -40°C on the ^{1}H NMR machine. This sample was originally prepared as a perchlorate salt. We prepared the new sample initially from the nitrate salt, and which upon metathesis with an aqueous sodium tetraphenylborate solution afforded the tetraphenylborate salt. The white solid was dissolved in d_6-acetone and so gave us a lower limit of -80°C.

As can be observed in figure 3.30, upon cooling to -80C, the amine proton singlet shifts upfield from 5.45ppm to 5.65ppm. The aliphatic multiplet at 3.85ppm merges to a broad singlet and starts to collapse into the baseline. When it reaches 193K this aliphatic peak shifts upfield slightly from 3.80ppm to 3.85ppm. We would predict that if we could cool the solution further, then this peak would collapse fully into the baseline and a sharp singlet would rise in the centre of the previous aliphatic peak. There was a trace of residual water at 2.5ppm which shifted to 3.45ppm when cooled to -80°C. This is perhaps indicative of hydrogen bonding to the $[(L^{33})Zn]^{2+}$ cation. There was no observed change in the aromatic region over the whole temperature range.

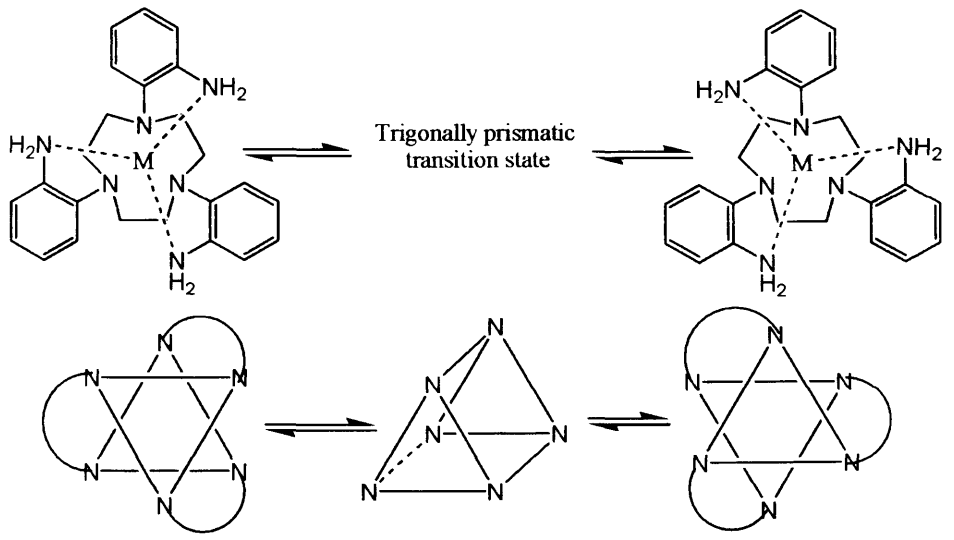

Figure 3.31: Bailar twist mechanism for interconversion of Λ to Δ for $[(L^{33})Zn]^{2+}$.

We propose that upon cooling, this fluxionality is reduced and so the stereochemical environment of the aliphatic protons approaches equivalence. At -80°C the macrocyclic protons present at 3.20ppm appear resemble the macrocyclic protons at -40°C. The rate at which these protons are merging is interesting as there are two different types present due to their position on the tacn ring. If we were able to run the ^{1}H NMR at a lower temperature, we feel that the aliphatic protons would resemble broad peaks, then collapse to the baseline, then rise as two singlets at ~3.85ppm and ~3.15ppm. Further discussion of like tacn and cyclen systems which exhibit the same behaviour has been investigated by Wainwright *et al*[98, 99, 100]. Wainwright shows this Δ↔Λ interchange with examples such as alkaline earth metal Δ-1, 4, 7, 10-tetrakis ((R)-2-hydroxy-2-phenylethyl)-1, 4, 7, 10-tetraazacyclododecane complexes[101].

Cadmium Complexes

The complexes of $[(L^{1/2/3})Cd](ClO_4)_2$ were all solved crystallographically and from this data it is observed that these complexes all exhibit geometry closest to trigonally prismatic. For $[(L^1)Cd](ClO_4)_2$ Φ =19°, $[(L^2)Cd](ClO_4)_2$ Φ = 5.8° and $[(L^3)Cd](ClO_4)_2.(MeCN)$ Φ = 2.4°. Comparison to the $[(L^{33})Cd](ClO_4)_2$ complex, the Φ of 0° displays the ideal trigonally prismatic geometry, with its fluorinated counterparts close to this value. Bond lengths for $[(L^3)Cd](ClO_4)_2$ (2.357Å) are comparable with bis (2-pyridylmethyl) amine cadmium complexes (2.350Å) synthesised by Hodgson *et al*[102], 3, 6, 14, 17, 23, 24-hexatricyclo [17.3.1.1^{8,12}] tetracosa-1 (23), 8, 10, 12, (24), 19, 21-hexaene (2.353Å) by Jackels et al[128], and tris ethylenediaminecadmium (2.35Å) by Malarova[103]. The $[(L^2)Cd](ClO_4)_2$ bond average is 2.361Å and so similar to Planalp[130] *et al*'s *N, N', N''*-tris (2-pyridylmethyl)-*cis, cis*-1, 3, 5-triaminocyclohexane (2.360Å). The $[(L^3)Cd](ClO_4)_2.(MeCN)$ complex exhibits

[98] Weeks J M., Buntine M A., Lincoln S F., Wainwright K P., *Inorg. Chim. Acta.*, 331, **2002**, 340-344.
[99] Weeks J M., Buntine M A., Lincoln S F., Tiekink E R T., Wainwright K P., *J. Chem. Soc., Dalton Trans.*, **2001**, 2157-2163.
[100] Dhillon., Lincoln S F., Madbak S., Stephens A K W., Wainwright K P., Whitbread S L., *Inorg. Chem.*, **2000**, 39, 1855-1858.
[101] Whitbread S L., Valente P., Buntine M A., Clements P., Lincoln S F., Wainwright K P., *J. Am. Chem. Soc.*, **1998**, 120, 2862-2869.
[102] Glerup J., Goodson P A., Hodgson D J., Michelsen K., Nielsen K M., Weihe H., Inorg. Chem., 1992, 31, 4611-4616.
[103] Malarova M., Kuchair J., Cernak J., *Acta. Cryst.*, **2003**, c59, m280-m282.

a bond length average of 2.372Å which is long but not uncommon as Bernhardt's[129] 6, 13-dimethyl-1, 4, 8, 11-tetraazacyclotetradecane-6, 13-diamine derivatives (2.379Å) shows similar bond lengths.

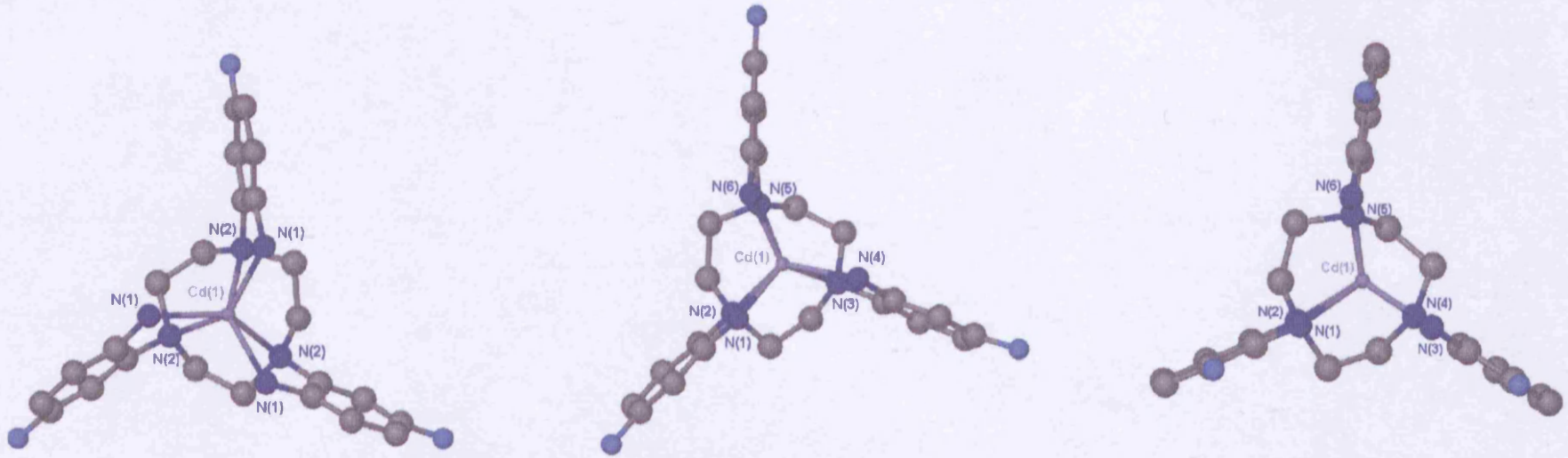

$[(L^1)Cd](ClO_4)_2$ **$[(L^2)Cd](ClO_4)_2$** **$[(L^3)Cd](ClO_4)_2.MeCN$**

Figure 3.32. $[(L^1)Cd](ClO_4)_2$ selected bond lengths; Cd(1)-N(1), 2.295(3), Cd(1)-N(2) 2.419(3). Crystal configuration is of the geometry (Λ). $[(L^2)Cd](ClO_4)_2$ selected bond lengths; Cd-N(1) 2.303(11), Cd-N(2) 2.419(10), Cd-N(3) 2.432(11), Cd-N(4) 2.283(12), Cd-N(5) 2.435(11) and Cd-N(6) 2.295(12). Crystal configuration is of the geometry (Δ). $[(L^3)Cd](ClO_4)_2.MeCN$ selected bond lengths; Cd-N(1) 2.410(4), Cd-N(2) 2.371(4), Cd-N(3) 2.293(4), Cd-N(4) 2.413(4),Cd-N(5) 2.441(4) and Cd-N(6) 2.302(5). Crystal configuration is of the geometry (Δ). Hydrogen atoms, counter ions and solvent molecules have been removed for clarity.

The non-bonding distances are F (1)-F (2) =7.724Å, F (1)-F (3) =7.843Å and F (2)-F (3) =8.149Å indicating an unequal puckering of the aromatic rings. The chelate formed is of (δδδ) for both $[(L^2)Cd](ClO_4)_2$ and $[(L^3)Cd](ClO_4)_2.(MeCN)$ structures shown but they are of an achiral spacegroup so are enantiomorphous. As with all of the L^1 metal complexes $[(L^1)Cd](ClO_4)_2$ is found to be chiral and so only (λλλ) is found within the crystal unit cell.

Mercury complexes

The fluorinated tris aniline tacn derivative of $[(L^1)Hg](ClO_4)_2$ afforded crystals of suitable for X-Ray diffraction. The mercury complex shows a geometry close to trigonal prismatic with an Φ angle of 18.7°. Although slightly smaller than the analogous Cd, we would predict the Φ for the $[(L^{2/3})Hg](ClO_4)_2$ analogues to be smaller than the Cd values and so closer to 0°.

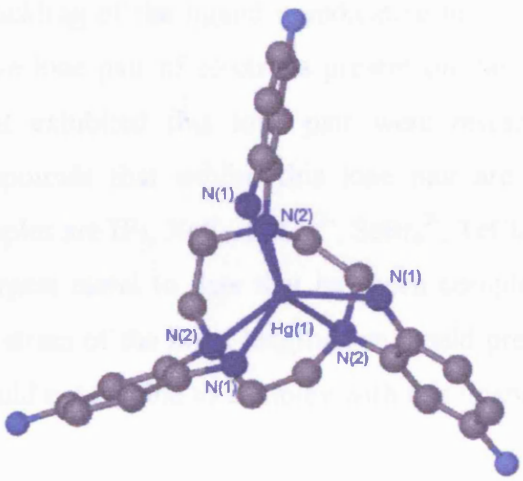

Figure 3.33. $[(L^1)Hg](ClO_4)_2$. Hydrogen atoms and counter ions have been removed for clarity. Selected Bond Lengths; Hg(1)-N(1) 2.320(5), Hg(1)-N(2) 2.509(5). Crystal configuration is of the geometry (Δ).

The complex $[(L^1)Hg](ClO_4)_2$ is found to be chiral and so only (δδδ) configuration of the chelate is found within the crystal unit cell. $[(L^1)Hg](ClO_4)_2$ was found to have an average bond length of 2.415Å which is highly comparable to the parent

$[(L^{33})Hg](ClO_4)_2$ complex (2.412Å), very similar to the L^{KW} complex[133] (2.427Å), and longer than triethylenediamine mercury perchlorate by Strasdeit[104]. Satellite peaks of ^{199}Hg isotope are either side the amine peak and exhibit coupling constants of $[(L^1)Hg](ClO_4)_2$ = 55.29Hz and $[(L^3)Hg](ClO_4)_2$ = 54.77Hz. For comparison, Wieghardt[133] reports coupling between the ^{199}Hg isotope in $[(L^{KW})Hg](ClO_4)_2$ with the amine protons (J_{HgH}=45Hz) and benzylic protons (J_{HgH}=58Hz).

Lead complexes.

The crystal data was obtained for the $[(L^3)Pb](ClO_4)_2$ complex (Figure 3.34), and produced an interesting result. The lead structure is the first of its kind for this class of compound to exhibit one of the aniline pendants to twist back against the natural rotation of the ligand, in which the complex does not conform to the usual Λ (δδδ) or Δ (λλλ) stereochemistry. All structures beforehand have been (Δ) or (Λ) in configuration. This buckling of the ligand is indicative to the accommodation of the stereochemically active lone pair of electrons present on the lead centre. Initial lead crystal structures that exhibited this lone pair were researched by Lawton and Kokotailo[105,106]. Compounds that exhibit this lone pair are generally main group compounds, and examples are IF_7, XeF_6, $SeCl_6^{2-}$, $SeBr_6^{2-}$, $TeCl_6^{2-}$ and $SbBr_6^{3-}$.

Lead is the largest metal to date that has been complexed with this class of ligand and due to the strain of the bond lengths, we would predict that metals of any larger ionic radius would not be able to complex with this ligand.

[104] Strasdeit H., Dahme A K., Weber M., Pohl S., *Acta Crystallogr.* **1992**, c48, 437.
[105] Lawton S L., Kokotailo G T., *Nature (London).*, **1969**, 221, 550.
[106] Lawton S L., Kokotailo G T., *Inorg. Chem.*, 11, 2, **1972**, 363-368.

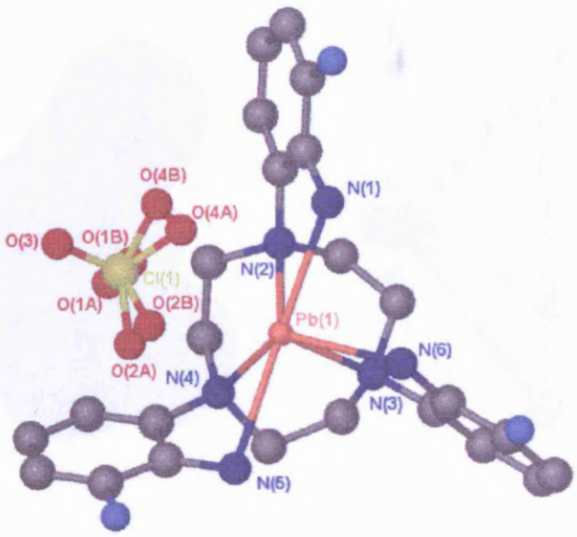

Figure 3.34. $[(L^3)Pb](ClO_4)_2$. Hydrogen atoms and one perchlorate counter ion have been removed for clarity. Selected Bond lengths; N(1)-Pb 2.691(3), N(2)-Pb 2.660(3), N(3)-Pb 2.649(3), N(4)-Pb 2.673(3), N(5)-Pb 2.697(3) and N(6)-Pb 2.539(3).

The average nitrogen-metal length for the Pb-N_{Ring} and Pb-$N_{Aniline}$ is 2.661Å, and 2.642Å respectively. This is in agreement with values in other complexes such as Schröder's[107] binuclear cofacial lead complex-2.68Å, and the "free" tacn-lead average bond lengths[108] are 2.44Å. Figure 3.35 depicts the Van Der Waals radii of the lead centre its nitrogen donors, clearly showing the cleft open on the right side.

[107] Tei L., Arca M., Aragoni M. C., Bencini A., Blake A. J., Caltagrione C., Devillanova F. A., Fornasari P., Garau A., Isaia F., Lippolis V., Schröder M., Teat S. J. and Valtanconi B., *Inorg. Chem.*, **2003**, 42, 8690-8701.
[108] Wieghardt K., Kleine-Boymann., Nuber B., Weiss J., Zsolnai L. and Huttner G., *Inorg. Chem.*. **1986**, 25, 1647-1650

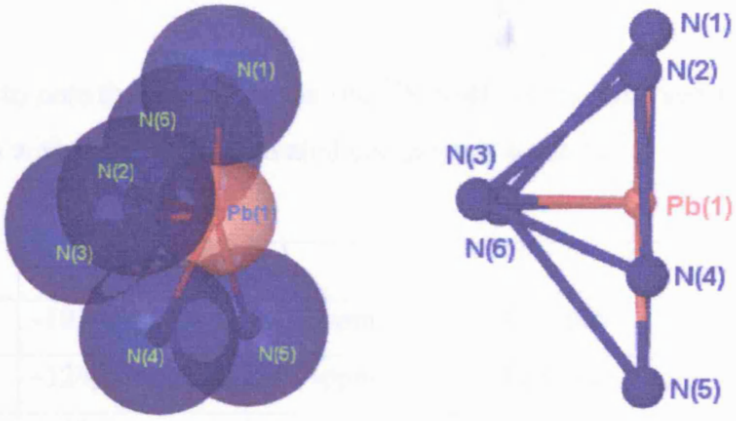

Figure 3.35. $[(L^3)Pb](ClO_4)_2$. This depicts the Van Der Waals radii of the lead and nitrogen donors at the complex centre (Left). Note the cleft of the open face of the lead centre.

The perchlorate-lead bond lengths range from 3.128Å-3.974Å. These are too long to be classed as bonds and so the complex is truly hexa-coordinated. The 1-(1-methylimidazol-2-ylmethyl)-1, 4, 7-triazacyclononane, Di Vaira[109] complex exhibits similar bonding with its perchlorate, but has shorter lengths (2.950Å-3.189Å). This we feel is due to the more flexible ligand allowing more accessibility to the lead centre, thus shorter bonding to its counterion. Our ligand is more rigid due to the phenyl rings and so this constraint prevents stronger bonding from the perchlorate ion. Other lead complexes have been synthesised which also exhibit this donor arrangement to accommodate the leads lone pairs[110, 111, 112].

[109] Di Vaira M., Guerra M., Mani F. and Stoppioni P. *J. Chem. Soc., Dalton Trans.*, **1996**, 1173-1179.
[110] Di Vaira, M., Mani F., Stoppioni P., *Eur. J. Inorg. Chem.*, **1999**, 833-837.
[111] Di Vaira M., Mani F., Stoppioni P., *J. Chem. Soc., Dalton Trans.*, **1998**, 3209-3213.
[112] Bazzicalupi C., Bianchi A., Berni E., Calabi L., Giorgi C., Mariani P., Losi P., Valtancoli B., *Inorg. Chim. Acta.*, 329, **2002**, 93-99.

^{19}F NMR shifts of mono and tris fluorinated zinc complexes.

It is of interest to note the similarities in the ^{19}F NMR shifts observed for these L^9 and L^{10} compounds with the triply fluorinated compounds L^1 and L^2.

	L^9	L^1	L^{10}	L^2
NO_2	-103ppm	-102ppm	-120ppm	-118ppm
NH_2	-124ppm	-124ppm	-123ppm	-117ppm
Zn	-112ppm	-112ppm	-114ppm	-113ppm

Figure 3.36: ^{19}F NMR comparison table for shifts.

The ^{19}F NMR shifts are very close to the triply fluorinated counterparts with only the amine version of L^{10} and L^2 slightly different (-123ppm-(-117ppm)). These trends show that when the fluorine is in the *meta* position to the amine moiety, no discernable shift is observed due to being deactivated by the amine group. The activating fluorine when *para* to the amine shows marked shifts when converted from the nitro to amine then complexed with zinc. We would expect that the mono *ortho* derivative, if synthesised would exhibit the biggest degree of shift in its ^{19}F NMR spectra.

Perchlorate counterion hydrogen bonding.

The crystal data obtained revealed that 6 structures exhibit significant hydrogen bonding with one of their perchlorate counterions. Figure 3.37 shows the lengths of the perchlorate-amine hydrogen bond distances.

Complex	Hydrogen Bond Length. (Å)	Figure
$[(L^1)Mn](ClO_4)_2$	2.186	3.38A
$[(L^1)Fe](ClO_4)_2.MeCN$	1.996+2.125+2.239	3.38B
$[(L^1)Ni](ClO_4)_2$	2.232	3.39A
$[(L^3)Ni](ClO_4)_2$	2.155+2.242	3.39B
$[(L^3)Cu](ClO_4)_2$	2.137+2.190	3.40A
$[(L^3)Zn](ClO_4)_2$	2.234+2.242	3.40B

Figure 3.37: Table of perchlorate-aniline hydrogen bond lengths.

The structures for $[(L^1)Mn](ClO_4)_2$, $[(L^1)Fe](ClO_4)_2.MeCN$, $[(L^1)Ni](ClO_4)_2$, all exhibit a "capping" mode as the three of the perchlorate oxygen's hydrogen bond to three of the exo-protons of the amine groups present on the anilines. These bond lengths are over the range of 1.996-2.239Å. The structures of $[(L^3)Ni](ClO_4)_2$, $[(L^3)Cu](ClO_4)_2$, and $[(L^3)Zn](ClO_4)_2$ all exhibit hydrogen bonding but not in the same fashion as the previous three examples. These structures show that only one oxygen on the perchlorate interacts with two amine protons on the aniline group. The counterion is now between two aniline protons and so they share the perchlorate oxygen by forming a bridging conformation. It is of interest to note that for the ligand L^3 as the fluorine is ortho to the amine and the hydrogen bonding is only through one perchlorate oxygen. We hypothesize due to the position of the fluorine, the "capping" mode of the perchlorate cannot be adopted due to electron repulsion. For the L^1 complexes the fluorine is para to the amine therefore sterically unhindered and not repulsed by the electron density of the fluorine. This space above the metal complex allows the threefold hydrogen bonding to occur. It is of interest to note that no counterion-aniline hydrogen bonding occurs with any of the cadmium compounds. In

the parent $[(L^{33})Cd](ClO_4)_2$ complex both its perchlorate counterions are seen to participate in hydrogen bonding by forming the N-H···O···H-N array. This perchlorate oxygen bridging is mirrored within the complex, but the parent complex exhibits perfect trigonal prismatic geometry with a twist angle of 0°. The complexes shown here have less than ideal twist angles (L^1=19°, L^2=6° and L^3=2°) and so the aniline protons are not as readily presented for hydrogen bonding in this fashion. The parent complex aniline protons are observed to point directly up and away from the plane of the aniline ring.

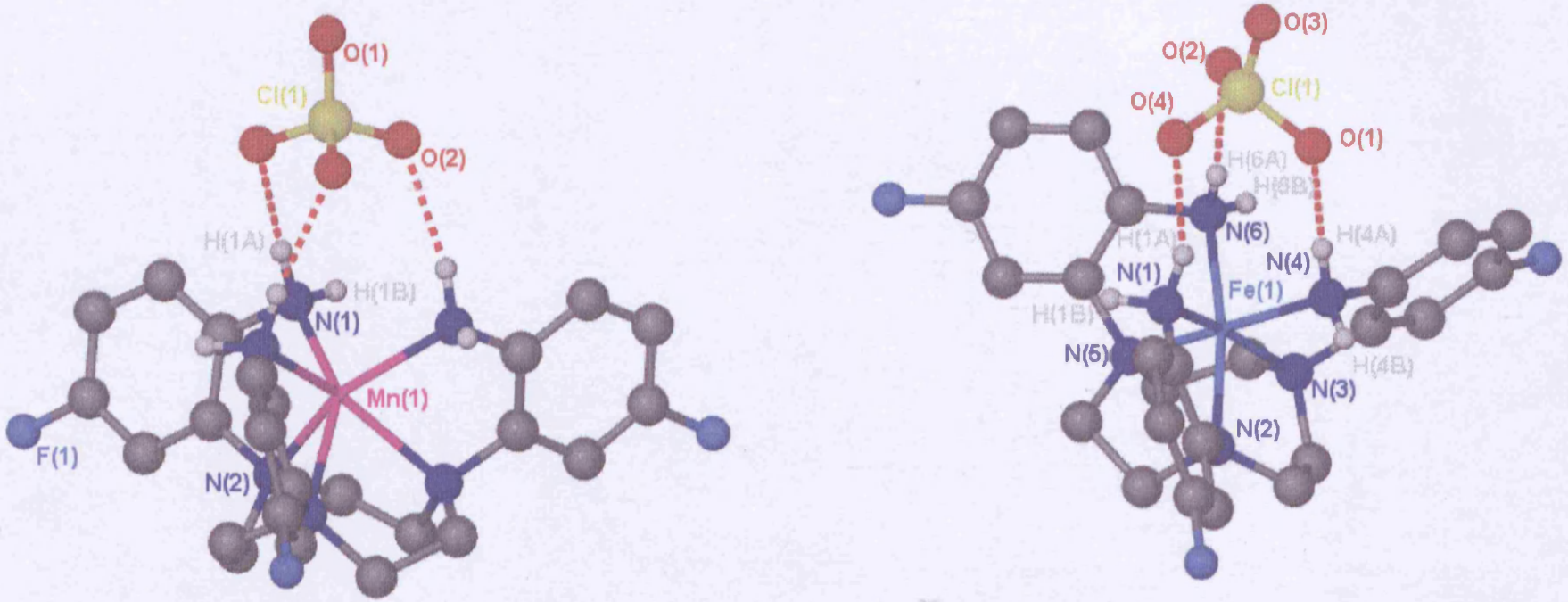

Figure 3.38: $[(L^1)Mn](ClO_4)_2$ crystal structure with one perchlorate capping the amine protons. The O-H distances are 2.186Å. $[(L^1)Fe](ClO_4)_2.(MeCN)$ crystal structure displaying the capping mode of the perchlorate counter ion. The O-H bond lengths are 1.996Å, 2.125Å and 2.239Å.

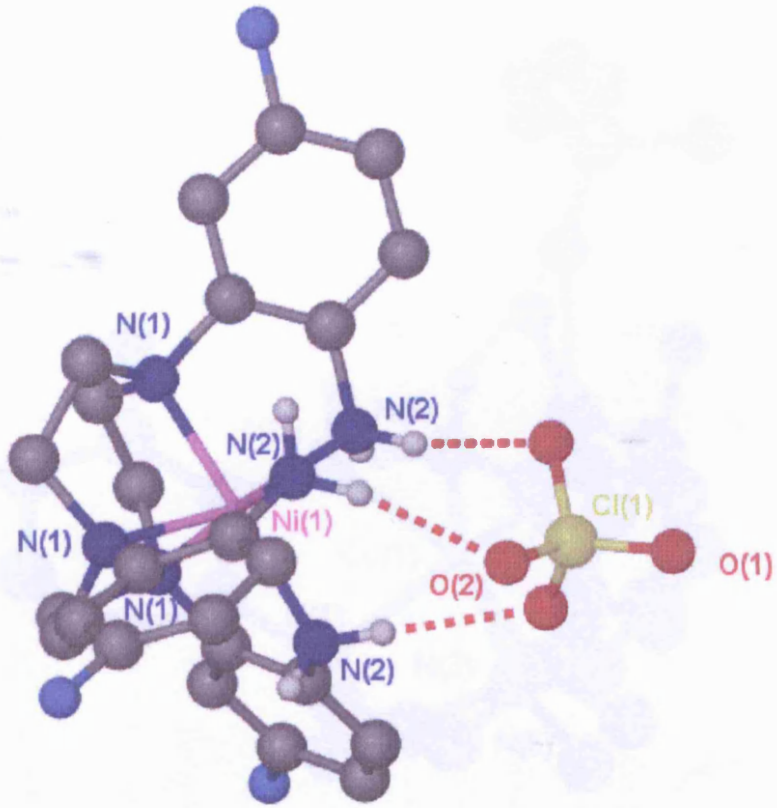

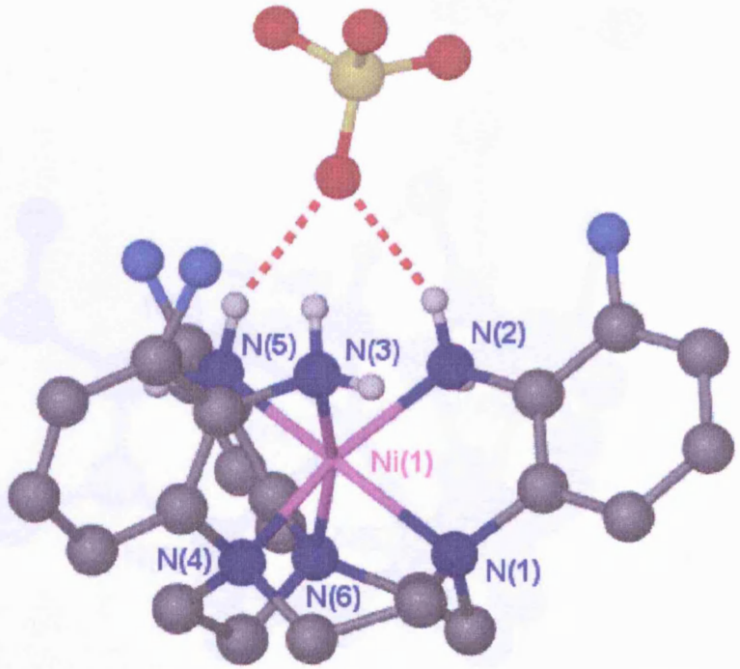

Figure 3.39: $[(L^1)Ni](ClO_4)_2$ with perchlorate counterion capping three *exo* aniline protons of a distance of 2.232Å. $[(L^3)Ni](ClO_4)_2$ perchlorate counter ion hydrogen bonding to aniline protons. Bond lengths are 2.137Å and 2.190Å.

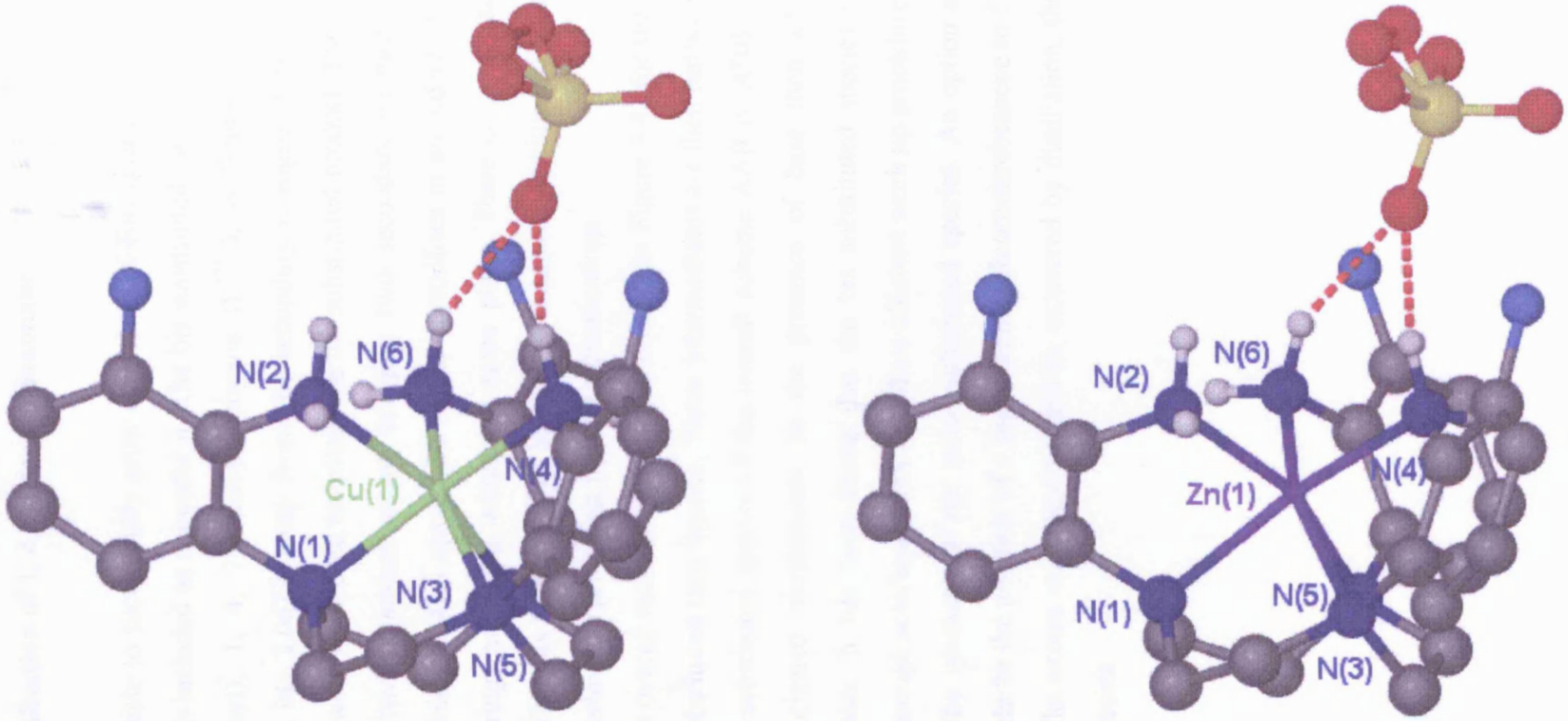

Figure 3.40: The hydrogen bonding modes between the perchlorate and the aniline protons of $[(L^3)Cu](ClO_4)_2$ and $[(L^3)Zn](ClO_4)_2$. Bond distances are 2.155Å + 2.242Å and 2.234Å + 2.242Å respectively.

Functionalisation of 1, 4, 7-triazacyclononane

We were able to successfully grow crystals of X-Ray quality of L^{32F2} and the crystal structure is included as appendix ii. The bis substituted ligand bis 1, 4-bis (2-nitro, 4-fluorophenyl), 1, 4, 7-triazacyclononane (L^{32F2}), is found to crystallise with a potassium ion 3.067Å away from the secondary nitrogen. This occurs due to the acid/base work up needed to isolate the bis-substituted product. The packing diagram indicates two potassium atoms bridging two secondary nitrogens thus the N-N distance being 4.243Å apart. The ligand crystallises in an ordered fashion, with the aromatic rings arranging within the same plane. There is no π stacking from the aromatic rings as they seem to stack in a staggered fashion and so are not directly above or below the preceding ligands aromatic rings.

An overall reaction scheme can be seen in Figure 3.41 for the routes to mono and bis substituted tacn ligands. These intermediates are then further reacted to form the triply substituted species of the overall scheme AAB or ABB. The addition of mono-fluorinated nitrobenzene in the presence of base then afforded the first intermediates. It has been found that the bis substituted species is more readily isolated through acid/base work up. More efficient work up procedures are needed to optimise the synthesis of the mono substituted species. An option available in the future could be the addition of 1 equivalent of fluoronitrobenzene to 5-10 equivalents of tacn. The excess macrocycle could be recovered by distillation, thus isolating the desired species.

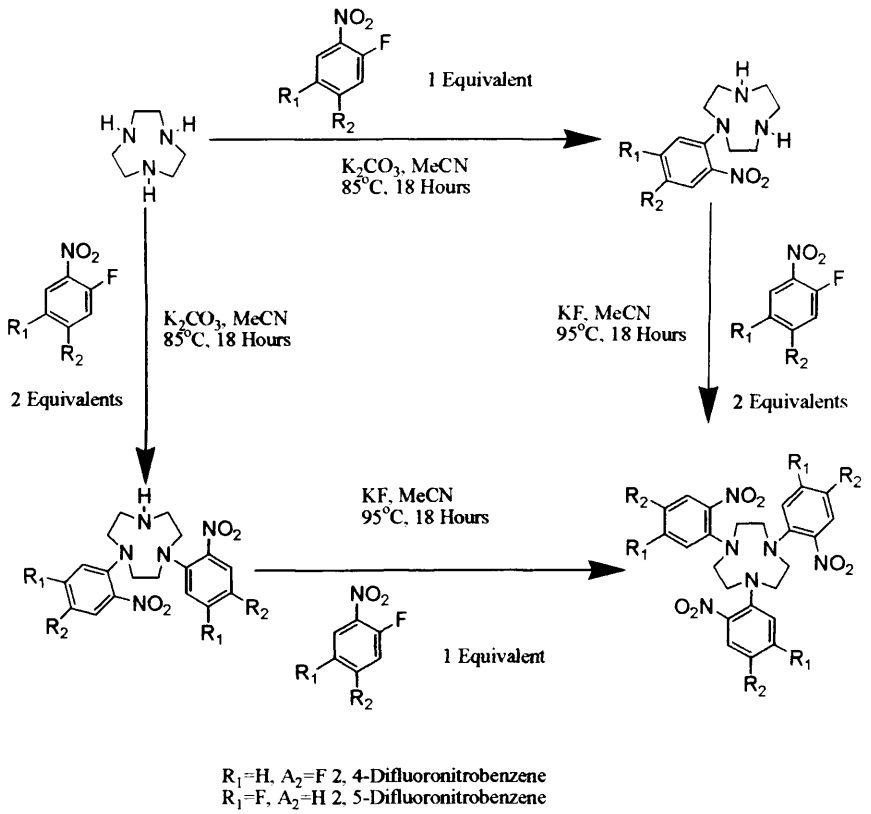

Figure 3.41: Reaction scheme of the formation of bis fluorinated, tris substituted tacn ligands.

We have developed a synthesis for the selective addition of differing fluorinated nitrobenzene derivatives, with the fluorines being present in the *ortho, meta* and *para* positions. Figure 3.42, shows this range of ligands. The fluorine position is with respect to the amine moiety of the aniline. To date we have synthesised tris, bis and mono fluorinated versions, but due to time constraints not all amine ligands were produced. We see no constraints as to why these could not be hydrogenated, and complexed. Also, extension of this class of ligands was not extended to the 2, 6-difluornitrobezene compound as due to its commercial availability. It is observed with the more activated ortho fluorine that the formation of bis tacn derivatives is more prevalent. This moiety could be added to the tacn ring, but under higher dilution conditions. Functionalisation of the tacn ring could be used as a useful tool to tuning the properties of the macrocycle, with the prospect of mixing different pendants. Developing a specific ligand could be achieved, as further groups and macrocycles

could be added by addition to the aniline rings, through further SNAr reaction with the activated ortho and para fluorines.

1st Nitrogen Site	2nd Nitrogen Site	3rd Nitrogen Site
Aniline	Aniline	Aniline
Aniline	Aniline	Para-Fluoro
Aniline	Para-Fluoro	Para-Fluoro
Para-Fluoro	Para-Fluoro	Para-Fluoro
Aniline	Aniline	Meta-Fluoro
Aniline	Meta-Fluoro	Meta-Fluoro
Meta-Fluoro	Meta-Fluoro	Meta-Fluoro
Meta-Fluoro	Meta-Fluoro	Para-Fluoro
Meta-Fluoro	Para-Fluoro	Para-Fluoro
Aniline	Meta-Fluoro	Para-Fluoro

Figure 3.42. Moiety table for differing tacn fluorinated aniline pendants.

Formation of the mono nitrobenzene tacn compound was synthesised under standard conditions, then one equivalent of 2, 5- difluoronitrobenzene was added and reacted further. Work up isolated the bis substituted compound, which was fully characterised, then reacted finally with one equivalent of 2, 4-difluoronitrobezene, to form the desired compound. The order of addition of the fluorinated nitrobenzene's was crucial, as if the bis fluorinated derivatives were added in reverse order, then chromatography would have had to have been employed to remove the mis-inserted product, thus drastically decreasing the overall yield.

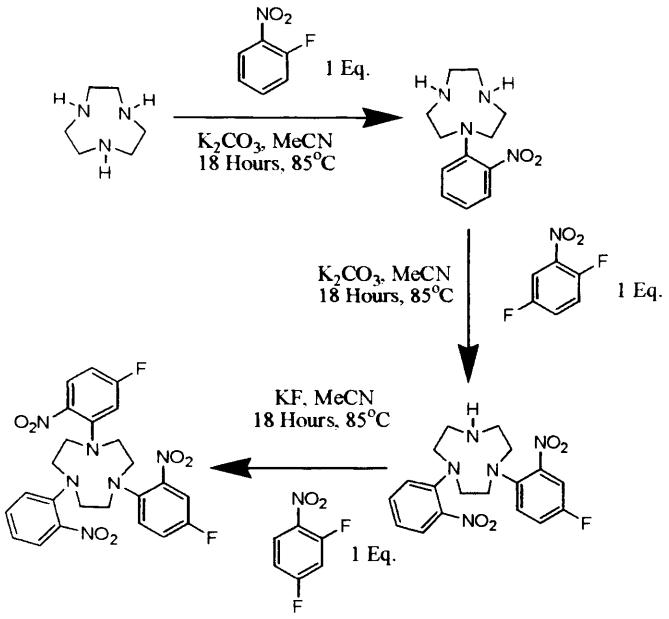

Figure 3.43: Substitution by three different fluoroaniline pendant groups onto a tacn ring.

We chose to add the 2, 4 difluoronitrobenzene last to maximise yield and minimise unwanted products. The overall yield is 7%, but we feel repeating this experiment would increase the yield of the second and third steps from 26% and 33% respectively. Unfortunately hydrogenation and complexation could not be attempted due to lack of sample and time constraints. It would be interesting to form a metal complex to observe the coordination environment of the metal with six unequal nitrogen donors. Repeating this methodology with 2, 6-difluoronitrobenzene, would increase the class of tris substituted compounds fourfold [nb=nitrobenzene (o/m/p), (o/m/nb) and (o/p/nb)].

	M^{2+} Ionic Radii (pm)	Para	Meta	Ortho	L^{33}
Mn	0.83	20.8	35.6	12.4	33.0
Fe	0.61 (0.55 ls Fe^{III})	47.5	46.6	NA	48.0
Ni	0.69	40.3	43.0	44.1	46.0
Cu	0.73	28.1	40.0	39.9	Fallis *et al*[57]
Zn	0.74	25.8	38.4	37.4	50.0
Cd	0.95	19.0	5.8	2.4	0
Hg	1.02	18.7	NA	Na	0

Figure 3.44: Twist angle (Φ) table for Mn, Fe, Ni, Cu, Zn, Cd and Hg complexes with fluorine in the *ortho, meta and para* positions, with respect to the aniline.

The twist angles (Φ) the complexes are summarised in figure 3.44. Metals with half or fully filled d orbitals (d^5-d^{10}), should be closer to trigonal prismatic orientation and the cadmium complexes show this with Φ of 19°, 5.8°, and 2.3°. The zinc complexes show higher Φ, (25.8, 38.4 and 37.4) closer to octahedral. The copper with *para* fluorine is a special case in its own right due to the solid state dynamic Jahn-Teller effect observed hence Φ of 28.1°, but from the table it can be seen that all the Fe, Ni, and Cu complexes are closer to octahedral orientation with Φ of 39.9°-47.5°.

Metal-Donor Set	Ligand	Average M-N	Reference
Mn^{II}-N_6	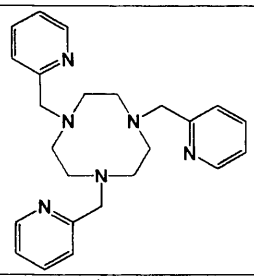	2.249	Wieghardt[113]
Mn^{II}-N_6	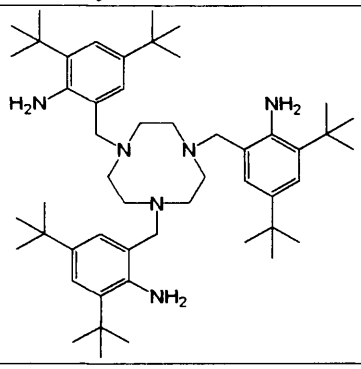	1.973	Wieghardt[114]
Mn^{II}-N_6	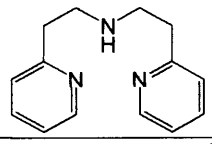	2.261	Weihe[115]
Fe^{II}-N_6	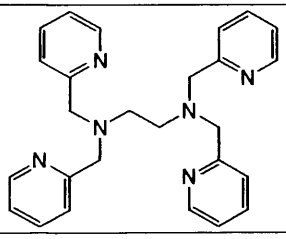	1.978	Toftlund[116]
Fe^{II}-N_6	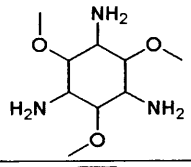	2.014	Sargeson[117]
Fe^{II}-N_6	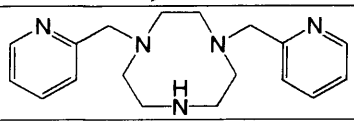	1.988	Spiccia[118]

[113] Wieghardt K., Schöffmann E., Nuber B., Wiess J., *Inorg. Chem.*, **1986**, 25, 4877-4883.
[114] Penkert E N., Weyhermuller T., Bill E., Hildebrandt P., Lecomte S., Weighardt K., *J. Am. Chem. Soc.*, **2000**, 122, 9663, 9675..
[115] Glerup J., Goddson P A., Hodgson D J., Michelson K., Nielsen K M., Weihe H., *Inorg. Chem.*, **1992**, 31, 4611-4616.
[116] Duelund L., Hazell R., McKenzie C J., Nielsen L P., Toftlund H., *J. Chem. Soc., Dalton Trans.*, **2001**, 152-156.
[117] Hegetschweiler K., Weber M., Huch V., Veith M., Schmalle H W., Linden A., Geue R J., Osvath P., Sargeson A M., Willis A., Angst W., *Inorg. Chem.*, **1997**, 36, 4121-4127.

Ni^{II}-N_6	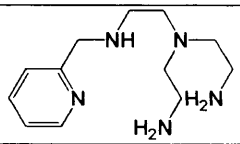	2.083	Spiccia[119]
Ni^{II}-N_6	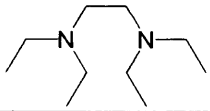	2.160	Sheldon[120]
Ni^{II}-N_6	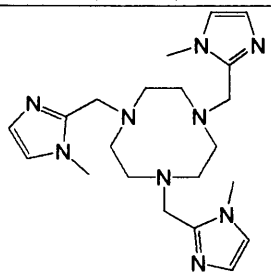	2.097	Di Vaira[121]
Cu^{II}-N_6	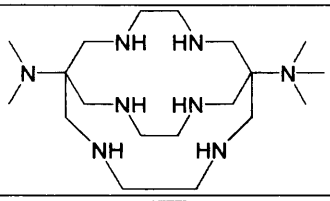	2.168	Sargeson[122]
Cu^{II}-N_6	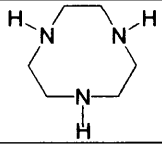	2.148	Wieghardt[123]
Cu^{II}-N_6	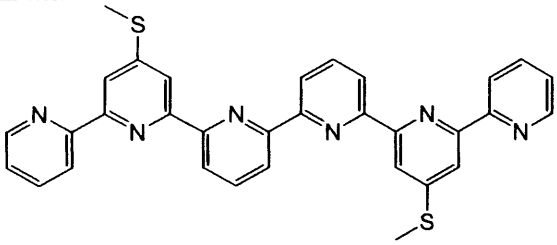	2.141	Potts[124]
Zn^{II}-N_6	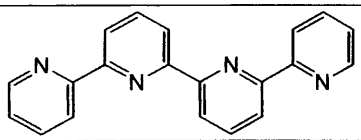	2.196	Dell' Amico[125]

[118] Spiccia L., Fallon G D., Grannas M J., Nichols P J., Teikink E R T., *Inorg. Chim. Acta.*, 279, **1998**, 192-199

[119] McLachlan G A., Fallon., Martin R L., Moubaraki B., Murray K S., Spiccia L., *Inorg. Chem.*, **1994**, 33, 4663-4668.

[120] Lever A B P., Walker I M., McCarthy P J., Mertes K B., Jircitano A., Sheldon R., *Inorg. Chem.*, **1983**, 22, 2252-2258.

[121] Di Vaira M., Mani F., Stoppioni P., *Inorg. Chim. Acta.*, 303, **2000**, 61-69.

[122] Bernhardt P V., Bramley R., Englehardt L., Harrowfiled J M., Hockless D C R., Korybut-Daszkiewicz B R., Krausz E R., Morgan T., Sargeson A M., Skelton B W., White A H., *Inorg. Chem.*, **1995**, 34, 3589-3599.

[123] Chaudhuri P., Oder K., Weighardt K., Weiss J., Reedijk J., Hindrichs W., Wood J., Ozarowski A., Stratemeier H., Reinen D., *Inorg. Chem.*, **1986**, 25, 2951-2958.

[124] Potts K T., Keshavarz-K M., Tham F S., Abruna H D., Arana C., *Inorg. Chem.*, **1993**, 32, 4436-4449.

Zn^{II}-N_6	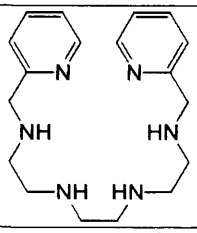	2.171	Barbier[126]
Zn^{II}-N_6	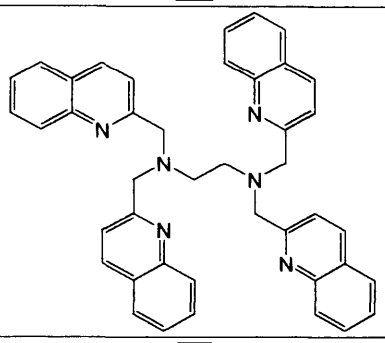	2.229	Yano[127]
Cd^{II}-N_6	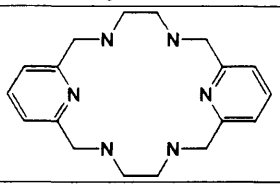	2.353	Jackels[128]
Cd^{II}-N_6	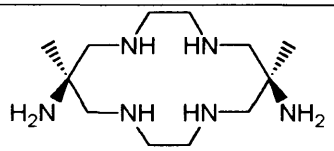	2.379	Bernhardt[129]
Cd^{II}-N_6	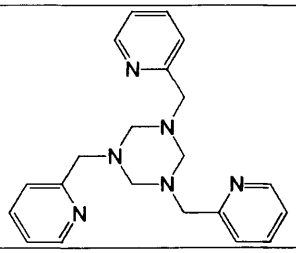	2.360	Planalp[130]
Hg^{II}-N_6	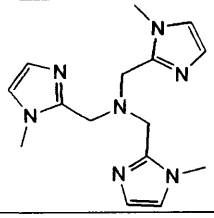	2.368	Butcher[131]

[125] Dell' Amico D B., Calderazzo F., Cuiardi M., Labella .L, Marchetti F., *Inorg. Chem.*, **2004**, 43, 5459-5465.
[126] Jubert C., Mohamadou A., Marrot J., Barbier J-P., *J. Chem., Dalton Trans.*, **2001**, 1230-1238.
[127] Mikata Y., Wakamatsu M., Yano S., *Dalton Trans.*, **2005**, 545-550.
[128] Bryant L H., Lachgar A., Jackels S C., *Inorg. Chem.*, **1995**, 34, 4230-4238.
[129] Bernhardt P V., Comba P., Hambley T W., Lawrance G A., Varnagy K., *J. Chem. Soc. Dalton Trans.*, **1992**, 355-359.
[130] Park G., Ye N., Rogers R D., Brechbiel M W., Planalp R P., *Polyhedron*, 19, **2000**, 1155-1161.
[131] Bebout D C., Garland M M., Murphy G S., Bowers E V., Abelt C J., Butcher R J., *Dalton Trans.*, **2003**, 2578-2584.

Hg^{II}-N_6	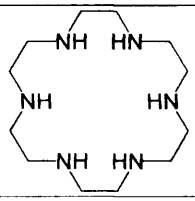	2.436	Santos[132]
Hg^{II}-N_6	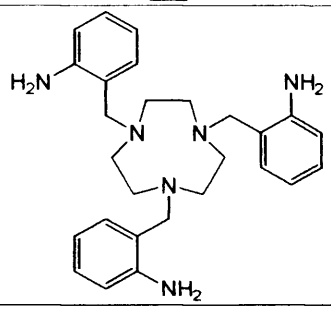	2.427	Wieghardt[133]
Pb^{II}-N_6	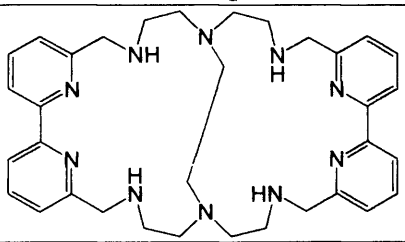	2.640	Valtancoli[134]
Pb^{II}-N_6	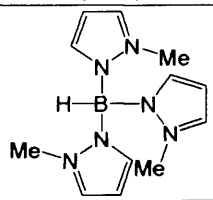	2.686	Reger[135]
Pb^{II}-N_6	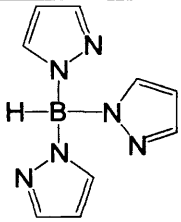	2.607	Reger[136]

Figure 3.52: Reference table for M-N_6 bond length comparison.

[132] De M A A F., Carrondo C T., Felix V., Duarte M T., Santos M A., *Polyhedron*, 12, 8, 931-937, **1993**.
133 Schlager O., Wieghardt K., Grondey H., Rufinska A., Nuber B., *Inorg. Chem.*, **1995**, 34, 6440-6448.
[134] Anda C., Bazzicalupi C., Bencini A., Berni E., Bianchi A., Fornasari P., Llobet A., Giorgi C., Paoletti P., Valtancoli B., *Inorg. Chim. Acta.*, 356, **2003**, 167-178.
[135] Reger D., Collins J E., Rheingold A L., Liable-Sands L M., Yap G P A., *Inorg. Chem.*, **1997**, 36, 345-351.
[136] Reger D L., Huff M F., Rheingold A L., Haggerty B S., *J. Am. Chem. Soc.*, **1992**, 114, 579-584.

Metal	Average M-N Bond Length Å	Metal	Average M-N Bond Length Å
L^1Mn	2.264	L^2Cu	2.141
L^2Mn	2.256	L^3Cu	2.136
L^3Mn	2.292	L^1Zn	2.183
L^1Fe	1.978	L^2Zn	2.170
L^2Fe	1.983	L^3Zn	2.168
L^3Fe	NA	L^1Cd	2.357
L^1Ni	2.103	L^2Cd	2.361
L^2Ni	2.105	L^3Cd	2.372
L^3Ni	2.099	L^1Hg	2.415
L^1Cu	2.141	L^3Pb	2.652

Figure 3.46: M-N bond length averages for all complexes.

The above table is a collation of all the average $M\text{-}N_6$ bond lengths for all the metal complexes present in this chapter. The average $N\text{-}_{Ring}$ and $N\text{-}_{Aniline}$ bond lengths are tabulated in Figure 3.47. From the postulates stipulated in the aims and objectives, we hoped to see a trend of short bond lengths when the fluorine was in a *meta* position to the nitrogen. From Figure 3.47 above all the average bond lengths which were shorter are present in bold. The average bond lengths prove our initial theories wrong as the *ortho* compounds should have the shortest $M\text{-}N\text{-}_{Ring}$ lengths but only the nickel compound exhibited this behaviour. The *meta* class should have had short $M\text{-}N_{Ring}$ bonds with the manganese, copper and zinc compounds possessing the shortest $M\text{-}N_{Aniline}$ bonds. The shortest M-N lengths should have been the $M\text{-}N\text{-}_{Ring}$ lengths, for the *para* class, but no complexes did. All compounds in the *para* class had shorter $M\text{-}N_{Aniline}$ bonds.

Ortho	Mn	Fe	Ni	Cu	Zn	Cd
M-$N_{Aniline}$	**2.256**	NA	2.106	**2.126**	**2.140**	**2.2322**
M-N_{Ring}	2.328	NA	**2.093**	2.146	2.195	2.2421

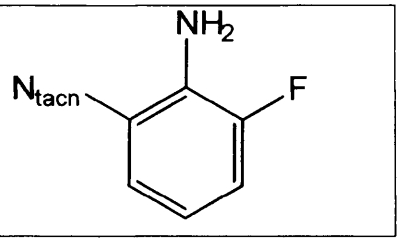

Meta	Mn	Fe	Ni	Cu	Zn	Cd
M-$N_{Aniline}$	**2.216**	2.010	2.106	**2.127**	**2.130**	2.379
M-N_{Ring}	2.297	**1.956**	**2.103**	2.155	2.209	**2.343**

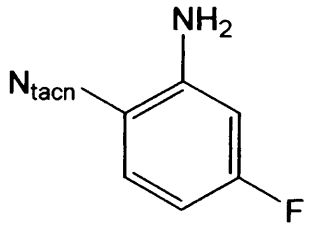

Para	Mn	Fe	Ni	Cu	Zn	Cd
M-$N_{Aniline}$	**2.219**	**1.949**	**2.092**	**2.106**	**2.125**	**2.295**
M-N_{Ring}	2.308	2.009	2.114	2.176	2.241	2.419

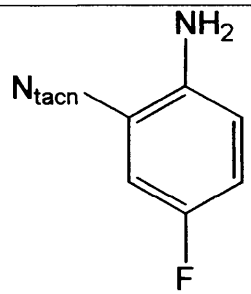

Figure 3.47: Individual bond length tables for all metal complexes present in the chapter.

These data show that the fluorine constituent present on the aniline ring do not affect the bond lengths of the complex, when related to current theories of aromatic ring activating/deactivating groups.

	L^1 (Para)	L^2 (Meta)	L^3 (Ortho)
NO_2	-102ppm	-118ppm	-122ppm
NH_2	-124ppm	-117ppm	-132ppm
Zn	-112ppm	-113ppm	-119ppm
Cd	-113ppm	-116ppm	-119ppm
Hg	-113ppm	N/A	-119ppm
Pb	-115ppm	N/A	-121ppm

Figure 3.48: Summary table of ^{19}F NMR shift in nitro precursors, amine ligand and metal complexes.

^{19}F NMR spectroscopy was carried out upon all derivatives and the shifts observed are summarised in Figure 3.48. There are no trends observed for the whole class of derivatives but the degree of shift can be explained by fluorine position and thus its activation of the nitro/amine moiety. The main observation is that L^2 has its fluorine *meta* to the nitro/amine and thus no discernable shift is observed in this class as when in this position as the nitro/amine does not activate the fluorine group[137,138]. The *meta* position is inactive to nucleophillic aromatic substitution as it cannot stabilize the anion intermediate through resonance reconfiguration. The greatest ^{19}F NMR shifts are observed with the L^1 compounds as the *ortho* fluorine is the most greatly activating and so nitro to amine conversion shows a downfield shift of 22ppm. Upon complexation, all metals show a similar shift of -112ppm-(-115ppm). The L^3 compounds exhibit similar but less pronounced activity in the ^{19}F NMR with nitro to amine shifting downfield 10ppm and its complexes appearing at -119pp-(-121ppm). L^2 complexes also show similar shifts of -113ppm-(-118ppm).

[137] Sokolowski A., Adam B., Weyhermuller T., Kikuchi A., Hildenbrand K., Schnepf R., Hildebrandt P., Bill E., Wieghardt K., *Inorg. Chem.*, **1997**, 36, 3702-3710.
[138] Kimura S., Bill E., Bothe E., Weyhermuller T., Wieghardt K., *J. Am. Chem. Soc.*, **2001**, 123, 6025-6039.

Other complexation studies

We have successfully complexed a variety of first row transition metal perchlorate salts, aswell as cadmium, mercury and lead. Complexation was also attempted with tin (II) sulphate, but unfortunately this reaction did not proceed under standard conditions. By following a standard method described in Vogel[139], the nitro precursor was mixed with sheet tin metal, and refluxed with concentrated HCl. We initially hoped to form the tin chloride complex, but a green solid was afforded, which had an unclear ^{1}H NMR spectra so conformation that complexation had occurred could not be determined.

It is interesting to note that for all complexes, the only mass spectrometry data to be successfully collected was for the copper samples. All other complexes were found to be demetallated, and so all showed a peak at 457 ($L+H^+$). We feel that this is not due to sample quality but to the actual chemical behaviour of the complex. Owing to the low quantities of sample required, upon sample preparation, it became demetallated due to the complex having a low formation value.

Upon complexation, a noticeable shift is observed of all aniline peaks of d^{10} complexes.

	NH_2	Zn	Cd	Hg	Pb
L^1	3.95ppm	5.45ppm	4.65ppm	6.65ppm	4.55ppm
L^2	4.40ppm	5.60ppm	4.75ppm	NA	NA
L^3	4.70ppm	4.60ppm	4.65ppm	4.90ppm	4.45ppm

Figure 3.49: Shift of NH_2 peak in ^{1}H NMR spectra.

The smallest deviation occurs within the L^3 class of diamagnetic complexes. The free ligand aniline peak occurs at 4.70ppm and complexation peaks are found within the range of 4.45-4.90ppm. Although there are no obvious trends with regards to the aniline peak, it can be seen that upon complexation with d^{10} metals, the peak shifts from its position for the free ligand for $L^{1/2}$ compounds.

[139] Vogel 5th Ed., Furniss B S., Hannford A J., Smith P W G., Tatchell A R., 892.

L^1	Mn	Fe	Ni	Cu	Zn	Cd	Hg
Department Code	0418	0402	KMAM	0413	KMAM	0412	0427
Crystal System	Cubic	Triclinic	Cubic	Cubic	Cubic	Cubic	Cubic
Space Group	P21/3	P-1	P21/3	P21/3	P21/3	P21/3	P21/3

L^2	Mn	Fe	Ni	Cu	Zn	Cd
Department Code	0405	0307	0301	0406	0404	0407
Crystal System	Triclinic	Triclinic	Triclinic	Triclinic	Triclinic	Monoclinic
Space Group	P-1	P-1	P-1	P-1	P-1	P2/c

L^3	Mn	Ni	Cu	Zn	Cd	Pb
Department Code	0416	0414	0415	0417	0421	0419
Crystal System	Triclinic	Orthorhombic	Orthorhombic	Orthorhombic	Orthorhombic	Monoclinic
Space Group	P-1	Pnab	Pnab	Pnab	P21/c	P21/c

Figure 3.50: Tables of crystal system and space group of $[(L^{1/2/3})M](ClO_4)_2$ complexes

Crystallography

From the crystal data obtained, several interesting trends have arisen from this class of compound.

All the L^1 complexes are of the cubic space group except the iron complex which is triclinic. All L^2 complexes are formed in the triclinic space group except the cadmium complex which is monoclinic. There is no definite trend with the L^3 with complexes forming in orthorhombic (Cu, Ni, Zn), monoclinic (Cd, Pb) and triclinic (Mn) spacegroups.

Conclusions

This chapter has shown that the fluorinated arylamine versions of L^{33} can be synthesised and from the crystallographic data obtained, shows small variations from the original parent ligand and its complexes. A dynamic Jahn-Teller distortion was found to be exhibited in the complex of $[(L^1)Cu](ClO_4)_2$, and a study must be carried out by Q-Band EPR spectroscopy to fully determine the behaviour of the complex. Q-Band EPR will determine if the structure does truly exhibit a dynamic Jahn-Teller distortion in solution, and not just in the solid state.

The $[(L^3)Pb](ClO_4)_2$ structure exhibits a typical stereochemically active lone pair, whereby the structure distorts to accommodate this feature, and thus forming the first buckled sample in the class of complexes.

After the results from the variable temperature ^1H NMR, we have developed a hypothesis as to why no discernable shift was observed even at -40°C. The sample run initially was the perchlorate salt, whereas this time the counterion was tetraphenylborate. It has been observed that in the crystal structure of the $[L^{33}(Zn)](ClO_4)_2$ compound, the counterion is bound by three hydrogen bonds from the oxygen's of the perchlorate to the *exo* protons of the three anilines. We suggest that the capping of this counterion somehow restricts the twisting of the complex by "locking" it into place. When the counterion was replaced with tetraphenylborate, due to the size of it, does not cap the aniline protons in the same fashion. We propose that

as this was then run; shifting of the peaks was observed even at -40°C and then to -80°C.

The ^{19}F NMR spectroscopy was found to be a useful tool in determining complexation among the d^{10} metals. Noticeable shifts were observed between nitro precursor, amine ligands and metal complexes. A minimal shift was observed for the fluorine *meta* to the aniline and so is concurrent with standard theories regarding nitro/amine activation of *ortho* and *para* positions.

The formation of Co samples completed but due to no crystals of X-Ray quality being forthcoming, such comparisons with the $[(L^{33})Co](ClO_4)_2$ and $[(L^{33-H})Co](ClO_4)_2$ structures obtained by Perkins[79] cannot be attempted. The UV/Vis spectrum of $[(L^{1/3})Co](ClO_4)_2$ indicates the same behaviour as the deprotonated complex reported by Perkins.

Ruthenium complexation was attempted with $RuCl_3.xH_2O$, $Ru(DMSO)_4Cl_2$ and $Ru(PPh_3)_3Cl_2$ in ethanol, but no complexation was observed in the ^1H NMR spectra. Further reaction by refluxing in MeCN did not generate the desired species. We feel alteration of the reaction conditions should produce the desired complex, but a ruthenium salt with more labile ligands should be tried. Research is still underway with the optimising of reaction conditions to try and achieve some degree of complexation with ruthenium and L^{33}.

From the work outlined within this chapter, it can be seen that the synthesis of triply substituted tacn derivatives can be achieved without the use of protecting groups. By employing strict reagent ratio methodologies, the desired *N*-aryl species can be isolated, and further reacted to produce multi-substituted ligands. The triply fluorinated ligands $L^{1/2/3}$ are all synthesised in good yield and further hydrogenated to form the amine species. Auto-catalytic oxidation is thought to degrade the ligand L^2 but research is currently underway to investigate the true nature of this chemical pathway. Complexation of the mono fluorinated ligands have shown by X-Ray crystallography that the metal complex does not deviate greatly from the triply fluorinated analogue, and this was reinforced by the ^{19}F NMR spectroscopy data which indicates like shifts. Further investigation into the bis fluorinated versions with fluorines in different positions should be pursued to fully gain an insight into this class of ligands.

Future Work

A majority of compounds synthesised exhibited a high degree of hydrogen bonding to their perchlorate counterions. Further investigation could be extended to the possibility of hydrogen bonding between the aniline protons and fluorine of the BF_4^- counterion.

This research was extended into the tetraazamacrocycle cyclen, and the possibility of producing 5, 6, 7 and 8-coordinate complexes has been explored by Fallis *et al*[140]. It is hoped that within the near future this area of work will be fully investigated and finished.

It would be of interest to synthesize the fluorinated versions of the tris aminobenzyl derivative L^{KW}, to explore the possible effects the fluorine has upon the amine group when the ligand has more flexibility to form complexes

[140] Fallis I A., Tatchell T., Gurden D L G., Malik K M A., Ooi L., *Unpublished Results.*, **2002**.

Chapter Four

Synthesis of metal-sulphonamide bond complexes

Guillotine, *n*. A machine which makes a Frenchman shrug his shoulders with good reason.
--Ambrose Bierce, The Devils Dictionary

My wife's jealousy is getting ridiculous. The other day she looked at my calendar and wanted to know who May was.
-- Rodney Dangerfield

Introduction

Synthesis of mono substituted tacn derivatives has been an area in which much effort has been paid in recent years [157]. Differing methods of protection[158] (L^a) and addition[159] (L^b) have been pursued in which to achieve the desired mono substituted species. Chong *et al*[160] have shown that firstly by functionalising an alkylamine with alkyl alcohols, benzyls, 1, 2-diols, and tertiary butyl esters, then using standard tacn formation preparations the mono pendant macrocycle was formed in high yields (81-92%). Using high excess methods, Fallis *et al*[161,162] used a 10 fold excess of the macrocycle with a long chained epoxide to form the desired mono substituted compound in excellent yield (93%).

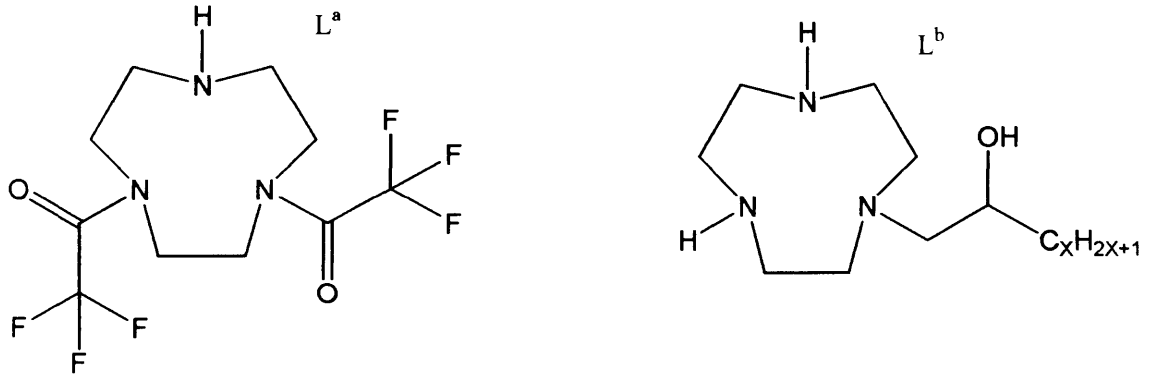

Figure 4.1: Protection and single pendant addition compounds.

The use of secondary sulphonamides as ligands is very rare and to date we have only found one such complex example by Fabbrizzi *et al*[174]. The use of tosyl in tacn chemistry has largely been employed as a protecting group[163,164,165].

---

[157] Lazar I., Takacs Z., *Synth. Commun.*, 31 (20), 3141-3144, **2001**
[158] Yang W., Giandomenico C M., Sartori M., Moore D A., *Tett. Lett.*, 44, **2003**, 2481-2483.
[159] Blake A. J., Danks J. P., Fallis I. A., Harrison A., Li W-S., Parsons S., Ross S. A., Whittaker G., Schröder M., *J. Chem.Soc., Dalton Trans.*, **1998**, 3969-3976.
[160] Chong H-S., Brechbiel M. W., *Synth. Commun.*, **2003**, 33, (7), 1147-1154.
[161] Fallis I A., Griffiths P C., Griffiths P M., Hibbs D E., Hursthouse M B., Winnington A L., *Chem Commun.*, **1998**, 665-668.
[162] Griffiths P C., Fallis I A., Willock D J., Paul A., Barrie C L., Griffiths P M., Williams G M., King S M., Heenan R K., Görgl R., *Chem. Eur. J.*, **2004**, 10, 2022-2028.
[163] Blake A. J., Danks J. P., Fallis I. A., Harrison A., Li W-S., Parsons S., Ross S. A., Whittaker G., Schroder M., *J. Chem.Soc., Dalton Trans.*, **1998**, 3969-3976.
[164] McAuley A., Subramanian S., *Inorg. Chem.*, **1990**, 29, 2830-2837.

Pentadentate ligand synthesis is an area researched by a few well known groups such as Spiccia[166], Fallon[167], and Schröder[168]. Mixed donor macrocycles have been synthesised bearing donors other than nitrogen such as oxygen, sulphur, selenium, and phosphorous. Within this chapter we will be focussing on pentatazamacrocycles, as we aim to replicate the Taube ruthenium salt chemistry.

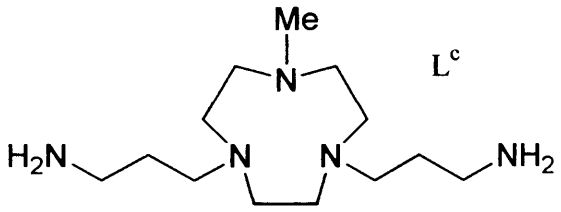

Figure 4.2: 1-Methyl, bis 4, 7-(3-aminopropyl) 1, 4, 7-triazacyclononane.

Schroder *et al*[169] produced the pentadentate ligand L^c via two routes. Firstly methylating ditosyl tacn by the Esweiler-Clarke method to block the third nitrogen site. Then after detosylation, the addition of 2 equivalents of acrylonitrile yielded the bis substituted ethylnitrile intermediate. Subsequent reduction of the nitrile groups with BH_3.THF afforded the amine moiety. The second route is acid hydrolysis of 1, 4, 7-triazatricyclo[5.2.1.$^{04.10}$]decane to yield the formyl tacn species. This formyl group blocks the third site and again addition of acrylonitrile, and reduction forms the ligand L^c. Work by the same group shows the tethering of two of these groups by the third free nitrogen. The addition of 1, 2-dibromoethane to 1, 4, 7-triazatricyclo[5.2.1.$^{04.10}$]decane forms the bis formyl tacn intermediate. Methods previously discussed formed the bis pentaazamacrocycle. Complexation with Cu^{II}

---

[165] Tei L., Blake A J., Devillanova F A., Garau A., Lippolis V., Wilson C., Schoder M., Chem. *Commun.*, **2001**, 2582-2583.
[166] Brundenell S J., Spiccia., Tiekink E R T., *Inorg. Chem.*, **1996,** 35, 1974-1979. Brundenell S J., Spiccia., Bond A M., Comba., Hockless D C R., *Inorg. Chem.* **1998**, 37, 3705-3713. Brundenell S J., Spiccia L., Hockless D C R., Teikink E R T., *J. Chem. Soc. Dalton Trans.* **1999**, 1475-1481.
[167] Fallon G D., McLachlan G A., Moubaraki B., Murray K S., O'Brien L., Spiccia L., *J. Chem. Soc. Dalton Trans.*, **1997**, 2765-2769. McLachlan G A., Fallon G D., Martin R L., Spiccia L., *Inorg. Chem.*, **1995**, 34, 254-261. McLachlan G A., Brundenell S J., Fallon G D., Martin R L., Spiccia L., Tiekink E R T., *J. Chem. Soc., Dalton Trans.*, **1995**, 439-447.
[168] Blake A J., Fallis I A., Gould R O., Parsons S., Ross S A., Schröder M., *J. Chem. Soc. Dalton Trans.*, **1996**, 4379-4387.
[169] Blake A J., Danks J P., Li W-S., Lippolis V., Schröder M., *J. Chem. Soc., Dalton Trans.*, **2000**, 3034-3040.

salts formed the desired complexes and were resolved via crystallographic methods. L^cCu exhibits a distorted square based pyramidal geometry, with two 6 membered chelates and one 5 membered chelate formed through the apical nitrogen. With the $Cu\text{-}_{(apical)}$ bond length being 2.257Å, its is comparable with long $Cu\text{-}N_{(apical)}$ distance of 2.337Å of the bis pentaazamacrocycle. The tethered version can be seen to have a weakly interacting acetonitrile solvent group, binding *trans* to the tertiary nitrogen at a distance of 2.710Å.

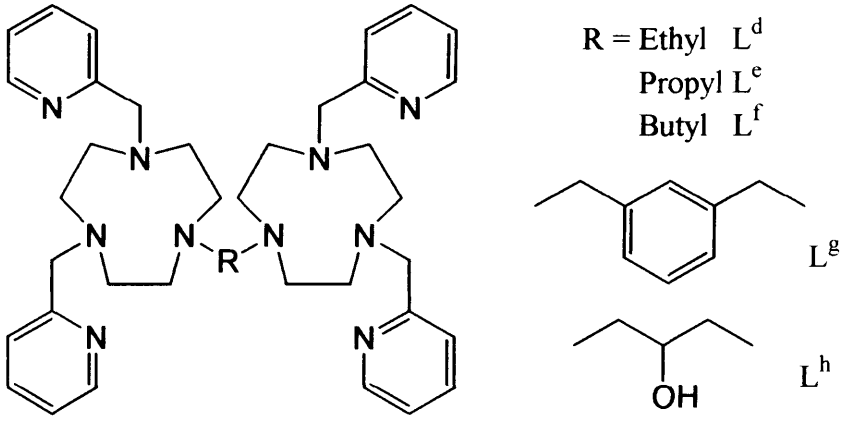

Figure 4.3: Tethered pentaazamacocycles.

Research by Spiccia *et al*[170] led to the development of $L^{d/e}$. The bis pentaazamacrocycle can bond to metals in a pentadentate fashion, or by the addition of base to the complex, form the μ-*oxo* bridged zinc species. They have shown that by altering the type of linker, the stereochemistry of the dimeric complexes can be controlled. The longer butyl chain L^f, rigid 1, 3 dimethylbenzene L^g, and propyl-2-ol L^h linker[171] can all be prepared by convenient routes.

[170] Brudenell S J., Spiccia L., Hockless D C R., Tiekink E R T., *J. Chem. Soc. Dalton Trans.*, **1999**, 1475-1481.
[171] Brudenell S J., Spiccia L., Bond A M., Mahon., Hockless D C R., *J. Chem. Soc. Dalton Trans.*, **1998**, 3919-3925.

Aims and Objectives

Preliminary ideas were to develop a rigid pentadentate ligand which complexed around a metal centre, with a high degree of steric hindrance. It was our aim to develop a new family of derivatives bearing an innocent pendant on the macrocycle ring, and through our methodologies, add two pendant aniline pendants, thus forming potential desired ligands.

We needed the steric bulk to stop dimerisation of the nitrous oxide between ruthenium complexes. Groves *et al*[172] have shown that by using tetramesityl porphyrin the two ortho methyl groups present on the mesityl groups are sufficient enough to prevent this dimerisation between the porphyrins.

Results and Discussion

The primary ligand ($L^{4'}$) in this class was prepared by SNAr reaction of two equivalents of nitrobenzene to mono tosyl tacn, then subsequent hydrogenation to give the desired amine moiety and finally complexation. A primary concern was that the sulphonamide nitrogen would be too electron deficient and thus not bond to the metal centre[173]. The only other example of a metal complex with the metal-2° sulphonamide bond was by Fabrizzi[174] *et al.* The Cyclam-Ni complex has a Ni-sulphonamide bond length of 2.36Å.

[172] Groves. J.T., Roman. J.S, *J. Am. Chem. Soc.* **1995**, 117, 5594-5595.
[173] Blake A J., Danks J P., Fallis I A., Harrison A., Li W-S., Parsons S., Ross S A., Whittaker G., Schroder M., *J. Chem. Soc., Dalton Trans.*, **1998**, 3969-3976.
[174] Calligaris M., Carugo O., Crippa G., De Santis G., Di Casa M., Fabrizzi L., Poggi A., Seghi B., *Inorg. Chem.*, **1990**, 29, 2964-2970.

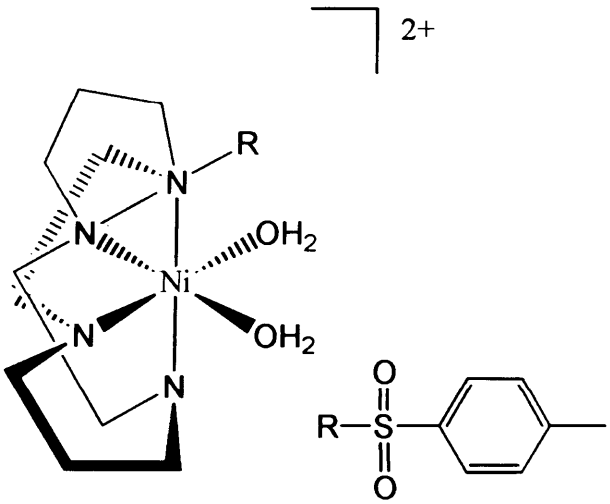

Figure 4.4: *N*-Tosylated Cyclam Nickel complex with Ts-N-Ni bond length 2.36Å.

Cyclam was tosylated in high dilution and complexed with nickel (II) chloride. This complex shows the water molecules in a *cis* arrangement, and the macrocycle adopts a folded conformation rather than co planar as the metal tries not to bond with the sulphonamide nitrogen. If we were to synthesize any complexes of this nature then could we alter the bond length of the metal sulphonamide by increasing/decreasing the electron withdrawing nature of the group present on the SO_2 moiety. The differing groups present will decrease in electron withdrawing nature (F>Me>OMe>), fluorine being the most electron withdrawing and oxymethyl being most electron donating. If this sphere of work was to prove fruitful then it could be extended to the bis tosyl tacn version[175,176,177]. We would like to investigate if metal complexes of this ligand could be made to see if it would be strong enough to bond twice to a metal centre.

Addition of 2 equivalents of 2-fluoronitrobenzene to mono tosyl tacn with potassium fluoride, afforded the nitro ligand ($L^{4'}$) in good yield. Hydrogenation under standard conditions ($Pt/C/H_2$) generated the aniline derivative. This was often delivered directly onto the metal perchlorate salt via cannula under anaerobic conditions, and stirred for 30 minutes. This THF:MeOH solution was removed *in vacuo*, degassed ethanol was added, and the reaction mix stirred for a further 18

[175] Pulachini S., Watkinson M., *Eur. J. Org. Chem.*, **2001**, (22), 4233-4238.
[176] Pulachini S., Watkinson M., *Tett. Lett.*, **1999**, 40 (52), 9353-9365.
[177] Weisman G R., Vachon D J., Johnson V B., Gronbeck D A., *J. Chem. Soc. Chem. Commun.*, **1987**, (12), 886-887.

hours, after which the metal complex precipitated from the ethanolic solution. This was filtered and washed with a small amount of diethyl ether. All complexes were found to be air stable, and formed in good yield (65-85%).

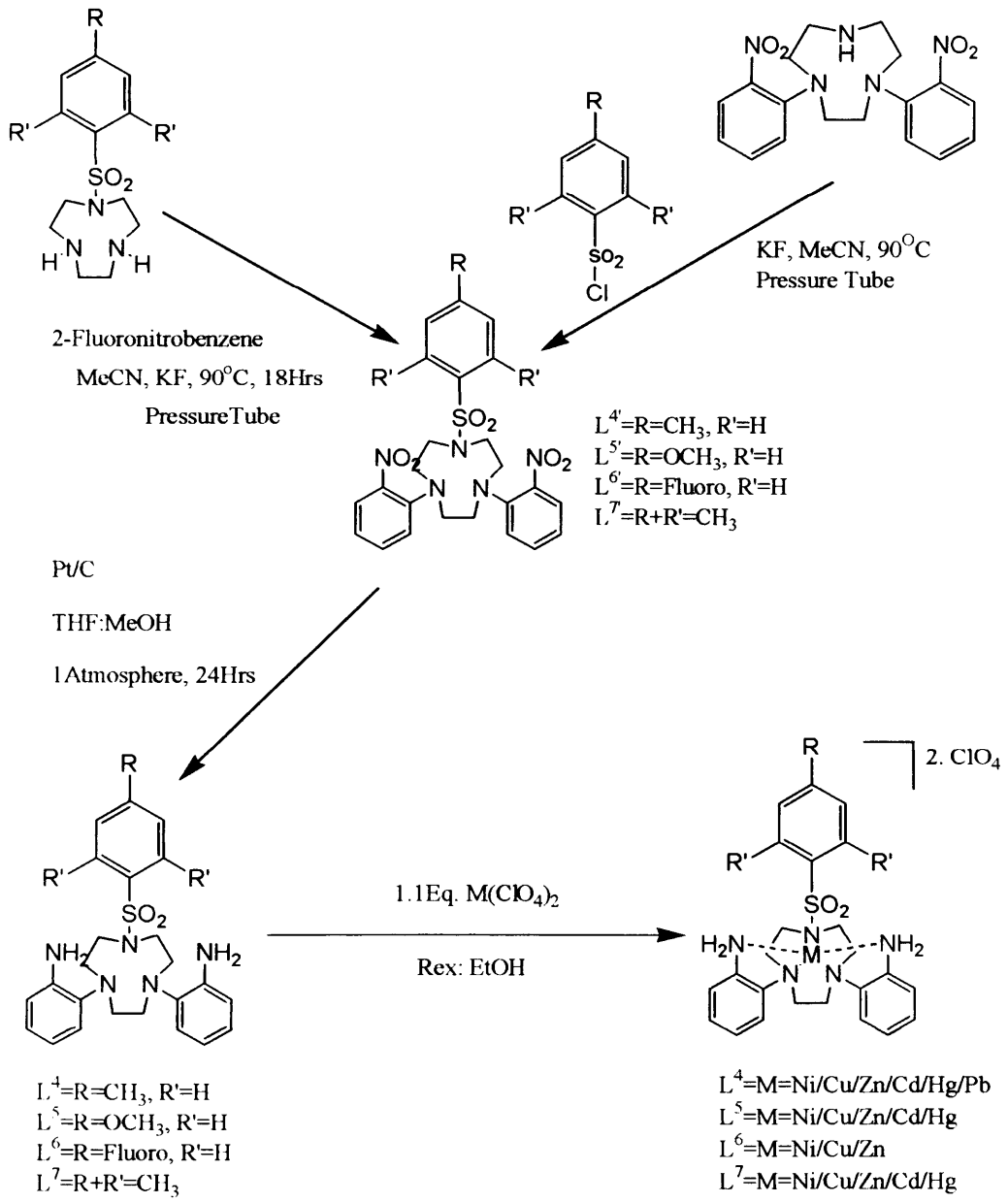

Figure 4.5: Reaction scheme for the synthesis of $[(L^{4/5/6/7})M](ClO_4)_2$ complexes.

Generation of the *para*-oxymethylphenyl (L^5), *para*-fluorophenyl (L^6), and 2-Mesityl (L^7) derivatives was achieved from addition of the chlorosulphonyl compound to 1, 4-bis (2-nitrophenyl), 1, 4, 7-triazacyclononane[178]. All derivatives were formed in good yield and the metal complexes formed were all air stable. Addition of the

[178] Fallis I A., Perkins W T S., Longhurst S., Malik K M A., *Unpublished Results*, **2001**.

chlorosulphonyl derivative to tacn to form the mono substituted macrocycle was attempted, but formed the mono, bis and tris substituted macrocycle, and was found to be difficult to purify by column chromatography. Addition the differing sulphonyl chlorides to L^{32} was found to be of a better methodology, as the nitro derivative could be synthesised in good yield and without column chromatography. Addition of the chlorosulphonyl compound to the ring formed no side products and so was employed for the synthesis of the other derivatives. We would predict that addition of tosyl chloride to bis 1, 4 (2-nitrophenyl) 1, 4, 7-triazacyclononane would also produce the ligand L^4.

Nickel complexes

This chapter will show, that a new class of metal complexes has been successfully explored. All complexes that were formed show from the crystal data that a bond exists between the metal centre and the sulphonamide nitrogen in the tacn ring.

To obtain a fully saturated coordination geometry, one molecule of acetonitrile bonds through the lone pair of the nitrogen to the metal centre. In all cases except $[(L^4)Cd.MeCN](ClO_4)_2$ the acetonitrile is bonded to the metal to form an unsymmetrical complex (point group=P21/n), with the anilines being inequivalent, thus bearing 4 chemically inequivalent protons.

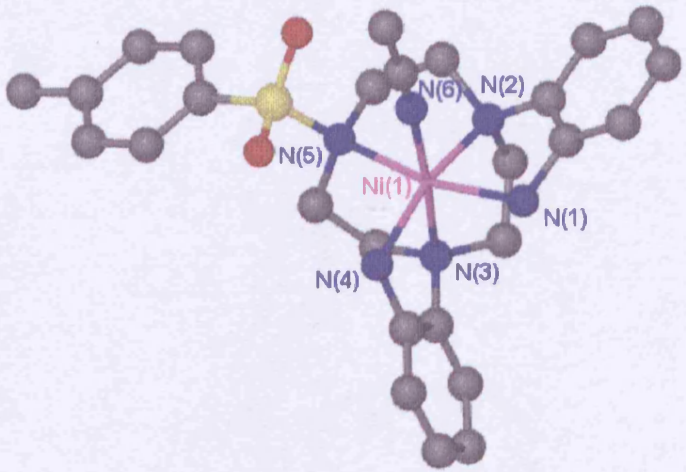

[(L^4)Ni.MeCN](ClO$_4$)$_2$.1(MeCN)

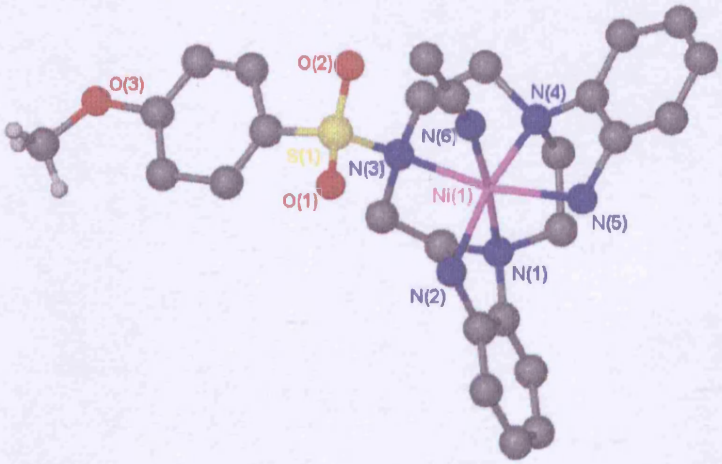

[(L^5)Ni.MeCN](ClO$_4$)$_2$.1(MeCN)

Figure 4.6. [(L^4)Ni.MeCN](ClO$_4$)$_2$.1(MeCN). Selected Bond lengths; N(1)-Ni 2.091(3), N(2)-Ni 2.088(3), N(3)-Ni 2.099(3), N(4)-Ni 2.078(3), N(5)-Ni 2.245(3) and N(6)-Ni 2.059(3). [(L^5)Ni.MeCN](ClO$_4$)$_2$.1(MeCN). Selected Bond lengths; N(1)-Ni(1) 2.100(5), N(2)-Ni(1) 2.054(5), N(3)-Ni(1) 2.232(7), N(4)-Ni(1) 2.074(6), N(5)-Ni(1) 2.089(7), N(6)-Ni(1) 2.076(6). Hydrogen atoms and solvent molecules have been removed for clarity.

The metal –sulphonamide bond length in $[(L^4)Ni.MeCN](ClO_4)_2.(MeCN)$ is 2.245Å, which is 0.115Å shorter than the bond present in the tosylated cyclam-nickel complex[174]. This could be due to the higher denticity of the macrocycle, therefore increasing the macrocycle effect and creating stronger bonds. The tosyl group may be coordinated weakly, or left free to dangle away from the meal centre. The complex crystallises with one MeCN molecule within the lattice. There is some hydrogen bonding present but will be discussed further in the hydrogen bonding section in this chapter.

The complex $[(L^5)Ni.MeCN](ClO_4)_2.(MeCN)$ also shows the same arrangement around its metal centre, again with the acetonitrile creating an unsymmetrical environment. There was no hydrogen bonding between counterions and complex present within the crystal structure.

The complex of $[(L^6)Ni.MeCN](ClO_4)_2.(MeCN)(H_2O)$ was the only structure achieved for this ligand to date. As fluorine is more electron withdrawing than OMe and Me, the weakest bond should be formed therefore keeping with the trend and being longer than the $[(L^4)Ni.MeCN](ClO_4)_2.(MeCN)$ bond 2.245Å. This length is 2.248Å and so for the nickel derivatives a trend can be seen to follow the electron withdrawing nature of the bond in relation to the bond length.

The structure of $[(L^7)Ni.MeCN](ClO_4)_2.MeCN$ was the only metal complex structure achieved to date for this ligand. The metal-$N_{Sulphonamide}$ length was 2.232Å which is identical to the $[(L^5)Ni.MeCN](ClO_4)_2.(MeCN)$ complex. It could be therefore perceived that these pendants are analogous with regard to their degree of electron withdrawing capabilities.

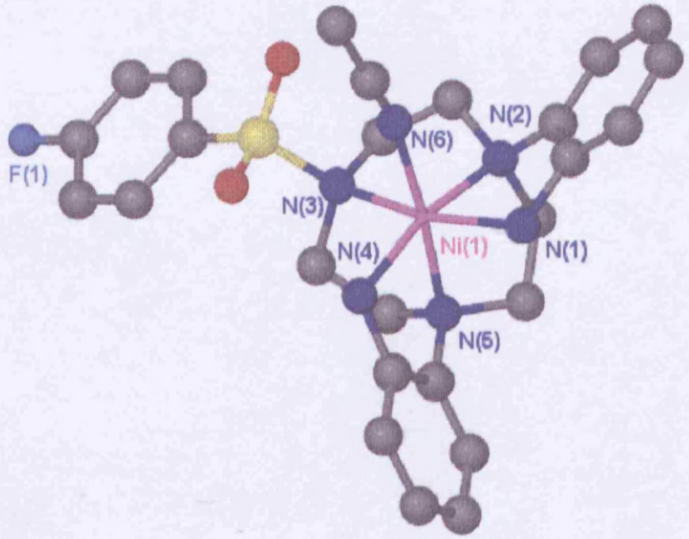

[(L^6)Ni.MeCN](ClO$_4$)$_2$.MeCN. H$_2$O

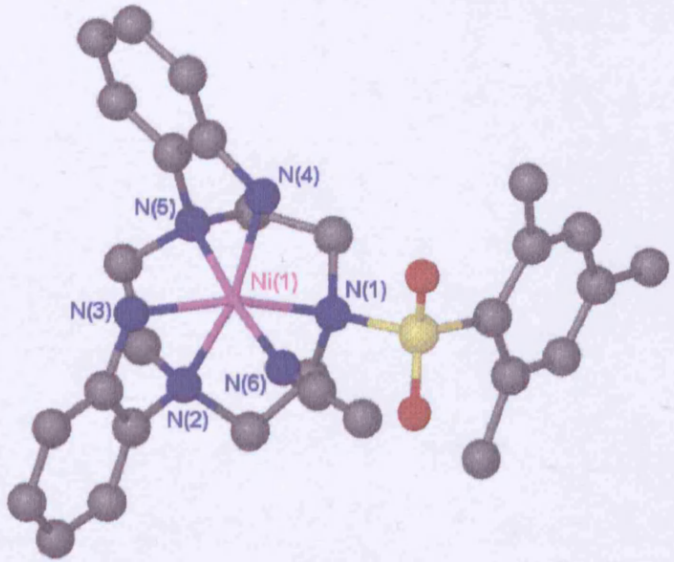

[(L^7)Ni.MeCN](ClO$_4$)$_2$.MeCN

Figure 4.7. [(L^6)Ni.MeCN](ClO$_4$)$_2$.MeCN. H$_2$O. Selected Bond lengths; N(1)-Ni(1) 2.094(3), N(2)-Ni(1), 2.081(3), N(3)-Ni(1) 2.248(3), N(4)-Ni(1) 2.061(3), N(5)-Ni(1) 2.094(3), N(6)-Ni(1)2.060(3). [(L^7)Ni.MeCN](ClO$_4$)$_2$.MeCN: N(1)-Ni(1) 2.232(4), N(2)-Ni(1) 2.096(3), N(3)-Ni(1) 2.092(4), N(4)-Ni(1) 2.081(4), N(5)-Ni(1) 2.100(4), N(6)-Ni(1) 2.063(4). Hydrogen atoms and solvent molecules have been removed for clarity.

Copper complexes

The crystal structure of $2[(L^4)Cu](ClO_4)_4.4(MeCN)$ MeOH exhibits a unique feature only observed for this class of compound. Within the cell, two of the same complexes are present, but both with slightly differing bond lengths and angles. Both metal centres are of distorted square based pyramidal arrangements, and the copper-nitrogen geometries are shown in figure 4.11.

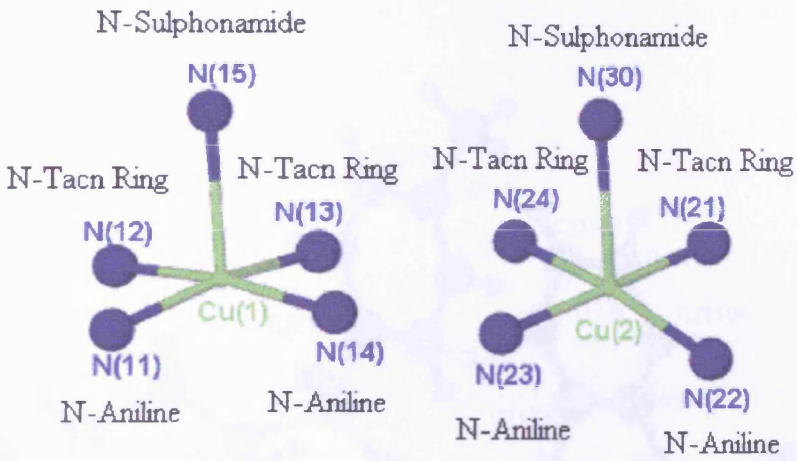

Figure 4.9: Copper and nitrogen donors in the complex of $2[(L^4)Cu](ClO_4)_4.4(MeCN)$ MeOH. The square based pyramidal structures are shown for both copper complexes present in the cell.

The relevant bond lengths and angles are shown in figure 4.10, and both show only minimal deviances in structure. This complex does not show any octahedral behaviour as no solvent donor is present to complete a hexadentate arrangement.

Cu(1)-N(14) 1.982(10)	Cu(2)-N(23) 1.967(10)
Cu(1)-N(11) 1.998(11)	Cu(2)-N(22) 1.988(11)
Cu(1)-N(13) 2.019(11)	Cu(2)-N(21) 2.025(10)
Cu(1)-N(12) 2.051(11)	Cu(2)-N(24) 2.041(10)
Cu(1)-N(15) 2.398(9)	Cu(2)-N(30) 2.453(11)
N(14)-Cu(1)-N(11) 99.9(4)	N(23)-Cu(2)-N(22) 99.9(5)
N(11)-Cu(1)-N(13) 165.2(4)	N(23)-Cu(2)-N(21) 171.4(5)

N(14)-Cu(1)-N(12) 167.1(4)	N(22)-Cu(2)-N(21) 86.1(4)
N(11)-Cu(1)-N(12) 84.5(4)	N(23)-Cu(2)-N(24) 86.2(5)
N(13)-Cu(1)-N(12) 86.2(4)	N(22)-Cu(2)-N(24) 162.5(4)
N(14)-Cu(1)-N(15) 108.1(4)	N(21)-Cu(2)-N(24) 86.4(4)
N(11)-Cu(1)-N(15) 109.4(4)	N(23)-Cu(2)-N(30) 100.6(4)
N(13)-Cu(1)-N(15) 80.5(4)	N(22)-Cu(2)-N(30) 117.0(4)
N(12)-Cu(1)-N(15) 81.4(4)	N(21)-Cu(2)-N(30) 81.9(4)

Figure 4.10: Table of bond distances and angles of both copper complexes present in $2[(L^4)Cu](ClO_4)_4.4(MeCN)$ MeOH crystal cell.

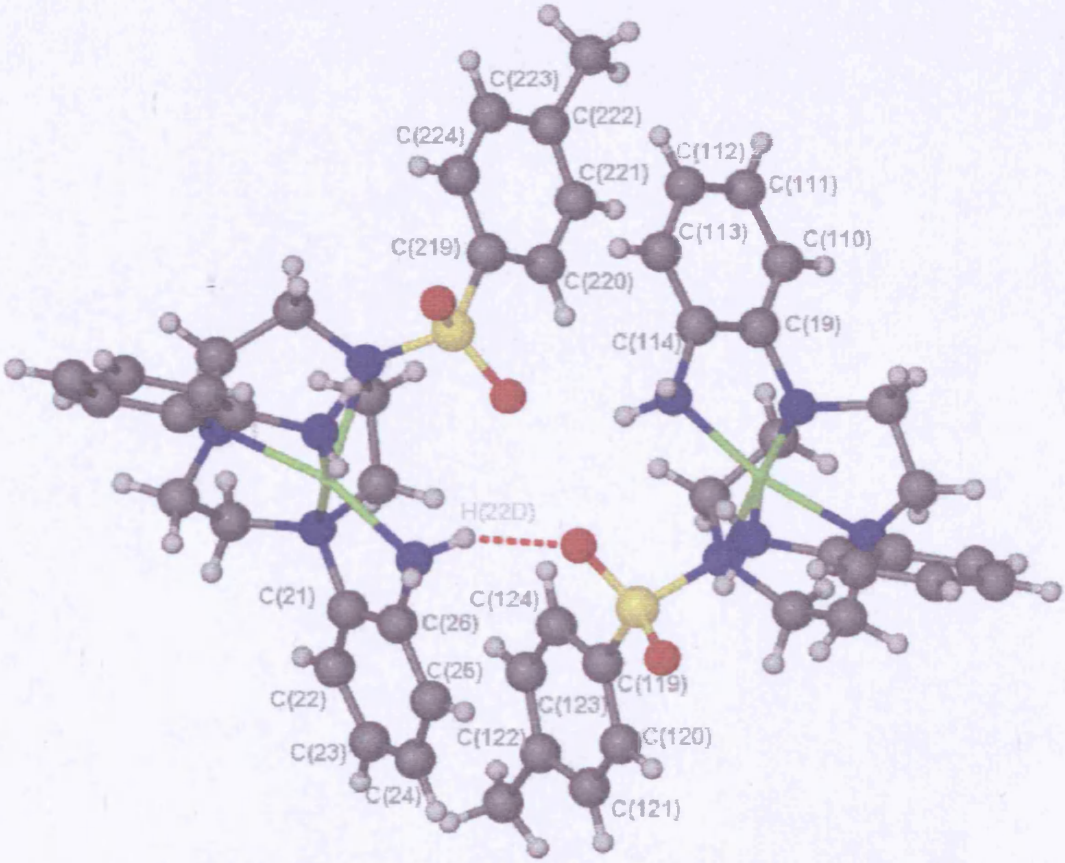

Figure 4.11: Both copper complexes $2[(L^4)Cu](ClO_4)_4.4(MeCN)$ MeOH present in the cell. All solvent and counter ions have been removed for clarity. Tosyl-phenyl ring non-bonding distances are C25-C120=3.802Å, C26-C119=3.893Å, C124-

C21=3.868Å, C24-C121=3.659Å, C123-C22=3.648Å, C122-C23=3.520Å, C110-C221=3.959Å, C111-C222=3.810Å, C112-C223=3.843Å, C113-C224=3.9131Å, C114-C219Å=4.018Å and C19-C220=4.046Å.

The tosyl and phenyl rings present in the cell appear to be π stacked [179] with the carbon distances ranging from 3.520Å-4.046Å. It can be imagined that due to the repulsion of the metal centres of the complexes, the stacking of the opposite tosyl-aniline aromatic rings is very weak with the strongest bonds occurring at the furthest opposing carbons in each pair. The shortest bonds are C111-C222=3.810Å and C122-C23=3.520Å. As a comparison, Riesgo *et al*[180] have observed π stacking in the crystal structure of 2, 2'-bibenzo[h] quinoline with an interplanar distance of 3.37Å. In a biological system, a slightly longer maximum of 3.5Å was noted by Shiraki *et al*[181] in the crystal structure of *Achromobacter* Protease, a Chymotrypsin-type serine. The π stacking occurs between Typ 169 and His 210 and the range of π stacking is 3.5Å-3.2Å.

The SO_2-H_2N distances for the compounds are 2.461Å, 2.548Å for one, and 2.380Å and 2.733Å for the other. Also within the cell, an aniline proton-oxygen hydrogen bond is present for opposing compounds with distances of 2.137Å and 2.272Å.

[179] Hunter C A., Sanders J K M., *J. Am. Chem. Soc.*, **1990**, 112, 5525-5534.
[180] Riesgo E C., Hu Y Z., Bouvier F., Thummel R P., Scaltrito D V., Meyer G J., *Inorg. Chem.*, **2001**, 40, 12, 3413-3422.
[181] Shiraki K., Norioka S., Li S., Yokota K., Sakiyama F., *Eur. J. Biochem.*, 269, **2002**, 4152-4158.

Zinc complexes

The crystal structure of $[(L^4)Zn.MeCN](ClO_4)_2.MeCN$ also exhibits an octahedral geometry with a molecule of acetonitrile bound via the lone pair of the nitrogen to the zinc centre. The $M\text{-}N_{sulphonamide}$ length is 2.404Å. The high resolution ^1H NMR data obtained shows an interesting display of doublets present in the aniline region (5.50-6.20ppm), which we find difficult to assign. We propose that due to the pair of inequivalent protons on the amine peaks should display a more complex arrangement than is actually observed in the spectra. The variable temperature ^1H NMR experiment was carried out on $[(L^4)Zn.MeCN](ClO_4)_2.MeCN$ to investigate the behaviour of the aniline protons. The spectrum is shown below in Figure 4.13. The temperature was increased stepwise from room temperature to 120°C and complete broadening of the aniline doublets was observed.

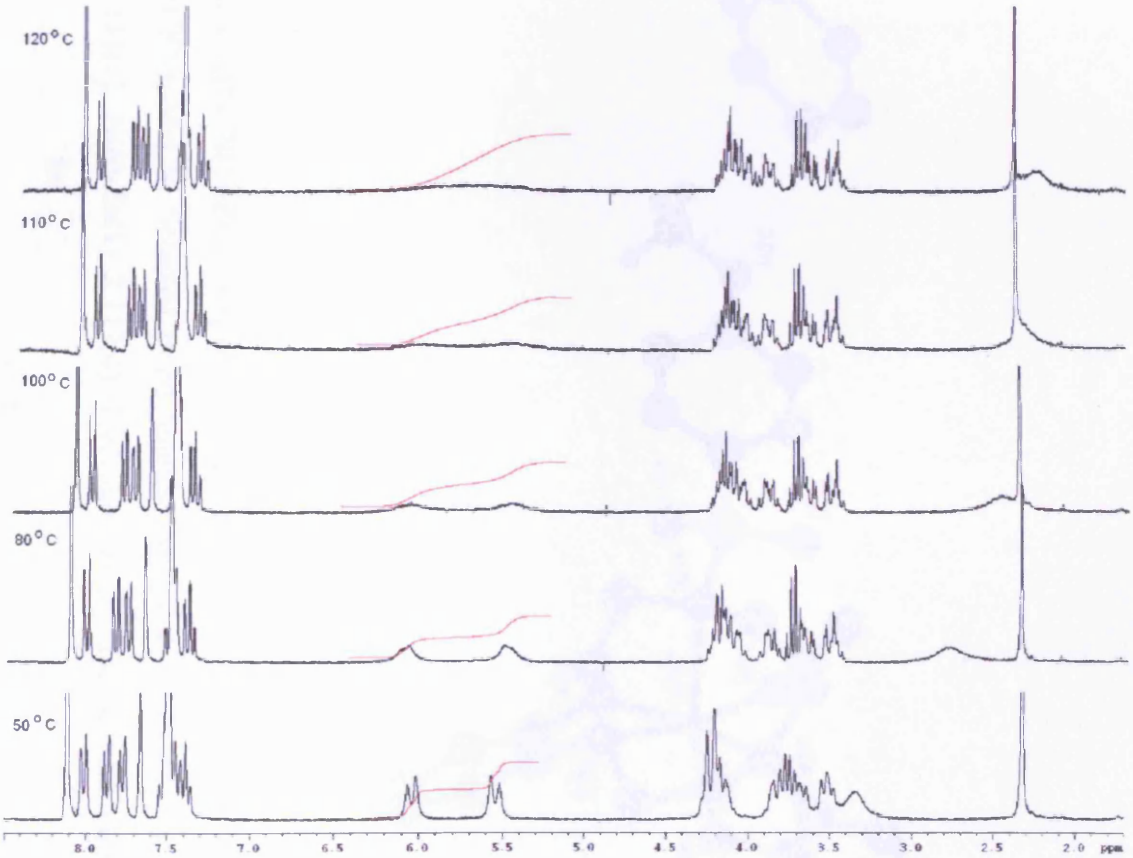

Figure 4.13: Variable Temperature ^1H NMR Spectra, 1.0ppm-6.5ppm for $[(L^4)Zn.MeCN](ClO_4)_2.MeCN$ in d^5 nitrobenzene.

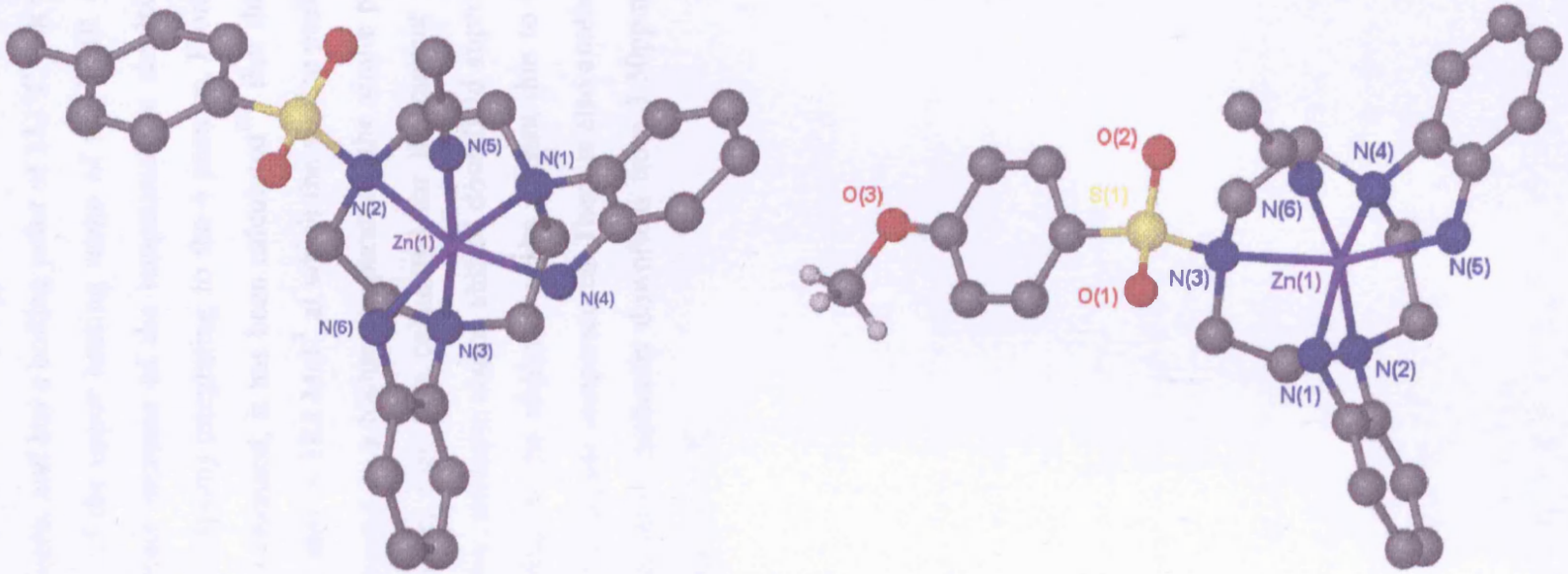

Figure 4.12. $[(L^4)Zn.MeCN](ClO_4)_2.MeCN$. Selected Bond lengths; N(1)-Zn 2.161(3), N(2)-Zn 2.404(2), N(3)-Zn 2.202(3), N(4)-Zn 2.113(3), N(5)-Zn 2.117(3) and N(6)-Zn 2.086(3). $[(L^5)Zn.MeCN](ClO_4)_2.MeCN$. Selected Bond lengths; N(1)-Zn(1) 2.066(3), N(2)-Zn(1) 2.199(3), N(3)-Zn(1) 2.410(3), N(4)-Zn(1) 2.134(3), N(5)-Zn(1) 2.131(3), N(6)-Zn(1) 2.117(4). Hydrogen atoms and solvent molecules have been removed for clarity.

As this increase occurred the doublets collapsing into the baseline. The deuterated solvent used was d_5-nitrobenzene, and has a boiling point of 211°C, but was not taken higher due to the restriction of the upper heating range of the NMR machine. We would predict that upon further increase of the temperature, a singlet would form between the aniline peaks (~5.8ppm) integrating to the 4 protons. From the variable temperature ^{1}H NMR spectra obtained, it has been calculated[182] that the temperature of coalescence is to be 81KJ Mol^{-1}± 1KJ Mol^{-1} at which the aniline peaks broaden. If the experiment could be repeated to a higher temperature, the single peak observed would generate a figure greater than that calculated for the current spectra. It is interesting to note also that the aromatic region shifted downfield approximately one ppm and there was sharpening of the aliphatic peaks present due to the increased fluxionality of the compound at higher temperatures. There is also another broad peak which we cannot assign that shifts gradually downfield from 3.50ppm to 2.45ppm, and a trace of water at 2.55ppm at 25°C.

[182] Iggo J., *NMR Spectroscopy in Inorganic Chemistry, Oxford Chemistry Primer*, Page 64.

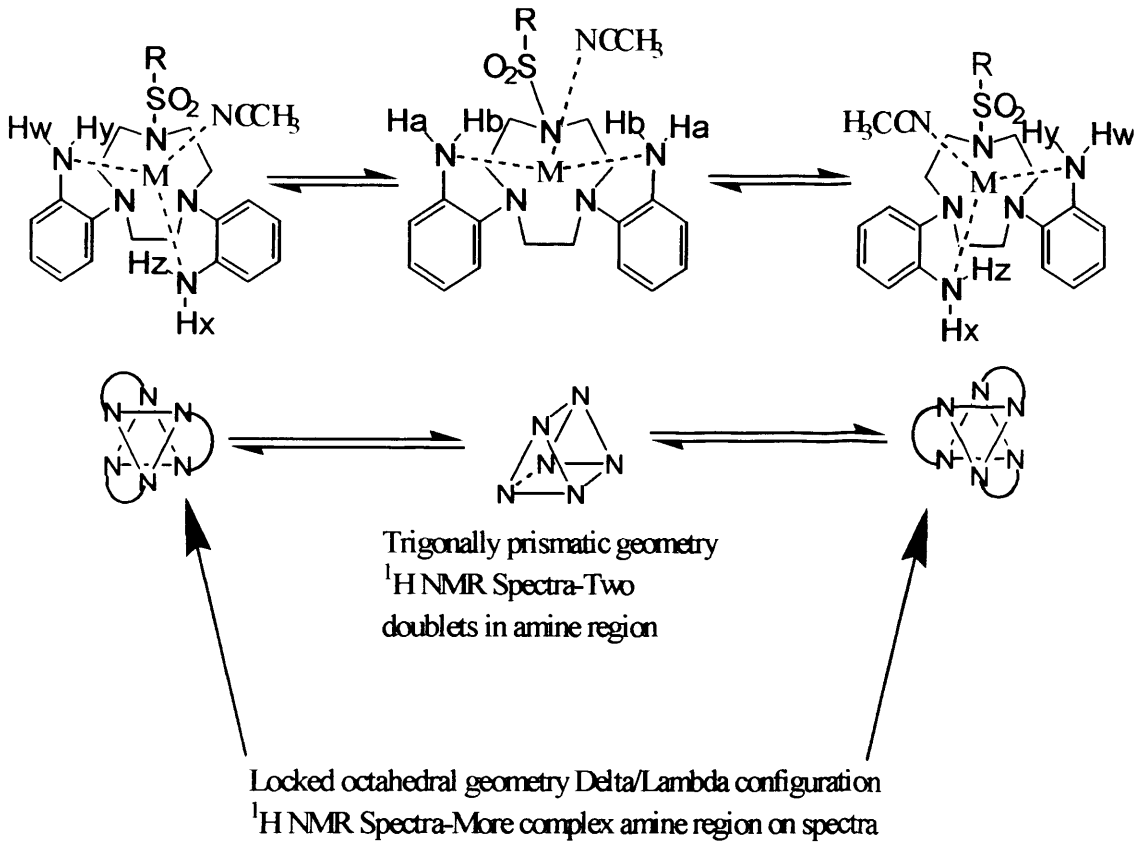

Figure 4.14: Labelling scheme for amine protons on symmetrical and unsymmetrical derivatives.

As can be seen from Figure 4.14, protons Ha and Hb would generate two doublets as observed in the $[(L^4)Zn.MeCN](ClO_4)_2.MeCN$, but the crystal structure shows an unsymmetrical arrangement in figure 4.14. This structure has 4 stereochemically inequivalent protons and so would generate a spectrum more complex than we actually observe. This spectrum we would predict would resemble four doublets.

The $[(L^5)Zn.MeCN](ClO_4)_2.MeCN$ crystal structure again indicates an octahedral environment with the inclusion of a bound acetonitrile molecule to the zinc centre. The bond length of the metal-sulphonamide is 2.410Å and so does not follow the trend as observed in the nickel analogue.

It is interesting to note a lack of apparent shifting in the ^{19}F NMR of $[(L^6)Zn.MeCN](ClO_4)_2.MeCN$. The nitro precursor (-104ppm), amine ligand L^6 (-

105ppm), and L^6Zn (-103ppm) show minimal deviation indicating a lack of interaction from the *para*-fluoro substituent.

Cadmium complexes

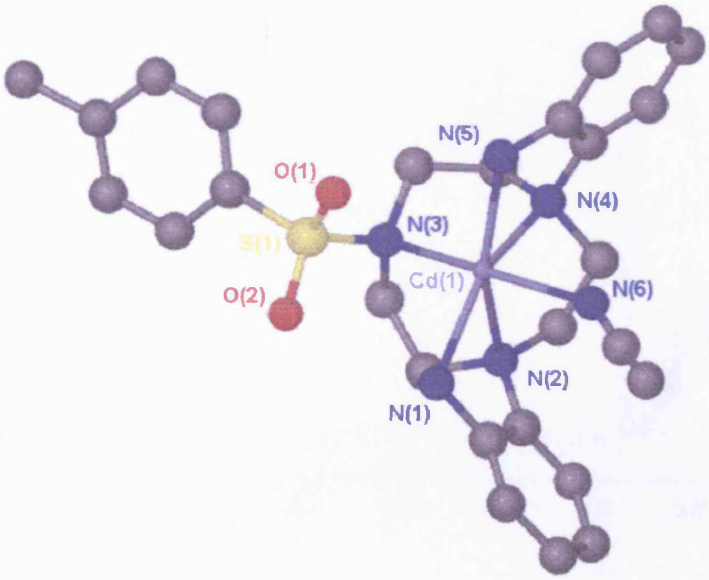

Figure 4.15. $[(L^4)Cd.MeCN](ClO_4)_2$. Hydrogen atoms and solvent molecules have been removed for clarity. Selected Bond lengths; N(1)-Cd(1) 2.243(4), N(2)-Cd(1) 2.508(3), N(3)-Cd(1) 2.631(4), N(4)-Cd(1) 2.412(4), N(5)-Cd(1) 2.241(4), N(6)-Cd(1) 2.347(16).

The crystal structure of $[(L^4)Cd.MeCN](ClO_4)_2$ shows a symmetrical arrangement, whereby an acetonitrile molecule is bound to the cadmium *trans* to the sulphonamide-metal bond of length 2.631Å. The spectra from the ^1H NMR is shown in figure 4.16, with an enlargement of the amine region shown in figure 4.17. The two broad peaks shown at 4.70ppm and 5.10ppm are tentatively assigned to the protons described in figure 4.14 as Ha and Hb.

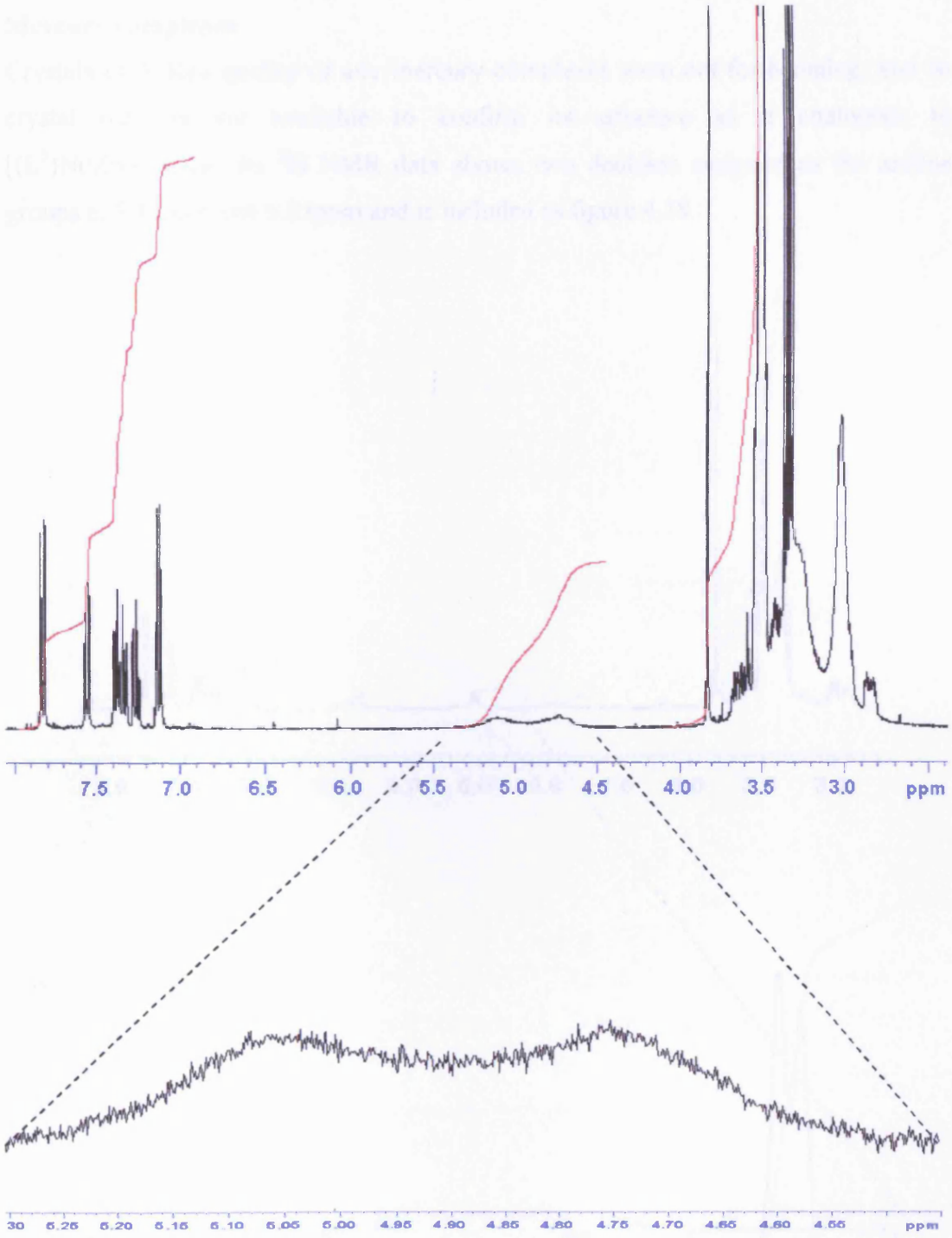

Figure 4.16A: ^{1}H NMR Spectra for $[(L^5)Cd.MeCN](ClO_4)_2$.

Figure 4.16B: ^{1}H NMR Spectra of aniline region (4.45ppm-5.30ppm) for $[(L^5)Cd.MeCN](ClO_4)_2$.

Mercury complexes

Crystals of X-Ray quality of any mercury complexes were not forthcoming, and so crystal data is not available to confirm its structure as if analogous to $[(L^5)Ni/Zn](ClO_4)_2$. Its ^1H NMR data shows two doublets assigned as the aniline groups at 5.13ppm and 6.33ppm and is included as figure 4.18.

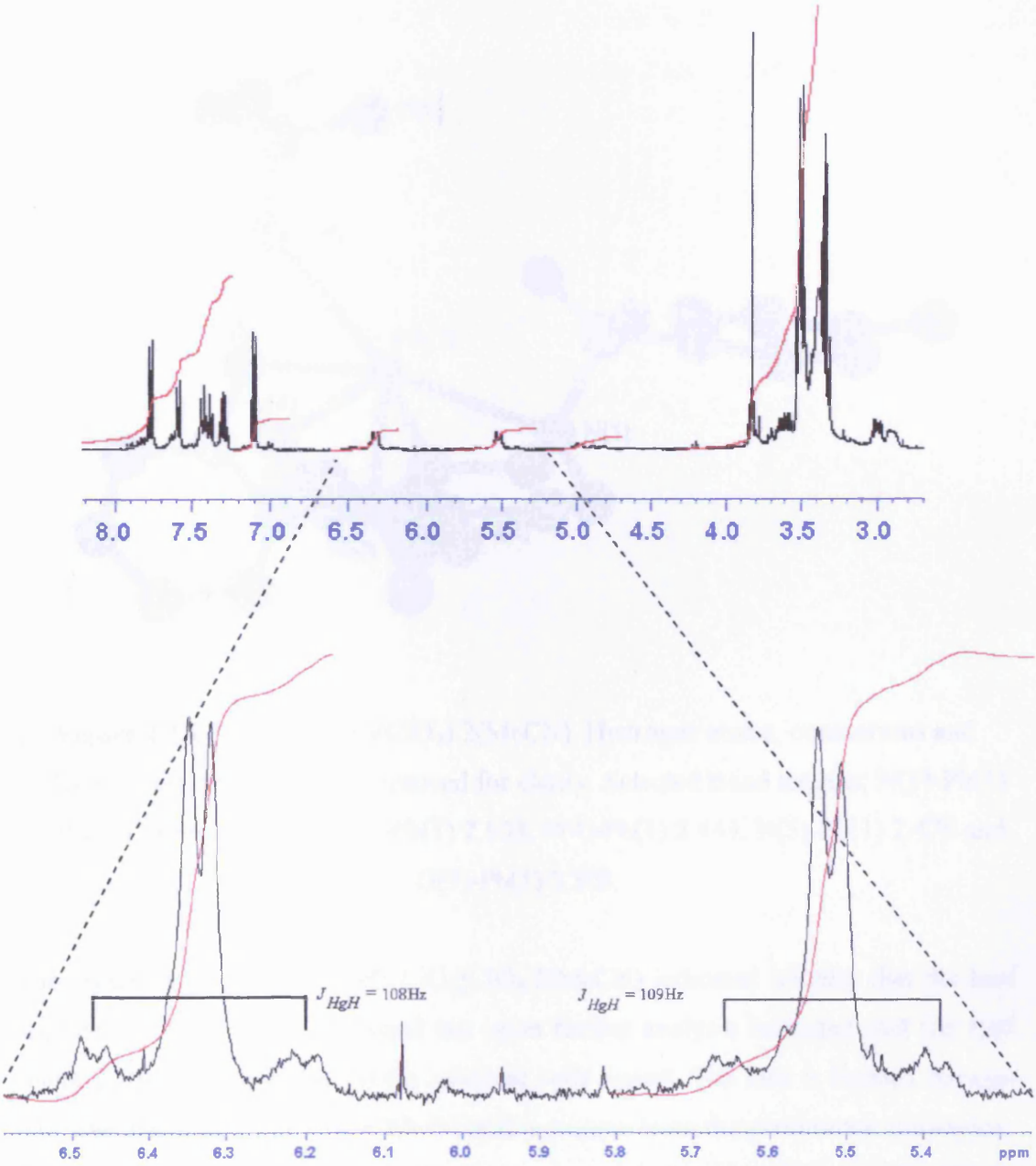

Figure 4.18: ^1H NMR Spectra of amine and Hg^{199} satellite region (5.30ppm-6.60ppm) for $[(L^5)Hg(ClO_4)_2$.

These are due to the J_{HgH} coupling between the ^{199}Hg isotope and the amine protons. Both coupling constants are similar with values of 109Hz and 108Hz.

Lead complexation

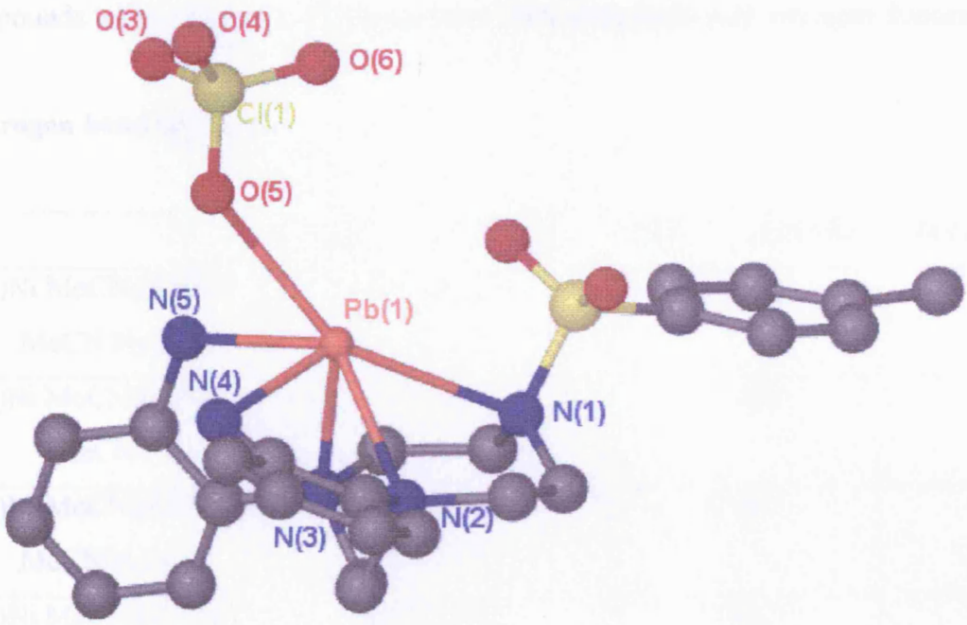

Figure 4.19. $[(L^4)Pb.ClO_4](ClO_4).2(MeCN)$. Hydrogen atoms, counterions and solvent molecules have been removed for clarity. Selected Bond lengths; N(1)-Pb(1) 2.953, N(2)-Pb(1) 2.584, N(3)-Pb(1) 2.633, N(4)-Pb(1) 2.443, N(5)-Pb(1) 2.476 and O(5)-Pb(1) 2.808.

The crystal structure of $[(L^4)Pb.ClO_4]ClO_4.2(MeCN)$ indicated initially that the lead ion was not bonded to the ligand but upon further analysis indicated that the lead centre in the cell is bonded to the adjacent cells ligand. The lead is bonded through four true bonds (N2-N5) and a Pb-O bond is present from the perchlorate counterion. A very long bond is present from the lead to the sulphonamide nitrogen with a length of 2.953Å and this completes a N_5O donor set. There is no hydrogen bonding evident from the crystallographic data and so the lead exhibits an unusual 6 co-ordinate geometry. It is unclear whether the lead's stereoactive lone pair of electrons is

dictating the geometry of the complex, but it could be perceived as being between and above the SO_2 group. The aniline pendant, when complexed to the lead centre, are rotated in one direction and so show the same metal-ligand geometry as the nickel and zinc complexes. The ^1H NMR spectra exhibits the same unusual amine splitting to that of the zinc and mercury counterparts. It is interesting to note the preference of the perchlorate oxygen over an acetonitrile solvent molecule to complete the 6 co-ordinate geometry. This deviance of metal donors is the first for this class of compounds where all other complexes have been completed with nitrogen donors.

Hydrogen bonding table

	ClO_4 - - -H_2N (Å)	SO_2 - - - H_2N (Å)	H_2O - - - H_2N (Å)
$[(L^4)Ni.MeCN](ClO_4)_2.$ $MeCN.H_2O$	2.116/2.130	2.508	NA
$[(L^5)Ni.MeCN](ClO_4)_2.$ MeCN	NA	2.342	NA
$[(L^6)Ni.MeCN](ClO_4)_2.$ $MeCN/H_2O$	NA	2.381	2.056
$[(L^7)Ni.MeCN](ClO_4)_2.$ MeCN	2.283/2.268	NA	NA
$2[(L^4)Cu](ClO_4)_4.4.Me$ CN.MeOH	2.137/2.272	2.461/2.548/2.380/ 2.733	NA
$[(L^4)Zn.MeCN](ClO_4)_2.$ MeCN	2.100/2.117/2.120/2.173	2.565	NA
$[(L^5)Zn.MeCN](ClO_4)_2.$ MeCN	2.100	2.566	NA
$[(L^4)Cd.MeCN](ClO_4)_2$	2.217	2.387/2.504	NA

Figure 4.20: Table of hydrogen bonding within crystal structures from this chapter.

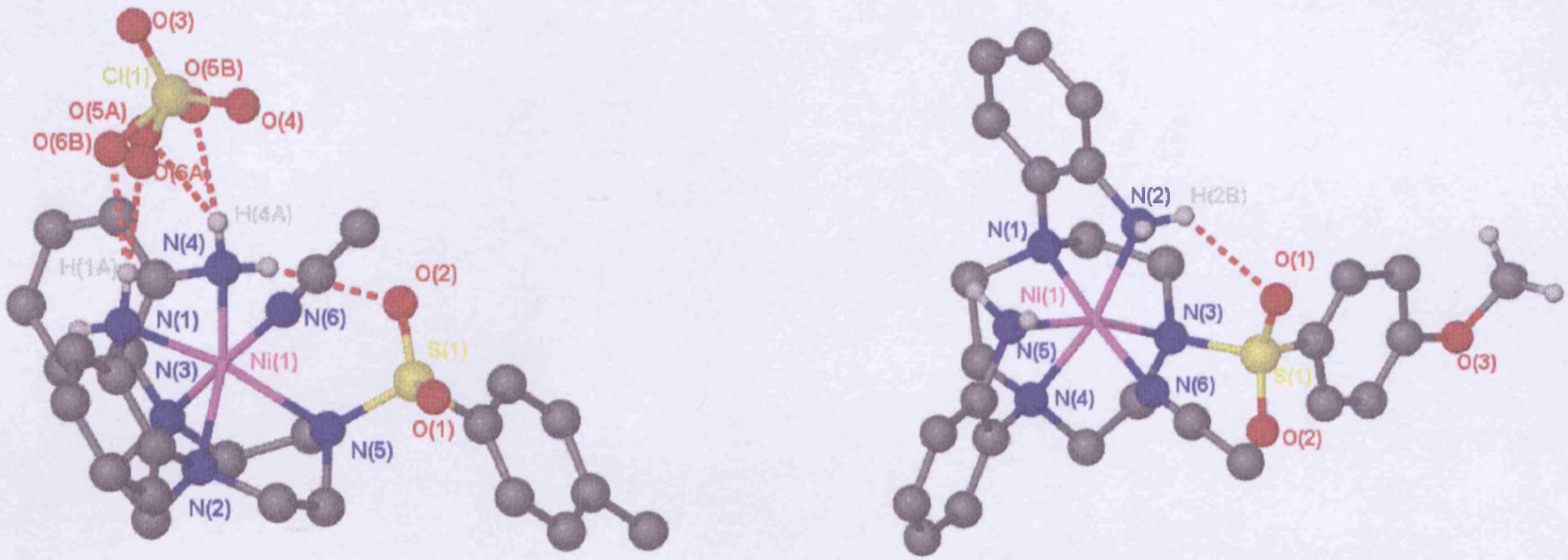

Figure 4.21: Hydrogen bonding present in $[(L^4)Ni.MeCN](ClO_4)_2.MeCN.H_2O$ and $[(L^5)Ni.MeCN](ClO_4)_2.MeCN$. Selected Counterions, hydrogen atoms and solvent molecules have been omitted for clarity.

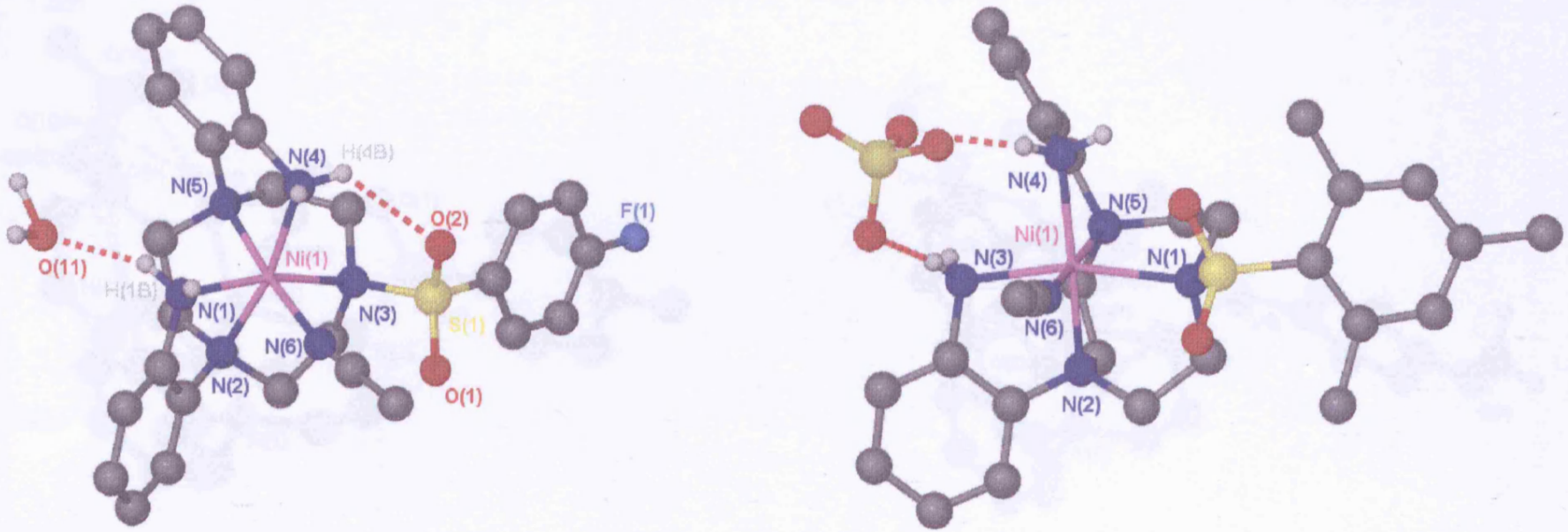

Figure 4.22: Hydrogen bonding present in $[(L^6)Ni.MeCN](ClO_4)_2.MeCN/H_2O$ and $[(L^7)Ni.MeCN](ClO_4)_2.MeCN$. Selected Counterions, hydrogen atoms and solvent molecules have been omitted for clarity.

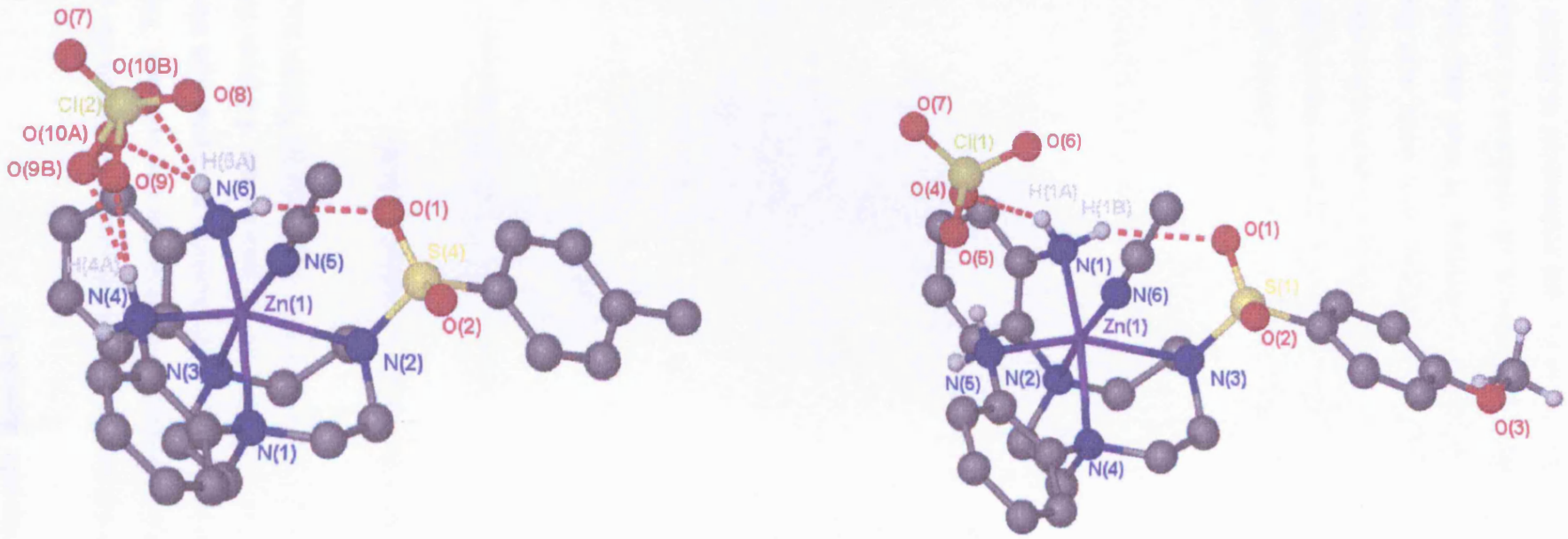

Figure 4.23: Hydrogen bonding present in $[(L^4)Zn.MeCN](ClO_4)_2.MeCN$ and $[(L^5)Zn.MeCN](ClO_4)_2.MeCN$. Selected Counterions, hydrogen atoms and solvent molecules have been omitted for clarity.

Bis-tosylated macrocyclic ligands L^8.

L^8 was synthesised via standard methodologies to investigate the possibilities of forming two metal sulphonamide binds within one complex. This would be a first for this area of research, but unfortunately no crystal data was forthcoming. There is a marked shift on the amine peaks from 4.20ppm for L^8 to 4.30-4.95ppm for $[(L^8)Zn](ClO_4)_2$ and 4.20-4.75ppm for $[(L^8)Cd](ClO_4)_2$.

Metal-Sulphonamide bond length comparison table.

Complex	Code	Metal-Sulphonyl bond length Å	Crystal System	Space Group
L^4Ni	0423	2.245	Monoclinic	P21/n
L^4Cu	0501	2.453	Triclinic	P-1
L^4Zn	0426	2.404	Monoclinic	P21/n
L^4Cd	0504	2.631	Triclinic	P-1
L^4Pb	0503	2.953	Triclinic	P-1
L^5Ni	0502	2.232	Triclinic	P-1
L^5Zn	0506	2.410	Monoclinic	P21/n
L^6Ni	0508	2.248	Triclinic	P-1
L^7Ni	0512	2.232	Monoclinic	P21/n

Figure 4.24. Table of Metal-Sulphonamide bond lengths, crystal system of cell and space group.

Attempts were made to synthesize the Mn, Fe and Co derivatives of this chapter, but employing the same methods and the relevant perchlorate salt did not produce any of the desired complexes. Complexation with ruthenium salts did not afford the desired complexes. Attempts were made with $RuCl_3.xH_2O$ and $Ru(DMSO)_4Cl_2$ and stirring with L^4 in ethanol. ^1H NMR data obtained indicated the presence of free ligand and showed no evidence of complexation. The reaction solution was dried *in vacuo*, and redissolved in MeCN and heated to

reflux, but again the ^{1}H NMR spectroscopic data showed no evidence of complexation. We feel that complexation should occur, but experimenting with differing reaction conditions is needed to generate the desired ruthenium complex.

Conclusions

A new class of substituted sulphonyl macrocyclic metal complexes has been described. From the crystal data obtained a range of metal-sulphonamide bond lengths (2.232Å-2.953Å) have been exhibited. We find that alteration of the substituents on the SO_2 group do not affect the bond length trend in relation to the electron-withdrawing nature of the substituted pendant. We would need more crystallographic evidence to fully explain and justify if this relation is coincidental or true to the previously stated hypotheses.

From the ^{1}H NMR spectra of the $[(L^{4/5/6/7})M](ClO_4)_2$ (M=Zn/Hg/Pb) derivatives compared to the Cd sample, we have concluded that the cadmium sample must be more fluxional in solution as the aniline protons show a broadened peak, whereas the aforementioned samples exhibited the pair of doublets. It is our interpretation that this doublet arrangement is an average of the Δ and Λ geometrical configurations and so a symmetrical, trigonal prismatic geometry is observed. We should carry out more varied temperature studies upon these samples to ascertain the point at which all samples exhibit the same doublet arrangement. It is unusual that only the cadmium sample shows this broadened peak and the mercury and lead samples do not. This anomaly could be attributed to the fact that the lead is not bound by six nitrogen ligators but five and a perchlorate oxygen. This difference in complexation may restrict the $[(L^4)Pb.ClO_4](ClO_4)$ sample to interchange when in solution, therefore exhibiting behaviour closer to that of the zinc and mercury samples. As we do not have the mercury crystal data, we cannot state with confidence why this trend arises as it does.

When we extended this investigation to the variable temperature ^{1}H NMR spectra of the $[(L^{4/5/6/7})Zn](ClO_4)_2$ samples, the results obtained we were most unexpected. If the complex were to be fluxional in solution, then we should have observed broadened peaks as those observed in the $[(L^4)Cd.MeCN](ClO_4)_2$

spectra. The peaks only started to look like those of the $[(L^4)Cd.MeCN](ClO_4)_2$ spectra at 100°C, and then the separation between the peaks did not reduce. This intense amount of energy needed to gain this result showed that the peaks were lost at 120°C and needed a calculated $\Delta G^{\ddagger}$ value of 81kJMol^{-1} to achieve this degree of fluxionality. As a comparison, Wieghardt *et al*[183] calculated a $\Delta G^{\ddagger}$ value of 55KJMol^{-1} for the merging of benzylic protons of $[(L^{KW})Zn](ClO_4)_2$. Over a temperature range of -36°C-40°C, the diastereotopic proton peaks merged to form a singlet. Our value shows that more energy is needed to achieve this and as stated before, the amine protons are still not in an equal environment. Our system is more strained as the 2 metal-ligand chelates are 5 membered, and the Wieghardt complex has 3 × 6 membered chelates. The barrier of rotation is currently being calculated by theoreticians at Cardiff University to see if the value agrees with data already collected.

[183] Schlager O., Wieghardt K., Nuber B., *Inorg. Chem.*, **1995**, 34, 6449-6455.

Chapter Five

Tetra-aza ligands and complexes

I don't deserve this award, but I have arthritis and I don't deserve that either.
-- Jack Benny

O Lord, help me to be pure, but not yet.
-- Saint Augustine

Chapter Five

Introduction

The research of porphyrins is extensive and varied[184,185]. As explained in chapter one, the need for sterically hindered ligands is paramount to the operation of our proposed system. Due to the inaccessibility of tetramesitylporphyrin in large quantities it is our aim to synthesize potential ligands that fit the criteria needed for the system (bulky groups to prevent dimerisation and nitrogen donors). Within this chapter we hope to show the possibility of producing such azamacrocyclic ligands that mimic porphyrin ligands, but that are more accessible and readily substituted.

Wieghardt *et al*[186] have shown that 6-membered chelates are formed upon complexation with the ligand 1, 4-bis(2-aminobenzyl)-1, 4-diazacyclohexane. Reaction of 2-nitrobenzyl bromide with piperazine afforded L^a and subsequent hydrogenation with graphite catalyst and hydrazine generated the amine derivative (L^b). Ethanolic solutions of the metal salts were reacted with L^b to afford the respective metal complexes in good yield (67-80%).

[184] Lindsey J S., *The Porphyrin Handbook*, **2000**, 45-117.
[185] Sessler J L., *J. Porphyrins Phthalocyanines*, 4, **2000**, 331-336.
[186] Schlager O., Wieghardt K., Rufinska A., Nuber B., *J. Chem. Soc., Dalton Trans.*, **1996**, 1659-1668.

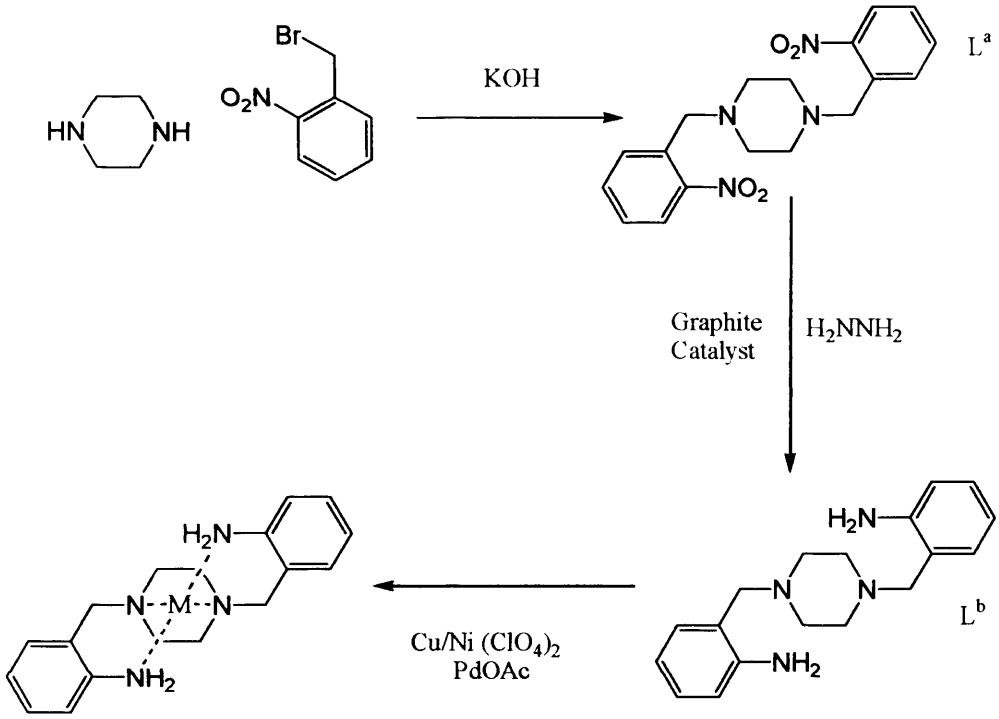

Figure 5.1: Synthesis of 1, 4-bis (2-aminobenzyl)-1, 4-diazacyclohexane complexes by Wieghardt *et al.*

Kimura *et al*[187] have developed a class of ligands to mimic carbonic anhydrase and have shown that a sulphonamide pendant inhibits this process. The process involves the formation of a Zn-OH species at pH 7 which has shown mimetic catalytic activity of carbonic anhydrase.

[187] Koike T., Kimura E., Nakamura I., Hashimoto Y., Shiro M., *J. Am. Chem. Soc.*, **1992**, 114, 7338-7345.

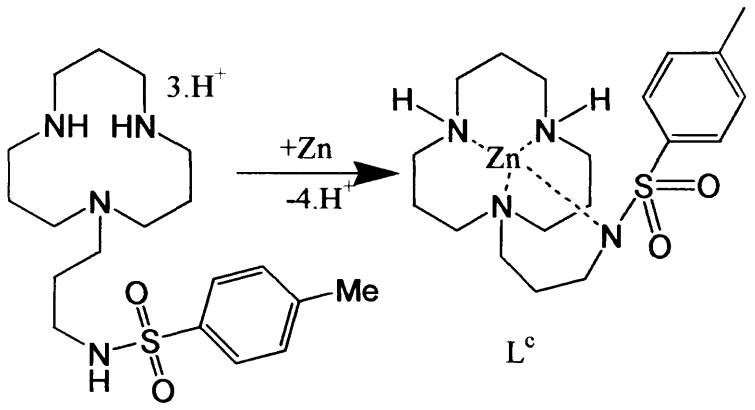

Figure 5.2: 12aneN$_3$ with a pendant propylamido *p*-tosyl, and its zinc complex.

Kimura and co-workers have shown that a sulphonamide pendant inhibits the process by forming a strong anionic nitrogen moiety and thus bonding with the zinc atom (L^c). The crystallographic data shows a tetragonally distorted geometry with the zinc-sulphonamide bond length 1.925Å.

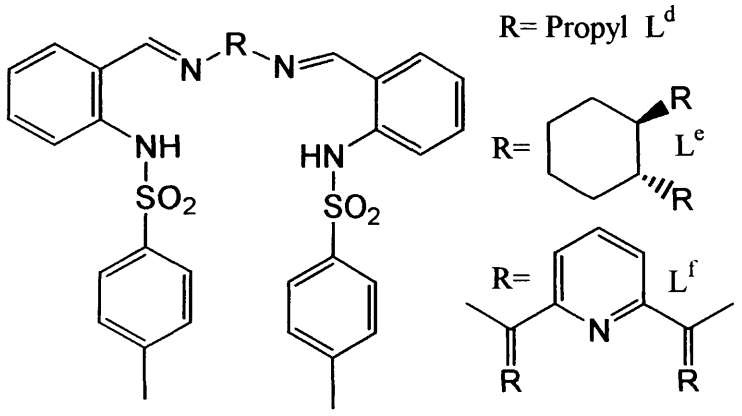

Figure 5.3: Ortho-tosylaniline derivatives with different Schiff base backbones.

A large amount of research has been carried out by Bermejo *et al*, on tosyl pendant containing ligands By differing the backbone group, they have been able to construct helical complexes with many transition metals. Employing the

flexible spacer of a propyl chain (L^d)[188] allowed the complexation of Mn/Fe/Co/Cu/Zn/Cd. It is interesting to note that the Co and Cu structures showed the formation of monomeric species whereas the Zn complex showed the binding of two Zn metals to two ligand chains, forming the [$L^d{}_2Zn_2$] complex. The [(L^d)Co] complex exhibits a metal sulphonamide length of 1.962Å, and the [(L^d)Cu] complex 1.980Å. The dimeric zinc compounds have an average metal-sulphonamide length of 1.978Å.

Complexes with the cyclohexane backbone have been investigated by both Bermejo L^e[189], and Lemaire L^e[190]. The formation of the [(L^d)Ni] and [(L^e)Cu] formed tetragonally distorted compounds with metal-sulphonamide bond averages of 1.922Å and 1.963Å respectively. The Lemaire group complexed the L^eCo compound which exhibited like geometry and bond averages of 1.995Å. Interestingly the Lemaire group could modify the sulphonyl moiety to add the triflate moiety using triflic anhydride, Et_3N in dichloromethane at -78°C. This ligand was reacted with $NiCl_2.6H_2O$ which formed the desired complex. X-Ray crystallography showed the metal-sulphonamide bonds to be very short at 1.908Å.

Bermejo *et al* extended their research further by incorporating a 2, 6-diacetylpyridine group between the tosylated anilines to form a new class of pentadentate ligand (L^f)[191]. Reaction group twelve metals afforded [(L^f)M] $(ClO_4)_2$ (M=Zn/Cd/Hg). X-Ray data was obtained for [(L^f)Zn]$(ClO_4)_2$ and [(L^f)Cd.H_2O]$(ClO_4)_2$ which showed distorted bipyramidal-trigonal and distorted pentagonal-pyramidal geometries respectively. Metal-sulphonamide averages are 2.012Å (L^fZn) and 2.291Å [L^fCdH_2O].

---

[188] Vasquez M., Bermejo M R., Fondo., Garcia-Deibe A., Gonzalez A M., Pedrido R., *Eur. J., Inorg. Chem.*, **2002**, 465-472.
[189] Vasquez M., Bermejo M R., Sanmartin J., Garcia-Deibe A M., Lodeiro C., Mahia J., *J. Chem. Soc. Dalton Trans.*, **2002**, 870-877.
[190] Karame I., Tommasino M L., Faure R., Lemaire M., *Eur. J. Inorg. Chem.*, **2003**, 1271-1276.
[191] Pedrido R., Bermejo M R., Garcia-Diebe A M., Gonzalez-Noya A M., Maniero M., Vasquez M., *Eur. J. Inorg. Chem.*, **2003**, 3193-3200.

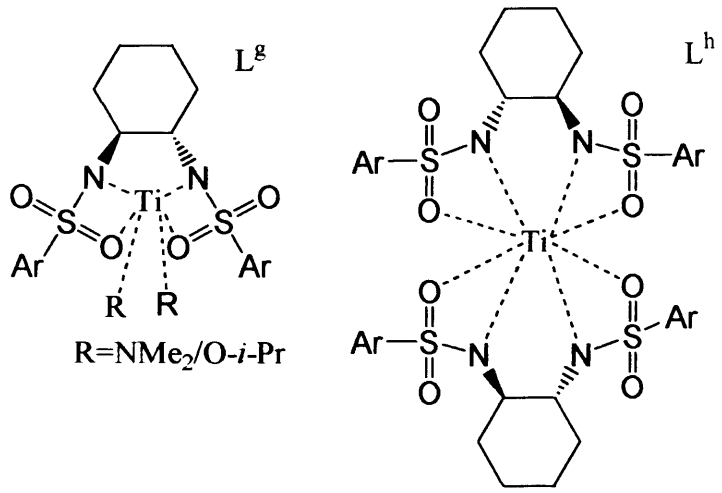

Figure 5.4: Titanium complexes bound by bis sulphonamide cyclohexyl ligands.

Walsh *et al*[192, 193] have developed titanium complexes ($L^{g/h}$) that are bound to a sulphonamide nitrogen for the catalytic asymmetric addition of diethylzinc to aldehydes[194]. It is of interest to note that an oxygen from the SO_2 group participates in binding to the titanium metal centre and forms octahedral and 8-coordinate complexes with highly defined geometrical orientations.

The catalytic behaviour of Salen derivatives in previous years has proved to be very selective in the resolving of racemic mixtures of epoxides. Chiral versions of Salen complexes have been found to resolve epoxides in high enantiomeric excess and high yield.

Recently Fallis *et al*[195] have shown that chiral vanadyl salen complexes can bind with different enantiomers and with the aid of EPR, can be distinguished by different characteristic spectra. The spectra indicate different interactions between the epoxides to the vanadyl salen catalyst, and also through the aid of DFT studies have confirmed the formation of diastereotopic complexes between the enantiomers of the vanadyl salen complex.

---

[192] Royo E., Betancourt J M., Davis T J., Carroll P., Walsh P J., *Organomet.* **2000**, 19, 4840-4851.
[193] Pritchett S., Gantzel P., Walsh P J., *Organomet.*, **1997**, 16, 5130-5132.
[194] Ojima I. Ed., *Catalytic Assymetric Synthesis*, VCH, New York, **1993**.
[195] Fallis I A., Murphy D M., Willock D J., Tucker R J., Farley R D., Jenkins R ., Strevens R R., *J. Am. Chem. Soc.*, 126, **2004**, 15660-15661.

Santos *et al*[196]investigated the effects of bridge constituents upon the stabilisation of the Ni^{3+} state. The crystal data obtained shows minimal deviation for L^j-L^k with average metal bond lengths of 1.845Å and 1.841Å respectively.

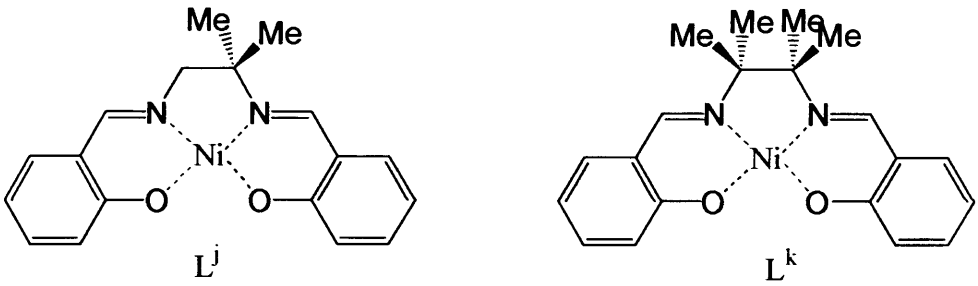

Figure 5.5: dimethyl and tetramethyl Schiff base (Salen) complexes of nickel.

Fajer *et al*[197] have investigated derivatives of porphyrins to see the effect non-planarity has upon the crystal packing of these complexes. These porphyrins are below and the N-Ni bond length averages are tabulated in figure 5.6.

1=2, 3, 7, 8, 12, 13, 17, 18-octaethyl, 5, 10, 15, 20-tetraphenylporphyrin.

2=2, 3, 7, 8, 12, 13, 17, 18-octapropyl, 5, 10, 15, 20-tetraphenylporphyrin.

3=2, 3, 7, 8, 12, 13, 17, 18-tetracyclohexenyl, 5, 10, 15, 20-tetraphenylporphyrin.

4=2, 3, 7, 8, 12, 13, 17, 18-octabromo, 5, 10, 15, 20-tetramesitylporphyrin.

5=2, 3, 7, 8, 12, 13, 17, 18-octabromo, 5, 10, 15, 20-tetrakis(pentafluorophenyl)porphyrin.

6=2, 3, 7, 8, 12, 13, 17, 18-octaethyllporphyrin.

---

[196] Santos I C., Vilas-Boas M., Piedade M F M., Freire C., Duarte M T., de Castro B., *Polyhedron*, 19, **2000**, 655-664.

[197] Barkinga K M., Renner M W., Furenlid L R., Medforth C J., Smith K M., Fajer J., *J. Am. Chem. Soc.*, **1993**, 115, 3627-3635.

1	2	3	4	5	6
1.906Å	1.902Å	1.914Å	1.916Å	1.903Å	1.952Å

Figure 5.6: Table for N-Ni average bond lengths for selected porphyrin complexes.

Aims and Objectives

Due to the problems associated (yields, chromatography) with synthesis of sterically hindered porphyrins and subsequent metallation, we decided to pursue our own area of research, through the formation of analogous tetraaza dianionic ligands and complexes.

Formation of the ligand *N, N'*-bis (2-aminophenyl) 1, 4-diazacycloheptane (L^{HP}) has been achieved previously by Fallis et al[198] and the N4 donor set could be perceived as analogous to the N4 donors of porphyrins.

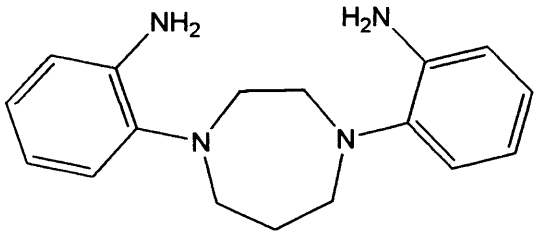

L^{HP}

Figure 5.7: *N, N'*-bis (2-aminophenyl) 1, 4-diazacycloheptane L^{HP}.

We felt with deprotonation to form the dianionic anilide species, we could form square planar complexes, and tailoring of the backbone or phenyl rings would allow us the possibility of creating sterically hindered ligands. Our ultimate goal would be to complex ruthenium in a sterically hindered ligand environment, and then begin testing of the compound for catalytic properties.

[198] Fallis I A., Perkins W T S., Malik K M A., *Unpublished Results.*, **2001**.

Results and Discussion

Complexation with these piperazine derivatives has been found in the past to not form complexes due to the restricted access to the macrocycles lone pair. The tight bite angle formed upon complexation is too strained and so the 5-membered chelate cannot be formed. Increasing the macrocycle from a 6 to 7-membered ring allows complexes to be formed but albeit strained. There are examples of piperazine macrocycles forming 5-membered chelates[199], but our *N*-Aryl derivative may be too rigid for such complexation. Larger 6-membered chelates have been formed with titanium by Mountford et al[200]. The ligand 1, 4-bis(2-amino-4-tert-butylbenzyl)piperazine has been crystallographically examined to show a square based pyramidal structure with a tertiary butyl ammonium counterion forming the apical donor. The 1, 5-diazacyclooctane macrocycle is large enough so when reacted forms metal complexes of square planar or octahedral geometries, by providing planar donors to the metal. Previous research by Fallis *et al*[201] has shown formation of the 1, 5-diazacyclooctane (daco) compounds[202], produces highly symmetrical square planar complexes.

[199] Ratilainen J., Airola K., Frohlich R., Nieger M., Rissanen K., *Polyhedron*, 18, **1999**, 2265-2273.
[200] Lloyd J., Vatsadze S Z., Robson D A., Blake A J., Mountford P., *J. Organomet. Chem.*., 591, **1999**, 114-126.
[201] Fallis I A., Perkins W T S., Malik K M A., *Unpublished Results*, **2000**.
[202] Halfen J A., Moore H L., Fox D C., *Inorg. Chem.*, **2002**, 41, 3935-3943.

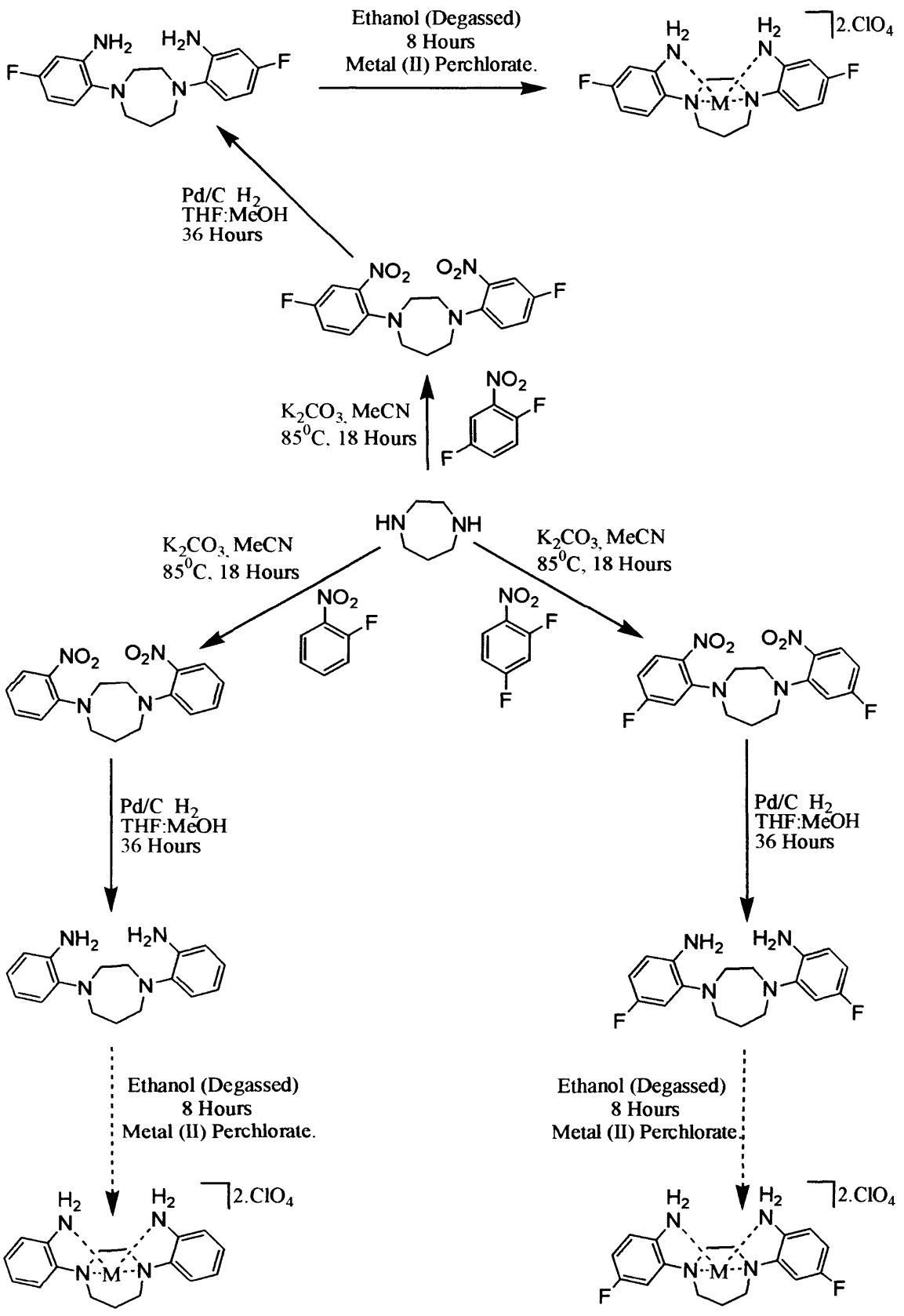

Figure 5.8: Reaction scheme for the synthesis of homopiperazine complexes.

Synthesis of the ligands produced highly coloured orange and yellow powders, except for 1-(2-nitrophenyl), 4-(2-nitro, 5-fluorophenyl)-homopiperizene which was afforded as a viscous orange oil. The hydrogenated ligands were found to be reasonably air stable but were manipulated under anaerobic conditions to reduce to possibility of any oxidised impurities catalytically degrading the samples. Complexation was carried out by stirring the ligand and metal perchlorate salt in an ethanolic solution. The crystal structure of L^{11NB} is attached as Appendix iii.

Nickel complexes.

$[(L^{11})Ni.2MeCN](ClO_4)_2$ was found to crystallise with two perchlorate counterions and two molecules of MeCN solvent. No hydrogen bonding was found within the cell. On comparison with the parent ligand L^{HP}, there are minimal bond length deviances but it is of interest to note an increase in the N_{ring}-Ni distances of 0.012Å and a decrease of 0.013Å in the $N_{aniline}$-Ni distances. This could be perceived as due to the fluorine being in the *para* position relative to the nitrogen in the homopiperazine ring, electron density is being withdrawn from the ring and weakening the N_{ring}-Ni bond, thus making it longer.

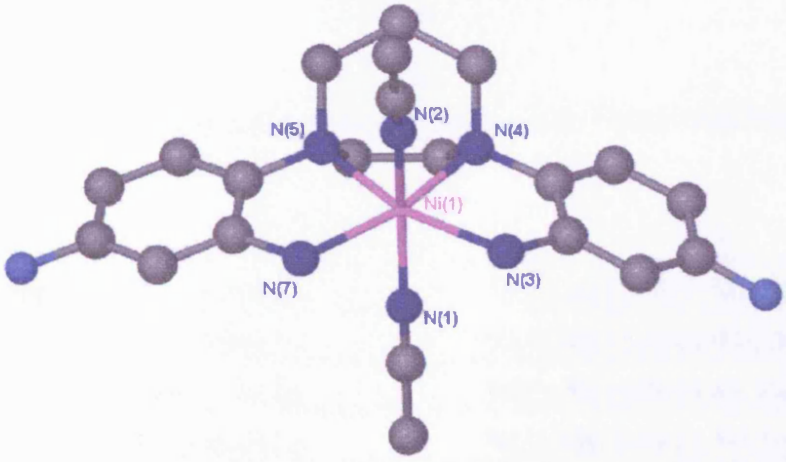

Figure 5.9: $[(L^{11})Ni\ 2.MeCN)](ClO_4)_2$. Hydrogen atoms and solvent molecules have been removed for clarity. N(1)-Ni(1) 2.129(4), N(2)-Ni(1) 2.127(4), N(3)-Ni(1) 2.080(4), N(4)-Ni(1) 2.094(4), N(5)-Ni(1) 2.092(4), N(7)-Ni(1) 2.071(4).

It would be of interest to observe other nickel derivatives with the fluorine in the *ortho* and *para* position to the aniline to hopefully note a trend in bond lengths when compared to the fluorine position. We would expect when the fluorine is *ortho* to the aniline the N_{ring} distances would be shortest and $N_{aniline}$ distances to be the longest. The octahedral geometry displayed is slightly distorted with the acetonitrile donors flexing out of the ideal position of 90° to all nitrogen donors of the ligand by ~5° away from the macrocycle ring.

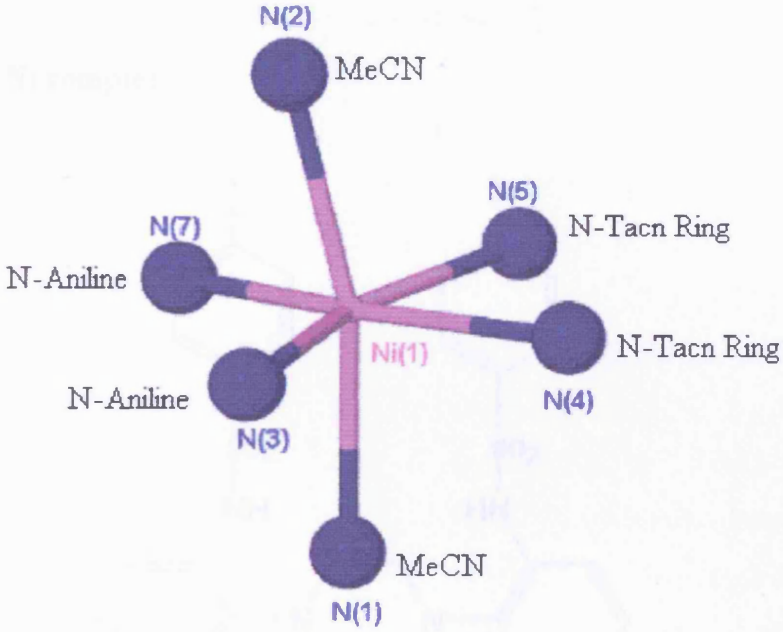

Figure 5.10: Distorted octahedral environment of $[(L^{11})Ni\ 2.MeCN)](ClO_4)_2$.

N(7)-Ni(1)-N(3) 114.40(16)	N(5)-Ni(1)-N(2) 96.29(15)
N(7)-Ni(1)-N(5) 84.49(15)	N(4)-Ni(1)-N(2) 99.02(15)
N(3)-Ni(1)-N(4) 83.43(15)	N(7)-Ni(1)-N(1) 85.59(15)
N(5)-Ni(1)-N(4) 77.63(15)	N(3)-Ni(1)-N(1), 86.39(15)
N(7)-Ni(1)-N(2) 87.17(15)	N(5)-Ni(1)-N(1) 94.11(14)
N(3)-Ni(1)-N(2) 86.46(15)	N(4)-Ni(1)-N(1) 91.28(14)

Figure 5.11: Bond angles for $[(L^{11})Ni\ 2.MeCN)](ClO_4)_2$.

Sample	Code	N-Tacn	N-Tacn	N-Aniline	N-Aniline	N-MeCN	N-MeCN
[L^{11}Ni 2.MeCN]	0419	2.094(4)Å	2.092(4)Å	2.071(4)Å	2.080(4)Å	2.129(4)Å	2.127(4) Å
[L^{HP}Ni 2.MeCN]	01IAF11	2.082(2)Å	2.080(2)Å	2.083(3)Å	2.094(3)Å	2.129(2)Å	2.117(3) Å
L^{HP}Ni	01IAF12	1.902(2)Å	1.893(2)Å	1.911(2)Å	1.911(2)Å	NA	NA

Figure 5.12: Comparison of bond lengths of [(L^{11})Ni 2.MeCN](ClO_4)$_2$, [(L^{HP})Ni 2.MeCN] (ClO_4)$_2$.and [(L^{HP})Ni] (ClO_4)$_2$.

Tosylated Ni complex.

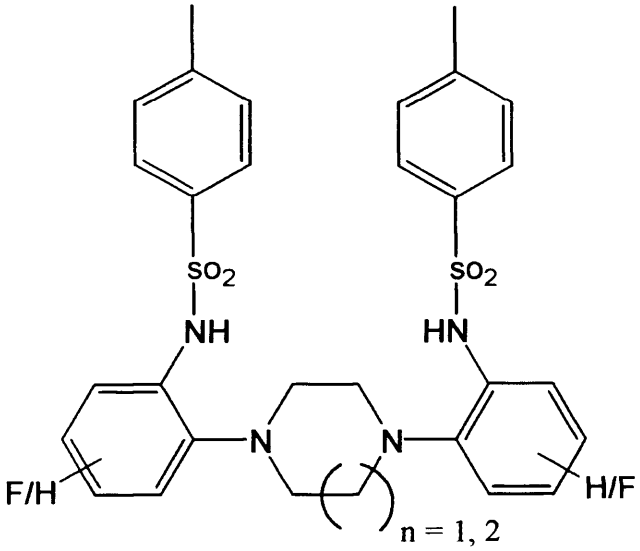

n = 1 = 1, 4-Diazacyclohexane = Piperazine
n = 2 = 1, 4-Diazacycloheptane = Homopiperazine

Figure 5.13: Schematic of functionalised diazamacrocycles piperazine and homopiperazine.

The synthesis of L^{12} was accomplished by the addition of tosyl chloride to L^{HP} under basic conditions. Work-up methods to date have produced the desired ligand but have not been optimised. Tosylation methods were modified from

procedures by Bermejo[188, 189, 191] and Goujon[203]. The metal salt was reacted with L^{12} in degassed acetone, and after the removal of solvent, the residue was taken up in MeCN and left to stand over the weekend. Fortunately crystals of X-Ray quality were afforded but this reaction was repeated with Zn, Mn and Cu and no positive results were obtained.

The bonds lengths for [L^{12}Ni] (IAF0402) are over a wide range (1.898Å-1.939Å), indicating a strained geometry. The plane of the nickel centre is slightly twisted and a plane drawn through N (2)-N (3) and N (4)-N (1), when measured as a torsion angle through the nickel centre gives an angle of 169°. This deviance from 180° shows a strain that could be due to the small ring size of the macrocycle, forcing the metal into a distorted square planar geometry. It is interesting to note the non-bonding distances for the oxygen's present in the SO_2 to the nickel centre are 3.180, 3.466, 4.230 and 4.292Å. This confirms that the geometry of the structure is truly a distorted square planar complex without axial ligands present.

Comparison of the N-Ni bond lengths is restricted due to the lack of like compounds in the literature. The crystal structure of L^{c}Ni by Bermejo[189] (Introduction, chapter five) shows bond lengths of 1.883Å, 1.925Å (cyclohexane amines) and 1.871Å and 1.919Å for the Ni-sulphonamide bonds. The [L^{12}Ni] Ni-sulphonamide bond length average is 0.024Å longer than [L^{c}Ni] structure. The [L^{c}Ni] complex shows a 6-membered chelate upon complexation, whereas [L^{12}Ni] is the more strained 5-membered chelate. The two bonds of [L^{12}Ni] are 1.939Å and 1.898Å and this big difference in like bonds could be due to the steric interference of the tosyl groups around the metal centre. The stress of the tosyl groups folding away from each other may lead to this inequivalence of bond lengths.

[203] Goujon J-Y., Zammattio F., Chretien J-M., Beaudet I., *Tetrahedron.*, 60, 18, **2004**, 4037-4039

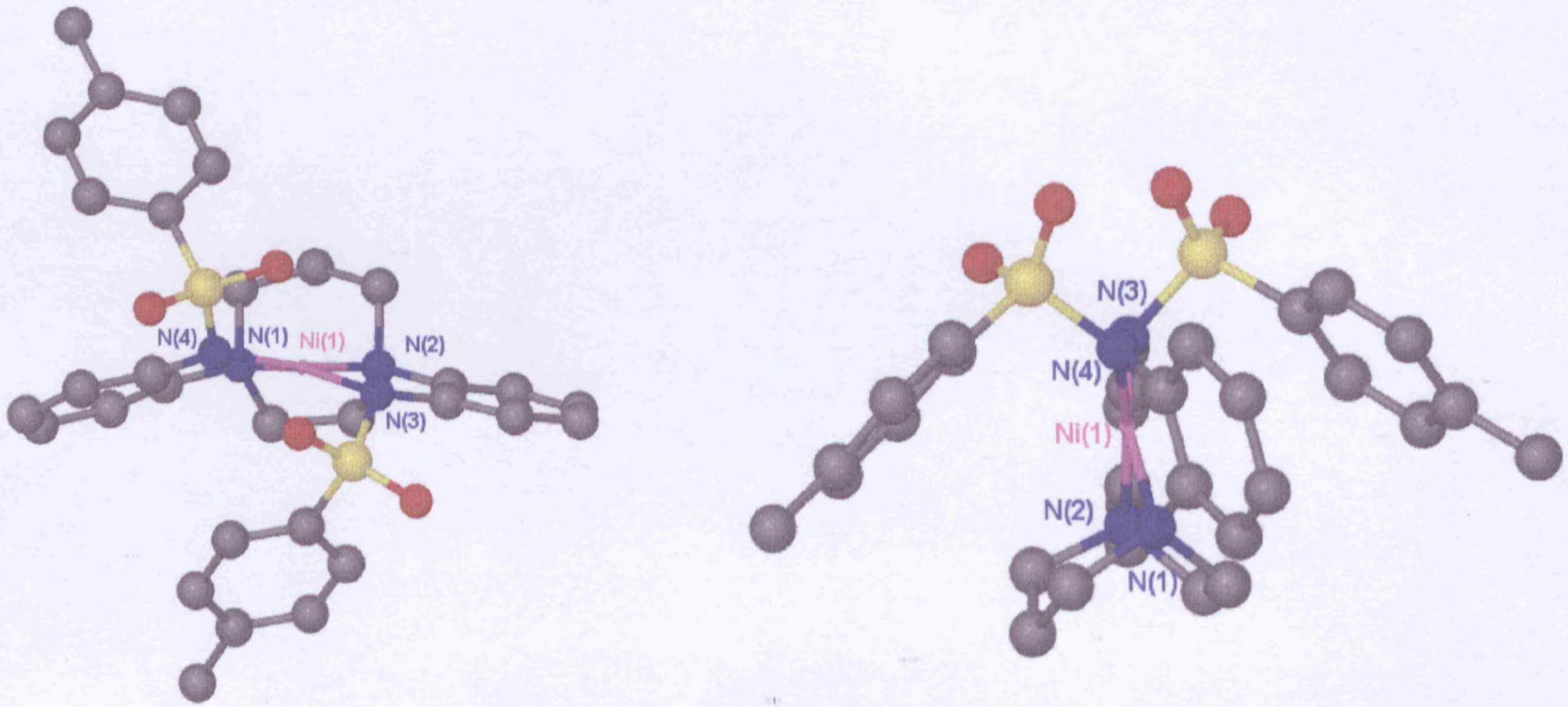

Figure 5.14. [(L^{12})Ni]. Hydrogen atoms have been removed for clarity. Selected bond Lengths: N (1)-Ni 1.912(3), N (2)-Ni 1.903(3), N (3)-Ni (1) 1.939 and N (4)-Ni 1.898(3). Image of [(L^{12})Ni] showing the SO_2 oxygen's not participating with bonding of the nickel centre.

Conclusions

This chapter has shown that there is a possibility of altering the macrocycle size, having fluorine present on the phenyl ring (which allows the possibility of further functionalisation), and the addition of different sulphonyl components, such as the derivatives researched (*p*-fluorophenylsulphonyl chloride, 2-mesitylsulphonyl chloride, and *p*-oxymethylphenylsulphonyl chloride) in chapter four.

Future Work

The outcome of this project has developed many new and interesting fields of research. The pursuit of a nitrous oxide sensor has led us to develop large classes of ligands and metal complexes but without a positive result for the actual complexation of ruthenium. We feel that through further research, an accessible ruthenium source would give the desired result and therefore further preliminary testing can proceed with the nitrous oxide screening. Many factors have influenced the path we have taken, such as the poor yield of tetramesitylporphyrin and difficult chromatography needed to isolate a pure sample. The most restricting factor was the metallation of the porphyrin. Current literature methods found were very vague and we feel yields quoted were ambitious. Attempts by us to form the desired metallated porphyrin failed, as the chromatography procedures followed were inaccurate.

This led us to pursue our own path with the study of potential Taube salt mimics, through the complexation of ruthenium with pentadentate azamacrocycles. Preliminary studies with different ruthenium sources, β-carotene, and silica/alumina mixed unfortunately produced no positive results. A main limiting factor could be that the previous studies by Yamada and Groves were all in the liquid phase, whereas we need our reaction to occur within the solid phase. If this were to work another drawback would be the level of detection needed to comply with current health and safety regulations. There are 11 olefin sites present on β-carotene, therefore epoxidation could occur many times per chromophore, but the degradation of the β-carotene would be unequal throughout the reagent spot. Research into other coloured olefins would be needed, so to produce a more straightforward catalytic cycle. Epoxidation of the olefin would have to incur the loss of the chromophore and so produce some sort of colour change.

Above all the biggest restriction would be the chemical inertness of nitrous oxide. Due to the lack of complexes formed with N_2O, our line of research has been restricted to ruthenium complexes. If in the future other complexes could be found, then more possible options would be available to the researcher.

Appendix i

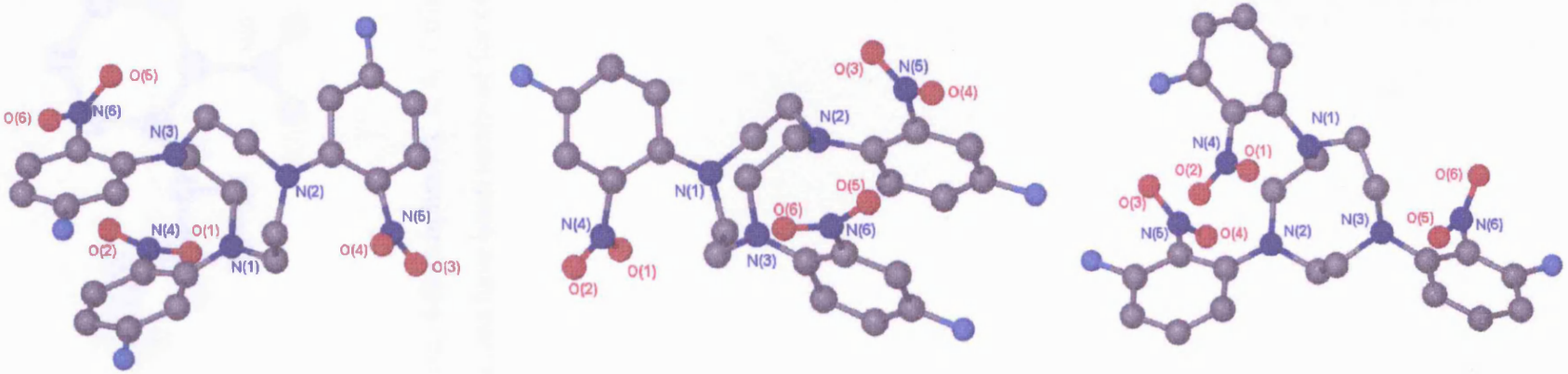

Figure i.1. The crystal structure of $L^{1'}$, $L^{2'}$ and $L^{3'}$. Hydrogen atoms have been removed for clarity.

Appendix ii

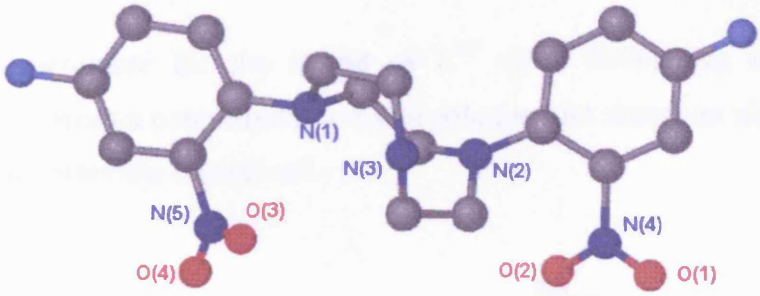

Figure ii.1. Bis 1, 4-bis (2-nitro, 4-fluorophenyl), 1, 4, 7-triazacyclononane (L^{32F2}). Hydrogen atoms have been removed for clarity.

Appendix iii

The crystal structure for the ligand of $L^{11'}$ (IAF 0308) was afforded by crystallisation from a concentrated ethanol solution and shows an almost planar arrangement within the crystal cell.

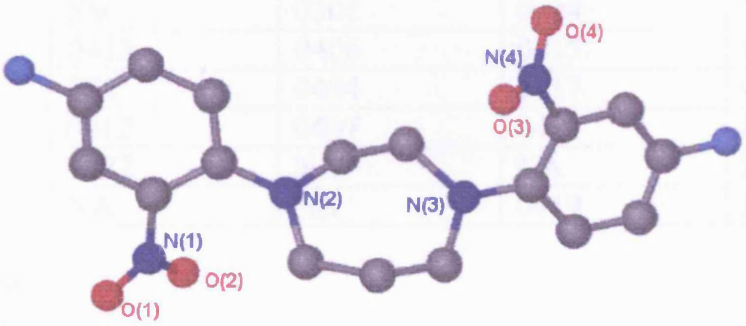

Figure iii.1. *N, N'*-bis (2-nitro, 4-fluorophenyl), 1, 4-diazacycloheptane. Hydrogen atoms have been removed for clarity.

Appendix iv

Crystal Departmental Codes

Chapter Two

	L^1	L^2	L^3	L^9
Ligand	0303	0402	0410	NA
Mn	0418	0405	0416	0422
Fe	0402	0307	NA	NA
Ni	S80	0301	0414	NA
Cu	0413	0406	0415	NA
Zn	S92	0404	0417	0420
Cd	0412	0407	0421	NA
Hg	0427	NA	NA	NA
Pb	NA	NA	0419	NA

Chpater Four

	L^4	L^5	L^6	L^7
Ni	0423	0502	0508	0512
Cu	0501	NA	NA	NA
Zn	0426	0506	NA	NA
Cd	0504	NA	NA	NA
Pb	0503	NA	NA	NA

Chapter Five

	L^{11}	L^{12}
Ni	0408	0409

Table 1. Crystal data and structure refinement for iaf0418.

Identification code	iaf0418	
Empirical formula	C24 H27 Cl2 F3 Mn N6 O8	
Formula weight	710.36	
Temperature	150(2) K	
Wavelength	0.71073 Å	
Crystal system	Cubic	
Space group	P 21 3	
Unit cell dimensions	a = 14.0658(8) Å	□= 90°.
	b = 14.0658(8) Å	□= 90°.
	c = 14.0658(8) Å	□ = 90°.
Volume	2782.9(3) $Å^3$	
Z	4	
Density (calculated)	1.695 Mg/m^3	
Absorption coefficient	0.748 mm^{-1}	
F(000)	1452	
Crystal size	0.28 x 0.25 x 0.25 mm^3	
Theta range for data collection	3.24 to 27.45°.	
Index ranges	-16<=h<=18, -12<=k<=18, -18<=l<=8	
Reflections collected	5092	
Independent reflections	2063 [R(int) = 0.0698]	
Completeness to theta = 27.45°	99.3 %	
Absorption correction	Semi-empirical from equivalents	
Max. and min. transmission	0.8351 and 0.8180	
Refinement method	Full-matrix least-squares on F^2	
Data / restraints / parameters	2063 / 0 / 133	
Goodness-of-fit on F^2	1.034	
Final R indices [I>2sigma(I)]	R1 = 0.0530, wR2 = 0.0918	
R indices (all data)	R1 = 0.0848, wR2 = 0.1043	
Absolute structure parameter	0.02(3)	
Largest diff. peak and hole	0.283 and -0.286 e.$Å^{-3}$	

Table 1. Crystal data and structure refinement for iaf0405.

Identification code	iaf0405
Empirical formula	C26 H30 Cl2 F3 Mn N7 O8
Formula weight	751.41
Temperature	150(2) K
Wavelength	0.71073 Å
Crystal system	Triclinic

Space group	P -1	
Unit cell dimensions	a = 10.8439(3) Å	□=
78.8550(10)°.		
	b = 11.0916(3) Å	□=
77.3900(10)°.		
	c = 14.1396(5) Å	□ =
73.3330(10)°.		
Volume	1574.30(8) $Å^3$	
Z	2	
Density (calculated)	1.585 Mg/m^3	
Absorption coefficient	0.666 mm^{-1}	
F(000)	770	
Crystal size	0.23 x 0.28 x 0.35 mm^3	
Theta range for data collection	2.98 to 27.44°.	
Index ranges	-14<=h<=14, -14<=k<=14, -18<=l<=18	
Reflections collected	19323	
Independent reflections	6930 [R(int) = 0.0619]	
Completeness to theta = 27.44°	96.6 %	
Absorption correction	Semi-empirical from equivalents	
Max. and min. transmission	0.8783 and 0.8783	
Refinement method	Full-matrix least-squares on F^2	
Data / restraints / parameters	6930 / 0 / 412	
Goodness-of-fit on F^2	1.041	
Final R indices [I>2sigma(I)]	R1 = 0.0658, wR2 = 0.1500	
R indices (all data)	R1 = 0.1031, wR2 = 0.1711	
Largest diff. peak and hole	0.935 and -0.798 $e.Å^{-3}$	

Table 1. Crystal data and structure refinement for iaf0416.

Identification code	iaf0416	
Empirical formula	C24 H27 Cl2 F3 Mn N6 O8	
Formula weight	710.36	
Temperature	180(2) K	
Wavelength	0.71073 Å	
Crystal system	Triclinic	
Space group	P -1	
Unit cell dimensions	a = 10.0430(2) Å	a=
84.6120(10)°.		
	b = 10.3171(2) Å	b=
77.8410(10)°.		

	c = 15.3839(4) Å	g =
67.7840(10)°.		
Volume	1442.38(5) $Å^3$	
Z	2	
Density (calculated)	1.636 Mg/m^3	
Absorption coefficient	0.721 mm^{-1}	
F(000)	726	
Crystal size	0.30 x 0.25 x 0.25 mm^3	
Theta range for data collection	3.02 to 27.39°.	
Index ranges	-12<=h<=12, -13<=k<=13, -18<=l<=19	
Reflections collected	21966	
Independent reflections	6437 [R(int) = 0.1169]	
Completeness to theta = 27.39°	98.5 %	
Absorption correction	Semi-empirical from equivalents	
Max. and min. transmission	0.8403 and 0.8127	
Refinement method	Full-matrix least-squares on F^2	
Data / restraints / parameters	6437 / 0 / 414	
Goodness-of-fit on F^2	1.071	
Final R indices [I>2sigma(I)]	R1 = 0.0676, wR2 = 0.1762	
R indices (all data)	R1 = 0.0935, wR2 = 0.1951	
Extinction coefficient	0.011(2)	
Largest diff. peak and hole	1.175 and -1.142 $e.Å^{-3}$	

Table 1. Crystal data and structure refinement for iaf0411.

Identification code	iaf0411	
Empirical formula	C26 H30 Cl2 F3 Fe N7 O8	
Formula weight	752.32	
Temperature	150(2) K	
Wavelength	0.71073 Å	
Crystal system	Triclinic	
Space group	P -1	
Unit cell dimensions	a = 8.8824(3) Å	a=
98.7030(10)°.		
	b = 9.8672(3) Å	b=
91.6510(10)°.		
	c = 18.3752(6) Å	g =
103.3510(10)°.		
Volume	1545.51(9) $Å^3$	
Z	2	

Density (calculated)	1.617 Mg/m^3
Absorption coefficient	0.740 mm^{-1}
F(000)	772
Crystal size	0.18 x 0.10 x 0.03 mm^3
Theta range for data collection	2.94 to 27.56°.
Index ranges	-11<=h<=11, -12<=k<=12, -22<=l<=23
Reflections collected	21961
Independent reflections	7002 [R(int) = 0.0873]
Completeness to theta = 27.56°	97.9 %
Absorption correction	Semi-empirical from equivalents
Max. and min. transmission	0.9782 and 0.8784
Refinement method	Full-matrix least-squares on F^2
Data / restraints / parameters	7002 / 12 / 422
Goodness-of-fit on F^2	1.031
Final R indices [I>2sigma(I)]	R1 = 0.0778, wR2 = 0.1642
R indices (all data)	R1 = 0.1408, wR2 = 0.1940
Largest diff. peak and hole	1.402 and -0.881 e.$Å^{-3}$

Table 1. Crystal data and structure refinement for iaf0307.

Identification code	iaf0307
Empirical formula	C26 H30 Cl2 F3 Fe N7 O8
Formula weight	752.32
Temperature	150(2) K
Wavelength	0.71073 Å
Crystal system	Triclinic
Space group	P -1
Unit cell dimensions	a = 10.4248(3) Å □= 81.1520(10)°.
	b = 10.9636(4) Å □= 77.3660(10)°.
	c = 14.2289(6) Å □ = 73.366(2)°.
Volume	1513.23(9) $Å^3$
Z	2
Density (calculated)	1.651 Mg/m^3
Absorption coefficient	0.755 mm^{-1}
F(000)	772
Crystal size	0.33 x 0.30 x 0.13 mm^3
Theta range for data collection	2.95 to 30.11°.

Index ranges	-14<=h<=14, -15<=k<=15, -19<=l<=20
Reflections collected	21147
Independent reflections	8484 [R(int) = 0.0941]
Completeness to theta = 30.11°	95.1 %
Absorption correction	Semi-empirical from equivalents
Max. and min. transmission	0.9082 and 0.7886
Refinement method	Full-matrix least-squares on F^2
Data / restraints / parameters	8484 / 0 / 413
Goodness-of-fit on F^2	1.020
Final R indices [I>2sigma(I)]	R1 = 0.0848, wR2 = 0.1981
R indices (all data)	R1 = 0.1464, wR2 = 0.2296
Largest diff. peak and hole	0.791 and -1.008 e.$Å^{-3}$

Table 1. Crystal data and structure refinement for 02IAF13.

Empirical formula	C24 H27 Cl2 F3 N6 Ni O8
Formula weight	714.13
Temperature	150(2) K
Wavelength	0.71073 A
Crystal system	Cubic
Space group	P2(1)3 (No. 198)
Unit cell dimensions	a = 14.0797(6) A alpha = 90 deg. b = 14.0797(6) A beta = 90 deg. c = 14.0797(6) A gamma = 90 deg.
Volume	2791.1(2) A^3
Z	4
Density (calculated)	1.699 Mg/m^3
Absorption coefficient	0.967 mm^-1
F(000)	1464
Crystal size	0.35 x 0.30 x 0.25 mm
Theta range for data collection	3.24 to 27.47 deg.
Index ranges	-13<=h<=18, -4<=k<=18, -12<=l<=18
Reflections collected	5062
Independent reflections	2102 [R(int) = 0.0504]

Max. and min. transmission	0.7940 and 0.7282
Refinement method	Full-matrix least-squares on F^2
Data / restraints / parameters	2102 / 0 / 133
Goodness-of-fit on F^2	1.043
Final R indices [I>2sigma(I)]	R1 = 0.0485, wR2 = 0.0881
R indices (all data)	R1 = 0.0642, wR2 = 0.0940
Absolute structure parameter	-0.02(2)
Largest diff. peak and hole	0.486 and -0.490 e.A^-3

Table 1. Crystal data and structure refinement for iaf0301.

Identification code	iaf0301	
Empirical formula	C26 H30 Cl2 F3 N7 Ni O8	
Formula weight	755.18	
Temperature	150(2) K	
Wavelength	0.71073 Å	
Crystal system	Triclinic	
Space group	P -1	
Unit cell dimensions	a = 10.7140(3) Å	□=
79.7670(10)°.		
	b = 10.9970(3) Å	□=
77.763(2)°.		
	c = 14.1370(4) Å	□ =
73.6170(10)°.		
Volume	1549.32(7) $Å^3$	
Z	2	
Density (calculated)	1.619 Mg/m^3	
Absorption coefficient	0.877 mm^{-1}	
F(000)	776	
Crystal size	0.28 x 0.18 x 0.08 mm^3	
Theta range for data collection	3.75 to 26.05°.	
Index ranges	-13<=h<=13, -13<=k<=13, -17<=l<=17	
Reflections collected	26169	
Independent reflections	6078 [R(int) = 0.0977]	
Completeness to theta = 26.05°	99.1 %	
Absorption correction	None	
Max. and min. transmission	0.9331 and 0.7913	
Refinement method	Full-matrix least-squares on F^2	

Data / restraints / parameters	6078 / 0 / 410
Goodness-of-fit on F^2	1.063
Final R indices [I>2sigma(I)]	R1 = 0.0650, wR2 = 0.1636
R indices (all data)	R1 = 0.1004, wR2 = 0.1867
Extinction coefficient	0.025(3)
Largest diff. peak and hole	0.989 and -0.742 e.$Å^{-3}$

Table 1. Crystal data and structure refinement for iaf0414.

Identification code	iaf0414	
Empirical formula	C24 H27 Cl2 F3 N6 Ni O8	
Formula weight	714.13	
Temperature	150(2) K	
Wavelength	0.71073 Å	
Crystal system	Orthorhombic	
Space group	P n a b	
Unit cell dimensions	a = 14.0676(2) Å	a= 90°.
	b = 14.4040(2) Å	b= 90°.
	c = 27.3974(6) Å	g = 90°.
Volume	5551.53(16) $Å^3$	
Z	8	
Density (calculated)	1.709 Mg/m^3	
Absorption coefficient	0.973 mm^{-1}	
F(000)	2928	
Crystal size	0.20 x 0.18 x 0.15 mm^3	
Theta range for data collection	3.55 to 26.37°.	
Index ranges	-17<=h<=17, -17<=k<=18, -24<=l<=34	
Reflections collected	29798	
Independent reflections	5655 [R(int) = 0.0613]	
Completeness to theta = 26.37°	99.6 %	
Absorption correction	Semi-empirical from equivalents	
Max. and min. transmission	0.8678 and 0.8292	
Refinement method	Full-matrix least-squares on F^2	
Data / restraints / parameters	5655 / 54 / 398	
Goodness-of-fit on F^2	1.047	
Final R indices [I>2sigma(I)]	R1 = 0.0760, wR2 = 0.1883	
R indices (all data)	R1 = 0.0966, wR2 = 0.2006	
Largest diff. peak and hole	1.297 and -0.898 e.$Å^{-3}$	

Table 1. Crystal data and structure refinement for iaf0413.

Identification code	iaf0413	
Empirical formula	C24 H27 Cl2 Cu F3 N6 O8	
Formula weight	718.96	
Temperature	150(2) K	
Wavelength	0.71073 Å	
Crystal system	Cubic	
Space group	P 21 3	
Unit cell dimensions	a = 13.9866(7) Å	a= 90°.
	b = 13.9866(7) Å	b= 90°.
	c = 13.9866(7) Å	g = 90°.
Volume	2736.1(2) $Å^3$	
Z	4	
Density (calculated)	1.745 Mg/m^3	
Absorption coefficient	1.076 mm^{-1}	
F(000)	1468	
Crystal size	0.25 x 0.20 x 0.20 mm^3	
Theta range for data collection	3.26 to 27.44°.	
Index ranges	-14<=h<=18, -14<=k<=17, -10<=l<=18	
Reflections collected	6098	
Independent reflections	2100 [R(int) = 0.0723]	
Completeness to theta = 27.44°	99.6 %	
Absorption correction	Semi-empirical from equivalents	
Max. and min. transmission	0.8136 and 0.7747	
Refinement method	Full-matrix least-squares on F^2	
Data / restraints / parameters	2100 / 6 / 133	
Goodness-of-fit on F^2	1.039	
Final R indices [I>2sigma(I)]	R1 = 0.0562, wR2 = 0.1226	
R indices (all data)	R1 = 0.0833, wR2 = 0.1362	
Absolute structure parameter	0.06(3)	
Largest diff. peak and hole	0.726 and -0.316 e.$Å^{-3}$	

Table 1. Crystal data and structure refinement for iaf0406.

Identification code	iaf0406
Empirical formula	C26 H30 Cl2 Cu F3 N7 O8
Formula weight	760.01
Temperature	150(2) K
Wavelength	0.71073 Å
Crystal system	Triclinic
Space group	P -1

Unit cell dimensions	a = 10.7705(2) Å	□= 79.101(1)°.
	b = 10.8796(2) Å	□= 77.203(1)°.
	c = 14.2665(3) Å	□ = 72.745(1)°.
Volume	1543.11(5) $Å^3$	
Z	2	
Density (calculated)	1.636 Mg/m^3	
Absorption coefficient	0.960 mm^{-1}	
F(000)	778	
Crystal size	0.25 x 0.15 x 0.10 mm^3	
Theta range for data collection	2.95 to 30.04°.	
Index ranges	-15<=h<=15, -15<=k<=15, -19<=l<=20	
Reflections collected	28588	
Independent reflections	8961 [R(int) = 0.0681]	
Completeness to theta = 30.04°	99.1 %	
Absorption correction	Semi-empirical from equivalents	
Max. and min. transmission	0.9101 and 0.7954	
Refinement method	Full-matrix least-squares on F^2	
Data / restraints / parameters	8961 / 0 / 425	
Goodness-of-fit on F^2	1.027	
Final R indices [I>2sigma(I)]	R1 = 0.0494, wR2 = 0.1085	
R indices (all data)	R1 = 0.0746, wR2 = 0.1190	
Largest diff. peak and hole	0.790 and -0.637 e.$Å^{-3}$	

Table 1. Crystal data and structure refinement for iaf0415.

Identification code	iaf0415	
Empirical formula	C24 H27 Cl2 Cu F3 N6 O8	
Formula weight	718.96	
Temperature	150(2) K	
Wavelength	0.71073 Å	
Crystal system	Orthorhombic	
Space group	P n a b	
Unit cell dimensions	a = 14.0450(2) Å	□= 90°.
	b = 14.3669(2) Å	□= 90°.
	c = 27.4338(5) Å	□ = 90°.
Volume	5535.68(15) $Å^3$	
Z	8	

Density (calculated)	1.725 Mg/m^3
Absorption coefficient	1.064 mm^{-1}
F(000)	2936
Crystal size	0.25 x 0.15 x 0.13 mm^3
Theta range for data collection	2.97 to 27.48°.
Index ranges	-18<=h<=18, -18<=k<=18, -31<=l<=35
Reflections collected	32388
Independent reflections	6338 [R(int) = 0.0962]
Completeness to theta = 27.48°	99.8 %
Absorption correction	Semi-empirical from equivalents
Max. and min. transmission	0.8741 and 0.7768
Refinement method	Full-matrix least-squares on F^2
Data / restraints / parameters	6338 / 0 / 408
Goodness-of-fit on F^2	1.037
Final R indices [I>2sigma(I)]	R1 = 0.0480, wR2 = 0.0983
R indices (all data)	R1 = 0.0714, wR2 = 0.1078
Largest diff. peak and hole	0.475 and -0.547 $e.Å^{-3}$

Table 1. Crystal data and structure refinement for 02IAF12.

Empirical formula	C24 H27 Cl2 F3 N6 O8 Zn
Formula weight	720.79
Temperature	150(2) K
Wavelength	0.71073 A
Crystal system	Cubic
Space group	P2(1)3 (No. 198)
Unit cell dimensions	a = 14.0172(5) A alpha = 90 deg. b = 14.0172(5) A beta = 90 deg. c = 14.0172(5) A gamma = 90 deg.
Volume	2754.13(17) A^3
Z	4
Density (calculated)	1.738 Mg/m^3
Absorption coefficient	1.168 mm^-1
F(000)	1472
Crystal size	0.20 x 0.15 x 0.10 mm
Theta range for data collection	3.25 to 27.47 deg.

Index ranges	-13<=h<=18, -11<=k<=18, -14<=l<=18
Reflections collected	5838
Independent reflections	1993 [R(int) = 0.0433]
Max. and min. transmission	0.8922 and 0.8000
Refinement method	Full-matrix least-squares on F^2
Data / restraints / parameters	1993 / 0 / 133
Goodness-of-fit on F^2	1.030
Final R indices [I>2sigma(I)]	R1 = 0.0389, wR2 = 0.0781
R indices (all data)	R1 = 0.0479, wR2 = 0.0821
Absolute structure parameter	0.009(18)
Largest diff. peak and hole	0.438 and -0.521 e.A^-3

Table 1. Crystal data and structure refinement for iaf0404.

Identification code	iaf0404	
Empirical formula	C26 H30 Cl2 F3 N7 O8 Zn1	
Formula weight	761.84	
Temperature	150(2) K	
Wavelength	0.71073 Å	
Crystal system	Triclinic	
Space group	P-1	
Unit cell dimensions	a = 10.8230(2) Å	a=
79.0690(10)°.		
	b = 11.0024(3) Å	b=
77.6390(10)°.		
	c = 14.0990(4) Å	g =
73.1250(10)°.		
Volume	1554.69(7) $Å^3$	
Z	2	
Density (calculated)	1.627 Mg/m^3	
Absorption coefficient	1.040 mm^{-1}	
F(000)	780	
Crystal size	0.20 x 0.20 x 0.20 mm^3	
Theta range for data collection	2.99 to 27.49°.	
Index ranges	-13<=h<=14, -13<=k<=14, -14<=l<=18	
Reflections collected	23557	
Independent reflections	6931 [R(int) = 0.0866]	

Completeness to theta = 27.49°	97.1 %
Absorption correction	Semi-empirical from equivalents
Max. and min. transmission	0.906 and 0.830
Refinement method	Full-matrix least-squares on F^2
Data / restraints / parameters	6931 / 0 / 450
Goodness-of-fit on F^2	1.076
Final R indices [I>2sigma(I)]	R1 = 0.0519, wR2 = 0.1012
R indices (all data)	R1 = 0.1167, wR2 = 0.1215
Largest diff. peak and hole0.519 and -0.536 e.$Å^{-3}$	

Table 1. Crystal data and structure refinement for iaf0417.

Identification code	iaf0417	
Empirical formula	C24 H27 Cl2 F3 N6 O8 Zn	
Formula weight	720.79	
Temperature	150(2) K	
Wavelength	0.71073 Å	
Crystal system	Orthorhombic	
Space group	P n a b	
Unit cell dimensions	a = 14.17760(10) Å	a= 90°.
	b = 14.25980(10) Å	b= 90°.
	c = 27.5815(3) Å	g = 90°.
Volume	5576.14(8) $Å^3$	
Z	8	
Density (calculated)	1.717 Mg/m^3	
Absorption coefficient	1.154 mm^{-1}	
F(000)	2944	
Crystal size	0.25 x 0.15 x 0.13 mm^3	
Theta range for data collection	3.00 to 27.49°.	
Index ranges	-18<=h<=18, -18<=k<=18, -35<=l<=35	
Reflections collected	48827	
Independent reflections	6364 [R(int) = 0.1131]	
Completeness to theta = 27.49°	99.2 %	
Absorption correction	Semi-empirical from equivalents	
Max. and min. transmission	0.8645 and 0.7613	
Refinement method	Full-matrix least-squares on F^2	
Data / restraints / parameters	6364 / 30 / 408	
Goodness-of-fit on F^2	1.084	
Final R indices [I>2sigma(I)]	R1 = 0.0601, wR2 = 0.1433	
R indices (all data)	R1 = 0.0825, wR2 = 0.1557	

Largest diff. peak and hole	0.954 and -0.734 e.Å^{-3}

Table 1. Crystal data and structure refinement for iaf0412.

Identification code	iaf0412	
Empirical formula	C8 H9 Cd0.33 Cl0.67 F N2 O2.67	
Formula weight	255.94	
Temperature	150(2) K	
Wavelength	0.71069 Å	
Crystal system	Cubic	
Space group	P 21 3	
Unit cell dimensions	a = 14.083(5) Å	□= 90°.
	b = 14.083(5) Å	□= 90°.
	c = 14.083(5) Å	□ = 90°.
Volume	2793.1(17) Å^3	
Z	12	
Density (calculated)	1.826 Mg/m^3	
Absorption coefficient	1.054 mm^{-1}	
F(000)	1544	
Crystal size	0.20 x 0.15 x 0.10 mm^3	
Theta range for data collection	3.23 to 27.46°.	
Index ranges	-18<=h<=18, -18<=k<=18, -18<=l<=13	
Reflections collected	27702	
Independent reflections	2149 [R(int) = 0.1407]	
Completeness to theta = 27.46°	99.8 %	
Absorption correction	Semi-empirical from equivalents	
Max. and min. transmission	0.9019 and 0.8168	
Refinement method	Full-matrix least-squares on F^2	
Data / restraints / parameters	2149 / 0 / 133	
Goodness-of-fit on F^2	1.076	
Final R indices [I>2sigma(I)]	R1 = 0.0384, wR2 = 0.0684	
R indices (all data)	R1 = 0.0547, wR2 = 0.0734	
Absolute structure parameter	-0.02(4)	
Largest diff. peak and hole	0.343 and -0.346 e.Å^{-3}	

Table 1. Crystal data and structure refinement for iaf0407.

Identification code	iaf0407
Empirical formula	C24 H27 Cd Cl2 F3 N6 O8
Formula weight	767.82
Temperature	150(2) K

Wavelength	0.71073 Å	
Crystal system	Monoclinic	
Space group	P 21/n	
Unit cell dimensions	a = 11.0887(5) Å	a= 90°.
	b = 21.7388(8) Å	b=
101.874(2)°.		
	c = 12.0387(6) Å	g = 90°.
Volume	2839.9(2) $Å^3$	
Z	4	
Density (calculated)	1.796 Mg/m^3	
Absorption coefficient	1.037 mm^{-1}	
F(000)	1544	
Crystal size	0.20 x 0.13 x 0.10 mm^3	
Theta range for data collection	3.58 to 25.03°.	
Index ranges	-12<=h<=12, -25<=k<=25, -14<=l<=14	
Reflections collected	24465	
Independent reflections	4895 [R(int) = 0.1128]	
Completeness to theta = 25.03°	97.4 %	
Absorption correction	Semi-empirical from equivalents	
Max. and min. transmission	0.9034 and 0.8195	
Refinement method	Full-matrix least-squares on F^2	
Data / restraints / parameters	4895 / 0 / 401	
Goodness-of-fit on F^2	1.156	
Final R indices [I>2sigma(I)]	R1 = 0.1164, wR2 = 0.2633	
R indices (all data)	R1 = 0.1444, wR2 = 0.2773	
Largest diff. peak and hole3.227 and -1.233 e.$Å^{-3}$		

Table 1. Crystal data and structure refinement for iaf0421.

Identification code	iaf0421	
Empirical formula	C25.50 H30.50 Cd Cl2 F3 N6.50 O8.50	
Formula weight	804.36	
Temperature	150(2) K	
Wavelength	0.71073 Å	
Crystal system	Monoclinic	
Space group	P 2/c	
Unit cell dimensions	a = 13.4616(2) Å	a= 90°.
	b = 8.9614(2) Å	b=
100.0520(10)°.		
	c = 26.6072(6) Å	g = 90°.

Volume	3160.48(11) $Å^3$
Z	4
Density (calculated)	1.690 Mg/m^3
Absorption coefficient	0.937 mm^{-1}
F(000)	1624
Crystal size	0.35 x 0.30 x 0.15 mm^3
Theta range for data collection	2.92 to 27.47°.
Index ranges	-17<=h<=17, -8<=k<=11, -34<=l<=34
Reflections collected	21407
Independent reflections	7192 [R(int) = 0.0813]
Completeness to theta = 27.47°	99.2 %
Absorption correction	Semi-empirical from equivalents
Max. and min. transmission	0.8722 and 0.7350
Refinement method	Full-matrix least-squares on F^2
Data / restraints / parameters	7192 / 37 / 422
Goodness-of-fit on F^2	1.068
Final R indices [I>2sigma(I)]	R1 = 0.0625, wR2 = 0.1581
R indices (all data)	R1 = 0.0835, wR2 = 0.1711
Largest diff. peak and hole2.823 and -1.489 e.$Å^{-3}$	

Table 1. Crystal data and structure refinement for iaf0427.

Identification code	iaf0427	
Empirical formula	C24 H27 Cl2 F3 Hg N6 O8	
Formula weight	856.01	
Temperature	150(2) K	
Wavelength	0.71073 Å	
Crystal system	Cubic	
Space group	P 21 3	
Unit cell dimensions	a = 14.0927(6) Å	a= 90°.
	b = 14.0927(6) Å	b= 90°.
	c = 14.0927(6) Å	g = 90°.
Volume	2798.9(2) $Å^3$	
Z	4	
Density (calculated)	2.031 Mg/m^3	
Absorption coefficient	5.771 mm^{-1}	
F(000)	1672	
Crystal size	0.15 x 0.15 x 0.10 mm^3	
Theta range for data collection	3.23 to 30.03°.	
Index ranges	-14<=h<=19, -19<=k<=18, -9<=l<=19	

Reflections collected	7072
Independent reflections	2722 [R(int) = 0.0724]
Completeness to theta = 30.03°	99.3 %
Absorption correction	Semi-empirical from equivalents
Max. and min. transmission	0.5961 and 0.4781
Refinement method	Full-matrix least-squares on F^2
Data / restraints / parameters	2722 / 0 / 133
Goodness-of-fit on F^2	1.035
Final R indices [I>2sigma(I)]	R1 = 0.0473, wR2 = 0.0802
R indices (all data)	R1 = 0.0611, wR2 = 0.0851
Absolute structure parameter	-0.017(11)
Largest diff. peak and hole	0.798 and -0.646 e.$Å^{-3}$

Table 1. Crystal data and structure refinement for iaf0419.

Identification code	iaf0419	
Empirical formula	C24 H27 Cl2 F3 N6 O8 Pb	
Formula weight	862.61	
Temperature	150(2) K	
Wavelength	0.71073 Å	
Crystal system	Monoclinic	
Space group	P 21/c	
Unit cell dimensions	a = 10.2444(2) Å	a= 90°.
	b = 18.7379(3) Å	b=
99.4060(10)°.		
	c = 14.9096(3) Å	g = 90°.
Volume	2823.54(9) $Å^3$	
Z	4	
Density (calculated)	2.029 Mg/m^3	
Absorption coefficient	6.245 mm^{-1}	
F(000)	1680	
Crystal size	0.23 x 0.15 x 0.10 mm^3	
Theta range for data collection	3.13 to 30.07°.	
Index ranges	-14<=h<=14, -18<=k<=26, -20<=l<=20	
Reflections collected	30488	
Independent reflections	8215 [R(int) = 0.1042]	
Completeness to theta = 30.07°	99.0 %	
Absorption correction	Semi-empirical from equivalents	
Max. and min. transmission	0.5740 and 0.3277	

Refinement method	Full-matrix least-squares on F^2
Data / restraints / parameters	8215 / 18 / 453
Goodness-of-fit on F^2	1.097
Final R indices [I>2sigma(I)]	R1 = 0.0361, wR2 = 0.0868
R indices (all data)	R1 = 0.0440, wR2 = 0.0910
Largest diff. peak and hole	1.081 and -2.251 e.$Å^{-3}$

Table 1. Crystal data and structure refinement for iaf0422.

Identification code	iaf0422	
Empirical formula	C24 H29 Cl2 F Mn N6 O8	
Formula weight	674.37	
Temperature	150(2) K	
Wavelength	0.71073 Å	
Crystal system	Cubic	
Space group	P 21 3	
Unit cell dimensions	a = 14.0304(6) Å	a= 90°.
	b = 14.0304(6) Å	b= 90°.
	c = 14.0304(6) Å	g = 90°.
Volume	2761.9(2) $Å^3$	
Z	4	
Density (calculated)	1.622 Mg/m^3	
Absorption coefficient	0.739 mm^{-1}	
F(000)	1388	
Crystal size	0.28 x 0.28 x 0.10 mm^3	
Theta range for data collection	3.25 to 27.48°.	
Index ranges	-14<=h<=18, -14<=k<=18, -8<=l<=18	
Reflections collected	5915	
Independent reflections	2106 [R(int) = 0.0658]	
Completeness to theta = 27.48°	99.4 %	
Absorption correction	Semi-empirical from equivalents	
Max. and min. transmission	0.9298 and 0.8199	
Refinement method	Full-matrix least-squares on F^2	
Data / restraints / parameters	2106 / 0 / 133	
Goodness-of-fit on F^2	1.073	
Final R indices [I>2sigma(I)]	R1 = 0.0687, wR2 = 0.1735	
R indices (all data)	R1 = 0.0813, wR2 = 0.1837	
Absolute structure parameter	0.05(5)	
Largest diff. peak and hole	1.443 and -0.458 e.$Å^{-3}$	

Table 1. Crystal data and structure refinement for iaf0420.

Identification code	iaf0420	
Empirical formula	C8 H9 Cl0.67 F0.33 N2 O2.67 Zn0.33	
Formula weight	227.60	
Temperature	150(2) K	
Wavelength	0.71069 Å	
Crystal system	Cubic	
Space group	P 21 3	
Unit cell dimensions	a = 13.952(5) Å	a= 90°.
	b = 13.952(5) Å	b= 90°.
	c = 13.952(5) Å	g = 90°.
Volume	2715.9(17) $Å^3$	
Z	12	
Density (calculated)	1.670 Mg/m^3	
Absorption coefficient	1.169 mm^{-1}	
F(000)	1400	
Crystal size	0.28 x 0.25 x 0.23 mm^3	
Theta range for data collection	2.92 to 27.47°.	
Index ranges	-13<=h<=18, -8<=k<=18, -17<=l<=14	
Reflections collected	5403	
Independent reflections	2070 [R(int) = 0.0574]	
Completeness to theta = 27.47°	99.8 %	
Absorption correction	Semi-empirical from equivalents	
Max. and min. transmission	0.7748 and 0.7355	
Refinement method	Full-matrix least-squares on F^2	
Data / restraints / parameters	2070 / 0 / 133	
Goodness-of-fit on F^2	1.039	
Final R indices [I>2sigma(I)]	R1 = 0.0685, wR2 = 0.1737	
R indices (all data)	R1 = 0.0857, wR2 = 0.1882	
Absolute structure parameter	-0.02(3)	
Largest diff. peak and hole	1.540 and -0.583 e.$Å^{-3}$	

Table 1. Crystal data and structure refinement for iaf0423.

Identification code	iaf0423
Empirical formula	C29 H37 Cl2 N7 Ni O10 S
Formula weight	805.33
Temperature	150(2) K
Wavelength	0.71073 Å

Crystal system	Monoclinic	
Space group	P 21/n	
Unit cell dimensions	a = 10.52110(10) Å	a= 90°.
	b = 26.9809(4) Å	b=
108.1560(10)°.		
	c = 13.1552(2) Å	g = 90°.
Volume	3548.42(8) $Å^3$	
Z	4	
Density (calculated)	1.507 Mg/m^3	
Absorption coefficient	0.820 mm^{-1}	
F(000)	1672	
Crystal size	0.30 x 0.20 x 0.20 mm^3	
Theta range for data collection	2.98 to 27.48°.	
Index ranges	-13<=h<=13, -34<=k<=35, -17<=l<=17	
Reflections collected	28941	
Independent reflections	8101 [R(int) = 0.0912]	
Completeness to theta = 27.48°	99.7 %	
Absorption correction	Semi-empirical from equivalents	
Max. and min. transmission	0.8531 and 0.7909	
Refinement method	Full-matrix least-squares on F^2	
Data / restraints / parameters	8101 / 30 / 473	
Goodness-of-fit on F^2	1.094	
Final R indices [I>2sigma(I)]	R1 = 0.0537, wR2 = 0.1309	
R indices (all data)	R1 = 0.0762, wR2 = 0.1421	
Largest diff. peak and hole	1.444 and -0.745 e.$Å^{-3}$	

Table 1. Crystal data and structure refinement for iaf0502.

Identification code	iaf0502	
Empirical formula	C31 H40 Cl2 N8 Ni O11 S	
Formula weight	862.38	
Temperature	150(2) K	
Wavelength	0.71073 Å	
Crystal system	Triclinic	
Space group	P -1	
Unit cell dimensions	a = 10.7650(3) Å	a=
93.5730(10)°.		
	b = 13.4460(4) Å	b=
98.8200(10)°.		
	c = 13.7870(5) Å	g =

106.899(2)°.

Volume	1874.77(10) $Å^3$
Z	2
Density (calculated)	1.528 Mg/m^3
Absorption coefficient	0.784 mm^{-1}
F(000)	896
Crystal size	0.23 x 0.18 x 0.08 mm^3
Theta range for data collection	3.53 to 26.37°.
Index ranges	-13<=h<=13, -16<=k<=16, -17<=l<=17
Reflections collected	29404
Independent reflections	7655 [R(int) = 0.0903]
Completeness to theta = 26.37°	99.6 %
Absorption correction	Semi-empirical from equivalents
Max. and min. transmission	0.9399 and 0.8402
Refinement method	Full-matrix least-squares on F^2
Data / restraints / parameters	7655 / 90 / 491
Goodness-of-fit on F^2	1.030
Final R indices [I>2sigma(I)]	R1 = 0.1052, wR2 = 0.2555
R indices (all data)	R1 = 0.1417, wR2 = 0.2797
Largest diff. peak and hole	2.264 and -0.995 e.$Å^{-3}$

Table 1. Crystal data and structure refinement for iaf0508.

Identification code	iaf0508	
Empirical formula	C28 H36 Cl2 F N7 Ni O11 S	
Formula weight	827.31	
Temperature	150(2) K	
Wavelength	0.71073 Å	
Crystal system	Triclinic	
Space group	P -1	
Unit cell dimensions	a = 10.7270(3) Å	a=
109.307(2)°.		
	b = 13.7960(4) Å	b=
111.184(2)°.		
	c = 14.0750(5) Å	g =
99.343(2)°.		
Volume	1736.43(9) $Å^3$	
Z	2	
Density (calculated)	1.582 Mg/m^3	
Absorption coefficient	0.846 mm^{-1}	

F(000)	856
Crystal size	0.18 x 0.15 x 0.15 mm^3
Theta range for data collection	3.52 to 26.37°.
Index ranges	-13<=h<=13, -17<=k<=17, -17<=l<=17
Reflections collected	26253
Independent reflections	7071 [R(int) = 0.0961]
Completeness to theta = 26.37°	99.6 %
Absorption correction	Semi-empirical from equivalents
Max. and min. transmission	0.8835 and 0.8626
Refinement method	Full-matrix least-squares on F^2
Data / restraints / parameters	7071 / 6 / 489
Goodness-of-fit on F^2	1.028
Final R indices [I>2sigma(I)]	R1 = 0.0518, wR2 = 0.0998
R indices (all data)	R1 = 0.0837, wR2 = 0.1110
Largest diff. peak and hole	0.494 and -0.543 e.$Å^{-3}$

Table 1. Crystal data and structure refinement for iaf0512.

Identification code	iaf0512	
Empirical formula	C31 H41 Cl2 N7 Ni O10 S	
Formula weight	833.38	
Temperature	150(2) K	
Wavelength	0.71073 Å	
Crystal system	Monoclinic	
Space group	P 21/n	
Unit cell dimensions	a = 10.51400(10) Å	a= 90°.
	b = 27.5370(4) Å	b=
108.4110(10)°.		
	c = 13.0140(2) Å	g = 90°.
Volume	3575.01(8) $Å^3$	
Z	4	
Density (calculated)	1.548 Mg/m^3	
Absorption coefficient	0.817 mm^{-1}	
F(000)	1736	
Crystal size	0.15 x 0.15 x 0.03 mm^3	
Theta range for data collection	3.60 to 26.37°.	
Index ranges	-13<=h<=13, -34<=k<=34, -16<=l<=16	
Reflections collected	27921	
Independent reflections	7281 [R(int) = 0.0557]	
Completeness to theta = 26.37°	99.6 %	

Absorption correction	Semi-empirical from equivalents
Max. and min. transmission	0.9759 and 0.8873
Refinement method	Full-matrix least-squares on F^2
Data / restraints / parameters	7281 / 0 / 464
Goodness-of-fit on F^2	1.037
Final R indices [I>2sigma(I)]	R1 = 0.0660, wR2 = 0.1692
R indices (all data)	R1 = 0.0874, wR2 = 0.1828
Largest diff. peak and hole	1.762 and -0.941 e.Å^{-3}

Table 1. Crystal data and structure refinement for iaf0426.

Identification code	iaf0426	
Empirical formula	C29 H37 Cl2 N7 O10 S Zn	
Formula weight	811.99	
Temperature	150(2) K	
Wavelength	0.71073 Å	
Crystal system	Monoclinic	
Space group	P 21/n	
Unit cell dimensions	a = 10.5744(2) Å	a= 90°.
	b = 26.9854(4) Å	b=
108.6140(10)°.		
	c = 13.2130(2) Å	g = 90°.
Volume	3573.16(10) Å^3	
Z	4	
Density (calculated)	1.509 Mg/m^3	
Absorption coefficient	0.959 mm^{-1}	
F(000)	1680	
Crystal size	0.30 x 0.23 x 0.10 mm^3	
Theta range for data collection	2.98 to 27.50°.	
Index ranges	-13<=h<=13, -33<=k<=35, -17<=l<=17	
Reflections collected	27943	
Independent reflections	8176 [R(int) = 0.0691]	
Completeness to theta = 27.50°	99.6 %	
Absorption correction	Semi-empirical from equivalents	
Max. and min. transmission	0.9102 and 0.7618	
Refinement method	Full-matrix least-squares on F^2	
Data / restraints / parameters	8176 / 36 / 474	
Goodness-of-fit on F^2	1.035	
Final R indices [I>2sigma(I)]	R1 = 0.0507, wR2 = 0.1172	
R indices (all data)	R1 = 0.0805, wR2 = 0.1306	

Largest diff. peak and hole	0.897 and -0.601 e.Å^{-3}

Table 1. Crystal data and structure refinement for iaf0506.

Identification code	iaf0506	
Empirical formula	C29 H37 Cl2 N7 O11 S Zn	
Formula weight	827.99	
Temperature	150(2) K	
Wavelength	0.71073 Å	
Crystal system	Monoclinic	
Space group	P 21/n	
Unit cell dimensions	a = 15.6220(2) Å	a= 90°.
	b = 12.9110(3) Å	b=
107.1190(10)°.		
	c = 18.4590(4) Å	g = 90°.
Volume	3558.15(12) Å^3	
Z	4	
Density (calculated)	1.546 Mg/m^3	
Absorption coefficient	0.967 mm^{-1}	
F(000)	1712	
Crystal size	0.43 x 0.23 x 0.20 mm^3	
Theta range for data collection	3.62 to 26.37°.	
Index ranges	-19<=h<=19, -16<=k<=16, -23<=l<=23	
Reflections collected	52914	
Independent reflections	7259 [R(int) = 0.2247]	
Completeness to theta = 26.37°	99.7 %	
Absorption correction	Numerical	
Max. and min. transmission	0.8302 and 0.6813	
Refinement method	Full-matrix least-squares on F^2	
Data / restraints / parameters	7259 / 18 / 463	
Goodness-of-fit on F^2	1.044	
Final R indices [I>2sigma(I)]	R1 = 0.0579, wR2 = 0.1355	
R indices (all data)	R1 = 0.0930, wR2 = 0.1514	
Largest diff. peak and hole0.521 and -0.501 e.Å^{-3}		

Table 1. Crystal data and structure refinement for iaf0501.

Identification code	iaf0501
Empirical formula	C57.50 H74.50 Cl4 Cu2 N13.50 O20.50 S2
Formula weight	1615.81
Temperature	150(2) K

Wavelength	0.71073 Å
Crystal system	Triclinic
Space group	P -1
Unit cell dimensions	a = 13.6500(5) Å a= 114.5540(10)°.
	b = 16.2300(5) Å b= 95.4010(10)°.
	c = 18.5970(7) Å g = 90.7610(10)°.
Volume	3724.5(2) $Å^3$
Z	2
Density (calculated)	1.441 Mg/m^3
Absorption coefficient	0.847 mm^{-1}
F(000)	1672
Crystal size	0.25 x 0.20 x 0.05 mm^3
Theta range for data collection	2.91 to 24.99°.
Index ranges	-16<=h<=16, -19<=k<=18, -22<=l<=22
Reflections collected	44248
Independent reflections	12915 [R(int) = 0.1416]
Completeness to theta = 24.99°	98.4 %
Absorption correction	Semi-empirical from equivalents
Max. and min. transmission	0.9589 and 0.8161
Refinement method	Full-matrix least-squares on F^2
Data / restraints / parameters	12915 / 60 / 915
Goodness-of-fit on F^2	1.138
Final R indices [I>2sigma(I)]	R1 = 0.1465, wR2 = 0.3461
R indices (all data)	R1 = 0.2056, wR2 = 0.3756
Largest diff. peak and hole	1.845 and -0.742 e.$Å^{-3}$

Table 1. Crystal data and structure refinement for iaf0504.

Identification code	iaf0504
Empirical formula	C26 H34.50 Cd Cl2 N5.50 O10.50 S
Formula weight	807.45
Temperature	150(2) K
Wavelength	0.71073 Å
Crystal system	Triclinic
Space group	P -1
Unit cell dimensions	a = 9.9690(2) Å a= 78.8950(10)°.

	b = 11.6260(2) Å	b=
86.0020(10)°.		
	c = 14.5400(3) Å	g =
84.0680(10)°.		
Volume	1642.63(6) $Å^3$	
Z	2	
Density (calculated)	1.633 Mg/m^3	
Absorption coefficient	0.954 mm^{-1}	
F(000)	822	
Crystal size	0.25 x 0.25 x 0.10 mm^3	
Theta range for data collection	3.08 to 27.34°.	
Index ranges	-12<=h<=12, -14<=k<=14, -18<=l<=18	
Reflections collected	27261	
Independent reflections	7338 [R(int) = 0.0935]	
Completeness to theta = 27.34°	99.0 %	
Absorption correction	Semi-empirical from equivalents	
Max. and min. transmission	0.9106 and 0.7964	
Refinement method	Full-matrix least-squares on F^2	
Data / restraints / parameters	7338 / 2 / 415	
Goodness-of-fit on F^2	1.042	
Final R indices [I>2sigma(I)]	R1 = 0.0513, wR2 = 0.1372	
R indices (all data)	R1 = 0.0692, wR2 = 0.1487	
Largest diff. peak and hole	1.919 and -0.939 e.$Å^{-3}$	

Table 1. Crystal data and structure refinement for iaf0503.

Identification code	iaf0503	
Empirical formula	C29 H37 Cl2 N7 O10 Pb S	
Formula weight	953.81	
Temperature	150(2) K	
Wavelength	0.71073 Å	
Crystal system	Triclinic	
Space group	P -1	
Unit cell dimensions	a = 11.7030(2) Å	a=
113.6220(10)°.		
	b = 12.3650(2) Å	b=
92.8370(10)°.		
	c = 14.0520(2) Å	g =
106.2030(10)°.		
Volume	1758.72(5) $Å^3$	

Z	2
Density (calculated)	1.801 Mg/m^3
Absorption coefficient	5.073 mm^{-1}
F(000)	944
Crystal size	0.33 x 0.28 x 0.25 mm^3
Theta range for data collection	2.95 to 27.47°.
Index ranges	-15<=h<=15, -16<=k<=16, -18<=l<=18
Reflections collected	28667
Independent reflections	7986 [R(int) = 0.0622]
Completeness to theta = 27.47°	99.3 %
Absorption correction	Semi-empirical from equivalents
Max. and min. transmission	0.3636 and 0.2853
Refinement method	Full-matrix least-squares on F^2
Data / restraints / parameters	7986 / 12 / 454
Goodness-of-fit on F^2	1.014
Final R indices [I>2sigma(I)]	R1 = 0.0318, wR2 = 0.0678
R indices (all data)	R1 = 0.0377, wR2 = 0.0703
Largest diff. peak and hole	1.574 and -1.084 e.$Å^{-3}$

Table 1. Crystal data and structure refinement for iaf0408.

Identification code	iaf0408	
Empirical formula	C24 H32 Cl2 F2 N9 Ni O8	
Formula weight	742.20	
Temperature	150(2) K	
Wavelength	0.71073 Å	
Crystal system	Triclinic	
Space group	P -1	
Unit cell dimensions	a = 8.44000(10) Å	□=
90.0000(10)°.		
	b = 25.0230(3) Å	□=
95.1530(10)°.		
	c = 15.2870(5) Å	□ =
90.0000(10)°.		
Volume	3215.48(12) $Å^3$	
Z	4	
Density (calculated)	1.533 Mg/m^3	
Absorption coefficient	0.841 mm^{-1}	
F(000)	1532	
Crystal size	0.20 x 0.18 x 0.15 mm^3	

Theta range for data collection	3.52 to 27.31°.
Index ranges	-9<=h<=10, -32<=k<=32, -19<=l<=17
Reflections collected	37832
Independent reflections	7185 [R(int) = 0.1415]
Completeness to theta = 27.31°	99.3 %
Absorption correction	None
Refinement method	Full-matrix least-squares on F^2
Data / restraints / parameters	7185 / 0 / 450
Goodness-of-fit on F^2	1.062
Final R indices [I>2sigma(I)]	R1 = 0.0723, wR2 = 0.1787
R indices (all data)	R1 = 0.1103, wR2 = 0.1973
Largest diff. peak and hole	1.547 and -0.714 e.$Å^{-3}$

Table 1. Crystal data and structure refinement for iaf0409.

Identification code	iaf0409	
Empirical formula	C31 H32 N4 Ni O4 S2	
Formula weight	647.44	
Temperature	150(2) K	
Wavelength	0.71073 Å	
Crystal system	Orthorhombic	
Space group	P 212121	
Unit cell dimensions	a = 8.4419(2) Å	a= 90°.
	b = 15.8586(3) Å	b= 90°.
	c = 21.2946(6) Å	g = 90°.
Volume	2850.85(12) $Å^3$	
Z	4	
Density (calculated)	1.508 Mg/m^3	
Absorption coefficient	0.873 mm^{-1}	
F(000)	1352	
Crystal size	0.15 x 0.15 x 0.13 mm^3	
Theta range for data collection	3.08 to 27.47°.	
Index ranges	-9<=h<=10, -20<=k<=20, -26<=l<=27	
Reflections collected	23848	
Independent reflections	6136 [R(int) = 0.0903]	
Completeness to theta = 27.47°	98.5 %	
Absorption correction	Semi-empirical from equivalents	
Max. and min. transmission	0.8950 and 0.8803	
Refinement method	Full-matrix least-squares on F^2	
Data / restraints / parameters	6136 / 0 / 381	

Goodness-of-fit on F^2	1.031
Final R indices [I>2sigma(I)]	R1 = 0.0511, wR2 = 0.0800
R indices (all data)	R1 = 0.1011, wR2 = 0.0944
Absolute structure parameter	-0.010(16)
Largest diff. peak and hole	0.400 and -0.439 e.A^{-3}

Table 1. Crystal data and structure refinement for iaf0302.

Identification code	iaf0302
Empirical formula	C24 H21 F3 N6 O6
Formula weight	546.47
Temperature	150(2) K
Wavelength	0.71073 Å
Crystal system	Triclinic
Space group	P -1
Unit cell dimensions	a = 7.8250(2) Å □=
88.754(1)°.	
	b = 7.9750(2) Å □=
85.637(1)°.	
	c = 20.5520(6) Å □ =
64.579(1)°.	
Volume	1154.92(5) $Å^3$
Z	2
Density (calculated)	1.571 Mg/m^3
Absorption coefficient	0.131 mm^{-1}
F(000)	564
Crystal size	0.25 x 0.18 x 0.15 mm^3
Theta range for data collection	3.55 to 27.45°.
Index ranges	-10<=h<=10, -10<=k<=10, -26<=l<=26
Reflections collected	18907
Independent reflections	5216 [R(int) = 0.1396]
Completeness to theta = 27.45°	98.7 %
Absorption correction	Semi-empirical from equivalents
Max. and min. transmission	1.265 and 0.769
Refinement method	Full-matrix least-squares on F^2
Data / restraints / parameters	5216 / 0 / 353
Goodness-of-fit on F^2	1.123
Final R indices [I>2sigma(I)]	R1 = 0.1577, wR2 = 0.4014
R indices (all data)	R1 = 0.1760, wR2 = 0.4083
Extinction coefficient	0.076(11)

Largest diff. peak and hole	0.815 and -0.541 e.Å^{-3}

Table 1. Crystal data and structure refinement for iaf0410.

Identification code	iaf0410	
Empirical formula	C24 H21 F3 N6 O6	
Formula weight	546.47	
Temperature	150(2) K	
Wavelength	0.71073 Å	
Crystal system	Orthorhombic	
Space group	P 212121	
Unit cell dimensions	a = 7.4079(2) Å	a= 90°.
	b = 13.7027(3) Å	b= 90°.
	c = 23.1595(5) Å	g = 90°.
Volume	2350.88(10) Å^3	
Z	4	
Density (calculated)	1.544 Mg/m^3	
Absorption coefficient	0.129 mm^{-1}	
F(000)	1128	
Crystal size	0.28 x 0.20 x 0.20 mm^3	
Theta range for data collection	3.52 to 26.37°.	
Index ranges	-9<=h<=9, -14<=k<=17, -28<=l<=27	
Reflections collected	19622	
Independent reflections	4782 [R(int) = 0.0786]	
Completeness to theta = 26.37°	99.6 %	
Absorption correction	Semi-empirical from equivalents	
Max. and min. transmission	0.9747 and 0.9649	
Refinement method	Full-matrix least-squares on F^2	
Data / restraints / parameters	4782 / 0 / 353	
Goodness-of-fit on F^2	1.002	
Final R indices [I>2sigma(I)]	R1 = 0.0459, wR2 = 0.0880	
R indices (all data)	R1 = 0.0999, wR2 = 0.1028	
Absolute structure parameter	-0.6(8)	
Extinction coefficient	0.0112(11)	
Largest diff. peak and hole	0.200 and -0.206 e.Å^{-3}	

Table 1. Crystal data and structure refinement for iaf0403.

Identification code	iaf0403
Empirical formula	C18 H19 F2 K N5 O4
Formula weight	446.48

Temperature	120(2) K	
Wavelength	0.71073 Å	
Crystal system	Monoclinic	
Space group	P 21/n	
Unit cell dimensions	a = 7.9432(3) Å	a= 90°.
	b = 13.4354(6) Å	b=
95.715(2)°.		
	c = 18.1300(7) Å	g = 90°.
Volume	1925.22(13) $Å^3$	
Z	4	
Density (calculated)	1.540 Mg/m^3	
Absorption coefficient	0.332 mm^{-1}	
F(000)	924	
Crystal size	0.25 x 0.25 x 0.08 mm^3	
Theta range for data collection	2.99 to 27.48°.	
Index ranges	-10<=h<=10, -15<=k<=17, -21<=l<=22	
Reflections collected	12440	
Independent reflections	4020 [R(int) = 0.0782]	
Completeness to theta = 25.00°	97.8 %	
Absorption correction	Semi-empirical from equivalents	
Max. and min. transmission	0.9739 and 0.9215	
Refinement method	Full-matrix least-squares on F^2	
Data / restraints / parameters	4020 / 0 / 271	
Goodness-of-fit on F^2	1.072	
Final R indices [I>2sigma(I)]	R1 = 0.0739, wR2 = 0.1864	
R indices (all data)	R1 = 0.1394, wR2 = 0.2251	
Largest diff. peak and hole	0.875 and -0.671 e.$Å^{-3}$	

Table 1. Crystal data and structure refinement for iaf0308.

Identification code	iaf0308	
Empirical formula	C17 H16 F2 N4 O4	
Formula weight	378.34	
Temperature	150(2) K	
Wavelength	0.71069 Å	
Crystal system	Triclinic	
Space group	P -1	
Unit cell dimensions	a = 8.212(5) Å	□=
93.416(5)°.		
	b = 8.535(5) Å	□=

77.309(5)°.

c = 11.798(5) Å □ =

82.241(5)°.

Volume	795.9(8) $Å^3$
Z	2
Density (calculated)	1.579 Mg/m^3
Absorption coefficient	0.130 mm^{-1}
F(000)	392
Crystal size	0.30 x 0.20 x 0.10 mm^3
Theta range for data collection	2.87 to 30.17°.
Index ranges	-10<=h<=10, -10<=k<=11, -11<=l<=15
Reflections collected	12904
Independent reflections	3559 [R(int) = 0.1069]
Completeness to theta = 25.00°	99.7 %
Absorption correction	Semi-empirical from equivalents
Max. and min. transmission	0.9871 and 0.9621
Refinement method	Full-matrix least-squares on F^2
Data / restraints / parameters	3559 / 0 / 245
Goodness-of-fit on F^2	0.982
Final R indices [I>2sigma(I)]	R1 = 0.0622, wR2 = 0.1330
R indices (all data)	R1 = 0.1651, wR2 = 0.1719
Extinction coefficient	0.026(4)
Largest diff. peak and hole	0.318 and -0.344 $e.Å^{-3}$